The Role of Novel Genes in CNS Axon Regeneration

By

Sharif H Almutiri

A thesis submitted to the University of Birmingham for the degree of

DOCTOR OF PHILOSOPHY

March 2017

Neuroscience and Ophthalmology
Institute of Inflammation and Ageing
College of Medical and Dental Sciences
University of Birmingham

Abstract

Unlike the peripheral nervous system, the spinal cord which forms part of the central nervous system (CNS) is unable to regenerate. Intrinsic and extrinsic environment changes following spinal cord injury are the main factors contributed to inhibit neuronal survival and axonal growth. However, manipulating the growth-relative genes in the CNS after injury can induce limited axon regeneration. In this study we demonstrate by manipulating expression of three protein molecules AMIGO3 (an amphoterin-induced gene open reading frame), RTN3 (Reticulon 3) and astrocyte elevated gene-1 (AEG-1/ also known as MTDH/LYRIC1)), where axon regeneration in the CNS is possible. Data from a microarray screen in regenerating and non-regenerating spinal cord injury models showed that low levels of AMIGO3 expression correlated with regenerating sciatic nerve (SN) and preconditioning SN+DC lesion models. Conversely, high levels of RTN3 and AEG-1 were found to be correlated with regeneration injury models. *In vitro* knockdown of AMIGO3 combined with neurotrophin 3 (NT3) has been shown to promote dorsal root ganglion neuron (DRGN) neurite outgrowth, and *in vivo* delivery of non-viral mediated shRNA/AMIGO3 plasmid to suppress AMIGO3 expression demonstrated significant DC axon regeneration. In addition, *in vitro* knockdown of both RTN3 and AEG-1 suppressed DRGN neurite outgrowth, demonstrating that they are required for axonal growth. The mechanisms by which AMIGO3, RTN3 and AEG-1 suppress or promote axonal regeneration is not yet known but we conclude that they play a major role in axonal regeneration and could be harnessed to promote regeneration of the CNS.

Dedication

I dedicate this work to my great mum ‘Fatimah’ and my lovely wife ‘Hanan’ without them I would not have been continued for higher education.

Acknowledgments

I am extremely thankful and always will be to Allah (Subhanah Wa Ta'ala) the almighty who gave me health and patience to complete this effort.

Then I would like to extend my huge thanks to my great supervisor Dr. Zubair Ahmed who has been an amazing supervisor throughout my PhD, provided me with endless support, guidance, knowledge, help and always welcoming me any time during his work; truly without him I would not be able to complete this work.

I'm truly grateful to my second supervisor Professor Ann Logan who provided me with the perfect amount of support and use of her lab during my study, and would also like to thank Professor Martin Berry, Dr Carolyn Jones, Dr Ghazzalah Begum, Dr Sarina Surey, Maryam Esmaeili, Adam Thompson, Simon Foale and all the members of Neuroscience and Ophthalmology group (past and present) who have always been happy to assist me with my experimental work.

Very special thanks to my amazing brothers and sisters who kept in touch and encouraged me to do this work, and finally not to forget my children Yazan and Almass who made me enjoy the rest of my time at home playing with them, and also causing a little delay to my work.

Table of contents

List of figures

List of tables

Abbreviations

AAV	Adeno-associated virus
AD	Alzheimer’s disease
AEG-1	Astrocyte elevated gene-1
AMIGO	Amphoterin-induced gene and open reading frame
ANOVA	Analysis of Variance
APP	Amyloid precursor protein
APS	Ammonium persulphate
ASIA	American Spinal Injury Association
Aβ	β-amyloid
BACE1	β-amyloid cleaving enzyme 1
BBB	Basso, Beattie, Bresnahan
BMP	Bone morphogenic protein
BSA	Bovine serum albumin
BSCB	Blood-spinal cord barrier
CAP23	Cytoskeleton associated protein-23
Caps	Capricious
CD	Cluster of differentiation
cDNA	Complimentary DNA
CEACAM1	Carcinoembryonic antigen-related cell adhesion molecule-1
CME	CNS myelin extracts

CNS	Central nervous system
CRELD1	Cysteine rich with EGF like domains 1
CSPG	Chondroitin sulphate proteoglycans
DC	Dorsal column
DEGA	Differentially expressed in gastric adenocarcinomas
DREZ	Dorsal root entry zone
DRG	Dorsal root ganglia
DRGN	Dorsal root ganglion neurons
EAA	Excitatory amino acids
EAAT	Excitatory amino acid transporter
ECL	Enhanced chemiluminescence
ECM	Extracellular matrix
EGFR	Epidermal growth factor receptor
ELISA	Enzyme linked immunosorbent assay
ER	Endoplasmic reticulum
ESC	Embryonic stem cells
FGF-2	Fibroblast growth factor-2
GAP43	Growth associated proteins-43
GAPDH	Glyceraldehyde 3-phosphate dehydrogenase
GFAP	Glial fibrillary acidic protein
GM	Gray matter
HAD	HIV-1 associated dementia

HIV-1	Human immunodeficiency virus-1
HMGB1	High-mobility group box-1
HSPGs	Heparan sulphate proteoglycans
IFNγ	Interferon gamma
Ig	Immunoglobulin
IL	Interleukins
KSPGs	Keratin sulphate proteoglycans
L	Lumber
LHD	Lung-homing-domain
LIF	Leukaemia inhibitory factor
LILRB	PirB paired-immunoglobulin-like receptor-B
LIMK	LIM-domain containing protein kinases
LRR	Leucine-rich repeat
LYRIC1	Lysine-rich CEACAM1 co-isolated
MAG	Myelin associated glycoprotein
MMP	Matrix metalloproteinase
mRNA	Messenger RNA
MTDH	Metadherin
NBA	Neurobasal-A
NDD	Neurodegenerative diseases
NF1	Neurofibromatosis type 1 gene
NGA2	Nerve-glial antigen 2

Ngn2	Neurogenic transcription factor
NgR1	Nogo receptor 1
NSCISC	The National Spinal Cord Injury Statistics Centre
NSP	Neuroendocrine-specific proteins
NT3	Neurotrophin 3
ODD	Order differential display
OMGp	Oligodendrocyte-derived myelin glycoprotein
OPC	Oligodendrocyte precursor cells
P	Probability
PBS	Phosphate buffer saline
PDL	Poly-D-lysine
PFA	Paraformaldehyde
PHFAs	Primary human fetal astrocytes
PNS	Peripheral nervous system
PVDF	Polyvinylidene fluoride membranes
RAGE	Receptor for advance glycation end products
RAGs	Regeneration-associated genes
RaSH	Rapid subtraction hypridization approach
RGC	Retinal ganglion cells
RHD	Reticulon homology domains
RIDNs	RTN3 immunoreactive dystrophic neurites
ROCK	Rho-associated kinase

RT	Room temperature
RTNs	Reticulons
RT-PCR	Reverse Transcriptase-polymerase chain reaction
SCI	Spinal cord injury
SDS	Sodium dodecyl sulphate
siRNA	Short interferon RNA
S	Sacral
SN	Sciatic nerve
T	Thoracic
TEMED	Tetramethylethylenediamine
TGFβ	Transforming growth factor beta
TID	Trypsin Inhibitor/DNase
TLR	Toll-like receptor
TNFα	Tumour necrosis factor alpha
Trk	Tropomyosin receptor kinases
TTBS	Tween-Tris buffered saline
WM	White mattter
YY1	Ying Yang-1

CHAPTER 1: General Introduction

1.1 The complex system of the CNS

The CNS comprises the brain and the spinal cord. The brain receives and processes sensory inputs from both the spinal cord and its own nerves whilst the spinal cord conducts sensory information to the brain and motor information from the brain to skeletal, cardiac and smooth muscle, and glands among other functions. These actions enable the CNS to control motor movement, regulate respiration, maintain homeostasis, and provide logical coordination of all bodily activity (Shoichet et al., 2008). Any injury to the CNS will thus result in the inability of the CNS to perform these actions leading to morbidity, and ultimately mortality. Accidents, stroke, trauma, and tumours among others can cause injuries to the CNS system.

1.2 Spinal cord anatomy

The spinal cord caudally extends below the brainstem, which is an essential part of the central nervous system. The spinal cord plays important roles in transmitting and integrating the sensory, motor and autonomic signals between the brain and the body. It is protected and supported by the bony structure of the vertebral column and like the brain, is encapsulated by three membranes of the CNS known as meninges, i.e, pia, arachnoid and dura mater. The pia mater, the innermost layer is extremely delicate and adheres to the surface of the spinal cord whereas the arachnoid mater is a web-like membrane that lies between pia and the tough outermost layer, the dura mater **(Figure 0.1)** (Nógrádi and Vrbová, 2006).

The cord contains regions of long myelinated fibers of inter-neurons that run in bundles refered to as tracts. These regions are refered to as white mattter (WM) as a result of their colouration due to the heavy degree of myelination. The WM is divided into three regions known as ventral (anterior), lateral and dorsal (posterior) culumns. The dorsal tracts bring messages from the periphary to the brain, hence termed ascending, with the ventral tract being predominantly concerned with relaying information from the brain to the periphery. The inner cord, is termed gray matter (GM), and is composed of nerve-cell bodies. Each spinal nerve emerging from the spinal cord is connected to it by short branches, one from the ventral region, and one from the dorsal region, called the dorsal and ventral roots. These roots join in the spinal nerve before the nerve leaves the vertabral column (Miele et al., 2012, Oke, 1844).

The vertebraes in the human spinal cord are comprised of 31 segments, which are divided into five groups; 8 cervical, 12 thoracic, 5 lumbar, 5 sacral and 1 coccygeal. In each vertebral level, there are entry and exit nerves of the spinal cord, motor and sensory nerve roots where they are named according to their emergence site. Cervical nerves mainly control neck, head and upper part of the human body, whilst thoracic spinal nerves provide control for abdominal muscles. Lumbar and sacral nerve levels mainly control lower organs and extremities.

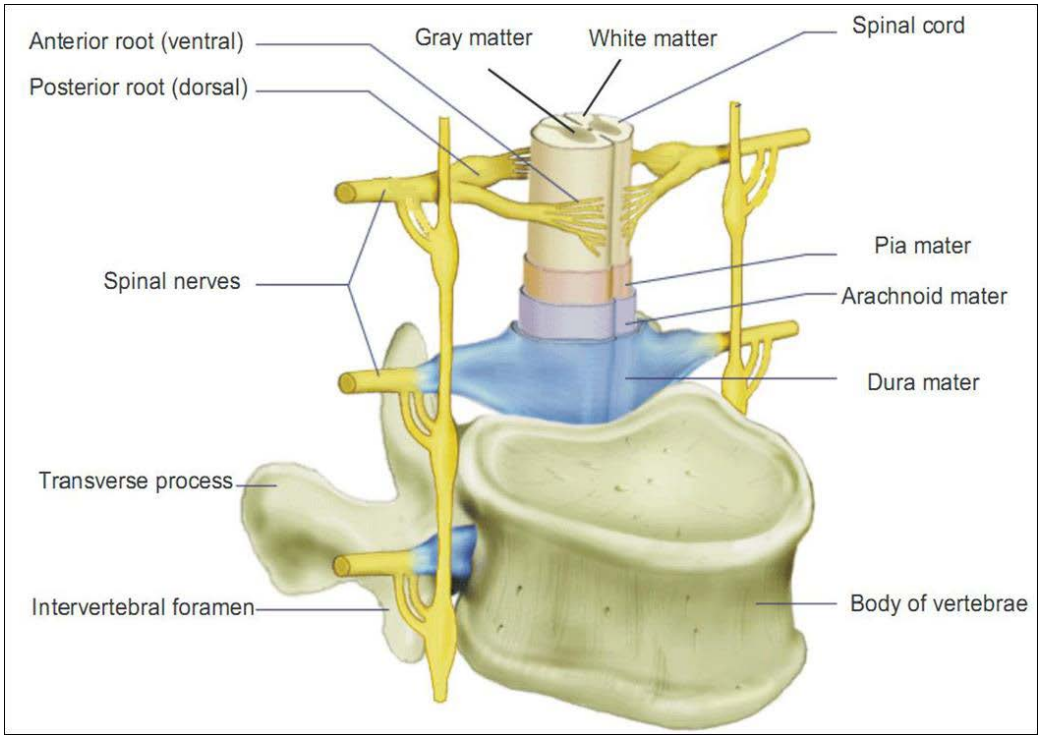

Figure 0.1: Anatomy of the spinal cord.

Illustrates the white and gray matter of the spinal cord together with the meninges (pia, arachnoid and dura maters) and surrounding vertebral column. Also presents dorsal (posterior) and ventral (anterior) roots that carry the sensory and motor signals. (Adapted from (Mohamad and Anuar, 2014)).

1.2.1 Dorsal root ganglion neurons (DRGN)

DRGN are sensory neurons that relay sensory inputs from the periphery of the body to the spinal cord and the brain with their cell bodies lying in the dorsal root ganglia lateral to the spinal cord (Saijilafu and Zhou, 2012). The axons of DRGN grow from the cell body and branch into two; one innervating the peripheral targets such as motor muscles and other body organs, and the other innervating the CNS

through the spinal cord. Since the cell bodies of DRGN lie outside the CNS, they are considered part of the peripheral nervous system (PNS) **(Figure 0.2)**. While successful regeneration of adult neurons in the CNS is limited, the peripheral DRGN projections are known to readily regenerate after injury (Wall, 1992). However, it has been shown that if damage to the peripheral DRGN projection occur prior to the CNS damage (pre-conditioning lesion), there is hastened recovery of the CNS neuron (Wall, 1992). This has led many researchers to hypothesize that DRGN have a role to play in the regeneration of the CNS neurons and understanding the environmental factors influencing the two neural systems and their interaction with each other may help improve the regenerative strategies of the CNS. For example, the central axons of the DRGN share the same environment as the axons of the CNS neurons in the spinal cord since the two form synapses (Wall, 1992). The molecular factors that influence the growth of the DRGN should therefore be the same as those that influence the growth of the CNS neurons in the spinal cord. Therefore, controlling and understanding the regeneration of DRGN can derive better methods of enhancing the growth of CNS neurons.

Peripheral conditioning lesions are one of the major tools being used to understand regenerative capacity of CNS neurons (Hollis and Zou, 2012). Many researchers tend to agree that injury to the peripheral DRGN projection regulates gene expression to increase the intrinsic growth capacity of the neurons to regenerate (Richardson and Issa, 1984). By providing permissive growth substrates, peripheral nerves can be stimulated to regenerate but the regeneration of the CNS through this method is still moderate. Also, by controlling the

environment, DRGN can be manipulated to create models of CNS neurons making regenerative studies possible.

For example, Chong *et al* (1999) found that the central axons of the DRGN regenerated after injury but only up to the dorsal root entry zone (DREZ) and were prevented from re-growing back into the spinal cord. By sectioning L4 and L5 dorsal roots in adult rats, they demonstrated that central axons of the DRGN were able to grow back into the spinal cord (Chong et al., 1999). Another study by Irina *et al* (2010) suggests that the response to growth factors responsible for the regeneration of the DRGN into the spinal cord is also dependent on the spinal level. Different regenerative responses may be observed in the DRGN compared to the CNS neurons under the same conditions, however, DRGN still provide good models for understanding axonal regeneration in the CNS (Vetter et al., 2010).

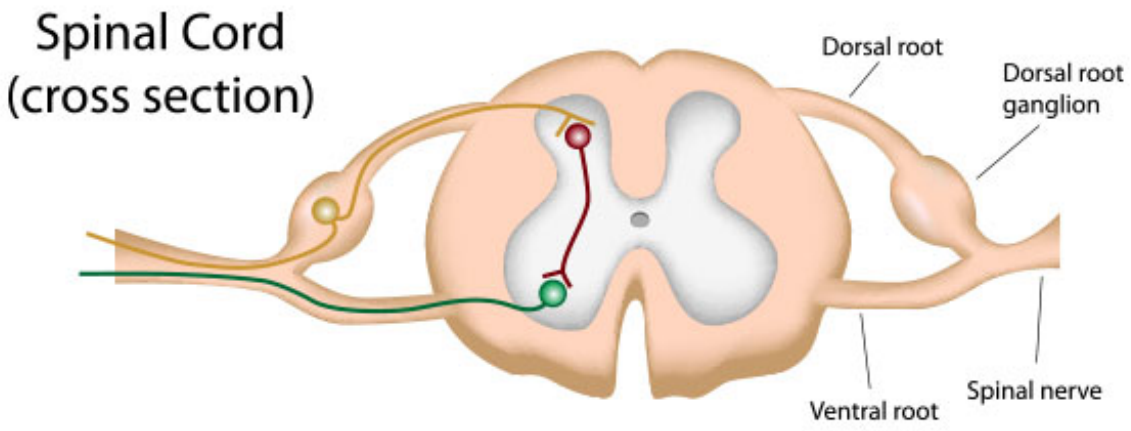

Figure 0.2: Diagram of spinal cord cross section showing dorsal root ganglion neurons (DRGNs).

DRGN are located in dorsal root ganglia and give rise to both peripherally and centrally directed axons. (Adapted from, www.socratic.org, 2016).

1.2.2 Ascending pathways in the dorsal column

The ascending pathway of the spinal cord mainly conducts the signals and information from receptors in the limbs and trunk to the brain. Two main groups found essential in the spinal cord ascending fibres, direct and postsynaptic dorsal column pathways. The ascending pathway in the direct dorsal column comprised of two branches from primary afferents of the sensory neurons. One innervates receptors in the muscle, skin while the other branches connected to the brain via the dorsal roots of the spinal cord (Waile et al., 1995, Willis Jr and Coggeshall, 2004).

The ascending branches from primary afferents mainly end in the gray matter of the spinal cord while a fraction of these branches project to the dorsal nuclei. A large number of DRGN that are based in the cervical region project directly to the dorsal nuclei compared with lumbar DRGN. Axons travelling within the dorsal column normally terminate in different areas of gray matter such as the ventral horn, dorsal horn and intermediate region (Smith and Bennett, 1987, Giuffrida and Rustioni, 1992, Willis Jr and Coggeshall, 2004). In the rat spinal cord, 25% of the dorsal column axons are unmyelinated, which suggests that these unmyelinated projections might carry information from visceral or nociceptors to the dorsal column nuclei (Chung et al., 1987, McNeill et al., 1988, Tamatani et al., 1989, Patterson et al., 1990). On the other hand, the postsynaptic dorsal column pathway is different from the direct pathway; here the pathway is formed by the axons of spinal neurons that travel to the dorsal column nuclei. These neurons are in the nucleus proprius, which reside ventral to the substantia gelatinosa and the postsynaptic pathway axons terminate at all rostrocaudal levels of the cuneate and

gracile nuclei (Giesler and Cliffer, 1985, Giesler et al., 1984, de Pommery et al., 1984).

1.3 Epidemiology of spinal cord injury (SCI)

SCI is one of the major types of CNS injuries that cause loss of autonomic, motor and sensory function, which lead to long-term personal difficulty to the patient. Patients with SCI normally have a permanent loss of function due to lack of effective treatments to repair and regeneration of the damaged axons or to prevent the secondary injury that normally results after SCI (Di Giovanni, 2006, Luo et al., 2009). It is estimated that each year there are 130,000 new cases of SCI around the world and approximately 40 new cases of SCI per million of the worldwide population (Illes et al., 2011, Forostyak et al., 2013). There are approximately 1000 new cases of SCI in UK alone and estimates of 12,000 new cases per year in the Unites States (Devivo, 2012).

The major causes of SCI include vehicular accidents, traumatic falls, violence and sports. The consequences of SCI are psychological, physical, and economical. Statistics show that only about 12% of people with SCI are able to maintain their employment after one year of injury. This employment rate increases to about 30% over a 20-year period but generally over 60% of these injured individuals are unable to work again during their lifetime. Loss of employment, together with lengthy periods of admissions in hospitals, the economic burden of SCI is estimated to average $70,000 per injured person per year. This translates to over $840 million every year (The National Spinal Cord Injury Statistics Centre (NSCISC)).

1.4 The pathological response to SCI

1.4.1 Phases of SCI

There are three generalised phases of responses after SCI, which extend from acute, secondary and chronic phases that respond to the primary injury event (Hulsebosch, 2002).

1.4.1.1 Acute phase

The acute phase begins from the moment of the injury and extends for few days, where different pathophysiological processes are activated. There is immediate mechanical disruption to the neurons among other soft tissue including endothelial cells of the surrounding vasculature. The mechanical damage in the immediate hours after SCI leads to cell loss including neurons and oligodendrocytes and necrosis (Hulsebosch, 2002, Di Giovanni, 2006). In the next few minutes of the insult, the injured neuron responds back by injury-induced barrage of action potentials accompanied with electrolyte shifts that contribute to spinal shock and functional neural failure, which is a generalized failure of circuitry in the spinal neural network, lasting for about 24 hours (Hulsebosch, 2002).

Furthermore, loss of micro-circulation by thrombosis, haemorrhage which is accompanied by oedema, loss of auto-regulation and vasospasm and mechanical damage further aggravate the neural injury. The acute phase usually persists for hours up to days before being subsequently resolved into the sub-acute phase (Mohamad and Anuar, 2014).

1.4.1.2 Secondary phase

The pathology of the secondary injury phase is an outcome of the molecular and cellular responses after mechanical trauma to the spinal cord. In the secondary phase, several pathologies processing continued from the acute phase, including oedema, cell death and electrolyte shifts (Lu et al., 2000). The cell death or necrosis is characterised by energy loss, swelling and intense damage of mitochondria which lead to cell lysis. The release of intracellular constituents due to cell rupture results in the induction of the inflammation processes, where the extracellular concentrations including excitatory amino acids (EAA) and glutamate reach toxic levels (Hulsebosch, 2002, Mohamad and Anuar, 2014).

Later on, apoptosis or programmed cell death occurs that is associated with increased expression levels of glial fibrillary acidic protein (GFAP), astrocyte proliferation that plays a role in oligodendrocytes death thus, axonal demyelination. Increasing the concentration of local chemokine and cytokines and invading inflammatory cells such as; lymphocytes and neutrophils leads to further necrosis and apoptosis. (Liu et al., 1997, Hulsebosch, 2002). The inhibitory molecules to axonal regeneration begin to be expressed surrounding the lesion area and subsequently enlargement of the lesion cavity/size results in further cell death and damage to the axonal architecture.

1.4.1.3 Chronic phase

The chronic phase of SCI lasts from weeks to years; apoptosis is continued in both orthograde and retrograde direction of the lesion site. Ion channels and other

different types of receptors become altered in their activation status and expression levels. These events lead to scar formation in the cord and conduction deficits due to demyelination as well as syringomyelia (a fluid-filled cyst formed and continue to enlarge). However, chronic pain syndrome occurs in most SCI patients due to neural circuit disruption in inhibitory and excitatory inputs (Christensen et al., 1996, Christensen and Hulsebosch, 1997, Hulsebosch, 2002, Bertram and Heil, 2017).

1.4.2 Inflammatory response

As with all forms of physical injury, spinal cord damage is followed by a significant inflammatory response. However, due to the highlighted specialised and sensitive nature of neural tissues, the nature and outcome of this secondary inflammation within the spine is highly pertinent to the overall outcome of the injury, and much research has been focused on elucidating the nature of the response and in finding ways to manipulate this response towards a less deleterious outcome (Ju et al., 2014). When a physical insult to the spinal cord occurs, the tissue, including the neural axons that travel longitudinally through the vertebral column are damaged, as are the glial cells, including the oligodendrocytes, astrocytes and microglia that sub-serve the neurons and maintain homeostasis within the tissue.

On a timescale of hours to days subsequent to the initial insult, secondary pathological processes occur including changes to the regional vasculature that affects blood flow to the wound environment. This includes obstruction of the vessels serving the wound site itself; changes in the availability of local

electrolytes, the generation of excess free radicals within the affected tissues, the generation of action potentials by excitotoxicity, and the cascades of molecules and cells that accompany a generic innate immune response (Cao and He, 2013, Ankeny and Popovich, 2009). During this second phase of damage to the spinal cord, the site of injury becomes a fluid filled cavity enclosed by a glial scar, which acts as an impediment for neuron growth and axonal regeneration (Ankeny and Popovich, 2009, Fawcett and Asher, 1999). Among the many processes which take place in the time immediately after SCI, the inflammatory cascades are perhaps the most damaging in terms of perturbing the repair processes that attempts to regenerate competent, preserved tissues (Hammond et al., 2014).

The initial disruption to the blood-spinal cord barrier (BSCB) which occurs during a SCI results in the migration of immune cells from the peripheral circulation into the site of inflammation as a result of chemotactic proteins generated from the complement cascade which is triggered at the time of the physical damage to the tissue (Hawthorne and Popovich, 2011). Following the initial influx of neutrophils, inflammatory cells secrete extracellular matrix (ECM) digesting elastases and matrix metalloproteinases (MMP), the site is then populated by macrophages and their precursors, monocytes, around 2 - 4 days after injury (Hawthorne and Popovich, 2011). These cells continues to migrate into the wound for a number of weeks after injury and following these, around 4 weeks post injury, adaptive immune cells such as T and B cells begin to migrate into the lesioned area.

1.4.3 Glial scar and cavity formation

The formation of scar tissue surrounding the lesion site is one of the many reactive changes that has received attention after SCI. This pathological response is also referred to 'glial scar' due to reactive astrocytes playing a prominent role in this process, however other studies have suggested that cells of pericyte origin are also involved in the scar formation (Goritz et al., 2011, Faulkner et al., 2004). The term reactive astrogliosis (will be discussed below in section 1.4.4.1 in more details) is a result of local astrocytes undergoing proliferation, hypertrophy and increased secretion of GFAP that respond to the injury (Pekny and Nilsson, 2005, Pekny et al., 2014). The formation of the glia scar has both advantages and disadvantages. The heavy glial scar that is formed surrounding the dying and damaged tissues at the lesion site have several advantages, including re-establishment of the BSCB, restrict the cytotoxic inflammatory response within this lesion, release anti-oxidants that help defend against oxidative stress and protects against glutamate excitotoxicity via glutamate uptake. On the other hand, the damaged area which is sealed by the scar continues to undergo apoptosis and necrosis. These processes produce a large quantity of tissue debris resulting in a fluid-filled cavity surrounded by a dense glial scar **(Figure 0.3)** (Fitch et al., 1999, Sofroniew, 2009, Karimi-Abdolrezaee and Billakanti, 2012, Fitch and Silver, 2008). The early formation of a physical barrier of glia scar by reactive astrocytes appear to be vital in limiting secondary damage after SCI. Once local homeostasis is re-established, the detrimental role of reactive astrogliosis becomes more apparent providing a physical barrier to axonal regeneration and secretion of several factors that inhibit cell replacement and axon growth (James, 2013).

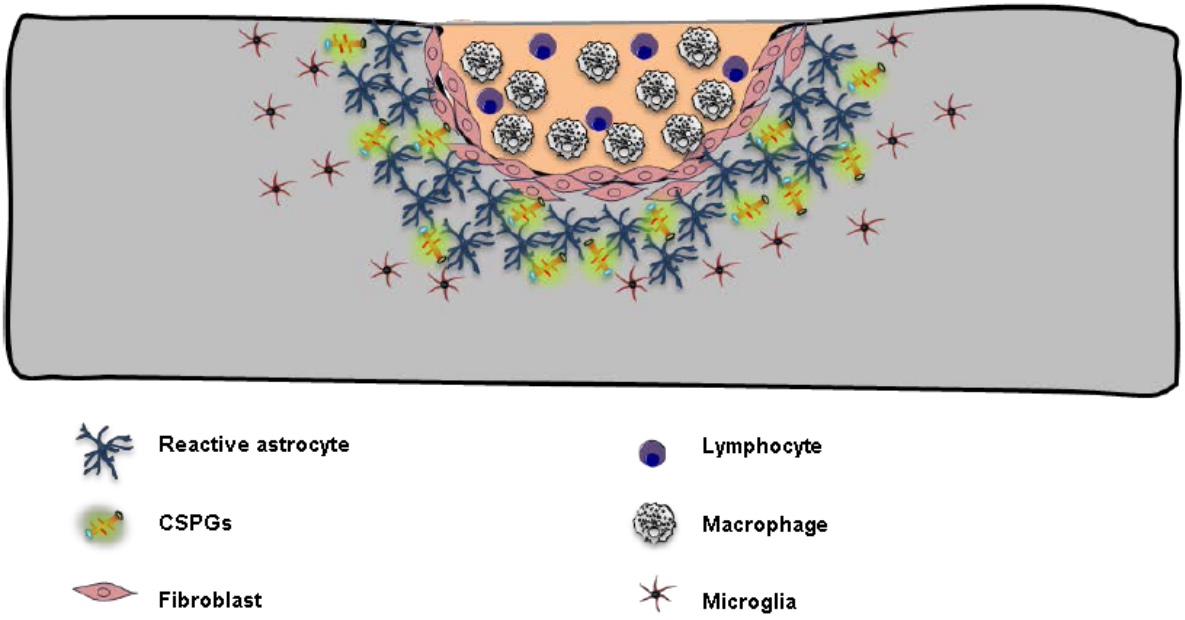

Figure 0.3: Illustration of glial scar processes at the lesion site.

Fibroblasts and reactive astrocytes start sealing off the lesion site, which form a glial fibrotic scar. Fibroblasts can be recruited either from perivascular scours e.g. contusion injury or from the meninges (if the meninges is damaged). The levels of Inhibitory chondroitin sulphate proteoglycans (CSPG) that are secreted from reactive astrocytes increase surrounding the injury area. Circulating lymphocytes, macrophages and microglia are also recruited to the injury site. Adapted from (James, 2013).

1.4.4 Glial cell responses after SCI

1.4.4.1 Astrocytes and reactive astrocytosis

The activation of astrocytes in the process of gliosis results in astrocytes with increased size, displaying a hypertrophic morphology, increased synthetic capacity, resulting from the transcription and secretion of proteins, and positive immunostaining for GFAP (Ridet et al., 1997, Sofroniew, 2009). These cells result from the activation of quiescent or resting astrocytes, which are perennially present with in the spinal cord tissue. Recently, these cells have been shown to express nestin and other markers of neural progenitor cells suggesting that the reactive process may involve dedifferentiation from astrocytes into neural stem cells (Lang et al., 2004, Robel et al., 2011). Reactive astrocytes have also been shown to express and secrete cytokines which contribute an inflammatory phenotype, such as tumour necrosis factor alpha (TNFα), and interleukins-1 and -6 (IL-1/-6). Reactive astrocytes have been demonstrated to produce CSPG and neurotropic factors and other factors that regulate axon growth, such as leukaemia inhibitory factor (LIF), ciliary neurotrophic factor and insulin-like growth factor (Ridet et al., 1997, Robel et al., 2011). It is thought however, that the diversity in the production of these factors produced during astrogliosis may result from heterogeneity in the population of astrocytes in the tissue, which become activated, resulting in a heterogeneous reactive response.

The mechanisms of astrocyte activation are complex and have not yet been comprehensively elucidated. Research to understand how these cellular responses are initiated and subsequently maintained, including the regulation of migration of reactive astrocytes is still on-going. However, numerous studies have

pointed at transforming growth factor beta (TGFβ/Smad) signalling for a key role in the process. Similarly, IL-1 and interferon gamma (IFNγ) have been shown experimentally to activate astrocytes (Ridet et al., 1997, Schachtrup et al., 2010, Sofroniew, 2009). Further work has demonstrated the mTOR signalling pathway is vital in the regulation of the gene expression profile associated with reactive astrocytes. Furthermore, the bone morphogenic protein (BMP) - microRNA-21 signalling axis has also been implicated in regulating gliosis, though the mechanisms remain elusive (Codeluppi et al., 2009, Sahni and Kessler, 2010, Sahni et al., 2010). However, experimental interference with these signalling networks was shown to significantly impede gliosis and glial scar formation after SCI.

In addition to the cytokines and transcription factors required to activate and maintain reactive astrocyte phenotype, cytoskeletal proteins such as vimentin and GFAP are required for the altered morphology of reactive astrocytes (Menet et al., 2003). In addition, the expression of matrix metalloproteinase-9 (MMP9) is thought to be important. MMP9 is capable of potently degrading ECM and is crucially important in the migration and invasion of cancer cells, as well as in wound healing. As such, expression of MMP9 in reactive astrocytes was shown to facilitate the migration of reactive astrocytes (Hsu et al., 2008).

While the process of astrogliosis is represents an evolutionarily derived and physiologically important process, it does present something of a double edged sword in the case of SCI. One particularly deleterious element of the reactive astrocyte response which has been shown to impede repair of axonal pathways is

the production of CSPG and keratin sulphate proteoglycans (KSPG) during gliosis. Both of these sulphated glycosaminoglycans are signalling and structural components of tissues throughout the body, but they are understood to act in an inhibitory fashion in the context of neural growth (Silver and Miller, 2004). Similarly, reactive astrocytes have been shown to produce Ephrin-B2 and Semaphorin 3A, both of which act as repellents to neuronal growth, preventing the regenerating neural axons from developing through and in the lesion, and newly formed scar tissue (Silver and Miller, 2004). Furthermore, astrocytes have been shown to secrete endothelin-1, which can directly inhibit myelination (Hammond et al., 2014).

On the other hand, however, reactive astrogliosis prevents further increases to the size of the cavity produced by the physical insult to the cord, and has been shown to modulate the extent and type of inflammation, inducing the migration and activity of innate cells within the tissue environment. In addition, astrocytes increase the uptake of glutamate from the extracellular compartment, induce angiogenic processes which aid healing and reduce ischemia, and perhaps most importantly rebuild the physical BSCB and the physical matrix which supports neurons within the tissue (Rolls et al., 2009). Indeed, experimental depletion of astrocytes in animal models has demonstrated that these cells required re-establishment of this barrier, and their absence from the lesion increases the migration of innate cells such as neutrophils and results in increased death of neurons and increases in demyelination of neurons. Animals which lack astrocytes have significantly reduced recovery of locomotion (Rolls et al., 2009).

1.4.4.2 Oligodendrocytes

As with other glial cell types located within the spinal cord, oligodendrocytes are susceptible to damage from primary and secondary injury after SCI. Numerous studies have shown that oligodendrocytes die as a result of necrosis and apoptosis after tissue injury, and given their role in providing the myelin sheath to nearby neurons, the death of these cells leads to demyelination of axons and impeded neuronal signalling (Casha et al., 2001, Kim et al., 2003). Indeed, this demyelination as a result of oligodendrogial death is a significant contributor to the secondary pathology of injury to the spinal cord (Casha et al., 2001).

Experiments conducted in rodents and cats have demonstrated that significant demyelination does indeed take place after experimentally induced spinal cord contusions, especially within the first 2 weeks following the insult (Gledhill et al., 1973, Blight, 1985). Furthermore, evidence from samples of human tissue have demonstrated that the damage to the myelination of axons after spinal injury can persist for up to 22 years. However, the extent of demyelination that takes place varies highly and depends on the extent of the lesion present (Guest et al., 2005).

It should also be noted that the failure of studies to observe extensive chronic demyelination post-SCI in humans is due to spontaneous remyelination by surviving oligodendrocytes (Guest et al., 2005). The ability of neurons to become remyelinated after injury was first observed in the sixties, demonstrating promise for experimental manipulation to increase healing potential and restore locomotion to victims of SCI (Bunge, 1960, Bunge and Bradbury, 1961). In humans, remyelination by oligodendrocytes is initiated by about two weeks after the initial

insult (Gledhill et al., 1973), however, it has been noted that remyelination frequently results in thinner sheaths and shorter internodes when compared to the myelin that preceded it (Gledhill et al., 1973). This is usually termed dysmyelination, or abnormal myelination. Interestingly, dysmyelination may prove to be worse than no myelination at all, as it leads to the production of incorrect signals being sent through the system (McDonald and Belegu, 2006).

On the other hand, Schwan cells (responsible glia for myelinated damaged axons in PNS) has been implicated in the myelinating central axons after SCI particularly DC that associated with peripheral myelin. The presence of Schwan cells in spinal cord could be concluded into two mechanisms; (1) might have access to SC due to injury to transition zone between CNS/PNS; (2) could be derived from CNS resident oligodendrocytes precursors by differentiation (Bartus et al., 2016).

While it has been understood that remyelination occurs after injury, the cells which were responsible for performing this task were unknown. Indeed, it was revealed in 1999 that oligodendrocytes are not actually the cells responsible for remyelination, but rather oligodendrocyte precursor cells (OPC) (Keirstead and Blakemore, 1999, Blakemore and Keirstead, 1999). Unlike oligodendrocytes, OPC maintain a proliferative state, whereas oligodendrocytes are post-mitotic (Keirstead and Blakemore, 1999). It is now been understood that after injury and during gliosis, these OPC which are present throughout the spinal cord, in both white and gray matter, become activated in response to demyelination and begin to proliferate and migrate into the zone of injury to replace the oligodendrocytes which have died in response to the secondary injury (Watanabe et al., 2002). OPC

are identified by their expression of nerve-glial antigen 2 (NGA2), are however thought to be a relatively heterogeneous population of cells and only a fraction of these respond to injury and are capable of remyelination (Nishiyama et al., 2009, Suzuki and Nishiyama, 2009). However, the understanding that this subset of OPC is responsible for myelination produces opportunities for therapeutic intervention to aid this process. Several molecules, have been identified which induce differentiation of $NGA2_+$ cells into OPC including epidermal growth factor receptor (EGFR), neurogenic transcription factor (Ngn2) and several other growth factors (Ohori et al., 2006, Aguirre and Gallo, 2007).

A number of relevant studies have addressed the role and therapeutic use of OPC post injury to the spinal cord. One rat model of spinal cord damage at the level of T9 has generated a number of interesting results. In a systematic analysis of collected data it was discovered that transplanted OPC introduced to the post injury scar were able to migrate throughout the injury site and ultimately differentiate into fully mature post-mitotic oligodendrocytes as opposed to other nervous tissue, such as neurons or astrocytes (Lee et al., 2005b). These transplants were also able to reduce functional recovery over time and resulted in a far higher number of new neuronal connections within treated tissue, indicating a positive effect on neuronal axon generation (Keirstead et al., 2005). In other work, embryonic stem cells (ESC) were differentiated into OPC *ex vivo* and subsequently transplanted into rat SCI sites at both 1 week and 10 week after injury. The transferred OPC demonstrated good overall survival and were shown to migrate into the scar where they differentiated into mature oligodendrocytes. Interestingly, similar results were obtained at both time-points after injury

(Faulkner and Keirstead, 2005, Nistor et al., 2005). Further work using this model of SCI has combined the transplant of OPC with treatment with neural growth factors. These experiments demonstrated both further increases in the formation of mature oligodendrocytes within the scar tissue but also increased numbers of ascending and descending axons and increased signalling, showing significant potential for interventions in humans (Sharp et al., 2010).

Progress has also been made in the implementation of such neuro-regenerative methodologies into the clinic, using the work performed in numerous animal models as the template. The American Spinal Injury Association (ASIA) approved a national phase-one trial, which was funded by the Geron Corporation. This trial was implemented to assess the tolerability and safety of human ESC-derived OPC-based therapies in patients with spinal injuries manifesting sub-acute thoracic damage, in which this trial have been reported to efficiently contribute to the functional improvement (Sypecka, 2011). Another trail is in progress by Asterias Biotherapeutic where they occupied the same stem cells that been used by Geron's trail and employs many of the same people (Willyard, 2013).

1.4.4.3 Microglia

Microglia are cells considered to be specialised components of the innate immune arm of the immune system. Like oligodendrocytes, these cells possess many branching processes and are phenotypically distinct (Cao and He, 2013). It is estimated that microglial cells make-up around 10% to 20% of all the cell types in the CNS (Hammond et al., 2014). Microglia are distinct from other cell types of the nervous system, in that they are derived from macrophages which emerge from

early haematopoiesis during development in the yolk sac, these then migrate to and undergo further differentiation within the developing neural tube to form microglia. This is distinct from other nervous system components which develop from neural stem cells. Interestingly, microglia revert back into macrophages during inflammation (Ransohoff and Cardona, 2010). Microglial cell populations within the spinal cord persist and are replenished from a local population of progenitor cells and distinct from this is a population, which is derived from bone marrow-derived monocytes, which consistently migrate into the CNS and differentiate into mature microglia, both homeostatically, and in response to injury (Ransohoff and Cardona, 2010, Aguzzi et al., 2013). Microglia are generally considered the first myeloid-derived cell to respond to SCI and quickly differentiate into activation of macrophages in response to early inflammatory signals. These early responding microglial-derived macrophages then cannot be differentiated in terms of morphology from peripherally recruited macrophages (Hawthorne and Popovich, 2011).

Within the cellular milieu which characterises the early inflammatory response after tissue damage at the spinal column, these resident microglial macrophages are key components, serving to determine changes to the immediate micro-environment in ways which are both beneficial and detrimental in terms of axon regeneration (David and Kroner, 2011). As with other types of macrophages in other tissues, microglial macrophages demonstrate significant plasticity in terms of their activation states. The traditionally accepted phenotypic characteristic of activated macrophages are termed M1 and M2, though it should be noted that these represent phenotypic extremes and it is now generally accepted that a full

scale of intermediate phenotypes between these two are produced depending on the specific signalling resulting from the stimulation by molecules in the immediate inflammatory milieu (Kigerl et al., 2009). M1 macrophages are generally known as classically activated, and are pro-inflammatory. These respond to toll-like receptor (TLR) signalling in response to lipopolysaccharide and other microbial pathogenic signals by activation and secretion of cytokines such as IFNγ, IL-1β, TNFα, all of which cause a further cascade of innate immune activation and increase inflammation within the area. Microglial macrophage M1 activation results from stimulation by pro-inflammatory cytokines, such as IL-12, IL-1β, TNFα and other small molecules known to induce M1 phenotypes (e.g. reactive oxygen species and reactive nitrogen species are frequently present in inflammation after spinal cord damage) (Kigerl et al., 2009, Ju et al., 2014). M1 activation not only leads to an increase in the secretion of further inflammatory molecules, but also leads to an increase in antigen presentation and phagocytic capabilities of the macrophages, which enables them to clear the surrounding tissue of cellular debris resulting from tissue damage, remove pathogens, and subsequently induce an adaptive response to any dangers present within the area. Alternatively, microglial macrophages can undergo an M2 type activation. This is usually in response to the stimulation by the cytokines, IL-4 and IL-13. In contrast to M1, M2 activated cells are generally anti-inflammatory and secrete the immune suppressive cytokines TGFβ and IL-10 which have been shown to lead to the resolution of inflammation (Lawrence and Natoli, 2011).

1.5 Limited regenerative capacity of CNS axons

Damage to the CNS causes permanent disabilities due to limited capacity of repair and functional recovery after CNS injury, in which the CNS enables a significant regenerative response to restore lesioned areas compared to PNS that launches a robust regenerative in response to injury (Huebner and Strittmatter, 2009, Giger et al., 2010, Kempf et al., 2013). Several factors contributed to the limited regenerative capacity of CNS neurons, which fall into two main categories; intrinsic growth limiting factors and extrinsic inhibitory factors present after SCI.

1.5.1 Intrinsic growth limiting factors

Many studies have attempted to regenerate CNS neurons after injury by providing growth permissive environments such as cell transplants and peripheral nerve grafts but, these attempts have shown feeble regeneration whist others showed no regenerative response (Richardson et al., 1980, David and Aguayo, 1981, Li et al., 1997, Houle et al., 2006, Grill et al., 1997, James, 2013). The key mechanism responsible for this failure is a pattern of proteins synthesis and gene regulation in axotomised neurons. The pattern of these factors becomes clear when comparisons are made with axotomised neurons in the PNS, where regeneration associated genes (RAGs) are elevated far early after PNS injury compared to the CNS (Huebner and Strittmatter, 2009). The upregulation of RAGs including genes that transcribe cytoskeletal proteins such as actin, tubulin, growth associated proteins-43 (GAP43) and cytoskeleton associated protein-23 (CAP23) were shown to play important roles in mediating growth cone elongation (Bulsara et al., 2002,

James, 2013). Moreover, PTEN is one of the RAGs that promoting axon regeneration and functional repair after adult spinal cord injury through PTEN/mTOR pathway (Liu et al., 2010). One of the other RAGs is Krüppel-like Transcription Factor 7 (KLF7), in which overexpression of KLF7 in adult rat RGCs, found to increase RGC survival and induce axon regeneration after optic nerve injury (Wang et al., 2013). Epothilone B (that reactivated neuronal polarization by inducing concerted microtubule polymerization into the axon tip) (Ruschel et al., 2015), pregabalin (Warner et al., 2017) and c-Jun (Fagoe et al., 2015) are other RAGs found recently that implicated in CNS axon regeneration.

In the development stage of the nervous system, most RAGs are found highly expressed and then decrease in the adult, while in the PNS RAGs are robustly re-expressed (Fernandes et al., 1999, Bulsara et al., 2002). The presence of RAGs and local protein synthesis in the CNS is necessary for rapid formation of growth cones, along with their guidance and elongation. In contrast, low levels of these factors and components would definitely contribute to the limited intrinsic growth capacity of CNS axons (James, 2013).

Another intrinsic mechanism that limits the growth in injured CNS axons is the response of microtubules to axotomy. After CNS injury, microtubules are unable to propel axon growth because they become depolymerised at the axon stump, resulting in formation of retraction bulbs (disorganised microtubules network) (Erturk et al., 2007). Retraction bulbs are not present in PNS injury since microtubules in the PNS are effective and quickly restore the organisation at the axon stump, leading to axon extension and a rapid growth cone formation

therefore, stabilisation and organisation of microtubules in CNS axons result in stimulation of axon extension and successful growth cone formation (Erturk et al., 2007, Hellal et al., 2011).

Furthermore, another key mechanism that may be responsible for regeneration failure of CNS axons is the activation and expression of different receptors e.g. high affinity neurotrophin receptors (tropomyosin receptor kinases (Trk)). Trk receptors have three forms including TrkA, TrkB and TrkC, which bind with specific neurotrophins. This binding promotes neurite outgrowth, enhances cell survival and regulates the advance of the growth cones (James, 2013). All forms of Trk receptors expression is lost after either contusion injury or spinal hemisection, therefore the reduced expression of these receptors after SCI leads to sequestration of neurotrophins, which clearly have negative outcomes on axonal growth and survival (King et al., 2000, Liebl et al., 2001, Widenfalk et al., 2001). Moreover, another receptor appears to negatively affect injured CNS axon is the integrins, these types of receptors bind with ECM molecules e.g. fibronectin, collagen and laminin and allow axonal elongation over ECM components. The levels of integrin receptors decrease in CNS axons after injury, which leaves the axons without the important adhesion molecules to grow back through the injury sites resulting in dramatic elevation of ECM components (Jones, 1996, Wallquist et al., 2004, Eva et al., 2012). The lack of these receptors after SCI leads to the accumulation of dense ECM at the lesion site, adding further difficulty of axons re-growing through the lesion area (Tan et al., 2011).

All of the above intrinsic mechanisms are found to contribute to limit the growth capacity of CNS neurons after injury. There are also large numbers of extrinsic inhibitory molecules available along with lack of trophic support present in the adult CNS which contributes to further lack of axonal repair after injury.

1.5.2 Extrinsic inhibitory factors

Damaged CNS axons are incapable of re-growing after injury with different degrees of success once provided with growth permissive substrates. Unfortunately, many CNS neurons have lower intrinsic capacity and are surrounded by extrinsic inhibitory factors after the injury, compared to their peripheral counterparts, but still they are able to grow if the regenerative growth environment is replaced with a PNS environment (Richardson et al., 1980, David and Aguayo, 1981, Houle et al., 2006). A wide range of research has been carried out to investigate the non-growth permissive environment correlated with CNS damage and why it is inhibiting axon regeneration especially after injury.

1.5.2.1 Myelin-associated inhibition

In 1982, Berry was the first person who suggested that CNS myelin may inhibit axonal growth after CNS injury, and indicated that non-myelinated CNS axons have the ability to regenerate after injury if surrounding myelin remains intact, but unable to regenerate if the myelin was disrupted, therefore speculating that myelin products were involved in axonal growth inhibition (Berry, 1982, James, 2013). Since then, the myelin-associated inhibitory molecules were identified; NogoA,

myelin associated glycoprotein (MAG) and oligodendrocyte-derived myelin glycoprotein (OMGp), which are considered to be the major CNS axon growth inhibitory factors (Hunt et al., 2002, Filbin, 2003, Sandvig et al., 2004). Each of these inhibitory molecules will be discussed below in more details.

The first myelin-associated inhibitors is Nogo, this protein belongs to the Reticulon protein family (RTN1, 2, 3 and 4), since Nogo has a similar gene structure to RTN4, which was characterised by its physiological role in maintaining the shape of the endoplasmic reticulum (ER) (Oertle and Schwab, 2003). Expression of Nogo is found on both inner and outer surfaces of myelin sheaths, as well as reduces axonal growth following CNS injury (Voeltz et al., 2006). Two main regions of Nogo are potentially responsible for inhibiting neurite outgrowth; the 66-amino acid loop region located at C-terminal and the region including two stretches at the N-terminal. These regions are found to induce neuronal growth cone collapse following CNS injury (Oertle and Schwab, 2003). Targeting Nogo also underwent clinical trial (see section 7.4).

The second myelin-derived inhibitor is MAG, which is a transmembrane glycoprotein expressed in oligodendrocytes at the axonal membrane between axons and the innermost myelin sheath. It acts to maintain the myelination of axons in the nervous system. However, MAG has been shown to inhibit neurite growth (Schnaar, 2010, McKerracher et al., 1994). In the context of axon regeneration, MAG can act as an inhibitor of axon remyelination and growth (Filbin, 2003, Gao et al., 2003). MAG has a dual role in axon growth, it is growth promoting on younger neurons while growth inhibitory on older neurons, with this transition in function occurring at or soon after birth (McKerracher et al., 1994).

MAG also signals through binding to ganglioside receptors, which has been shown to mediate MAG's role in inhibition of myelination (Quarles, 2002). It has been postulated that integrin receptors may also mediate the inhibitory functions shown by MAG (Hu and Strittmatter, 2008). However, its role in regeneration is likely far more complex and not fully understood, having multiple roles in axonal responses after injury in the adult CNS (Nguyen et al., 2009).

The glycoprotein, OMGp is the third myelin-derived inhibitor, which was originally discovered as a peanut agglutinin-binding protein found in CNS myelin preparations (Mikol et al., 1988). It is now known that OMGp is also expressed prominently in neurons (Habib et al., 1998). Studies are only now beginning to garner useful insights into the physiological role of OMGp. In the OMGp knockout mouse, axons exhibit significant overgrowth causing a deleterious phenotype, and suggesting that OMGp serves as an inhibitor to axon growth (Gil et al., 2010). The OMGp gene is found in an intron of the neurofibromatosis type 1 gene (NF1) (Viskochil et al., 1991) so it was initially postulated to play a role in the induction of neurofibromatosis. OMGp was reported to inhibit aberrant collateral sprouting from the nodes of Ranvier, by its expression in oligodendroglia-like cells which ensheathe the nodes during development (Voeltz et al., 2006, Schnaar, 2010).

All of these three myelin molecules are able to bind with the same GPI-linked protein (Nogo receptor 1 (NgR1)) (Domeniconi et al., 2002, Fournier et al., 2001). NgR1 forms a complex signalling receptor with p75 or TROY and LINGO-1 to mediate the inhibitory signals generated by these ligands (Mi et al., 2004, Park et al., 2005, Wong et al., 2002). Furthermore, PirB paired-immunoglobulin-like

receptor-B (LILRB) was discovered to bind and act as receptor for Nogo, MAG and OMgp, and when binding takes place in conjunction with NgR1, it was shown to mediate potent myelin-associated axon growth inhibition (Atwal et al., 2008). More recently, AMIGO3 has been identified to substitute LINGO-1 in the acute phase of SCI acting as a co-receptor for p75 and NgR1, since LINGO-1 was raised 2 weeks after SCI (Ahmed et al., 2013).

However, the activation of the complex receptors leads to downstream signalling via the activation of RhoA (**Figure 0.4)** (Ahmed et al., 2013). Since RhoA exists in equilibrium between active GTP complexed (Rho-GTP) and inactive GDP complexed (Rho-GDP), a guanine-nucleotide exchange factor (Rho-GEFs) activates Rho-A by converting Rho-GDP to Rho-GTP (Overbeck et al., 1995, Schmidt and Hall, 2002). Rho-GTP active form leads to activate a number of signalling pathways contributed in growth cone collapse via Rho-associated kinase (ROCK). ROCK has two subtypes but they are considered as together, and has two major functions: formation of stress fibres and inhibition of actin depolymerisation (Schmandke et al., 2007). Many pathways can regulate actin polymerisation but the most important pathways are LIM-domain containing protein kinases 1 and 2 (LIMK) and cofilin, in which activation of ROCK leads to phosphorylation of LIMK result in deactivation of cofilin by phosphorylation (Maekawa et al., 1999, Zhao and Manser, 2005, Schmandke et al., 2007). Although actin cytoskeleton plays an important role in neuronal morphology and growth cone extension, actin can be affected due to deactivation of cofilin causing neuronal growth cone collapse and axon degeneration (Mizuno, 2013).

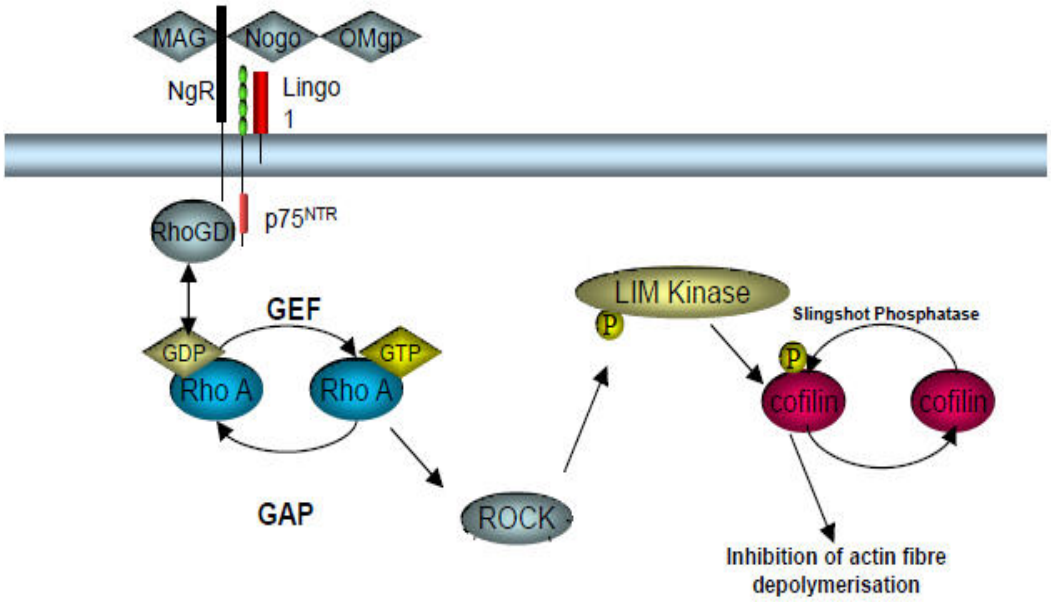

Figure 0.4: The signalling pathway activated by myelin molecules when bound with NgR1/LINGO-1/p75 complex receptors.

This binding complex leads to displacement of Rho-GDI (Rho GDP-dissociation inhibitor) from Rho-GDP leading to activation of Rho-GTP by GEF. This activates ROCK leading to inhibition of actin depolymerisation by phosphorylation of LIM Kinase and cofilin result in occurrence of growth cone collapse and inhibition of its motility. Figure provided by Dr Zubair Ahmed.

1.5.2.2 Inhibitory guidance molecules

There are a number of axon guidance molecules which play a role in restricting axonal growth after CNS injury; in contrast, they also play a vital role in correct wiring of the CNS during development. An example of these guidance molecules is the Semaphorin family, which contribute in developing CNS shape by deflecting axons from inappropriate areas and potent repellents of axon growth during development (Messersmith et al., 1995, Behar et al., 1996). Semaphorin-3A is expressed in the glial scar by meningeal fibroblasts and inhibition of Semaphorin-3A after CNS injury was found to promote axon regeneration (Pasterkamp and Verhaagen, 2001, Kikuchi et al., 2003).

There are other important inhibitory guidance molecules such as; eph receptor tyrosine kinases and their ligands. Eph receptors are upregulated after SCI and some ephrins are expressed by astrocytes at the lesion site (Willson et al., 2002, Bundesen et al., 2003). Genetic knockout studies of the ephrin and EPHA4 and application of a blocking peptide of these proteins showed enhanced regeneration of CNS axons after injury (Goldshmit et al., 2004, Fabes et al., 2007). Moreover, a genetic knockout of EPHB3 enhanced regenerative response after spinal hemisection and optic nerve crush (Duffy et al., 2012). Therefore blocking these molecules lead to provide better growth permissive for injured CNS axons.

1.5.2.3 Proteoglycans

As previously mentioned, glial cells form a physical barrier to axonal regeneration in response to SCI, however these cells (particularly reactive astrocyte) also create a chemical barrier to regeneration by producing a number of inhibitory ECM molecules (Fitch and Silver, 2008, Sharma et al., 2012). In the context of SCI, the most widely studied of these upregulated ECM inhibitory molecules are proteoglycans (Jones and Tuszynski, 2002). Proteoglycans can be chondroitin sulphate, keratin sulphate, heparan sulphate or dermatan sulphate, in which chondroitin sulphate proteoglycans (CSPGs), heparan sulphate proteoglycans (HSPGs) and keratin sulphate proteoglycans (KSPGs) are all induced after CNS injury (Jones et al., 2003, Ramer et al., 2005).

CSPG and its family molecules (neurocan, aggrecan, brevican and versican) are the most abundant proteoglycans in the CNS and are secreted by glia scar cells creating CSPG rich ECM surrounding lesion site (Jones et al., 2003), NG2 is other CSPGs are expressed in glial cell membranes and react rapidly to CNS injury (Fidler et al., 1999, Tang et al., 2003). CSPGs have been observed to have a role in axon growth inhibition, for example: *in vitro* evidence demonstrates that a normal growth permissive substrate containing CSPGs prevent sensory neurons extending neurites (Snow et al., 1990) as well as, disrupt growth cone dynamics of adult CNS neurons and prevent their neurite extension in the presence of explanted glial scars (James, 2013).

Furthermore, *in vivo* studies show axons of transplanted adult sensory neurons will extend in the CNS, however these axons will form dystrophic end bulbs and

halt abruptly upon reaching the reactive gliosis site correlating with areas of induced CSPG expression (James, 2013). Disruption and degradation of CSPG and its inhibitory interaction either by antibody neutralisation, targeting downstream effector molecules or by enzymatic degradation enhanced axonal growth both *in vitro* and *in vivo* (Grimpe and Silver, 2004, Shen et al., 2009, Fisher et al., 2011, Bradbury et al., 2002). The sustained and dramatic elevation of CSPGs along with multi-faceted inhibitory actions of these molecules following injury remain a key target for the development of potential therapeutic interventions for use in SCI (James, 2013). In vivo study, a mammalian-compatible engineered chondroitinase ABC (ChABC) has been delivered using lentiviral vector (LV-ChABC) to explore the consequences of large-scale CSPG digestion for SC repair. The results demonstrate significantly reduced secondary injury pathology in adult rats injected LV-ChABC with after spinal contusion injury, with reduction of the cavitation and enhanced preservation of spinal neurons and axons at twelve weeks post-injury (Bartus et al., 2014). Manipulating these molecules along with inhibitory factors listed earlier lead to the promotion of regeneration of injured CNS axons.

1.6 CNS repair and axon regeneration

Due to long-term disabilities resulting from damage to the CNS, it was initially thought that the adult CNS has no ability to repair itself. However, in 1928 Ramon Y Cajal (Ramón y Cajal et al., 1991) observed that the CNS may actually have the ability to repair itself given the right environmental conditions. Regeneration of the CNS is first of all dependent on whether the neural cell itself survives the injury.

The other factors are the availability of molecules involved in axon growth and guidance, and the local permissive and inhibitory signalling cascades. Aguayo *et al* (Richardson et al., 1980) later replicated Ramon Y Cajal's findings and further established that the inability of the CNS to regenerate was the result of a local environment that was always altered in response to the injury. Aguayo's group was able to observe elongation of regenerative axonal "sprouts" in both the CNS and PNS after injury (Richardson et al., 1980). They determined that neuronal responses to injury were possibly influenced by glial cells, growth factors and target tissues such as smooth muscle cells.

This has since led to a number of investigations into axonal regeneration of the CNS with the aim of developing regenerative strategies that could be adopted for therapeutic applications. Because of the fact that neuronal regeneration requires the neural cell to be alive in the first place, any successful regenerative strategy are likely to benefit SCI rather than brain injuries.

Any regenerative strategy employed must take into consideration the viability of the neuronal cells, the availability of target tissues, the elongation of the cut axon and dendrites, re-myelination and the formation of new synapses for total recovery of function that may have been lost after injury. Regeneration in the adult CNS is therefore a step wise process that involves factors which affect the parameters listed above. Therefore, most of the strategies currently being employed are aimed at stimulating "cellular replacement, neurotrophic factor delivery, axon guidance and removal of growth inhibition, manipulation of intracellular signalling, bridging and artificial substrates, and modulation of the immune response (Horner and Gage, 2000)".

To replace neuronal and glial cells lost during CNS injury, researchers have considered the use of fetal tissue grafts (Richfield, 2000) and neural stem cells (Gage, 2000). Stem cells have the ability to differentiate into glial and neural cells once transplanted into the brain and given the right neurotropic factors. However, ethical, physical and mechanical difficulties still limit the use of fetal tissue grafts and restoration of function after cell replacement using neural stem cells still has to be proved (Horner and Gage, 2000). These hurdles still put to question whether cellular replacement is viable in CNS axon regeneration. This takes us back to the first requirement that for any viable regeneration of the CNS to occur, the neuronal cell has to have survived the initial injury. Once the cell is alive, neurotrophic factors are believed to be able to signal axonal regrowth. Neurotrophins however, are said to induce axonal growth only when the permissive factors provided by for example Schwann cells are present (Xu et al., 1995). Despite the ability of neurotrophins to generally induce axonal growth, the need to direct regenerating axons into the injured CNS begs the question of axonal guidance factors and removal of any inhibitory signals. Growth promoting molecules including ECM molecules, immunoglobulin, inflammatory cytokines and tyrosine kinase receptors among others are some of the molecules that are responsible for axonal growth and guidance (Horner and Gage, 2000). All these factors explained above are extracellular. However, there are intracellular factors that are vital in cellular survival and axonal growth, and their roles have to be understood as well if regeneration of the CNS is to be understood. Some of these factors can influence apoptotic cell death in response to injury thus minimizing any chances of regeneration. Manipulation of these factors is important in stimulating the cells to start regenerating. Immune responses activated by the body to remove

necrotic tissues, may in turn lead to progressive damage to the CNS thus preventing neuronal repair (Bredesen, 1995).

In general, the CNS is a complex system whose regeneration is possible but dependent on a number of factors both extrinsic and intrinsic to the damaged cell. Research has shown that these regenerative factors can be induced both *in-vivo* and *in-vitro*. Restoration of damaged cells however cannot be taken as restoration of function and functional deficiencies may still exist even after CNS repair.

1.7 SCI models

Over the past century, SCI models have evolved since Allen in 1911 developed the first SCI model by weight-drop contusion model. Complete and incomplete SCI models been developed in animals, which aimed to understand the biological and anatomical consequences of SCI and resemble human SCI as closely as possible. Rat models are most commonly used in preliminary studies of SCI since they are readily available, inexpensive, easily housed and can be studied in large numbers. Mice are useful for genetic studies and are also implemented in SCI research. Large animals such as dogs and pigs can be used for SCI models but it is rare because they require expensive housekeeping, care and stringent ethical considerations. The only use for large mammals is for further validation required of some experimental conditions. Currently, researchers are using a range of SCI models that includes contusion, compression and complete spinal cord transection models among others. The reason behind the variety of these models is that they never truly express the human condition (Allen, 1911, Metz et al., 2000, Jakeman

et al., 2000, Talac et al., 2004, Davoody et al., 2011, Kundi et al., 2013, Cheriyan et al., 2014).

1.7.1 Limitations of SCI models

In the contusion models, it may be hard to assess pain behaviour, since pain sometimes is not appear from weight that released from short distance to precise area (Nakae et al., 2011). Although, contusion models mainly performed in thoracic level of the spinal cord, as a contusion to cervical level affects cardiovascular and respiratory functions, which can be a life threating of the animal (Yisheng et al., 2007). However, a contusion controlled by a computer is useful model that obtain a reliable SCI and reduces experiment variability but it is expensive method to use and requires sophisticated equipment (Jakeman et al., 2000, Ma et al., 2001). Other limit of using computer-controlled method in axon regeneration study is that distinguish between spared and regenerating axons is difficult at produced lesions (Talac et al., 2004).

In addition, complete transection model is usually used to study regeneration in present of scaffolds, biomaterials and stem cells, but it causes a large scar at the lesion surface therefore produces a sever model that dedicated an intensive care after surgery (De Winter et al., 2002, Talac et al., 2004, Lee and Lee, 2013). Other than evaluation of axon regeneration and devices implantation, this models is rarely reported in human thus, has no clinical relevance (Talac et al., 2004). On the other hand, injury induced by photochemical model is extent and difficult to be

controlled, since this method producing large area that may affected by the ischemic environment created by this model (Surey, 2015).

Furthermore, anaesthesia and laminectomy are two factors limiting the models that rely on these factors, which they play crucial role in SCI experiments, since they not mimicking the clinical injury of humans. For example, CNS pathology and recovery after the injury can be affected following anaesthesia that includes respiratory rate, blood pressure metabolism. Each of these symptoms affected differently either directly or indirectly depends on different concentrations of the same anaesthetic procedure (Akhtar et al., 2008). The other factor is laminectomy when it has performed in humans it can cause spinal instability, beside that local trauma can be increased. Instability of the spine can occur when the bone, ligaments and muscles are removed surrounding the injury during operation, in which removal of these components can alter the physiological responses following SCI (Akhtar et al., 2008, Surey, 2015).

There are variations between clinical and experimental models in behavioural assessments and functional outcomes of SCI, since it is easy for human to express the symptoms and pain correlates with injury compare to animal models where it is difficult. Therefore, specific tests and analysis methods been created and applied after injury to carry out behavioural patterns correlated with SCI (Blight, 2000). The Basso, Beattie, Bresnahan (BBB) rating scale method is a locomotor activity evaluation that used to assess the functional outcomes of animals. This analysis was originally developed in Ohio State University and aims to evaluate the hind limb and forelimb movements of the animal following injury to express recovery. While this method is reproducible and reliable, it has been

tested in mild severity condition but whenever the condition become more severs, the reproducibility is decrease. Although it is, only assess hind limb function it does not consider other symptoms that require coordinated spinal cord activity such as bladder, bowel and pain function (Basso et al., 1995, Basso et al., 1996, Barros Filho and Molina, 2008, Akhtar et al., 2008).

1.7.2 Non-regeneration (DC) and regeneration (SN, pSN+DC) injury models.

1.7.2.1 Dorsal column injury model (DC)

Dorsal column (DC) including the Gracile and Cuneate Fasciculi are part of the spinal cord white matter. In this PhD, we used our well-established DC injury model to investigate genes related to axon growth inhibition/promotion and to observe axon regeneration at the lesion site following manipulation of some of these genes in DRGN. This method was used by us to study axon regeneration and to document cellular responses after SCI injury (Lagord et al., 2002, Ahmed et al., 2011a, Ahmed et al., 2013). However, the model is limited since there are no behavioural deficits in terms of responses to thermal or mechanical allodynia but does serve as a useful model to study long tract DRGN axon regeneration (Surey et al., 2014). The injury was performed by identifying the 13th rib of rats externally, using this as a landmark to count to the T8 vertebrae. After sterilising the surgery site, a 4-5 cm skin incision was made and the erector spinae muscles removed as much as possible to be able to reach the T8 vertebra. By using rongeurs, the T8 vertebra was gently removed along with lamina (partial laminectomy) and the spinal cord was exposed, and crushed bilaterally with a calibrated watchmaker's

forceps (for 10s), inserted through the spinal cord meninges to a depth of 1mm (**Figure 0.5**). The erector spinae muscles were closed with absorbable sutures and skin overlaid using staples.

1.7.2.2 Sciatic nerve injury (SN)

Much investigation on neuronal response after peripheral nerve injury includes sciatic nerve, aimed at studying the mechanism of neuropathic pain rather than the mechanisms of regeneration. Studies that aimed to examined the change in gene expression of DRGN that associate with neuropathic pain caused by SCI, have subsequently able to identify novel regeneration-associated gene following sciatic nerve injury (Blain, 2009). This model was also used by us in this study and others (Ahmed et al., 2011a, Ahmed et al., 2013) to investigate the genes associated with SN axon regeneration. The SN injury was performed at the left posterior thigh to greater trochanter in the level of sacrotuberous ligament (**Figure 0.6**). After sterilising the operating area, approximately 2cm skin incision was made and gluteal muscles were split using retractors. The SN was then exposed unilaterally and crushed using calibrated forceps for 10s (**Figure 0.7)**. After crush, gluteal muscles and the skin were closed by absorbable sutures; animals were monitored until recovery from anaesthesia and allowed to survive for 7 days then L4/5 DRGN collected for further analysis.

A

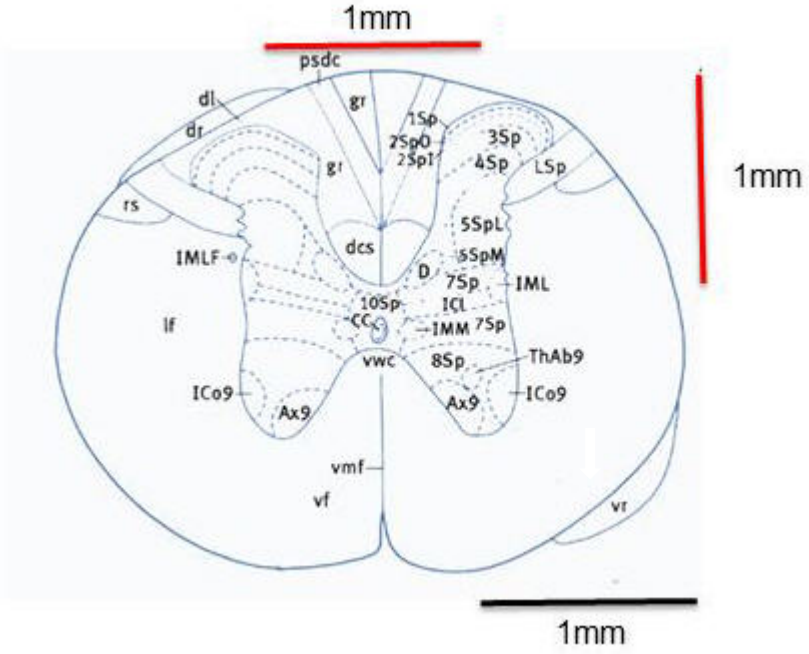

B

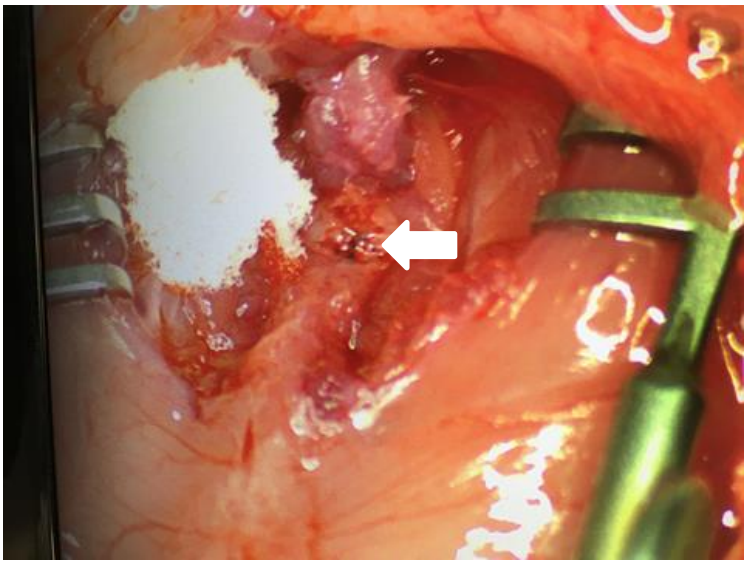

Figure 0.5: Dorsal column crush at T8 vertebrae in female Sprague-Dawley rats.

(A) Diagram of cross-section of rat spinal cord at T8 with width and depth of 1mm used to perform the injury in dorsal funiculus, (Adapted from (Surey, 2015). (B) Spinal cord exposed after 4-5 cm skin incision and removal of erector spinae muscles followed by insert of calibrated watchmaker forceps (white arrow marks the crush site).

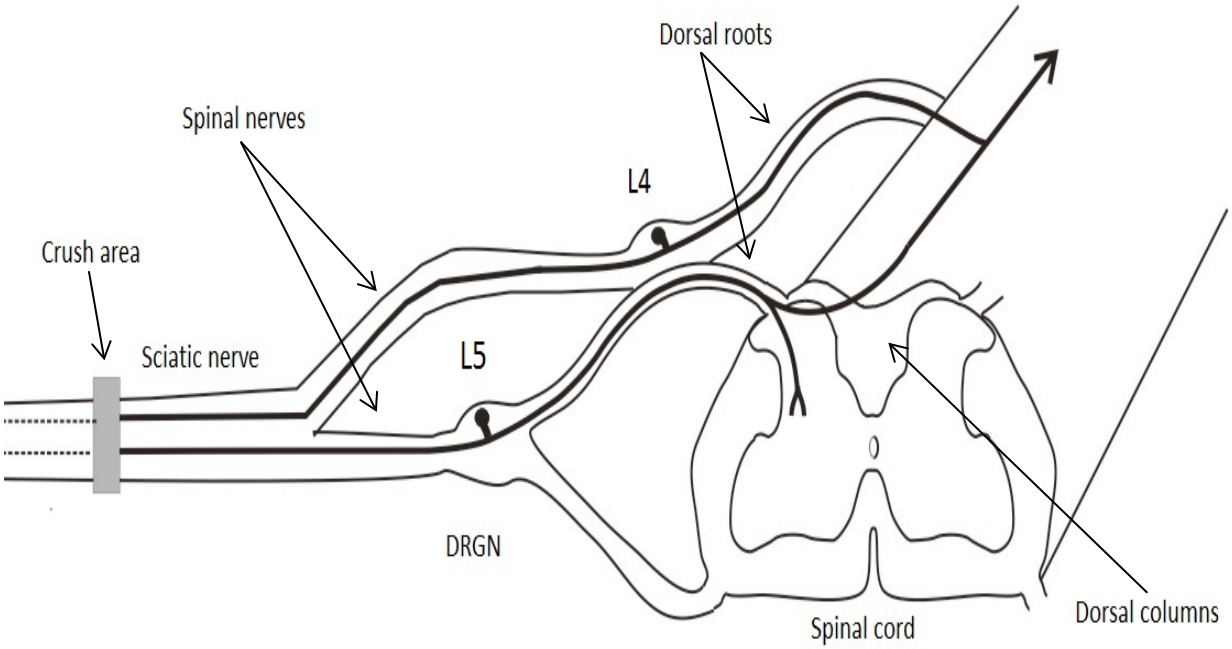

Figure 0.6: Diagram of cross section of the spinal cord showing the site of SN injury and relevant anatomical features of the injury.

Adapted and modified from (Blain, 2009).

A B

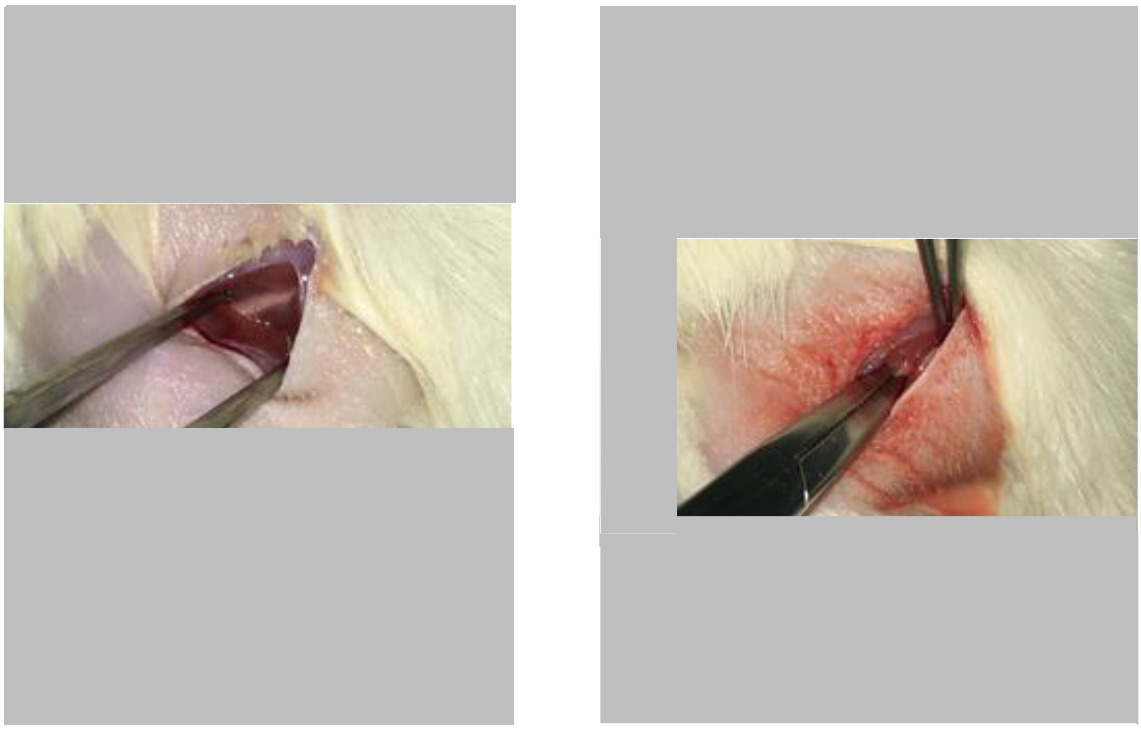

Figure 0.7: Operation images for left SN crush in adult Sprague-Dawley rat.

(A) About 2cm of skin incision at the left posterior thigh to greater trochanter followed by gluteal muscles cut then sciatic nerve was exposed after gently removal of the muscles. **(B)** Crush step using calibrated forceps for 10s.

1.7.2.3 Preconditioning sciatic nerve injury (pSN+DC)

Since DRGN branched two projections one to periphery and other to central nervous system, injured peripheral branch found capable to regenerate whereas central not. However, if PNS injured before CNS (precondition) those cells found primed to sprout some central fibres demonstrate that central branches are capable to regenerate (Case and Tessier-Lavigne, 2005). As stated above this injury model was used to study gene relative to axon regeneration and to model a preconditioning injury, the SN was crushed 7 days prior to DC injury as described above.

1.8 Main hypothesis

In a microarray screen in regenerating and non-regenerating models of SCI (described above), approximately 350 genes were observed to correlate with axon regeneration. Therefore, understanding the contribution of these genes and manipulation of these genes either by knockdown or overexpression may lead to the promotion of axon regeneration and enhanced regenerative responses after SCI. This led to hypothesis that manipulating some of the most highly regulated genes (i.e. AMIGO3, RTN3 and AEG-1) will promote enhanced DRGN axon regeneration after DC injury.

1.9 Main aims

- To determine protein and messenger RNA (mRNA) levels of these genes in both regenerating and non-regenerating SCI models after 7 days post injury.
- To knock down these genes using siRNA in an *in vitro* model of SCI using cultured primary DRGN in the presence of an axon growth inhibitory CNS myelin extract (CME) and observe how they regulate neurite outgrowth.
- Supress or overexpress these gene *in vivo* depending on how they regulate disinhibited DRGN neurite outgrowth and determine their effects on promoting DC axon regeneration *in vivo*.
- To assess the inflammatory responses including glial activity, macrophages and T cells after injection of plasmids encoding shAMIGO3.

CHAPTER 2: Materials and Methods

2.1 *In vivo* methods

2.1.1 Animal surgery

All animal procedures were licensed and approved by the University of Birmingham's Ethical Review Committee and by the UK Home Office. Adult female Sprague-Dawley rats were used in these experiments weighing between 180-250g (Charles River, Margate, UK). Prior to surgery animals were injected with 0.05ml of Buprenorphine for analgesia and then placed in a chamber for anaesthesia using 5% of Isoflurane, 1.8/mg of O_2 and monitoring body temperature and heart rate during surgery.

2.1.2 Injury models

The T8 DC model, SN and pSN+DC models have been described in the introduction (see section 1.7.2). (all injuries were performed by Dr Zubair Ahmed)

2.1.3 Intra-DRG injection

While the animal was under deep anaesthesia we preformed intra-DRG injection to lumbar (L)4/5 DRG ganglia after DC injury. At the level of midline lumbar region about 4-5 cm skin incision was made and erector spinae muscles were removed and split using retractor to visualise the contralateral side at lumbar level. The L4 vertebra was marked and approximately 2cm paramedian incision was made from left of the spinous processes down to the articulating surfaces of the facet joints. Ligaments attached to the articular surfaces were removed by using rongeurs and further dissection was made to reach the lateral vertebra which was then removed

to reveal the ventral L4/5 rami. By further gentle dissection, the L4/5 DRG was exposed in the intervertebral foramina and 2µl of plasmids or PBS solution, depending on the experiment was injected using microglass needle attached to a 20ml syringe. It is sign of successful process if the DRG ganglia was observed to swell during the injection (**Figure 2.1**), finally retractor was removed and muscle was closed using absorbable suture followed by skin closure using staples. (Intra-DRG injections were performed by Dr Zubair Ahmed).

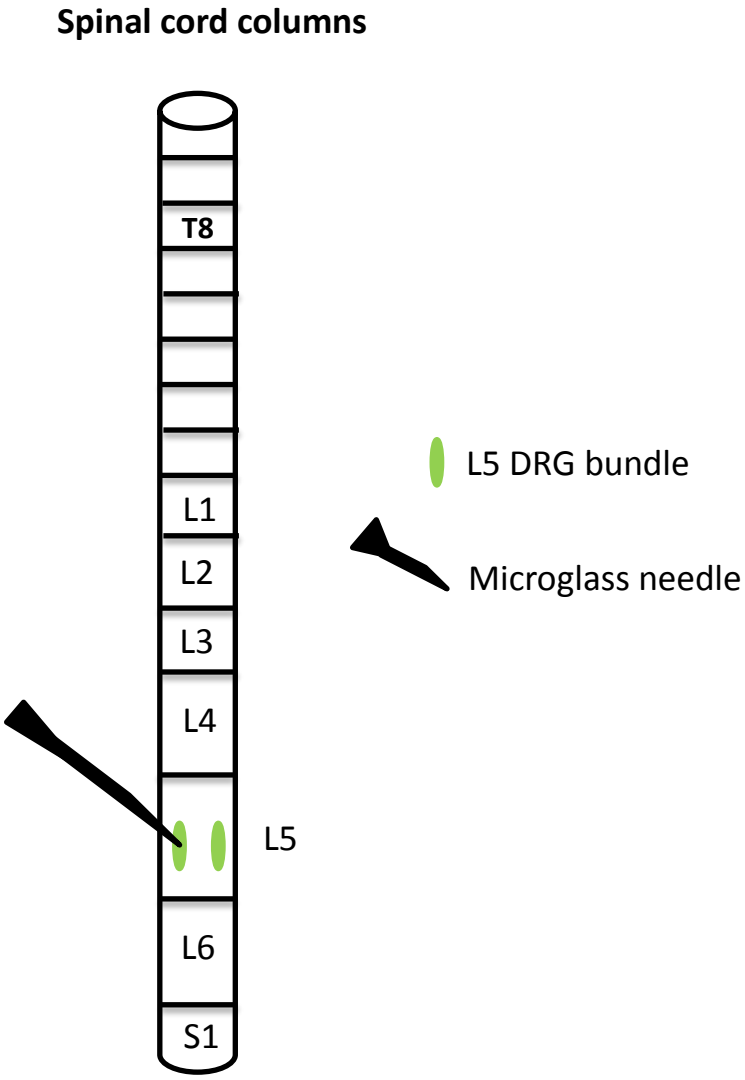

Figure 2.1: Injection paradigm showing anatomic level of intra-DRG injection preformed in this study.

2.1.4 Experimental design for in vivo experiments

Different surgical procedures have been carried out in this thesis that includes injury models, microarrays, injection of different plasmids. In injury models three different crushes were performed (DC, SN and pSN+DC) and DRG ganglia were collected at day 7, in which pSN+DC model preformed 7 days prior to DC injury **(Figure 2.2A)** to preform microarray screening and validate the highlighted genes using immunohistochemistry, western blot and RT-PCR. However, down-regulate and overexpression using plasmid injection was carried out in two chapters in this thesis; (1) down-regulate AMIGO3 after DC injury for 29 days (2) overexpress RTN3 after pSN+DC for 21 days **(Figure 2.2B, C).**

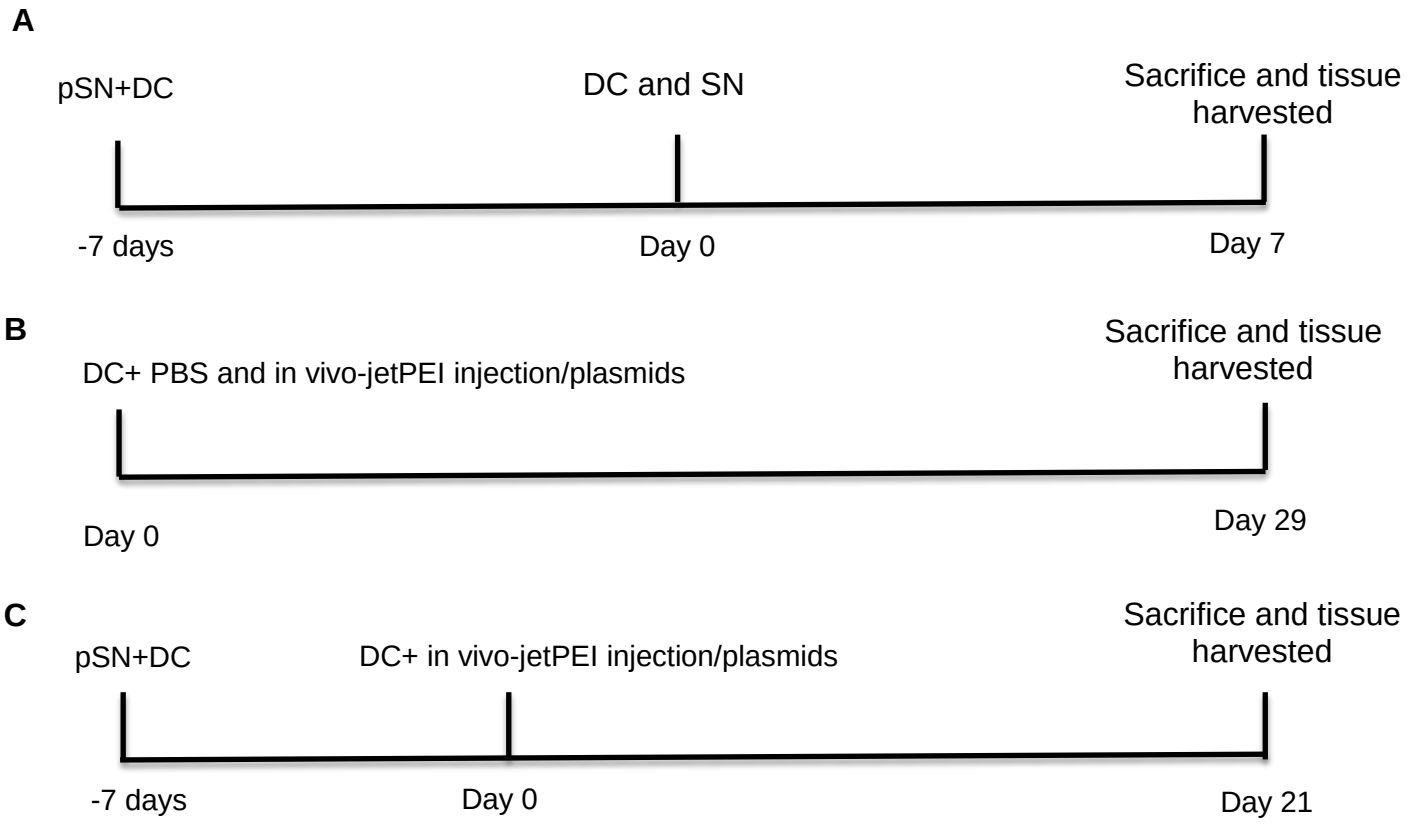

Figure 2.2:Timelines for in vivo surgical procedure. (A) Timeline for microarray and genes validation, (**B)** timeline used in chapter 3,**(C)** timeline used in chapter 5.

2.2 *In vitro* methods

2.2.1 Tissue processing and sectioning

For microarrays, RT-PCR and western blot, animals were killed at 7 days after injury by rising CO_2 levels and fresh DRG tissue were collected and immediately frozen in liquid N_2. Samples were stored at -80^{o}C until required.

2.2.2 Intracardic perfusion

For immunohistochemistry, animals were intracardially washed with phosphate buffer saline (PBS) and then perfused using 4% formaldehyde (PFA: TAAB Laboratories, Berkshire, UK). Once animals were perfused DRG and injury sites were dissected out and postfixed for 2 hours at room temperature (RT). Tissues were washed in 3 changes of PBS for 30mins each, and cryoprotected in 10%, 20% and 30% sucrose solutions diluted in PBS. Tissues were then embedded in OCT and cut at 15µm thick using a cryostat (Bright Instrument, Cambridgeshire, UK), adhered onto Superfrost plus slides (Fisher Science, Loughborough, UK) and stored at -20^{o}C until required.

2.2.3 Immunohistochemistry

Sections were thawed for 30 mins at RT then washed twice in PBS for 5 mins each. Sections were permeabilized in 0.1 Triton X-100 (Sigma, Pool, UK) in PBS for 10 mins at RT, washed twice for 5 mins in PBS and then blocked for 30 mins at RT using PBS containing 0.5% bovine serum albumin (BSA; Sigma, Pool, UK) and 0.05% Tween 20. Appropriate primary antibodies, diluted in PBS containing 0.5%

BSA and 0.05% Tween 20 were incubated overnight at 4^{o}C in a humidified chamber (**Table 2.1**). Sections were then washed three times in PBS for 5 mins each, and relevant secondary antibodies were applied to the sections and incubated at RT for 1 hr (**Table 2.1)**. Sections were then washed 3 x 5 mins in PBS and mounted in Vectashield with DAPI (Vector Laboratories, Peterborough, UK).

2.2.4 Protein extraction and western blot analysis

2.2.4.1 Homogenisation of spinal cords

To extract total protein, DRG were cut and placed in ice for at least half an hour, 200µl of ice-cold lysis buffer (1M Tris HCL pH7.4, 5M NaCL, 0.5M EDTA, .025M EGTA, 1%NP-40, 5µl/ml protease inhibitor) was added to each sample and homogenised for 1 min at 4000g. Samples were left on ice for a furhter 30 mins and then transferred to eppendorf tubes and clarified by centrifugation at 17680g for 30 mins at 4^{o}C. The supernatant was removed and 5µl/ml of protease inhibitor cocktail (Sigma, Pool, UK) was added to inhibit protein degradation, aliquoted and stored at -20^{o}C until required.

2.2.4.2 Protein concentration assay

Using a 96 well plate microassay, 5µl of tissue lysates or protein standards were added, followed by 20µl reagents A, B and S (BioRad, Hertfordshire, UK) were added to the rest of the well as following (20µl of A and S (20µl of reagent S per 1ml of reagent A) and 160µl of reagent B). The plate was kept in the dark for 15

mins for colour to develop and the absorbance at 750nm was read using a plate reader within 1 hr (Bio-Rad, Hertfordshire, UK).

2.2.4.3 Gel casting

A 12% polyacrylamide gel was cast in 1mm disposal cassettes (Fisher Scientific, Loughborough, UK). Each gel was composed of resolving and stacking gel. The resolving gel comprised 2.75ml Protogel (Geneflow, Fradley, UK), 1.65ml of 1.5M Tris-HCL pH 8.8, 2.2ml MilliQ water, 66µl 10% sodium dodecyl sulphate (SDS) (Fisher Scientific, Loughborough, UK), 23.1µl 10% ammonium persulphate (APS) and 9.9µl Tetramethylethylenediamine (TEMED, VWR International, Lutterworth, UK), all these components mixed and approximately 2/3 of resolving gel was loaded onto the cassette. Seventy present ethanol was layered onto resolving gel in order to exclude air bubbles during polymerisation. While resolving gel was polymerising, a stacking gel was prepared as following; 0.4ml Protogel, 1.85ml 0.5M Tris-HCL pH 6.8, 0.75ml MilliQ water, 30µl 10% SDS, 15µl 10% APS, 7.5µl TEMED, then layered ethanol was removed followed by loading of stacking gel. Then a 1mm 10 well comb was inserted and the gel was allowed to polymerise at RT.

2.2.4.4 Western blot

Western blot gels were made at least 20 mins before running the procedure. Protein samples were prepared by adjusting the protein concentration by dilution with 2X sample Lamelli loading buffer (4% SDS, 20% glycerol, 10% 2-mercaptoethanol, 0.004% bromphenol blue and 0.125 M Tris HCl, pH about 6.8

(Sigma, Pool, UK)) and denatured at 90^{o}C for 4 mins. Five microlitre of molecular weight standard markers (Rainbow markers, Invitrogen) and 20µl of protein samples were loaded onto gels and proteins separated for 2 hr at 125V, 18mA, 2.1W under running buffer containing of 25mM Tris-base, 192mM glycine and 0.01% SDS.

Proteins were then transferred from gels onto immobilon polyvinylidene fluoride membranes (PVDF), which were activated by soaking in 100% methanol for 1min followed by a 1min wash in MilliQ water then 5min in transfer buffer containing 25mM Tris-base, 192mM glycine, 20% methanol and 0.02% SDS, at 25V for 2hr. Membranes were then washed with Tween-Tris buffered saline (TTBS (0.12% Tris-base, 0.88% NaCl, pH 7.4, 0.05% Tween 20)) for 5 mins, incubated in a 5% non-fat milk blocking solution (Marvel, Lincolnshire, UK) for 1 hour at RT, and then incubated overnight at 4^{o}C with relevant primary antibodies (**Table 2.2:** . Membranes were then washed with TTBS 3 times and incubated with relevant secondary antibodies conjugated to HRP (1:1000, GE Healthcare, Buckinghamshire, UK) for 1hr at RT (**Table 2.2:** .

Membranes were then incubated for 1min in 2ml of enhanced chemiluminescence (ECL) solution (GE Healthcare, Buckinghamshire, UK) at RT. The membranes were then placed in a transparent bag and exposed onto Kodak Biomax film (Kodak) to visualise the protein bands.

2.2.4.5 Stripping blots

Membranes may be stripped of primary and secondary antibodies using a low pH stripping solution (25Mm Glycine-HCL, pH2, 1% SDS) for 1hr at RT. Blots were then washed with TTBS for 5 mins and blocked in 5% non-fat milk solution for 1 hour at RT and then incubated with relevant primary and secondary antibodies as described above (**Table 2.2).**

2.2.5 Antibodies specificity

AMIGO3: same antibody has been used from (Ahmed et al., 2013) were the author used blocking peptide in rat DRG sections for antibody specificity.

RTN3: according to the manufacturer RTN3 antibody has been tested using western blot analysis of human brain tissue extract.

AEG-1: the manufacturer reported specificity for AEG-1 using immunohistochemistry of tissue section of human skin cancer that fixed with formalin and embedded with paraffin.

CRELD1: a 45kDa was specific binding in mouse heart tissue lysate of CRELD1 using western blot according to the manufacturer.

2.2.6 Antibodies used

2.2.6.1 Immunohistochemistry antibodies

Antibody (Cat No)	Dilution Factor	Species	supplier
		Primary Antibody	
AMIGO3 (sc-49881)	1:200	Goat	Santa Cruz, USA
NT3 (ab6203)	1:100	Rabbit	AbCam, Cambridge, UK
NF200 (N4142)	1:400	Mouse	Sigma-Aldrich, Poole, UK
AEG-1 (ab45338)	1:200	Rabbit	AbCam, Cambridge, UK
RTN3 (sc-33599)	1:200	Rabbit	Insight Biotech, UK
CRELD1 (ab131286)	1:200	Rabbit	AbCam, Cambridge, UK
β-III-tubulin (T2200)	1:400	Mouse	Sigma-Aldrich, Poole, UK
GAP43(SAB1405847)	1:200	Goat	Sigma-Aldrich, Poole, UK
CD68/ED1 (MCA341R)	1:100	Goat	Serotec, UK
CD8 (MCA1226)	1:100	Goat	Serotec, UK
CD4 (MCA1267)	1:100	Goat	Serotec, UK
GFAP (AB5804)	1:200	Mouse	Sigma-Aldrich, Poole, UK
		Secondary antibody	
Alexa Fluor 488	1:400	Goat, Rabbit	Invitrogen Ltd, Paisley, UK
Alexa Fluor 594	1:400	Mouse	Invitrogen Ltd, Paisley, UK
Texas Red	1:400	Mouse, Rabbit	Molecular Probes, UK

Table 2.1: Primary and secondary antibodies used for staining and detecting proteins in immunohistochemistry (IHC).

2.2.6.2 Western blot antibodies

Antibody (Cat No)	Dilution Factor	Species	supplier
Primary Antibody			
AMIGO3 (sc-49881)	1:1000	Goat	Santa Cruz, USA
NT3 (ab6203)	1:1000	Rabbit	AbCam, Cambridge, UK
AEG-1 (ab45338)	1:1000	Rabbit	AbCam, Cambridge, UK
RTN3 (sc-33599)	1:1000	Rabbit	Insight Biotech, UK
MBP (ab40390)	1:1000	Rabbit	AbCam, Cambridge, UK
OMGp (ab78595)	1:1000	Mouse	AbCam, Cambridge, UK
CSPGs (C8035)	1:1000	Mouse	Sigma-Aldrich, Poole, UK
CRELD1 (ab131286)	1:1000	Rabbit	AbCam, Cambridge, UK
Actin β (A5441)	1:1000	Mouse	Sigma-Aldrich, Poole, UK
Secondary antibody			
HRP- anti mouse	1:1000	Mouse WB	GE Healthcare, Buckinghamshire, UK
HRP- anti-rabbit	1:1000	Rabbit WB	GE Healthcare, Buckinghamshire, UK
HRP- anti-goat	1:1000	Goat WB	GE Healthcare, Buckinghamshire, UK

Table 2.2: Primary and secondary antibodies used for detecting proteins in Western blot (WB).

2.2.7 Dorsal Root Ganglion Neuron (DRGN) culture

2.2.7.1 Dissection and well preparation

Animals were killed in a chamber by a rising concentrations of CO_2 and T13-L5 dorsal root ganglia (DRG) were dissected out from the spinal cord. DRG ganglia were washed in Neurobasal-A (NBA; Invitrogen Ltd, Paisley, UK), then digested in 1.8ml of NBA media and 200µl of collagenase (1.125% concentration) for 2 hrs at 37^{o}C. DRG were then moved into a screw capped tube containing 10ml of Neurobasal-A to wash out the collagenase enzyme, the media was then removed and 2 ml of supplemented NBA (24.2mls NBA, 500ul B27 supplement, 62.5ul L-Glutamine (200mM), 125ul Gentamicin) was added and DRG and dissociated into single cells by trituration. The DRGN suspension was then layered onto a BSA gradient (1ml 30% BSA, 1ml NBA) and centrifuged at 120 x g for 10 min. The supernatant was removed and 100µl of Trypsin Inhibitor/DNase (TID) (0.01ml HBSS, 0.89ml MilliQ water, 0.46µl sodium bicarbonate, 0.3mg BSA, 0.25mg Trypsin inhibitor, 0.05mg Deoxyribonuclease and 10µl 3.8% $MgSO_4$) was added to prevent cell adhesion and thus clumping and then DRGN were resuspended with NBA for cell counting (as described below).

2.2.7.2 Chamber slide preparation and Cell counting

Chamber slides were pre-coated with 150µl of poly-D-lysine PDL (100ug/ml) for 1 hour at RT. Wells were then washed with PBS 3 x and 150µl of Laminin was added to each well and left at RT in readiness for cell seeding. For DRGN counting 10µl of cell suspension was added to an eppendorf tube and mixed with 10µl of Trypan blue, and a Haemocytometer was used to count the number of live

cells. 300 DRGN/well were plated in a total of 500µl of supplemented NBA for the neurite outgrowth experiments. Cells were grown in the presence or absence of 100µg/ml CME (described below).

The same protocol was used to prepare DRGN after pSN+DC lesions. For these experiments, the SN was preconditioned for 7 days and DRG were collected 7 days after DC lesion to mimic the *in vivo* scenario.

2.2.7.3 siRNA transfection

DRGN were removed from the incubator after 1 day of seeding and left for 20 min at RT to settle. Short interferon RNA (siRNA) (**Table 2.3**) was prepared in Lipofectamine 2000 reagent (Invitrogen Ltd, Paisley, UK). The concentration of siRNA required to cause maximal knockdown was pre-optimised using different concentrations ranging from 10 – 150nM in Lipofectamine 2000, and optimal concentration of siRNA was determined as 50-100nM/well.

The siRNA was prepared in 100µl of NBA while 6µl of Lipofectamine 2000 (Invitrogen Ltd, Paisley, UK) was mixed with 100µl NBA. These were allowed to settle for 5 min prior to mixing the two tubes and incubating at RT for 20min to allow siRNA to enter within the liposome formed by Lipofectamine 2000 reagent. The medium from cells was removed and 200µl of NBA containing the siRNA/ Lipofectamine 2000 reagent were used to transfect the cells for 5 hours at 37^{o}C and 5% CO_2. Each well was then supplemented with 300µl of supplemented NBA and incubated for a further 3 days at 37^{o}C and 5% CO_2.

siRNA (Cat No)	sequence	Isoform accession No	Stock concentration	supplier
siAMIGO3 isoform 1 (sc-60166)	GGCTGCTCGATCTATCATCTA	NM_198722	10µM	Santa Cruz, USA
siRTN3 isoform 3 (orb298058)	GGTTTCTCTTGCAGCTGACAT	NM_080909.3	5nmol/µl	Biorbyt, USA
siAEG-1 isoform 1 (sc-77797)	GAGCGAGGAACAGAAGAAGAA	NM_178812	10µM	Santa Cruz, USA

Table 2.3: Small/Short interferon RNA (siRNA) used in this study.

2.2.7.4 Immunocytochemistry

DRGN were fixed in 4% paraformaldehyde (PFA) for 10 min, washed in three changes of PBS. Non-specific staining was then blocked in 3% BSA and 0.1% of Triton X-100 for 10 min at RT, followed by incubation in primary antibody (diluted 1:200) for 1 hour at RT (**Table 2.1)**. After 3 washes in PBS for 10 min each, DRGN were incubated with secondary antibody, diluted 1:400 (**Table 2.1)**. After 3 further washes in PBS, coverslips were mounted in Vectamount with DAPI (Vector Laboratories).

2.2.7.5 Measurement of neurite outgrowth

Each chamber slide was divided into 9 fields and 9 images were randomly captured from each quadrant using an Axioplan 200 fluorescent microscope, equipped with an Axiocam HRc and Axiovision software (all from Carl Zeiss, Hertfordshire, UK). The longest neurite from 30 DRGN/well were measured using the built-in facilities in Axiovision and recorded (**Figure 2.3)**. The number of DRGN with neurites and DRGN survival were also counted. Each experiment was performed in duplicate and repeated on 3 independent occasions.

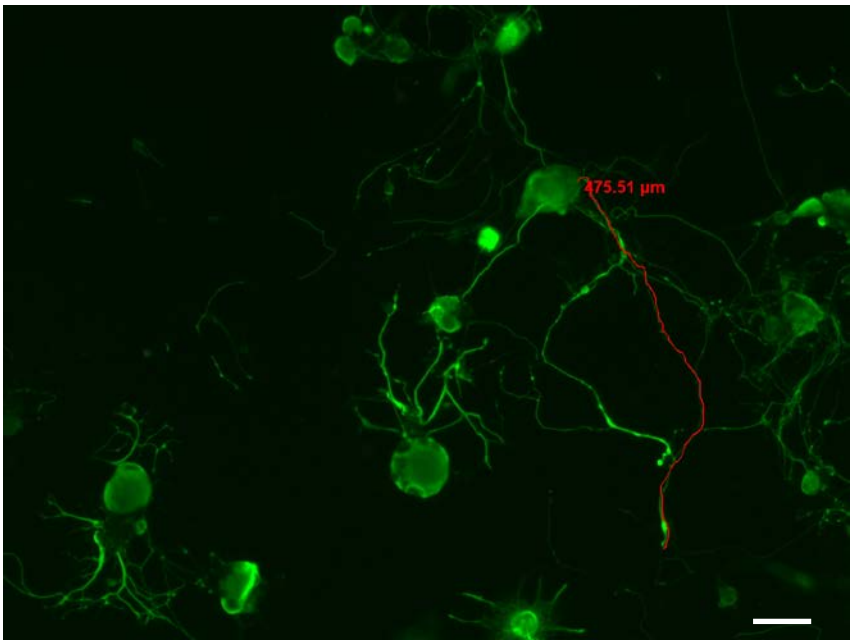

Figure 2.3: neurite outgrowth measured using built-in facilities in Axiovision

Image presented shows an example of a primary cultured DRGN followed by immunostaining with βIII-tubulin. The longest neurite outgrowth of each neuron was measured and recorded. Scale bar = 50µm.

2.2.8 Image capture for analysis of *in vivo* GFP expression

Images of whole DRG ganglia at x10 magnification from each animal group (n=6/group) were captured using an Axioplan 200 fluorescent microscope, equipped with an Axiocam HRc and Axiovision Software (all from Carl Zeiss, Hertfordshire, UK). Images were combined in Adobe Photoshop (Adobe Systems Incorporated) using the automated Photomerge feature. Composite images of the whole DRG ganglia were then used for analysis, including the number of gfp^+ DRGN**,** total number of DRGN and quantification of DRGN diameter.

2.2.9 Measurement of DRGN diameters

DRGN have high heterogenic size distribution since most of the literature classified DRGN as small and large (Schmalbruch, 1987). DRGN were divided by size into small, medium and large according to the following measurements: small (0-29 μm), medium (30-59 μm), large (> 60 μm) (Jacques et al., 2012a). DAPI channel images of the whole DRGN ganglia were converted to grayscale and DRGN were identified as a large round empty cell body surrounded by satellite cells (**Figure 2.**). Images were then examined using ImagePro image analysis software (Media Cybernetics Inc., Maryland, USA) to obtain diameter measurements.

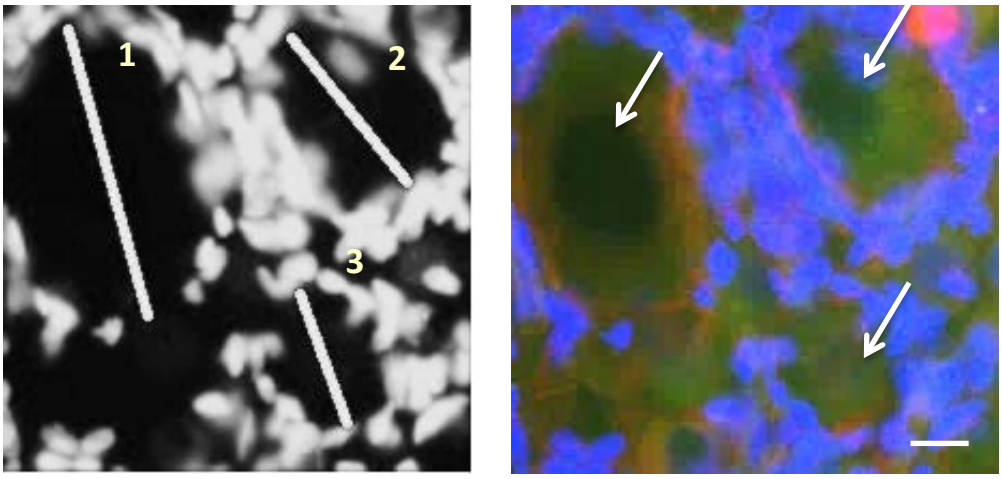

Figure 2.4: Method to measure DRGN diameter.

(A) DAPI channel for DRGN converted to grayscale and shown visible as empty areas with different diameter (1-3) large, medium and small. (B) Confirmation of DRGN nucleus not glia cells (arrow), Scale bar = 50µm.

2.2.10 Quantification of axons

Axon regeneration in the spinal cord was quantified according to the methods of Hata et al., (2006) (Hata et al., 2006). Serial parasagittal sections were completely reconstructed by collecting all serial 50-µm-thick sections (~20–30 sections per animal; n = 6 animals/treatment). On each section, the number of intersections of $GAP43^{+}$ fibers with a dorsoventral line was counted from 4 mm above to 4 mm below the lesion site (**Figure 2.)** . Axon number was calculated as a percentage of the fibers seen 4 mm above the lesion, where the DC was intact. The distance beyond the epicenter of the lesion was scored as positive and otherwise as negative distance.

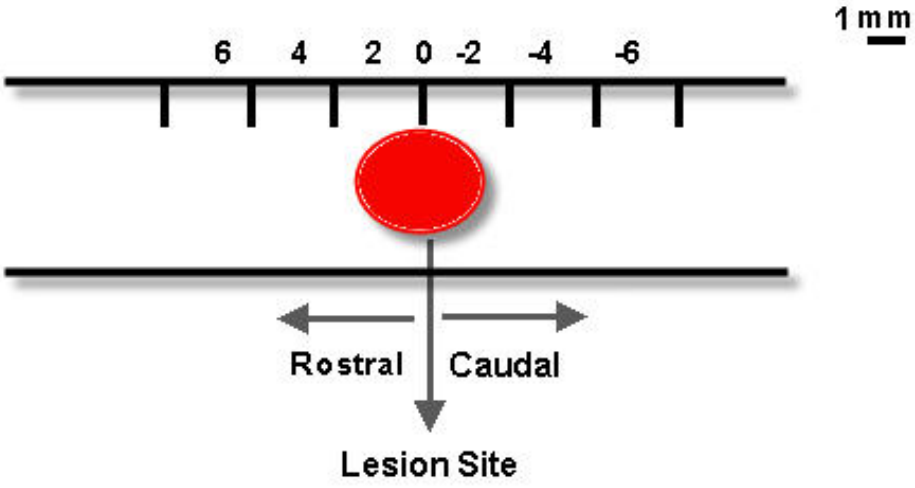

Figure 2.5: Paradigm of axon quantification in injured spinal cord.

2.2.11 Preparation of CNS myelin extracts (CME)

Myelin is a white insoluble precipitate and includes Nogo-A, myelin associated glycoprotein (MAG), and oligodendrocyte-derived myelin glycoprotein (OMgp). In this project, we extracted myelin from approximately 5 adult Sprague-Dawley rat brains as described previously (Ahmed et al., 2005). Brains were chopped into small pieces and homogenated in 10% (0.32M Sucrose, 1mM EDTA, pH 7.0) at 4^{o}C, then centrifuged at 800g (586 rpm) (< 10^{o}C) for 10 min. The resultant supernatant was collected and the pellet was re-suspended in the original volume before centrifugation at 800g (586 rpm) (< 10^{o}C) for 10 min. The supernatant was again collected and combined with the first supernatant and centrifuged at 13,000g (9533 rpm) for 20 min. The supernatant was removed and the pellet was re-suspended in 0.9M Sucrose to the original volume (10x tissue weight) and overlaid with 1-2ml of 0.32M Sucrose and centrifuged at 20,000g (14,666 rpm) for 60 min using ultra-centrifuge (Beckman centrifuge, UK). The white material at the interface was carefully collected in the minimum volume possible and dispensed in 20 volume of 0.32M Sucrose then centrifuged at 13,000g (9533 rpm) for 25 mins. Again, the white material was collected and diluted in 25 volumes of pure water and left on ice for 30 min before being centrifuged at 20,000g (14,666 rpm) for 25 min. The final white pellet, containing the CME was re-suspended in a small volume of pure water and kept in -80^{o}C freezer until required.

2.2.11.1 Procedure for using myelin on cells

Aliquoted CME were defrosted at 4^{o}C overnight and then triturated as follows to ensure a homogenous preparation: 200µl pipette tip (7-10 times), 19G needle (2-3 times), 23G needle (2-3 times). Myelin was then exposed to UV irradiation for 1 minute for sterilization and was then ready to be added onto cultured cells. At the required concentration, myelin can be either added directly to adhered DRGN or mixed with culture medium when medium replaced. Since myelin is an insoluble precipitate, the mixture of DRGN and CME was swirled every 24 hours to ensure equal distribution across the well.

2.2.12 Reverse Transcriptase-polymerase chain reaction (RT-PCR)

2.2.12.1 RNA extraction

All RNA samples were extracted from either L4/5 DRG ganglia or cultured DRGN. Two methods described below have been used in the project to obtain best RNA quality and quantity.

2.2.12.1.1 TRIAZOL method

DRG ganglia were thawed for 30mins (for DRG culture, media was aspirated out and cells were ready to be used for extraction methods). 1ml of TRIAZOL (Invitrogen Ltd, Paisley, UK) was added to the cells and incubated for 5mins at RT. Samples were then transferred to a new eppendorf tube and 200µl/1ml of chloroform were added in a fume hood and then vortexed for 15 seconds. Tubes

were then incubated at RT for 2-3 mins then centrifuged at 16200g for 20 mins at RT.

The overlying solution was carefully collected and transferred to a sterile Eppendorf tube. 500µl of isopropanol was added and mixed well, then kept for 30 mins at RT before storing at -20^{o}C overnight. The next day, tubes were centrifuged at 16200g for 20 mins at 4^{o}C and supernatant was removed and pellet was re-suspended for washing in 75% ethanol, mixed well and then centrifuged at 10800g for 20 mins at 4^{o}C.

Ethanol was removed and the pellet was left to dry for 15-30 mins at RT before 30-50µl of RNase free water added to dissolve the pellet. Water was passed well through the pellet and incubated for 10-20 mins at RT then the RNA concentration was determined by loading about 2µl of RNA solution into Nanodrop spectrophotometer (NanoDrop Lite; Thermo Scientific, USA) to measure the absorbance at 260nm. Sample purity was also performed using Nanodrop machine by measuring the 260/280nm absorbance ratio, RNA with a purity value of >1.8 was used in all experiments

2.2.12.1.2 Qiagen RNeasy kit

Approximately 350µl of RTL buffer was added to the samples (buffer was added directly to the cell samples and vortexed at high speed, while buffer was added and disrupted using homogenizer on tissue samples). One volume of 70% ethanol was added to the lysate and mixed well by pipetting. Total volume of 700µl of the samples were transferred including any precipitate to an RNeasy mini spin column

and placed in a 2ml Eppendorf tube then centrifuged at 10800g for 15 seconds. The supernatant was discarded and 700µl of RW1 buffer was added before centrifugation at 10800g for 15 seconds. Pellet was kept and 500µl of RPE buffer was added then centrifuged at 10800g for 15 seconds, which was repeated but centrifuged for 2 mins. RNeasy spin columns were removed and placed in a new 1.5ml Eppendorf tube and 30-50µl RNase-free water was added directly then centrifuged at 10800g for 1 min. Then RNA concentration and purity was measured using Nanodrop spectrophotometer (NanoDrop Lite; Thermo Scientific, USA) as described above.

2.2.12.2 cDNA synthesis

After extraction of total RNA from DRG using the methods described above, complimentary DNA (cDNA) single strand was synthesised by reverse transcription using the SuperScript First-Strand Reverse Transcription System for RT-PCR (Invitrogen Ltd, Paisley, UK). The reaction master mix mixture was prepared as shown in (**Table 2.4**), mixed briefly, and then combined with 12µl of RNA (1µg/12µl RNase free water) in a PCR tubes then placed at room temperature for 2 min. The PCR tubes were then transferred to PCR thermal cycler machine for preforming reverse transcription as shown in (**Table 2.5**). The reverse-transcribed first strand cDNA was stored at -20°C until use for RT-PCR.

Components	Volume (µl) per reaction
Reverse Transcription Buffer	4
10mM dNTPs	1
Random Primers	1
DTT	1
Superscript Reverse Transcriptase	1
Total per reaction	20 include 12µl of RNA

Table 2.4: RT master mix used for cDNA synthesis.

Steps	1	2	3	4
Temperature °C	25	37	85	4
Time/min	10	120	5	∞

Table 2.5: Thermal cycler setting used for the reaction.

2.2.12.3 Semi-quantitative RT-PCR

Primer concentrations were normalised by mixing 5 pmol/μl of forward and reverse primers (**Table 2.8),** where all primers design to detect all isoforms. An ABI Prism SDS 7000 PCR machine was used to set up the PCR program shown in (**Table 2.6**). The reaction master mix mixture was prepared in sterilised PCR tubes as shown in (**Table 2.7**). PCR reaction product was then analysed on 1% agarose gels (Bioline Ltd, London, UK) at either 3 or 5 cycle intervals to ensure exponential PCR product amplification, in which this step done by Dr Zubair Ahmed.

Steps	1	2 (35-40 cycles)	3	4
Temperature °C	96	96 58 72	72	4
Time	2min	30s 30s 45s	5min	∞

Table 2.6: PCR thermal cycles settings used for PCR.

Reagent	**Volume (μl)**
Buffer + MgCl 1.5mM	5
dNTPs	3
cDNA	3
Forward primer	1
Reverse primer	1
Taq polymers	0.2
H_2O	11.8
Total per reaction	**25**

Table 2.7: PCR master mix reagents volumes.

Primer name	Sequence (5’-3’)	Accession No
AMIGO3	Forward: GAATCGGCTCTACTTGCACA	NM_178144.1
	Reverse: AAGTCGTGCAGAGCACTTAG	
AEG-1	Forward: GGCGGATCCGCTGGGCCGCGGCTTGC	NM_133398.1
	Reverse: GGCGTCGACTCACGTTTCTCGTCTGGC	
RTN3	Forward: TCAGTCTTCCGAACAGGCTA	NM_001009953.3
	Reverse: AATCAGATCATGCACCGCAC	
CRELD1	Forward: CTAAAACAATGGGCTGACGC	NM_001024783.1
	Reverse: CTGGAAAAGCCAGCCGTAG	
GAPDH	Forward: CTCTGCTCCTCCCTGTTCTA	NM_017008.4
	Reverse: CGTTGATGGCAACAATGTCC	
NT3	Forward: CGCAGTGAGGATTACGGAAA	NM_031767.1
	Reverse: CCAAGATCAGCTTTGCAGGA	

Table 2.8: Forward and reverse primers used in PCR reactions

2.2.13 Densitometry

Bands detected by western blot and RT-PCR were both scanned using Adobe Photoshop (Adobe Systems Inc, San Jose, CA, USA) keeping all scanning parameters constant. ImageJ (NIH, USA, http://imagej.nih.gov/ij) was used to quantify the bands using the built-in-gel plotting macros (**Figure 2.)**. Each densitometric value was derived from 3 independent experiments and normalised to loading controls either to β-actin in western bolts or glyceraldehyde 3-phosphate dehydrogenase (GAPDH) in RT-PCR. The densitometric values were also normalised to the densities of the relevant intact controls for each experiment and presented as mean ± SEM.

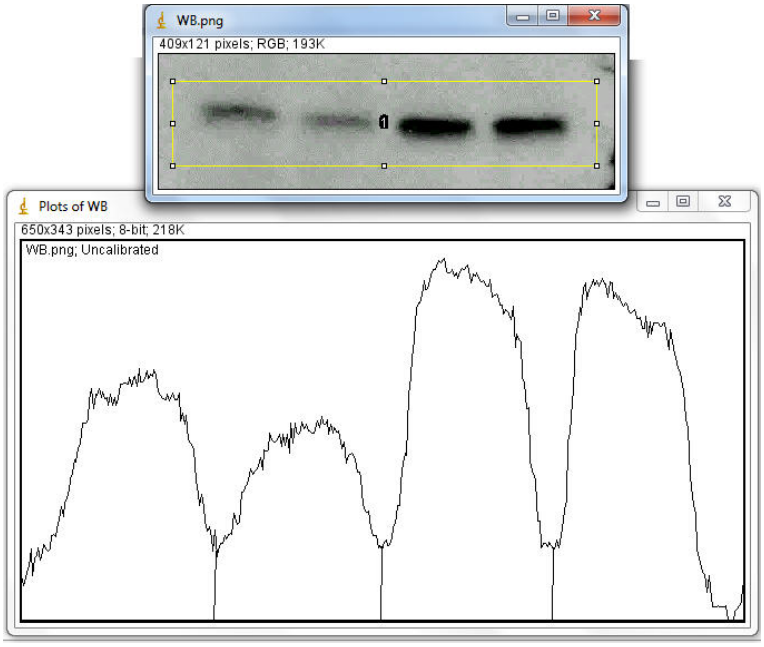

Figure 2.6: Illustration of how densitometry obtained using built-in macro function of ImageJ program.

Peaks of interest were enclosed by drawing a line then peaks area were measured using Wand tool to define the integrity.

2.2.14 Enzyme linked immunosorbent assay (ELISA)

A sandwich ELISA was used to measure neurotrophin 3 (NT3) level in NBA media following transection of CMV-shAMIGO3/nt3-gfp plasmid to DRGN cultures. All the reagents with kit provided from (R&D Systems, Abingdon, UK). Coated sterile 96-well plats (Nunc, Loughborough, UK) with polyclonal antibody against NT-3 was sealed with Parafilm (Pechiney Plastic Packaging Company, Chicago, IL, USA) and incubated at 4°C overnight, then washed 3 times with wash buffer. 300µl of block reagent was added in each well and incubated for 1hr at RT, followed by washing step. 100µl of NT-3 standards and samples were added to each well followed by incubation period 2-4hrs on a shaker at RT. After this, around of wash was performed and 100µl of detection monoclonal antibody at a dilution of 1:4000 was added to each well then incubated at 4°C overnight. The plate was washed then a 100µl of HRP-conjugated mouse IgG was added to each well at dilution of 1:100 and the plate was placed on shaker for 2hrs at RT followed by three times washing. After this, each well received a 100µl of substrate solution and incubated on a shaker for 20mins at RT, and then 100µl of stop solution was added and mixed gently on a shaker. The absorbance of the plate was then measured within 30mins in microplate reader set to 450 nm (Victor3, Perkin Elmer). The standard curve of NT-3 concentration vs absorbance was the plotted using Excel, the curve was used to determine the concentration of NT-3 in each sample.

2.2.15 Microarray analysis

The rat genome AROS V3.0 set has 26962 long-mer probes containing 27044 gene transcripts were purchased form Operon Biotechnology (Operon Biotechnology GmbH, Cologne, Germany). The microarray reaction was performed and prepared by the Functional Genomic Lab (University of Birmingham, UK). By using Pronto Universal slide spotting solution (Fisher Science, Loughborough, UK) oligonucleotides were resuspended and subsequently spotted onto UltraGAPS coated slides with Bar code (Fisher Science) using BioRobotic microgrid II spotter (Genomic Solution Ltd, Huntington, UK). The amount of 0.5-1 ug of the total extracted RNA form each animal (n=6) was amplified and then labelled with either Cy3 orCy5 dye (GE Healthcare, Little Chalfont, UK) following the protocol. By using the dye incorporation calculator (www.ambio.com/tools/dye) the frequency was calculated with frequencies of 30-60 dye molecules per 1000 nucleotides. The probes were resuspended in hybridization buffer (Corning BV, Koolhovenlaan, UK) and microarray was performed using Pronto Kit following the manufacturer's protocol. Slides were then scanned and images were analysed using GenePix software. The microarray was performed by Dr Martin Read using previous BBSRC funding obtained by Prof Ann Logan.

Data from the microarray were analysed using GenSpring GX7 (Agilent) and normalised to intact controls (Sohaib Mir PhD Thesis, 2009). Excel spread sheets were then created with fold changes of gene expression listed from the highest to the lowest. These spread sheets were interrogated for regeneration-related genes in this project.

2.2.16 Statistical analysis

All experiments were repeated on 3 independent occasions and no efforts were made to avoid bias. Statistical analyses were performed using IBM SPSS software (version 15). These analyses were applied to confirm whether the needed statistical significant differences observed between untreated controls and treated groups were real. The data from multiple treatment groups were analysed using one-way Analysis of Variance (ANOVA) combined with Games Howell post-hoc test, whereas t-test was applied to compare data from 2 experimental treatment groups. Data was then considered to be statically significant if the probability (p) was less than the specified significance levels (where *$p \leq 0.05$, **$p \leq 0.001$, ***$p \leq 0.0001$).

CHAPTER 3: Suppression of AMIGO3 promotes dorsal column axon regeneration after spinal cord injury

Sections of this chapter are included in the following paper:

Almutiri S., Berry M., Logan A., Ahmed .,Z (2017). Non-viral-mediated suppression of AMIGO3 promotes disinhibited NT3-mediated regeneration of spinal cord dorsal column axons. *Submitted to ELife.*

3.1 Introduction

3.1.1 Leucine-rich repeat (LRR) family of proteins

The leucine-rich repeat (LRR) containing motif is found in a family of proteins classified as synaptic proteins that play a role in “axonal guidance, target selection, synapse formation and stabilization of connections” (de Wit et al., 2011, de Wit and Ghosh, 2014). There is also some evidence that LRR may be involved in neurodegenerative disorders (Seeger et al., 1993). Therefore LRR plays a role in neural development, function and disorders. The LRR proteins are 20-30 amino acids in length and their concave/convex nature allows them to interact with a vast number of ligands making them a very efficient and versatile protein interaction motif.

Because of the rather elaborate role of LRR, understanding the mechanisms that enable these molecules to perform these functions may help provide information about axonal regeneration in the CNS. Proteins with LRR domains are found to be suited for communication between cells and cell adhesion and their diverse cellular interactions and ligand-binding specificity has been cited in directing neural connectivity, which is a major aspect in formation of neural circuitry. The role played by Slits and Robo receptors in axonal guidance are not disputed (Luo

and Flanagan, 2007). Slits contain four LRR proteins and Robo proteins have a high binding affinity to the Slit proteins. These therefore form a Slit-Robo pair, which is responsible for axonal guidance and dendritic arborisation (Cho et al., 2007). Trk receptors, another family of LRR proteins are also found to be involved in axonal guidance and targeting (de Wit and Ghosh, 2014, de Wit et al., 2011).

Target selection is another role played by LRR proteins in neuronal development involving a global targeting role played by molecular gradients and a specific targeting role played by discrete molecular cues. Slit has been cited as a molecular cue involved in global targeting while Capricious (Caps) has been found to act as a discrete cue in studies carried out in drosophila olfactory and visual systems (Luo and Flanagan, 2007). Slit and Caps are both LRR proteins, yet again entrenching the role of LRR proteins in axonal target selection.

3.1.2 leucine-rich repeat and immunoglobulin domain-containing Nogo receptor-interacting protein-1 (LINGO-1)

LINGO-1 was identified based on its symmetry to the guidance molecule Slit. LINGO-1 is located in 15q24 chromosome and belongs to the LRR protein family, consisting of twelve LRRs and a type 1 transmembrane with one immunoglobulin (Ig) right after the transmembrane segment (Mi et al., 2004, Carim-Todd et al., 2003). There are three human homologs of LINGO-1; LINGO-2, LINGO-3 and LINGO-4. LINGO-1 is predominantly expressed in the CNS including brain and spinal cord: no expression of LINGO-1 is detectable in non-neuronal tissues. Not much is known about LINGO-2, LINGO-3 and LINGO-4 expression, but studies

revealed that they expressed in far lower levels compared to LINGO-1 in the CNS (Haines and Rigby, 2008, Llorens et al., 2008). Human LINGO-1 consists of 614 amino acids and is a co-receptor of the NgR1 receptor (Nogo-66 receptor). The extracellular LRR domain of LINGO-1 interacts with NgR1 LRR domain and activates the signalling pathway of NgR1 in the CNS (Zhou et al., 2012).

The LRR domain of this protein is implicated in protein-protein interactions and in cell adhesion/signaling in specific areas of the brain. Most studies have revealed that the role of LINGO-1 is in axon growth inhibition, distribution of oligodendrocyte myelination and differentiation (Meabon et al., 2016, Mi et al., 2005, Zhang et al., 2015).

LINGO-1 is a signaling co-receptor with NgR1 and $p75^{NTR}$ or TROY/TAJ after spinal cord injury (Mi et al., 2004). However, the low intrinsic capacity of the spinal cord to regenerate is combined with a non-permissive environment which contain myelin inhibitors Nogo-A (Voeltz et al., 2006), MAG (Schnaar, 2010), and OMgps (Gil et al., 2010). All of these inhibitory ligands bind to the NgR1/$p75^{NTR}$/LINGO-1 tripartite receptor complex (McKerracher and Winton, 2002) and activate axon growth cone collapse through the RhoGTPase pathway (Ahmed et al., 2013). Rho-A binding to its Rho domain leads to activation of Rho kinase (ROCK-1) which activates LIM-kinase-1 (LIMK-1) thus results in phosphorylation by inactivation of cofilin (Yang et al., 1998). Inactivation of cofilin leads to polymerization of actin filaments, which inhibit the growth of axons (Lingor et al., 2007).

Although, LINGO-1 is implicated in axon degeneration after CNS injury, studies revealed that LINGO-1 also contributed in myelination and differentiation of oligodendrocytes. Since LINGO-1 is detected in neurons and oligodendrocytes, inhibition of LINGO-1 enhances the development of myelinated axons by promoting outgrowth of oligodendrocytes processes (differentiation) (Mi et al., 2008, Mi et al., 2007). The full mechanism of how LINGO-1 promotes oligodendrocyte differentiation and myelination remains to be elucidated. However, a recent study showed that LINGO-1 blocked the β1-integrin signalling pathway which negatively regulated oligodendrocytes differentiation (Mi et al., 2016). The integrin pathway is known to play an important role in oligodendrocytes differentiation and survival and β1-integrin is required for oligodendrocyte precursor cell (OPC) differentiation. LINGO-1 was found to interact and reduce β1-integrin expression whereas anti-LINGO-1 antibodies induced β1-integrin levels and enhanced both differentiation and myelination of oligodendrocyte (Mi et al., 2016).

3.1.3 Amphoterin-induced gene and open reading frame (AMIGO)

Amphoterin is a heparin binding protein known as high-mobility group box-1 (HMGB1) proteins, first isolated in 1987 as a neurite outgrowth-promoting factor from perinatal rat brain (Rauvala and Pihlaskari, 1987, Merenmies et al., 1991, Kuja-Panula et al., 2003). Amphoterin-induced gene and open reading frame (AMIGO) was first identified by Juha *et al,* the author binds Amphoterin to RAGE (receptor for advance glycation end products) in E18 rat hippocampal neurons, then was able to identify AMIGO using order differential display (ODD) screening

technique. By cloning AMIGO, Juha *et al* were subsequently able to find two other proteins, AMIGO2 and AMIGO3, all transmembrane proteins containing six LRRs and a type 1 transmembrane domain with one immunoglobulin Ig domain right after the transmembrane segment and implicated in axonal growth (**Figure 3.1**) (Kuja-Panula et al., 2003, Chen et al., 2006, Kajander et al., 2011). AMIGOs refer to LRRs protein family and immunoglobulin (Ig) superfamily due to multi LRR and immunoglobulin (Ig) found in their domain structure. While AMIGO is said to promote axonal growth, AMIGO3 on the other hand has been found to inhibit axonal growth after CNS injury (Kuja-Panula et al., 2003, Ahmed et al., 2013).

3.1.3.1 AMIGO1

AMIGO1 is involved in cell adhesion that manage axon fasciculation and extension via promoting neurite outgrowth through its extracellular region by homophilic binding. The ectodomain part of AMIGO1 was also shown to enhance attachment and neurite outgrowth of hippocampal neurons in culture (Kuja-Panula et al., 2003). Moreover, in cultured DRGN AMIGO1 showed to co-expressed with other LRRIG protein TrkA where the binding or co-expression was nearly all in $TrkA^+$ neurons including a subset of medium and large diameter $TrkA^-$ DRGN. The interaction or binding with TrkA may contribute to the development of sensory and motor neurons via modulating the functions of Trks and Ret receptor tyrosine kinases through distinct phases of axonal guidance, extension and target innervation (Mandai et al., 2009, Zhao, 2016).

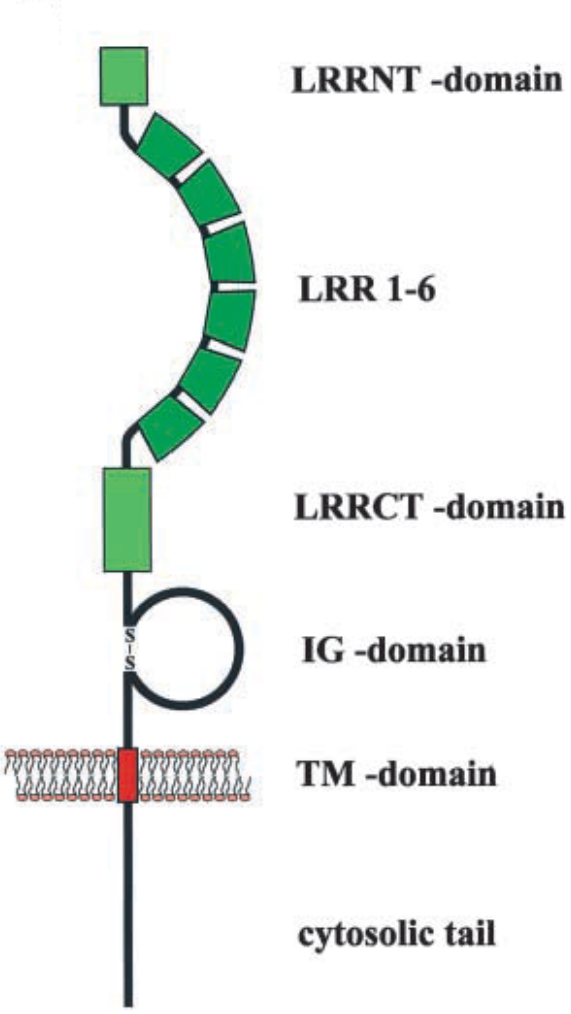

Figure 3.1: Schematic represents AMIGOs containing six LRRs and type1 transmembrane with one immunoglobulin (Ig) right after transmembrane segment.

(Adapted from (Kuja-Panula et al., 2003).

However, recently AMIGO1 was found to co-localise with Kv2.1 potassium channel in hippocampal neurons indicating that AMIGO1 takes part in neuronal channel function. Both AMIGO1 and Kv2.1 was found to be co-expressed in axon initial segment and dendrites where they may modulated action potential frequency, where Kv2.1 known as susceptibility gene for schizophrenia spectrum disorders. Therefore, Kv2.1 and AMIGO1 may provide a new therapeutic drug for neuronal excitability (i.e. psychiatric disorders and epilepsy) (Peltola et al., 2011, Peltola et al., 2016)

3.1.3.2 AMIGO2

Three different research groups have independently identified AMIGO2, otherwise known as Alivin1 and DEGA (differentially expressed in gastric adenocarcinomas) (Kuja-Panula et al., 2003, Ono et al., 2003, Rabenau et al., 2004). As mentioned above Kuja-Panula et al (2003) used ODD screening on hippocampal neurons in the presence of Amphoterin where they were able to identify AMIGO1, AMIGO2 and AMIGO3. Ono et al (2003) was able to identified Alivin1 gene that played a role in depolarization-dependent survival of cerebellar granule neurons and then two other similar genes were also isolated namely Alivin2 and Alivin3. Rabenau et al (2004) found Alivin1 to be differentially expressed in about 45% of human gastric adenocarcinomas (termed DEGA from differentially expressed in gastric adenocarcinomas). DEGA and Alivin1 were found to be identical to AMIGO2 (Laeremans et al., 2013).

During adulthood, AMIGO2 mRNA is expressed in neurons, astrocytes and oligodendrocytes whislt no expression of AMIGO2 was detectable in the spinal cord (Homma et al., 2009, Chen et al., 2012).

3.1.3.3 AMIGO3

Little is known about the function and implication of AMIGO3, which forms a complex with NgR1-p75/TROY after spinal cord injury, and inhibiting axon regeneration (Ahmed et al., 2013). The levels of LINGO-1 expression in the spinal cord after a spinal cord injury do not increase until 14 days (Mi et al., 2004), this is because it is likely that during the critical stages after CNS injury other NgR1 co-receptors that mediate the inhibition of axon growth are expressed and able to function. In the acute stage of spinal injury, LINGO-1 was reported to substitute by AMIGO3 in centrally axotomized DRGN and retinal ganglion cells (RGC). Immediate responses to inhibition of axon growth to CNS myelin are mediated by the NgR1-p75/TROY-AMIGO3 receptor complex. As much as LINGO-1 is an agreed upon as co-receptor in the NgR1-p75/TROY receptor complex which signals inhibition of the CNS axon growth, its patterns of expression after an injury in the spinal cord are not in line with its proposed function. This is because LINGO-1 levels do not increase in an appreciable rate in the DRGN until after 14 days, therefore other molecules may contribute in signaling the axon growth inhibition in the acute stage of spinal injury (Ahmed et al., 2013). Disinhibition on its own is not enough to propel the outgrowth of the neurites in the presence of CNS myelin but addition of relevant neurotrophic factors is necessary to drive the growth (Berry et al., 1996). When combined, disinhibition and neurotrophic factors

propel regeneration of the CNS axon. Therefore, AMIGO3 is a receptor complex that in a big way signals the inhibition of ligands derived from CNS myelin.

Suppression of the function of AMIGO3 rather than LINGO-1, when it is combined with NTF may be an effective acute therapeutic method in the promotion of CNS axon regeneration after injury.

3.1.4 Hypothesis

We hypothesise that AMIGO3 substitutes for LINGO-1 in acute phase of spinal cord injury by forming complex receptors with NgR1/p75-TROY, and that suppression of AMIGO3 together with driving regeneration by NTF will promote CNS axon regeneration.

3.1.5 Aims

- To confirm the levels of AMIGO3 increased in non-regenerating (DC) injury models.
- To promotes DRGN neurite outgrowth by knocking down AMIGO3 in presence of CME and Fibroblast growth factor-2 (FGF-2).
- To determine the optimal does of DNA plasmids in DRGN transfection by *in vivo*-jetPEI delivery vector.
- Validate the efficiency of non-viral delivery of CMV-shAMIGO3-nt3 plasmids to promote DRGN neurite outgrowth in presence of CME.

- Validate the efficiency of non-viral CMV-nt3/gfp plasmids to overexpress NT3 levels in DRGN culture and *in vivo*.
- Validate the efficiency of non-viral delivery of CMV-shAMIGO3/gfp to supress AMIGO3 levels *in vivo*.
- To assess which of DRGN diameters (small, medium and large) are GFP^+ after injection with plasmids (mentioned below in methods section).
- To promote dorsal column axon regeneration after DC lesion by *in vivo*-jetPEI-shAMIGO3/*nt3* plasmid delivery.

3.2 Materials and Methods

Please refer to the main materials and methods chapter for standard and detailed protocols.

3.2.1 Experimental design

The experiment in this chapter comprised 6 groups each contain n = 6 rats/group, as follows:

- Group 1 = intact control (IC) to detect baseline levels.
- Group 2 = DC transected controls (DC) to detect injury-mediated changes.
- Group 3 = DC+intra-DRG injection of *in vivo*-jetPEI-*gfp* (DC+PEI-*gfp)* to detect if transfection of *gfp* caused adverse effects and monitor DRGN transduction efficiencies. This experimental groups in which the DC was transected and DRG were injected with plasmid-containing *in vivo*-jetPEI complexes, comprised: DC+intra-DRG injection of *in vivo*-jetPEI-*gfp*
- Group 4 DC+*in vivo*-jetPEI -*nt3/gfp* to monitor DRGN transduction and NT3 over-expression
- Group 5 DC+*in vivo*-jetPEI-shAMIGO3/*gfp* (DC+PEI-shAMIGO3*/gfp)* to monitor AMIGO3 knockdown in DRGN and to establish if AMIGO3 knockdown without concomitant stimulation with NT3 promotes DRGN axon regeneration.
- Group 6 DC+intra-DRG injection of *in vivo*-jetPEI-shAMIGO3/*nt3 (*DC+PEI-shAMIGO3*/nt3)* to determine if AMIGO3 knockdown and simultaneous stimulation with NT3 is required for DRGN axon regeneration).

3.2.2 Plasmids construction

Several plasmids were created expressing control *gfp*, sh*gfp*, shAMIGO3/*gfp*, nt3/*gfp*, shAMIGO3/*nt3,* in different combinations based on their experimental use. This is because we are currently restricted to the delivery/expression of two transgenes in target tissues. Plasmids were produced as described previously (Feng et al., 2009). To construct bi*cis*tronic plasmids (pH1-shAMIGO3-CMV-*gfp* (shAMIGO3/*gfp*) and pH1-shAMIGO3-CMV-*nt3 (*shAMIGO3/*nt3*): shAMIGO3 encoding complementary DNA sequences were designed using the online Ambion software and shAMIGO3 oligonucleotides were cloned into pRNAT-H1.1/shuttle along with cDNA for either nt3 or gfp (Addgene, Cambridge, MA, USA). To create pCMV-*nt3*-*gfp* (*nt3*/*gfp*), the coding sequence of rat NT3 and the nerve growth factor signal sequence (Zhou et al., 2003) were cloned into pIRES-EGFP (Clonetech, Mountain View, CA, USA).

3.2.3 Preparation of *in vivo*-jetPEI vector

In vivo-jetPEI (Polyplus Transfection, New York, USA) was prepared according to the manufacturer's instructions. For example, for intra-DRG injection, 2µg/µl of DNA plasmid was added to 4µl of 5% glucose solution and 0.24µl 100mM of *in vivo*-jetPEI was added to 4µl of 5% glucose in separate tubes then vortexed well. Tubes were mixed and incubated for 15mins at RT before injection (5µl total volume).

3.2.4 Optimal concentration of plasmid

DRGN were transfected with 0.5, 1, 2, 3 and 4µg of plasmid DNA containing either a control sh*gfp* (PEI-sh*gfp*) or shAMIGO3/*nt3* (PEI-shAMIGO3/*nt3*). Additional controls included untreated DRGN (Untreated), DRGN transfected with *in vivo*-jetPEI only (Sham), and *in vivo*-jetPEI-shAMIGO3/*gfp* (PEI-shAMIGO3/*gfp*). DRGN were allowed to incubate for 3 days prior to harvesting of cells and extraction of total RNA for validation of shAMIGO3 knockdown using RT-PCR (refer to section 2.2.11 for more details).

To monitor NT3 production and disinhibited DRGN neurite outgrowth after shAMIGO3 knockdown and NT3 stimulation in cultures, DRGN were transfected with the optimal dose of plasmid DNA (2 µg) and incubated for 3 days in the presence of 100 µg/ml CME (Ahmed et al., 2005), prior to harvesting culture supernatant to detect NT3 production by ELISA (see section 2.2.13) and neurite outgrowth by immunocytochemistry (more details in section 2.2.6.4).

3.3 Results

3.3.1 AMIGO3 levels increased in non-regeneration models after 7 days post injury

We used double immunohistochemistry for AMIGO3 and neurofilament-200 in DRGN sections in regenerating (SN and pSN+DC) and non-regenerating (DC) models after 7 days post injury to detect AMIGO3 levels. No changes of AMIGO3 levels in intact DRGN were present, but higher levels of AMIGO3 were found in non-regenerating DRGN (DC injury alone) (**Figure 3.2)**. By contrast, lower levels of AMIGO3 were seen in regenerating SN paradigm compared to those seen in non-regenerating DRGN. However, regenerating DRGN after preconditioning lesions (pSN+DC) showed absence of AMIGO3 levels (**Figure 3.2)**, suggesting depressed AMIGO3 levels correlate with enhanced axon regeneration.

3.3.2 Knockdown of AMIGO3 enhances disinhibited DRGN neurite outgrowth only in the presence of FGF-2

In primary DRGN, AMIGO3 protein was localised in approximately 90% of βIII-tubulin^{+} DRGN (**Figure 3.3)**. In addition, transfected DRGN with Lipofectamine 2000, siGFP, and siAMIGO3 did not show enhanced neurite outgrowth in the presence of CME. However, disinhibited DRGN neurite outgrowth from around 45% of DRGN were observed when transfected with shAMIGO3 only in the presence of FGF-2 compare to DRGN treated with FGF-2 alone, demonstrating that knockdown of AMIGO3 in presence of CME and driven by FGF-2 enhanced disinhibited DRGN neurite outgrowth. The results in (**Figure 3.2, Figure 3.3 and Figure 3.4)** have been repeated from (Ahmed et al., 2013) to confirm that suppression of AMIGO3 is required to enhance CNS axon regeneration before establishing the *in vivo* study.

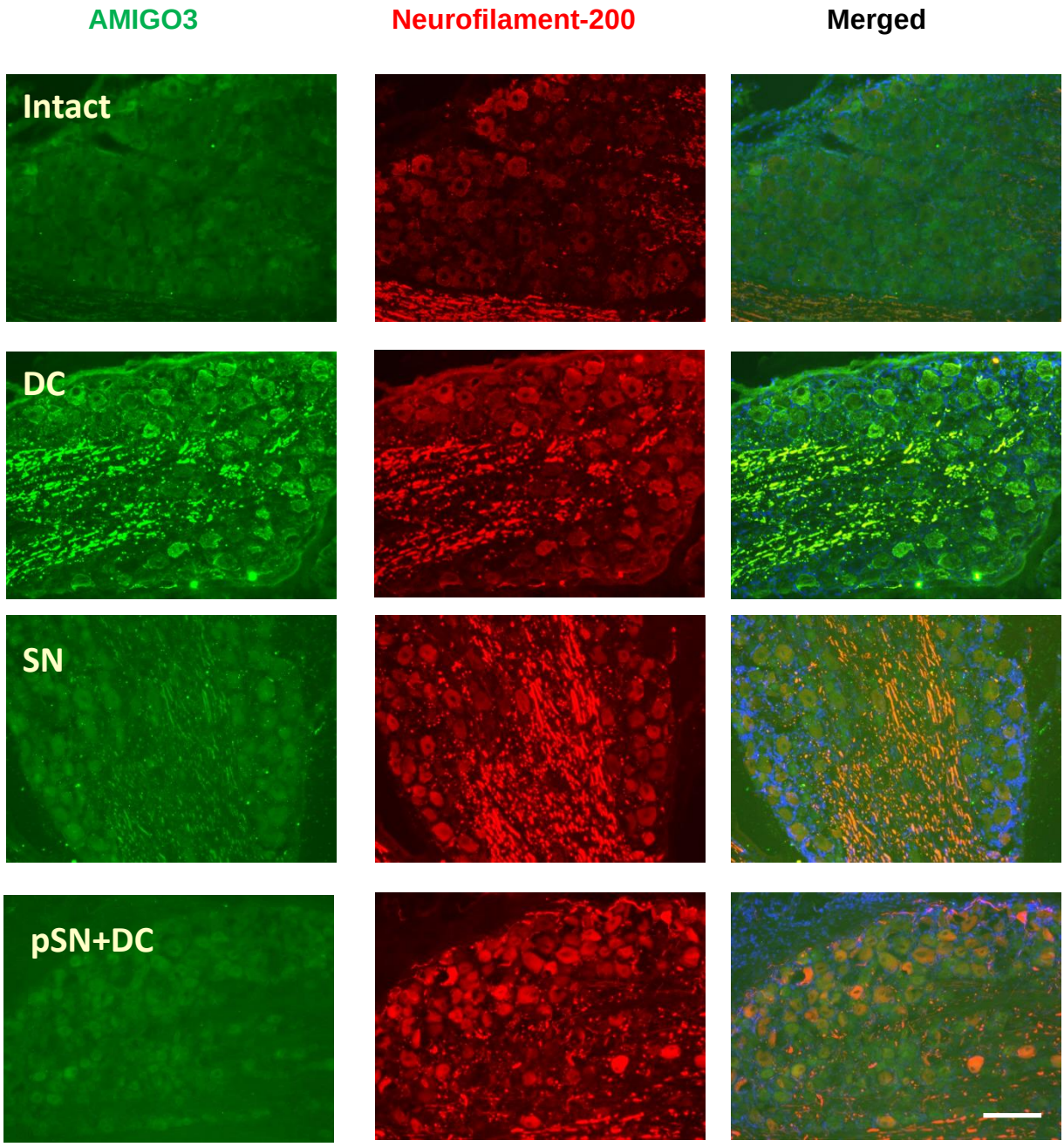

Figure 3.2: AMIGO3 levels in intact, non-regeneration and regeneration DRGN models at 7 days after injury.

Double immunohistochemistry for AMIGO3 and neurofilament-200 in DRGN sections showed high level of AMIGO3 protein in non-regeneration (DC) compare to intact and regeneration (SN and pSN+DC). Scale bar = 500 µm. (n=3)

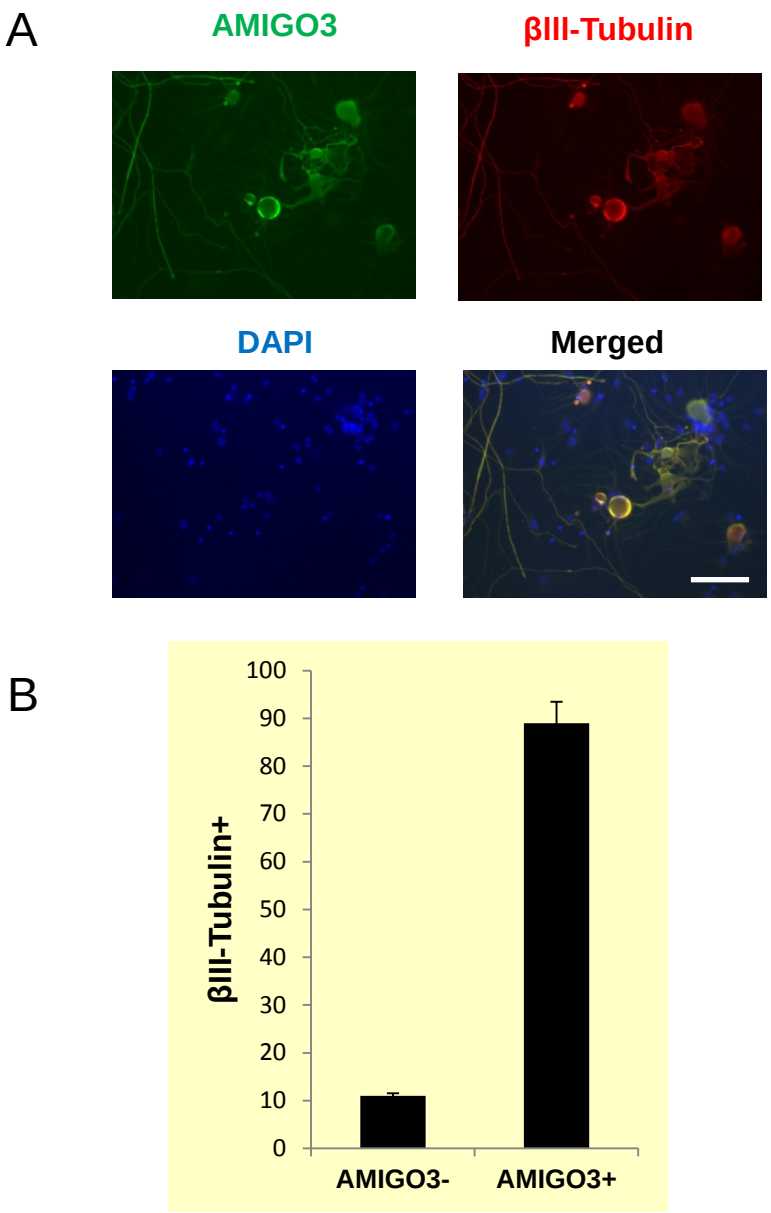

Figure 3.3: localisation of AMIGO3 in DRGN primary cultured for 3 days.

(A) Double immunohistochemistry showed that AMIGO3 was co-localised in βIII-tubulin^{+} DRGN **(B)** the proportion of AMIGO3 with βIII-tubulin co-localised DRGN was 88%. Estimate scale bar = 500µm. (n=3)

A

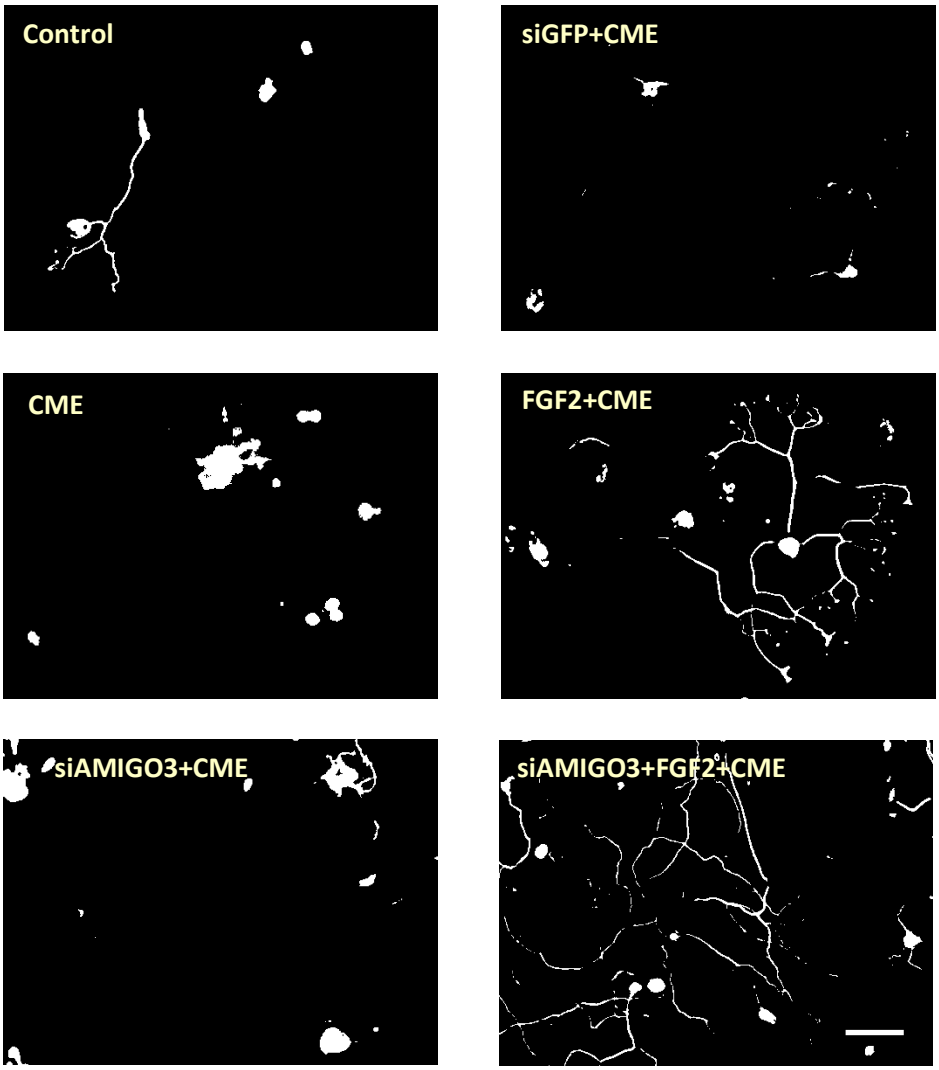
Control
siGFP+CME
CME
FGF2+CME
siAMIGO3+CME
siAMIGO3+FGF2+CME

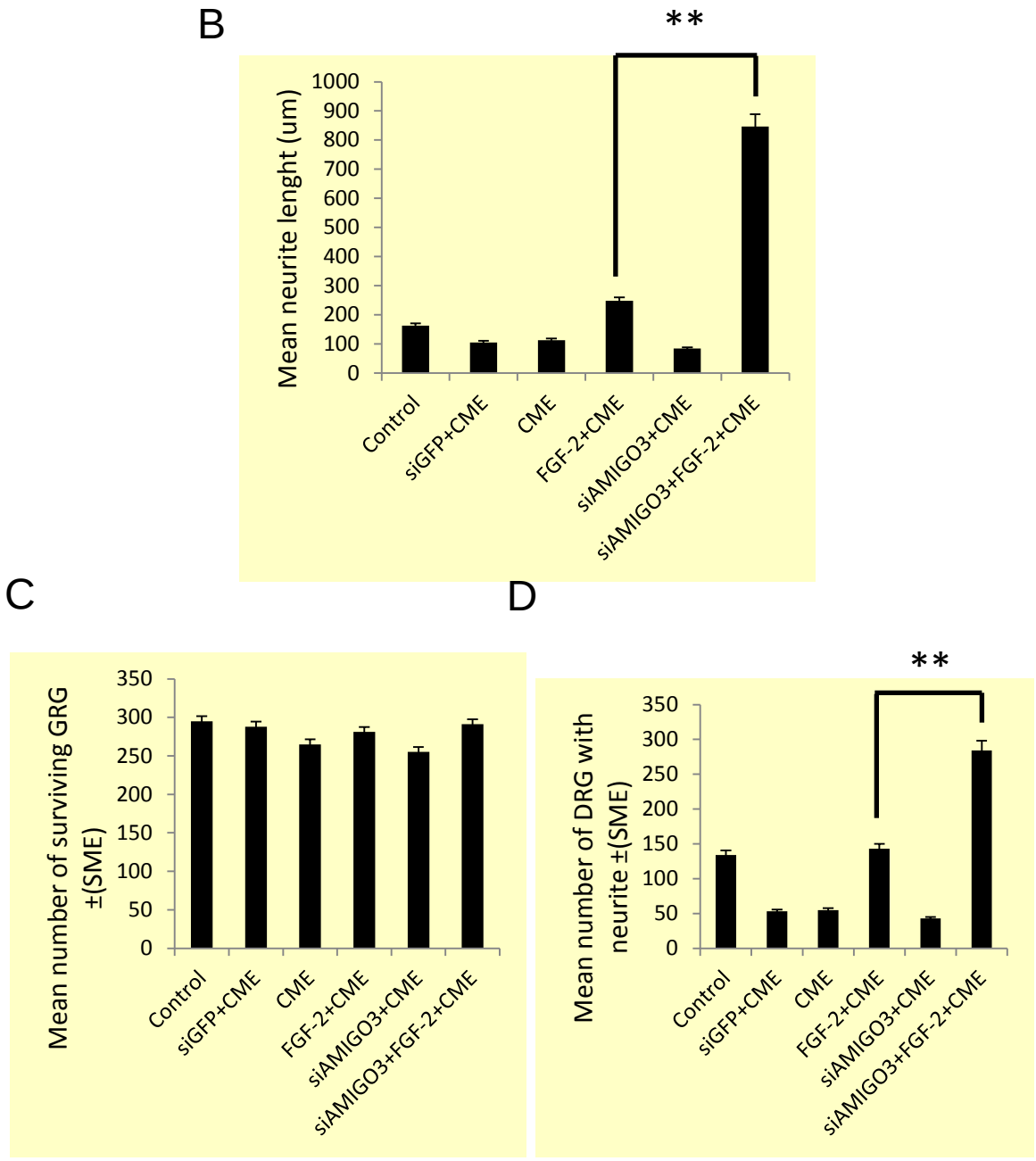

Figure 3.4: Knockdown of AMIGO3 promotes neurite outgrowth in presence of CME and stimulated by FGF-2.

(A) Representative photomicrograph of βIII-tubulin+ DRGN neurite outgrowth in transfected with Lipofectamine-2000, siGFP, CME, FGF-2, siAMIGO3 and siAMIGO3+CME+FGF-2. **(B)** Quantification of the mean DRGN neurite length and (**C**) mean the number of surviving DRGN **(D)** mean the proportion of DRGN with neurites. . **P<0.001, Analysis of Variance, scale bar = 50µm. (n=3)

3.3.3 *In vivo*-JetPEI delivered plasmids into primary culture DRGN knocked down AMIGO3 mRNA and increased NT3 secretion in media

Adult primary DRGN cultured used to test the efficacy of shAMIGO3 plasmid to supress mRNA levels of AMIGO3 following transfection with *in vivo*-jetPEI vector. In untreated, sham and non-specific sh*gfp* 1µg control-treated DRGN, there were no change in mRNA for AMIGO3 suggesting that none of these treatments had any non-specific effects on AMIIGO3 mRNA (**Figure 3.5)**. Treatment with increasing amounts of shAMIGO3 plasmid caused a dose-dependent decrease in AMIIGO3 mRNA to a maximum observed with 2µg of plasmid DNA, correlating with 80% knockdown compared to untreated, sham or sh*gpf* controls (**Figure 3.5A)**. Increasing the amount of plasmid DNA above the optimal amount did not decrease AMIIGO3 mRNA level, suggesting that 2µg of plasmid DNA was optimal.

On the other hand, overexpression of NT3 in untreated, non-specific PEI-sh*gfp* 1µg and PEI-shAMIGO3/*gfp*-treated DRGN cultured was observed, little or no NT3 was detected by ELISA in culture supernatant. However, in culture media from DRGN treated with 2µg of PEI-shAMIGO3/*nt3* plasmid DNA the production and release of significant amounts of NT3 were detected, where 164 ± 24 ng/ml of NT3 was detected by ELISA. These results suggest that 2µg of plasmid DNA is optimal for AMIGO3 mRNA knockdown and NT3 production (**Figure 3.5B).**

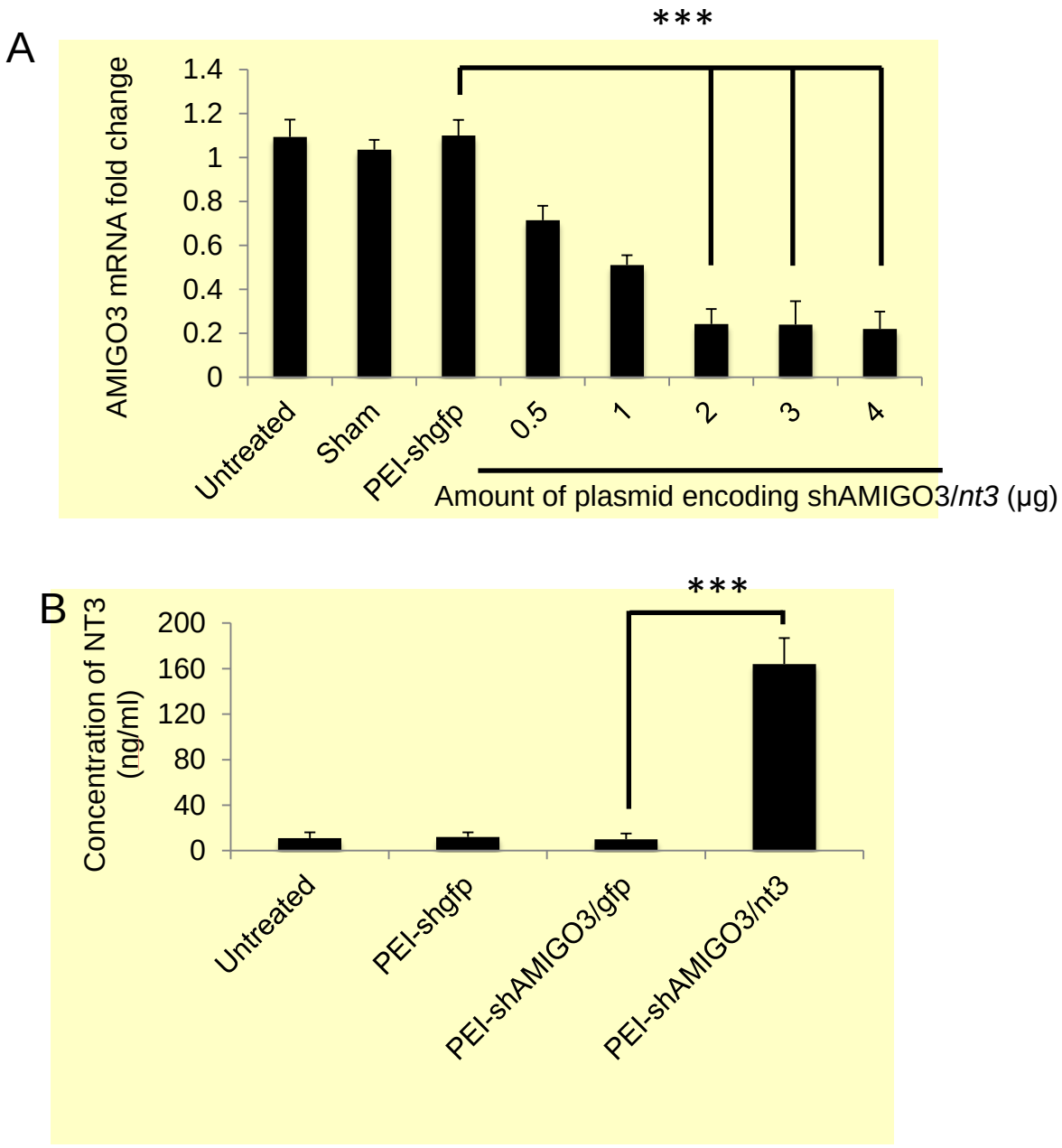

Figure 3.5: Knockdown of AMIGO3 and NT3 overexpression by *in vivo* jetPEI-delivered plasmid DNA.

(A) Increasing concentrations of plasmid DNA encoding shAMIGO3/*nt3* efficiently suppress AMIGO3 mRNA in cultured DRGN. **(B)** Plasmids encoding *nt3* induce the production of significant titre of NT3 in DRGN culture media. ***P<0.0001, Analysis of Variance. (n=3).

3.3.4 Knockdown of AMIGO3 and concomitant stimulation with NT3 promotes disinhibited DRGN neurite outgrowth

In PEI-sh*gfp*- or PEI-shAMIGO3/*gfp*-treated DRGN cultures, little or no disinhibited DRGN neurite outgrowth was observed (**Figure 3.6A-C)**. However, treatment of cultures with PEI-shAMIGO3/*nt3* caused significant disinhibited DRGN neurite outgrowth in terms of both neurite length, increasing significantly to 448 ± 31µm compared to PEI-shAMIGO3/*gfp*, and the proportion of DRGN with neurites, increasing significantly to 82 ± 8% compared to PEI-shAMIGO3/*gfp*; (**Figure 3.6A-C)**. These results suggest that delivery of shAMIGO3/*nt3* plasmids in primary DRGN culture by *in vivo*-jetPEI significantly enhances disinhibited DRGN neurite outgrowth.

3.3.5 *In vivo*-jetPEI/plasmids targeted large diameter DRGN

Sections of DRG from intact controls showed an absence of gfp^+ localisation in DRGN (**Figure 3.7A)** whilst DRG injected with DC+PEI-*gfp* containing plasmids showed number gfp^+ DRGN (**Figure 3.8A)**. Animals treated with the DC+PEI-*nt3/gfp* plasmid showed some gfp^+ DRGN (**Figure 3.9A)** whilst DRGN treated with DC+PEI-shAMIGO3*/gfp* showed wide spread of gfp^+ localisation in DRGN (**Figure 3.10A).** Intact control DRGN had no gfp^+ DRGNFigure 3.7B, whilst DRG injected with DC+PEI-*gfp* plasmids, approximately ≤2% of gfp^+ DRGN were classified as small, ≤3% as medium and ≤5% as large (**Figure 3.8B)**. In DRG injected with DC+PEI-*nt3/gfp* plasmid, gfp^+ DRGN were decreased. A small number of DRGN were transfected compared to medium (≤1%) and large diameter DRGN (≥3%) (**Figure 3.9B)**. Interestingly the transection rate was

significantly increased following DC+PEI-shAMIGO3-*nt3/gfp* injected plasmids such that ≤ 4% were small gfp^+ DRGN, ≤12% were medium and and ≤ 22% were large diameter DRGN (**Figure 3.10B)**. The total gfp^+ DRGN after DC+PEI-*gfp* plasmid injection was ≤4% compared to DC+PEI-*nt3/gfp* plasmid where ≤2% DRGN were transfected. Interestingly the total number of gfp^+ DRGN in the DC+PEI-shAMIGO3*/gfp* group was significantly higher (≤12%) demonstrating the highest proportion of transfection compared to other groups.

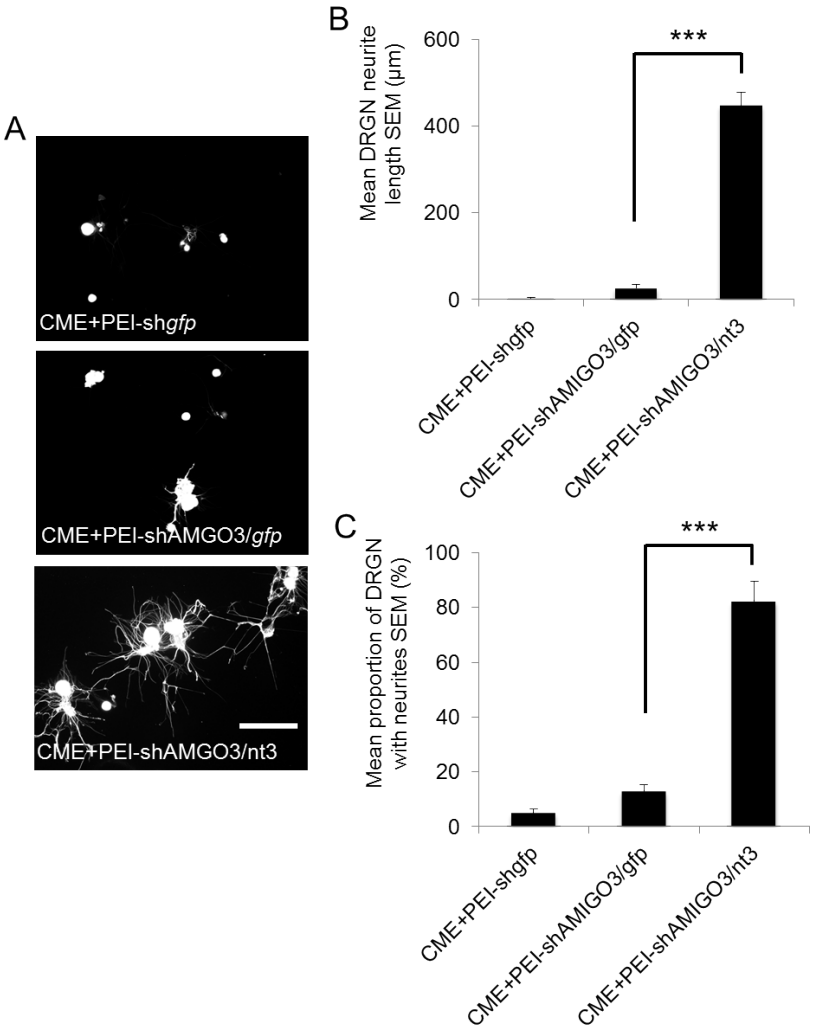

Figure 3.6: Knockdown of AMIGO3 and overexpression of NT3 by *in vivo* jetPEI-delivered plasmid DNA disinhibited DRGN neurite outgrowth.

(A) Representative images to show in presence of CME, plasmid DNA encoding *gfp* or shAMIGO3/*gfp* were unable to disinhibit DRGN neurite outgrowth, but plasmids encoding shAMIGO3 and NT3 promote disinhibited DRGN neurite outgrowth. **(B)** Quantification of the mean DRGN neurite length and **(C)** the proportion of DRGN with neurites showing that AMIGO3 suppression combined with *nt3* overexpression promotes significant disinhibited DRGN neurite outgrowth. Scale bar = 50µm. (n=3).

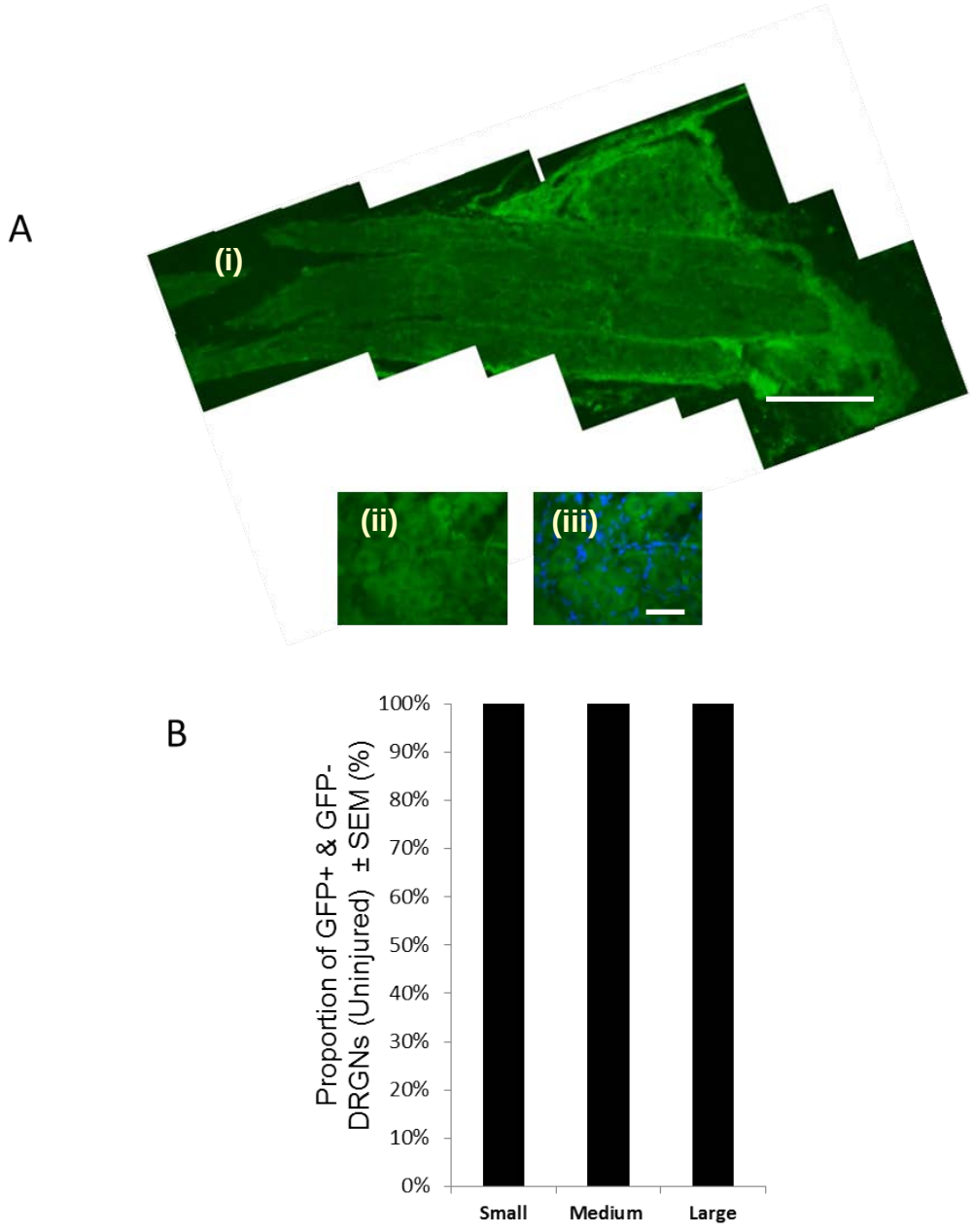

Figure 3.7: GFP expression in DRGN section of intact control (IC) group.

(A(i), (ii), (iii)) DRGN section represent GFP^+ DRGN and **(B)** the proportion of GFP^+ and size distribution; small (0-29µm), medium (30-59µm) and large (> 60µm) diameter DRGN (green bar); % total GFP^+/GFP^- small, medium and large DRGN (black bar). Scale bar in **(i)**=500µm, in **(ii)** and (**iii)**=50µm. (n=6).

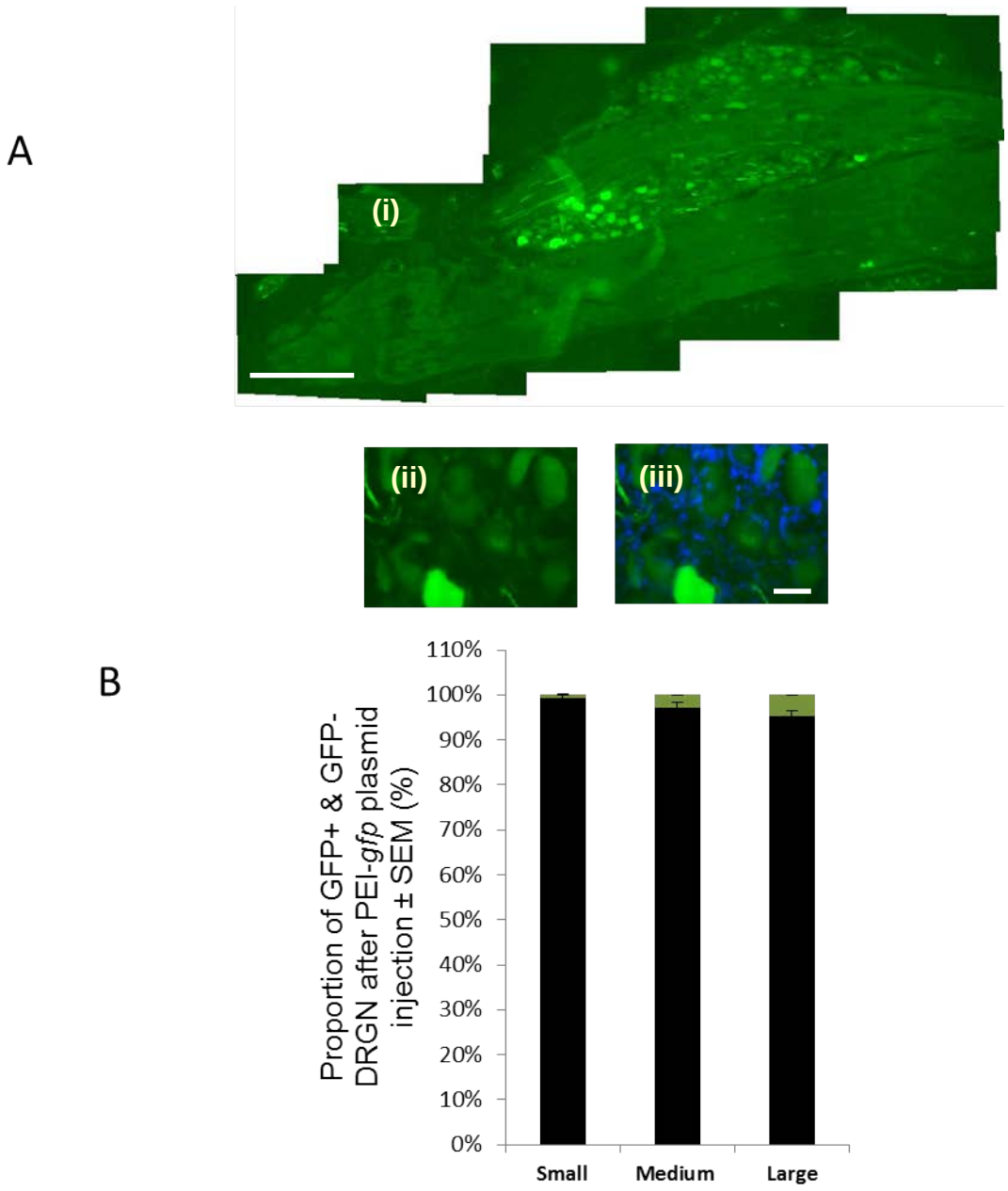

Figure 3.8: GFP expression in DRGN section of DC+PEI/gfp group.

(A(i), (ii), (iii)) DRGN section represent GFP^+ DRGN and **(B)** the proportion of GFP^+ and size distribution; small (0-29µm), medium (30-59µm) and large (> 60µm) diameter DRGN (green bar); % total GFP^+/GFP^- small, medium and large DRGN (black bar). Scale bar in **(i)**=500µm, in **(ii)** and (**iii)**=50µm. (n=6).

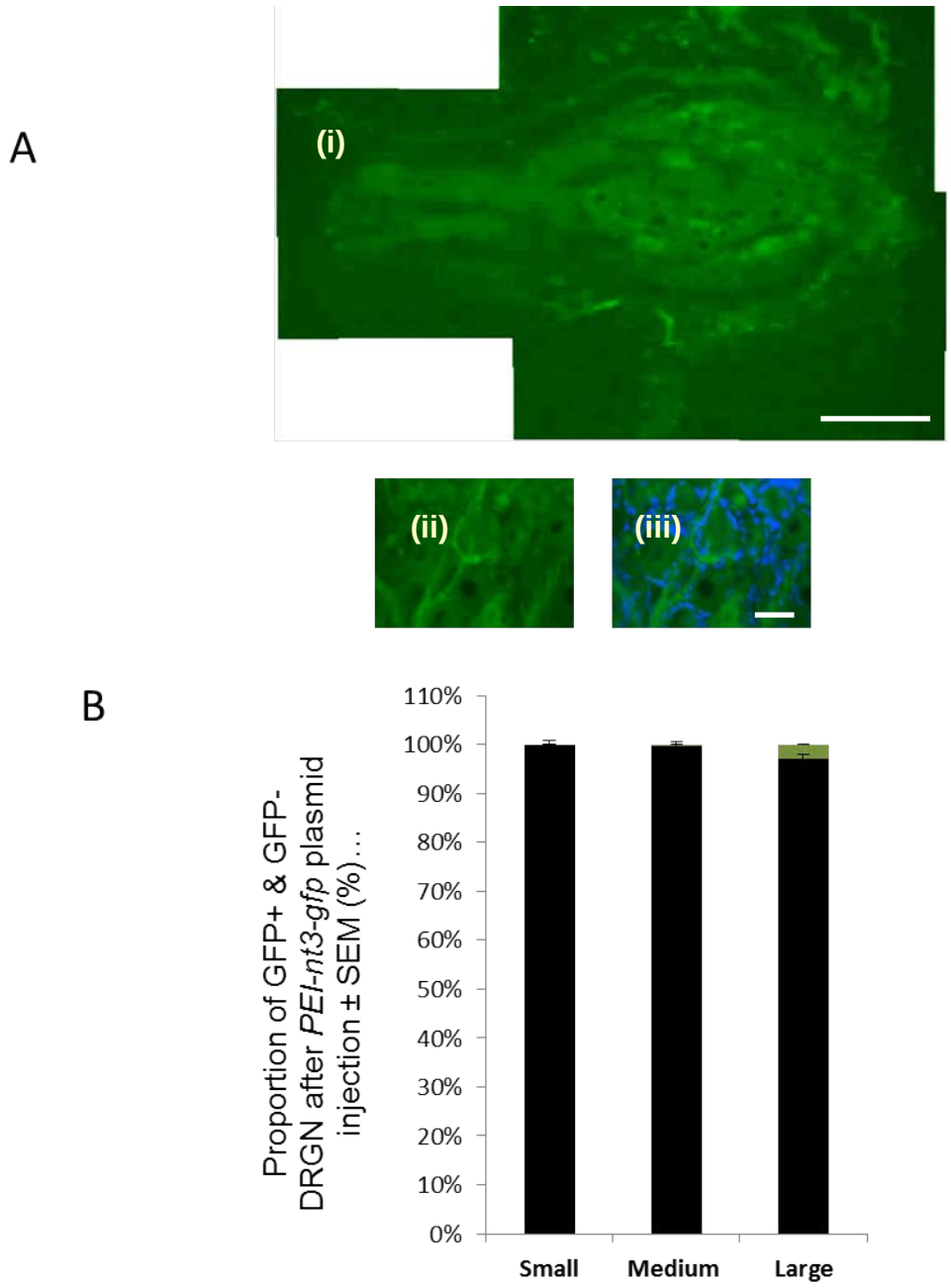

Figure 3.9: GFP expression in DRGN section of DC+PEI-nt3-*gfp* group.

(A(i), (ii), (iii)) DRGN section represent GFP^+ DRGN and **(B)** the proportion of GFP^+ and size distribution; small (0-29µm), medium (30-59µm) and large (> 60µm) diameter DRGN (green bar); % total GFP^+/GFP^- small, medium and large DRGN (black bar). Scale bar in **(i)**=500µm, in **(ii)** and (**iii)**=50µm. (n=6).

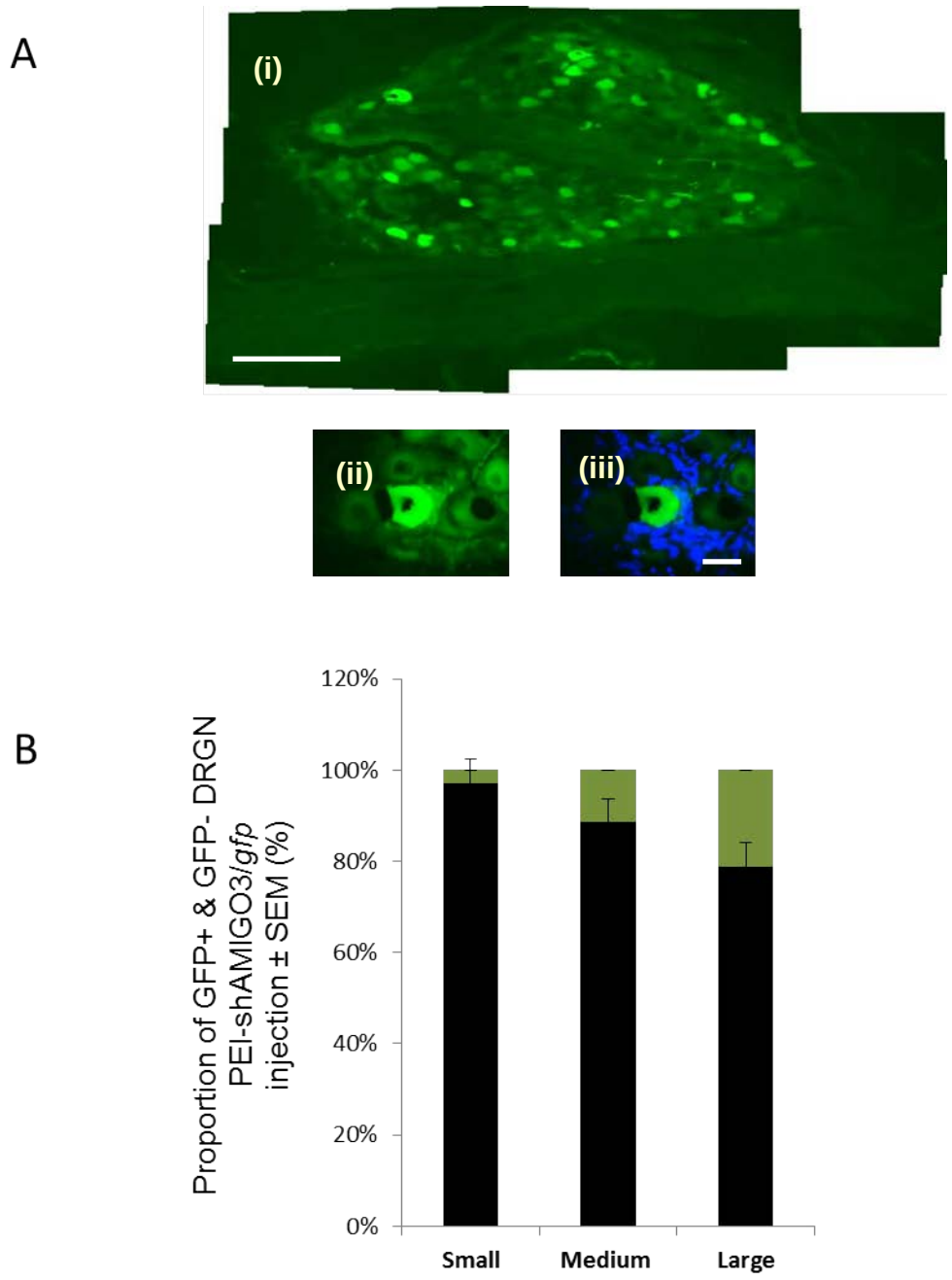

Figure 3.10: GFP expression in DRGN section of DC+PEI-shAMIGO3/*gfp* group.

(A(i), (ii), (iii)) DRGN section represent GFP^+ DRGN and **(B)** the proportion of GFP^+ and size distribution; small (0-29µm), medium (30-59µm) and large (> 60µm) diameter DRGN (green bar); % total GFP^+/GFP^- small, medium and large DRGN (black bar). Scale bar in **(i)**=500µm, in **(ii)** and (**iii)**=50µm. (n=6).

3.3.6 *In vivo*-jetPEI/shAMIGO3 down regulated AMIGO3 in DRGN

By using semi-quantitative RTPCR the levels of AMIGO3 mRNA increased significantly after injury and by 7.54 ± 0.33 and 7.42 ± 0.33-fold in both DCC and DC+PEI-*gfp*-treated DRG compared to those observed in intact controls (**Figure 3.11A)**. However, AMIGO3 mRNA levels were suppressed by nearly 11-fold in DRG treated with PEI-shAMIGO3/*nt3* compared to DC+PEI-sh*gfp*; (**Figure 3.11A)**. Immunohistochemistry detected high levels of AMIGO3 in DCC and DC+PEI-*gfp*-treated DRG in all DRGN, however in the DC-PEI-*gfp* group **(Figure 3.11B(iv)-(vi))** almost 30% of GFP^+/$AMIGO3^+$ DRGN were observed in DRG although the remaining $AMIGO3^+$ DRGN were GFP^-. In the DC+PEI-shAMIGO3/*gfp* group, similar numbers of DRGN as in the DC+PEI-*gfp* group were GFP^+ but little or no $AMIGO3^+$ DRGN were observed **(Figure 3.11B(i)-(iii) and (iv)-(vi))**,.

These results demonstrate that: (1), *in vivo*-jetPEI delivered plasmids encoding shAMIGO3 efficiently knocked down AMIGO3 protein in DRGN and that: (2), knockdown of AMIGO3 occurs in both transfected and un-transfected DRGN.

.

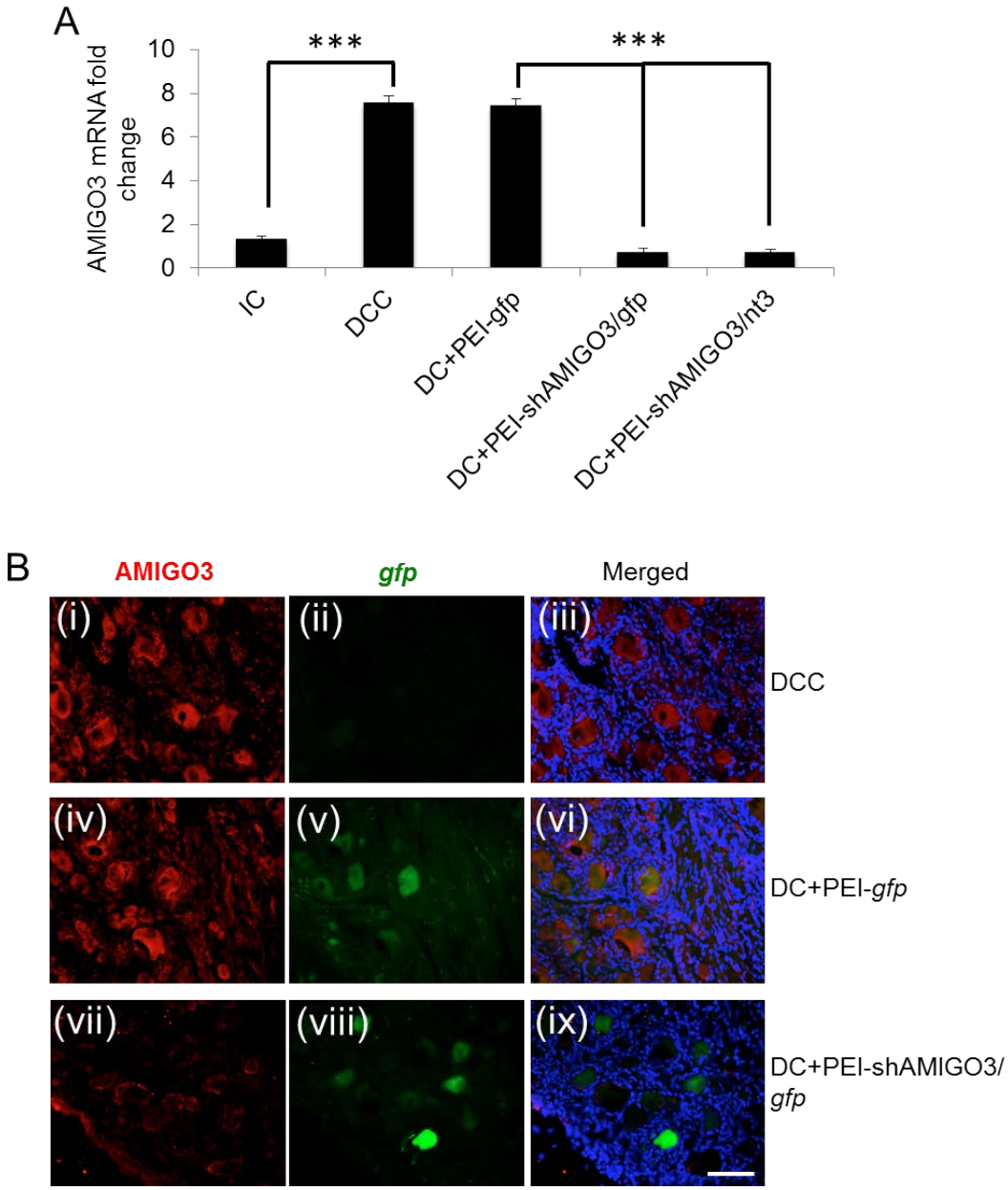

Figure 3.11: AMIGO3 levels are suppressed in DRGN after injection of *in vivo-jet*PEI transduced plasmids encoding shAMIGO3.

(A) Low levels of AMIGO3 mRNA in intact controls increased significantly after DCC injury and remained unaffected in DC+PEI-*gfp*. AMIGO3 mRNA levels reduced significantly in both DC+PEI/shAMIGO3/*gfp* and DC+PEI-shAMIGO3/*nt3* groups. **(B)** Immunohistochemistry for AMIGO3 showed high levels of AMIGO3 in DRGN after DCC (**B(i)**), which were *gfp*$^{-}$ (**B(ii)**). AMIGO3 levels remained high in

DC+PEI-*gfp* groups (**B(iv)**), with *gfp* expression in some DRGN (**B(v)**). AMIGO3 levels were suppressed in DRGN from DC+PEI-shAMIGO3/*gfp* groups (**B(vii)**), with *gfp* expression in some DRGN (**B(viii)**). B(iii), B(vi) and B(ix) are merged images from the red and green channels. Scale bar = 500μm. *** = P<0.0001, Analysis of Variance. (n=3).

.

3.3.7 NT3 levels in DRGN after *in vivo*-jetPEI-shAMIGO3/nt3 transfection

The levels of NT3 mRNA remained low and unchanged in intact control, DCC and DC+PEI-*gfp*-treated DRG. However, in DRGN treated with DC+PEI-shAMIGO3/*nt3*, *nt3* mRNA levels increased significantly and by 33 ± 1.35-fold, compared to DC+PEI-*gfp*-treated DRGN (**Figure 3.12A)**. Little or no NT3 immunoreactivity was present in DRGN in DCC and DC+PEI-*gfp* groups **(Figure 3.12B(i)-(iii)** and (iv)-(vi), respectively). However, in the DC+PEI-*nt3*/*gfp* groups, high levels of NT3 immunoreactivity were observed in both GFP^+ and GFP^- DRGN **(Figure 3.12B(vii)-(ix))**.

These results demonstrate that: (1), *in vivo-j*etPEI successfully transfected DRGN with plasmids encoding NT3 resulting in NT3 protein expression and that; (2), NT3 immunoreactivity was present in both transfected and un-transfected DRGN

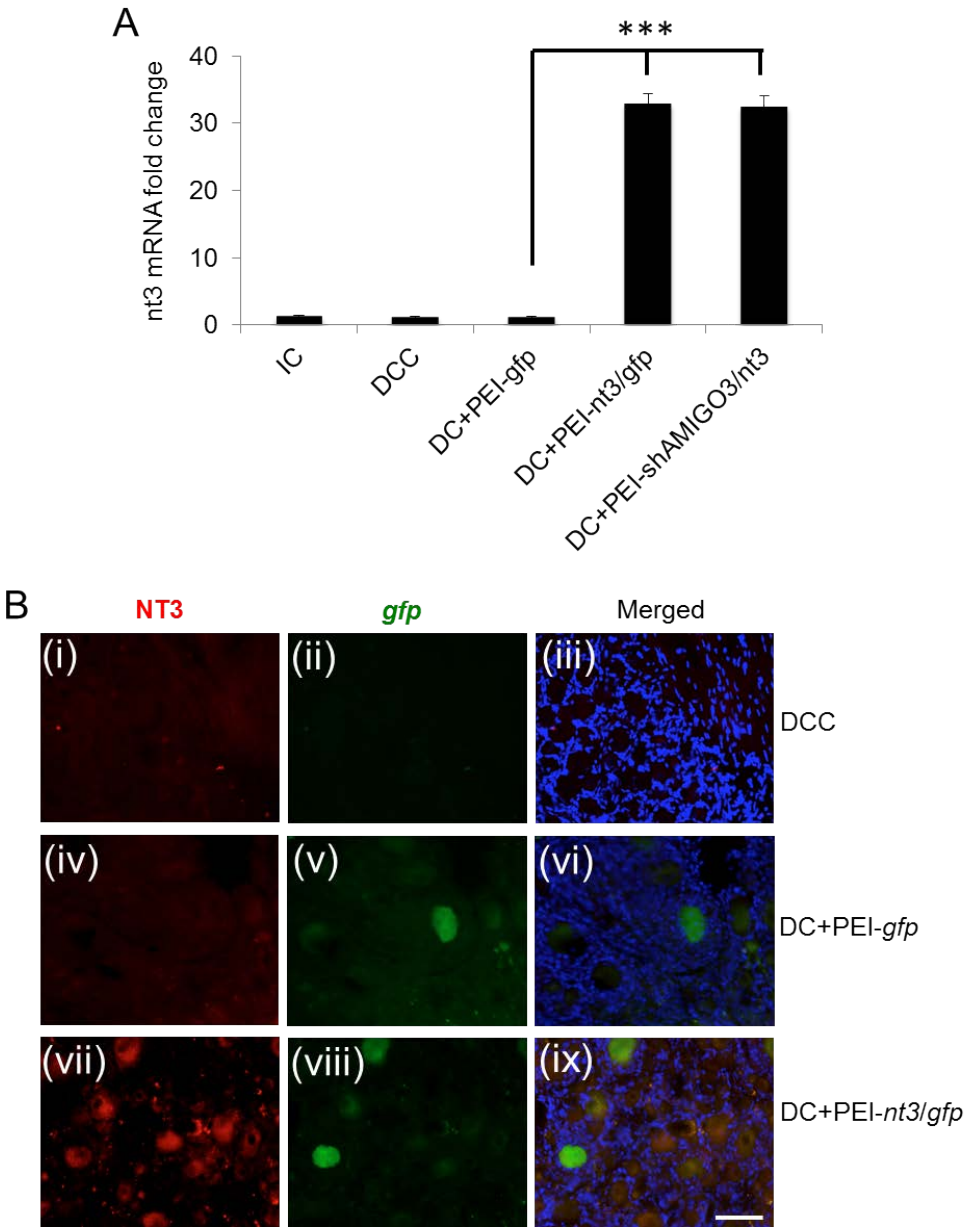

Figure 3.12: NT3 levels are overexpressed in DRGN after injection of *in vivo-jet*PEI transduced plasmids encoding shAMIGO3.

(A) Low levels of NT3 mRNA were detected in DCC and DC+PEI-*gfp* groups, whilst significantly higher levels were detected in DC+PEI-nt3/*gfp* and DC+PEI-shAMIGO3/*nt3* groups. **(B)** Immunohistochemistry for NT3 showed low levels of NT3 in DRGN after DCC (**B(i)**), which were *gfp*$^{-}$ (**B(ii)**) and in DC+PEI-gfp groups (**B(iv)**), with *gfp* expression in some DRGN (**B(v)**). NT3 levels (**B(vii)**) were high in

both gfp$^+$ and gfp$^-$ DRGN (**B(viii)**). Scale bar = 500μm. *** = P<0.0001, Analysis of Variance. (n=3).

3.3.8 PEI-shAMIGO3/nt3 transfected DRGN regenerate axons in the DC

After DC injury, a large cavity was present at the lesion site in the cords of DC+PEI-shAMIGO3/*gfp* groups, with little or no immunoreactivity for regenerating GAP43$^+$ axons (**Figure 3.13A)**. By contrast, in the injured cords of the DC+PEI-shAMIGO3/*nt3* groups, no cavities developed and many regenerating GAP43$^+$ axons were seen in the caudal segment and some traversed the lesion site, growing for long distances into the rostral segment of the spinal cord (**Figure 3.13B)**.

Many axons could be seen traversing through the lesion site, following an arduous path and exiting the lesion site in the distal cord (**Figure 3.13C)**; high power magnification). Quantification of the number of GAP43$^+$ DC axons regenerating through the lesion site shows that 24.5 ± 4.2, 18.0 ± 2.1, 12.7 ± 3.3 and 9.3 ± 3.1% of axons regenerated 0, 2, 4 and 6mm beyond the lesion site, respectively, in DC+PEI-shAMIGO3/*nt3* whilst no axons were present in DC+PEI-shAMIGO3/*gfp* (**Figure 3.14)**. These results demonstrate that PEI-shAMIGO3/*nt3* plasmids promote significant DC axon regeneration after DC injury.

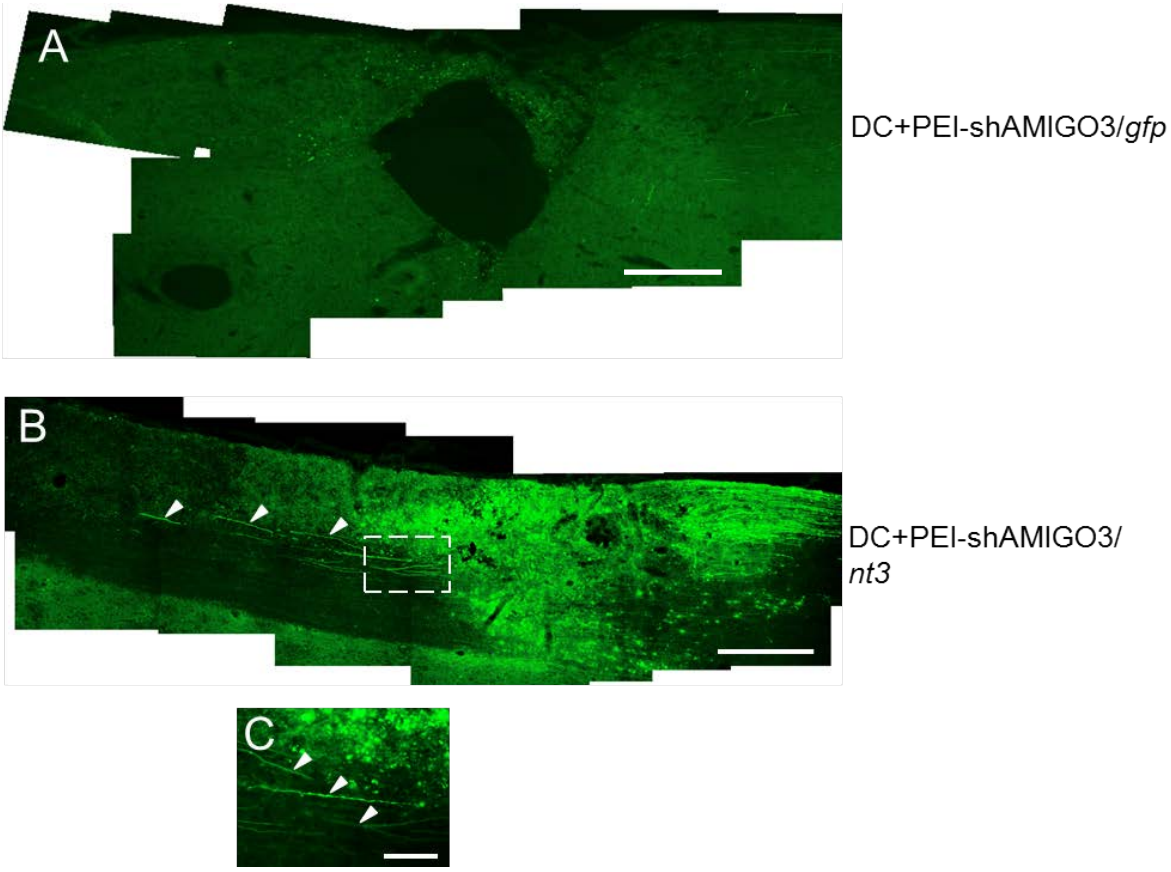

Figure 3.13: Suppression of AMIGO3 in DRGN promotes DC axon regeneration.

(A) There were no GAP43^{+} regenerating axons in the DC of the PEI+shAMIGO3/*gfp* group with a large cavity present at the lesion site. **(B),** However, knockdown of AMIGO3 and co-incident up-regulation of NT3 in the DC+shAMIGO3/*nt3* group promoted GAP43^{+} DRGN axon (arrowheads) regeneration through the DC lesion site (**B** and **C** (high power view of axons emanating from the lesion site)), with the absence of a cavity in the lesion site. Scale bar in A and B=500μm; in C = 50μm. (n=6)

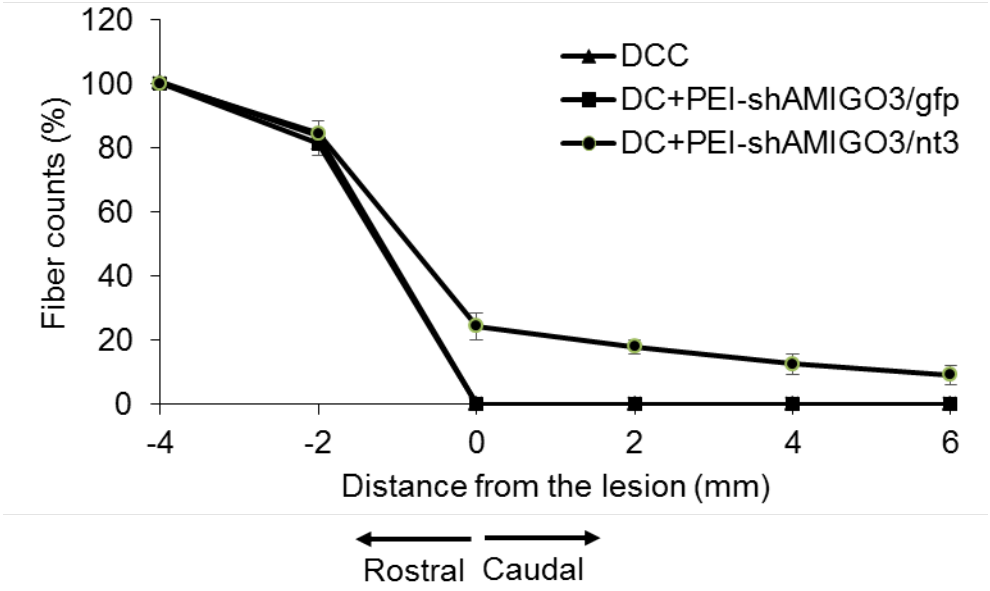

Figure 3.14: Quantification of GAP43^{+} axon fibre counts.

The quantification was done at various distance from the lesion site showed a significant proportion of axons present at 2, 4 and 6mm caudal to the lesion site. (n=6).

3.4 Discussion

Viral vectors are commonly used to transfect CNS cells with shRNA to inhibit target mRNA translation (Davidson and Breakefield, 2003, Raoul et al., 2006, Reynolds et al., 2004). One drawback of viral vectors, such as adeno-associated virus (AAV), is limited multiple gene transfection engendered by a restricted insert capacity and shRNA delivery delays suppression of translation of targeted mRNA by 14-28d, retarding the therapeutic effect and reducing their translational potential (Miyagoe-Suzuki and Takeda, 2010, Mason et al., 2010, McCarty et al., 2001). Another significant barrier to their use *in vivo* is that transgene expression requires 7-14 days to reach a maximum and hence are limited in acute conditions.

Non-viral gene delivery vectors include cationic lipid agents and a more recently formulated non-lipid polymer, polyethylenimine (*in vivo*-jetPEI) which transfects cells both *in vitro* and *in vivo* (Wiseman et al., 2003, Boussif et al., 1995). *In vivo* jetPEI has high transfection efficiency and results in up to 4X higher transfection rates than naked DNA (Wiseman et al., 2003). Moreover, jetPEI is easy to prepare, stable, and safe, and jetPEI/shRNA transfection induces faster suppression of mRNA translation than viral vectors giving immediate therapeutic benefit (Lungwitz et al., 2005). In the CNS, Liao and Yau reported that Melanopsin expression is rapidly abolished in RGC after intravitreal injection of *in vivo*-jetPEI-shMelanopsin (Liao and Yau, 2007).

In this study, AMIGO3 levels were elevated in non-regenerating (DC) compare to intact and regenerating (SN and pSN+DC) injury models by immunohistochemistry, also AMIGO3 was localised in DRGN cultured and used siRNA specific to AMIGO3 in presence of CME and stimulated by FGF-2 to promotes neurite outgrowth, these findings were repeated from results published in (Ahmed et al., 2013).

In addition, the use of a non-viral vector to deliver several genes to DRGN was investigated and showed that large diameter DRGN were preferentially transduced and that an shRNA knocked down AMIGO3 levels and at the same time up-regulated NT3 in DRGN, inducing DC axon regeneration. *in vivo*-jetPEI delivered shAMIGO3/*nt3* plasmid DNA: (1), efficiently knocks down AMIGO3 while at the same time increases *nt3* mRNA, both *in vitro* and *in vivo*; (2), transduces a significant proportion of large diameter DRGN; (3) ehances disnhibited DRGN neurite outgrowth and axon regeneration..

3.4.1 *In vitro* findings

In this report, the efficiency of *in vivo*-jetPEI-delivered plasmids has been tested to suppress AMIGO3 and at the same time upregulate NT3 in DRGN cultures. It has been recognised by us and others that a combinatorial strategy will be required to promote optimal CNS axon regeneration due to the complexity of the injury. For example, we have shown that suppression of axon growth inhibitory molecules combined with neurotrophic factor stimulation promotes significant disinhibited

DRGN neurite outgrowth in the presence of CME (Ahmed et al., 2005, Ahmed et al., 2006, Ahmed et al., 2009, Ahmed et al., 2011b). Here that 2µg of plasmid DNA encoding shAMIGO3 was sufficient to significantly knock down AMIGO3, to similar levels that we observed with siAMIGO3 (Ahmed et al., 2013). The same amount of DNA was also able to promote overexpression of NT3 in DRGN such that DRGN produced significant titres of NT3 in culture.

Similar to our previous observations with siAMIGO3, knockdown of AMIGO3 using an shAMIGO3 alone however, was insufficient in overcoming CME-mediated neurite inhibition, requiring simultaneous stimulation with NT3 to promote DRGN neurite outgrowth. Our results confirm that disinhibition alone in insufficient to promote DRGN neurite outgrowth in the presence of CME but that concomitant stimulation of growth is required.

3.4.2 *In vivo* findings

In vivo-jetPEI is increasingly being used as safer alternative to viral vectors that pose safety question, including induction of immune responses and virus-associated pathogenicity (Nayak and Herzog, 2010, Mingozzi and High, 2013, Daya and Berns, 2008). *In vivo*-jetPEI is a cationic polymer and has a high cationic charge density potential allowing it to condense DNA to form stable complexes, promoting gene transfer into cells (Demeneix et al., 1998, Wightman et al., 2001). *In vivo*-jetPEI has been used to deliver a variety of genes including siRNA to tissues such as (Acosta et al., 2014, Bivas-Benita et al., 2013, Ellermeier et al., 2013, Wahlquist et al., 2014, Zuckermann et al., 2015). Additionally, *in vivo*-

jetPEI is also being tested in human applications, including the treatment of cancer and for genetic vaccination treatments (Lisziewicz et al., 2001, Ziller et al., 2004). On the other hand, short hairpin RNA (shRNA) has been used in this study to supress AMIGO3 and it is know that foreign RNA induced endogenous immune response such as interferon and PKR. For example, lentiviral encoding shLINGO-1 was used to enhance CNS axon regeneration but however the vector increase neurons death even at low transfection doses (Hutson et al., 2012, Hutson et al., 2014). Here the endogenous immune response include interferon have not determined due to lack of time but however, it has been suggested that in vivo jetPEI vector does not induced inflammatory cytokines (Bonnet et al., 2008)

Several studies have referred to the analysis of DRGN sizes as small, medium and large due to the high heterogeneity of DRGN in size distribution (Schmalbruch, 1987, Jacques et al., 2012b). The implication here is that our plasmids mainly targeted large diameter DRGN. Surprisingly, however, these results are entirely consistent with previously reported levels of viral vector-mediated transfection rates and DRGN diameters, where used AAV8 to deliver *gfp* (Jacques et al., 2012b). It is possible that, as was concluded for AAV8-mediated transfection of large diameter DRGN that the large surface area exposed to the plasmid resulted in a higher chance of these DRGN being transfected (Jacques et al., 2012b). In addition, it is also well established that the majority of the DRGN that project their axons in the ascending tract of the DC are the large diameter DRGN and hence high transfection rate by our plasmids is actually beneficial, since our DC injury transects these particular axons, and any beneficial effects of axon regeneration may be derived from these DRGN. Another possible advantage of targeting of the large diameter DRGN is that growth of small diameter DRGN in

response to, for example NGF, has been linked to nociception and hence this may be avoided by this preferential targeting of our plasmids (Lewin et al., 1993, Eskander et al., 2015). Having said this, all DRGN may be affected by preferential transfection of large diameter DRGN through the local production of NT3 and paracrine effects on neighbouring DRGN.

Not only did the *in vivo*-jetPEI-delivered shAMIGO3 suppress AMIGO3 levels by greater than 80% in DRGN, immunoreactivity for AMIGO3 were reduced in both *gfp*$^{+}$ (both low and high *gfp* expressing DRGN) and gfp^{-} DRGN. This suggests that the plasmid efficiently suppressed AMIGO3 levels in both transduced and non-transduced DRGN. At present it is difficult to explain why non-transduced DRGN showed reduced AMIGO3 levels but to our knowledge this is the first report to show such an effect. It may suggest that suppression of AMIGO3 in DRGN has paracrine effects on neighbouring DRGN, representing an intriguing observation that suggest that not all DRGN in the DRG need to be targeted to promote therapeutically effective outcomes. Similarly, overexpression of NT3 was also apparent in both *gfp*$^{+}$ and *gfp*$^{-}$ DRGN suggesting that both transfected and non-transfected DRGN produced high titres of NT3. Our results therefore demonstrate that *in vivo*-jetPEI efficiently knocked down AMIGO3 and up-regulated NT-3 in DRGN.

Knockdown of AMIGO3 and simultaneous stimulation with NT3 promoted significant DRGN axon regeneration after DC injury. This is the first demonstration that knockdown of AMIGO3 promotes DRGN axon regeneration *in vivo* and demonstrates that AMIGO3 is an additional molecule that might require targeting

to promote CNS axon regeneration. We previously showed that AMIGO3 could substitute for LINGO-1 in binding to $p75^{NTR}$ and NgR1 to induce RhoA activation in response to CME. Our current results are consistent with these findings. Axons regenerated for up to 6mm caudal to the lesion site but unfortunately behavioural analysis could not be performed since the T8 DCC model does not lead to measurable functional deficits, including mechanical and thermal hyperplasia (Kanagal and Muir, 2008, Surey et al., 2014).

As it's been observed previously in DRGN cultures grown in the presence of CNS myelin extracts, that knockdown of AMIGO3 promoted signifcant DRGN neurite outgrowth, our current study demonstrates *in vivo* proof-of-principal. Namely, that knockdown of AMIGO3 together with co-incident growth stimulation (here by NT-3) promotes signficant DC axon regeneration. In addition, spinal cord cavitation was reduced as a result of AMIGO3 knockdown and NT-3 overexpression and instead the lesion site was filled with invading cells. However we do not know why this happen but suggesting a further therapeutic use of AMIGO3/NT-3 in spinal cord injury.

CHAPTER 4: Inflammatory-induced responses after non-viral mediated suppression of AMIGO3

4.1 Introduction

4.1.1 Inflammation

Inflammation is one of the human body's natural responses against injury, infection and is involved in pathogeneses of neurodegenerative disease, stroke and cancer among others. Inflammation aims to initiate the healing response and restore the damaged tissues back to normal through removal of harmful stimuli. The acute phase inflammation requires rapid influx of blood granulocytes, typically neutrophils, followed promptly by monocytes that mature into inflammatory macrophages.

The acute phase of inflammation results in signs such as heat, pain, swelling and redness, symptoms typically associated with inflammation and surrounding the injury /infection area (Ricciotti and FitzGerald, 2011, Surey, 2015). After removing the harmful stimuli by phagocytosis, the inflammation process starts to resolve which allows lymphocytes and macrophages to return to normal phenotypes and pre-inflammatory numbers.

The rapid resolution of tissue damage results from a successful acute inflammation, but dysfunction and persistent inflammation leads to scarring and loss of organ function and therefore leads to chronic inflammation (Nathan, 2002). Long lasting chronic inflammation can cause not only autoimmune diseases e.g. rheumatoid arthritis but also could lead to cancer (Surey, 2015).

4.1.2 Inflammation markers

The inflammatory mediators after SCI can be localised using inflammatory markers including CD68, GFAP, CD4 and CD8. Cluster of differentiation 68 (CD68) also named ED-1 was identified originally as a marker for macrophages, which can be used to mark the recruitment and activation after infection/injury, especially after inflammation of neurodegenerative disease (Perego et al., 2011, Holness and Simmons, 1993). CD68 is also expressed in active endothelial cells and human fibroblasts (Kunz-Schughart et al., 2002, Beranek, 2005) and can be used as a marker of active phagocytosis after infection/injury (Perego et al., 2011).

GFAP is expressed in different glial cell sub-types in the CNS including astrocytes and ependymal cells. GFAP is an intermediate filament protein and generally high levels of GFAP represent activation of glial cells and astrocytes in neurodegenerative disease (Roessmann et al., 1980, Jacque et al., 1978, Brahmachari et al., 2006). A study investigated neuropathic pain, observed that GFAP was expressed mainly by astrocytes in dorsal horn of the rat spinal cord following SC injury models (Silva et al., 2015). GFAP also expressed DRGN satellite cells following injection of relevant doses of Paclitaxel (known to induce neuropathic pain) for ten days (Peters et al., 2007).

Between 1-3 days after SCI, there are fewer macrophages/monocytes found where a significant number of $CD68^{+}$ microglia are present in the injury site and these last in the cord from weeks to months. The accumulation of activated macrophages and microglia is thought to be implicated in the progression of secondary injury after SCI (Fleming et al., 2006, Blight, 1992, Blight et al., 1995).

Cluster of differentiation 4 and 8 (CD4 and CD8) are used as markers of T cells after injury. Both CD4 and CD8 are transmembrane glycoprotein where CD4 is known as a marker for T 'helper' cells that activate B cells, whereas CD8 are T 'cytotoxic' cells and kill other target cells (Okoye and Wilson, 2011, Alberts et al., 2002). T-cell infiltration in rats was elevated between 3-7 days after SCI but then dropped by 50% after 3 weeks (Surey, 2015).

4.1.3 Hypothesis

In vivo-jetPEI is increasingly being used *in vitro*/*vivo* studies and used as a safer alternative to viral vectors in terms of the non-specific immune responses that some viruses elicit. This leads to hypothesis that *in vivo* suppression of AMIGO3 in DRGN using *in vivo*-jetPEI vector seen in Chapter 3 will not induce an overt inflammatory response.

4.1.4 Aims

- To assess inflammatory responses in glia, macrophages and T cells in L4/5 DRGN after intra-DRG injection with PEI-shAMIGO3-*nt3/gfp* seen in Chapter 3 using immunohistochemistry.
- To compare the inflammatory response with intact animals and those injected with PBS using immunohistochemistry.

4.2 Results

4.2.1 Characterisation of the inflammatory response after suppression of AMIGO3

Macrophages (CD68): Intact animals showed infiltration of $CD68^+$ macrophages in DRGN sections (**Figure 4.1A)** whereas animals receiving PBS through intra-DRG route, higher numbers of $CD68^+$ macrophages could be seen compared to intact animals (**Figure 4.3B)**. A slight increase in $CD68^+$ immunoreactivity was observed in DRG sections of the animals injected with DC+PEI-gfp, DC+PEI-nt3/gfp and DC+PEI-shAMIGO3/gfp plasmids *via* intra-DRG injection route compared to animals receiving PBS **(Figure 4.5A, Figure 4.7A and Figure 4.9A)**.

Glial fibrillary acidic protein (GFAP): The immunoreactivity of $GFAP^+$ glial cells was virtually absence in intact animals (**Figure 4.1B)** compared to animals that received PBS. In PBS injected animals $GFAP^+$ was slightly increased (**Figure 4.3B)**. Interestingly, $GFAP^+$ immunoreactivity was confined in DRGN sections of those that received PBS with no apparent differences between PBS and animals injected with DC+PEI-gfp, DC+PEI-nt3/gfp and DC+PEI-shAMIGO3/gfp plasmids (**Figure 4.5B, Figure 4.7B and Figure 4.9B)**.

Resident T-cells: $CD8^+$ a marker for T 'cytotoxic' cells were absent in DRGN sections of intact animals (**Figure 4.2A)** whilst, no significant increase was observed in CD8 immunoreactivity in animals receiving PBS after 29 days (**Figure 4.4A)**. Interestingly, CD8 immunoreactivity in DRGN sections of animals treated with DC+PEI-gfp, DC+PEI-nt3/gfp and DC+PEI-shAMIGO3/gfp plasmids

was identical to that of intact animals (**Figure 4.6A, Figure 4.8A and Figure 4.10A)**. These results suggested that *in vivo*-jetPEI did not induce T cell immunoreactivity in DRGN after intra-DRG injection over the time-course of the experiment.

Furthermore, $CD4^+$ resident T 'helper' cells showed a similar pattern as that observed with $CD8^+$ T 'cytotoxic' cells; no significant differences were observed in treated animals compared to intact (**Figure 4.2B)**, PBS (**Figure 4.4B)** or in animals injected with DC+PEI-gfp, DC+PEI-nt3/gfp and DC+PEI-shAMIGO3/gfp plasmids (**Figure 4.6B, Figure 4.8B and Figure 4.10B)**.

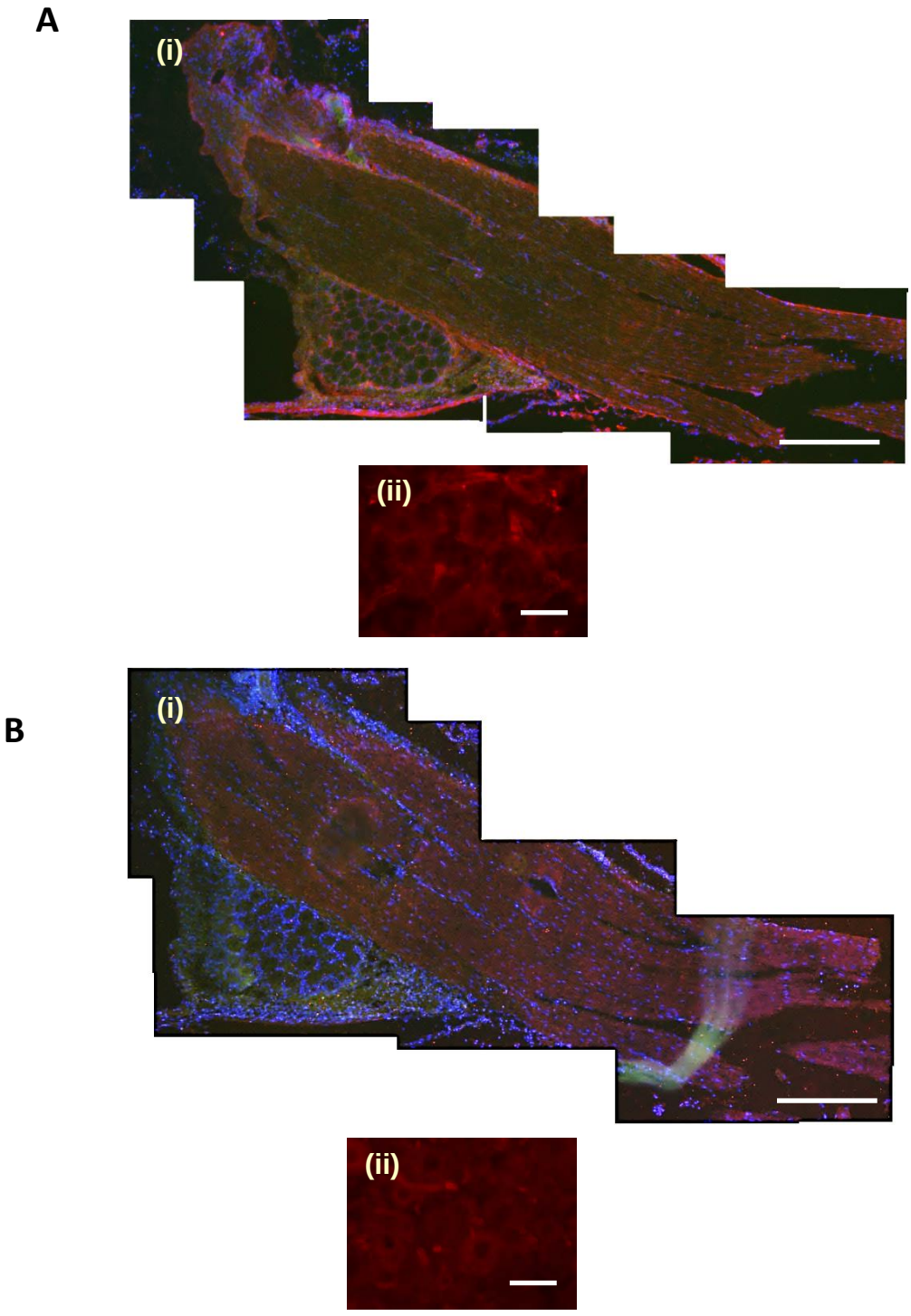

Figure 4.1. Localisation of CD68^{+} and GFAP^{+} inflammation responses in DRGN sections.

(A) Immunohistochemistry of CD68 macrophages (RED) for intact animals. **(B)** immunoreactivity of GFAP glial cells (RED) for intact animals. Scale bar in **(i)** =500μm and in **(ii)** =50μm. (n=6)

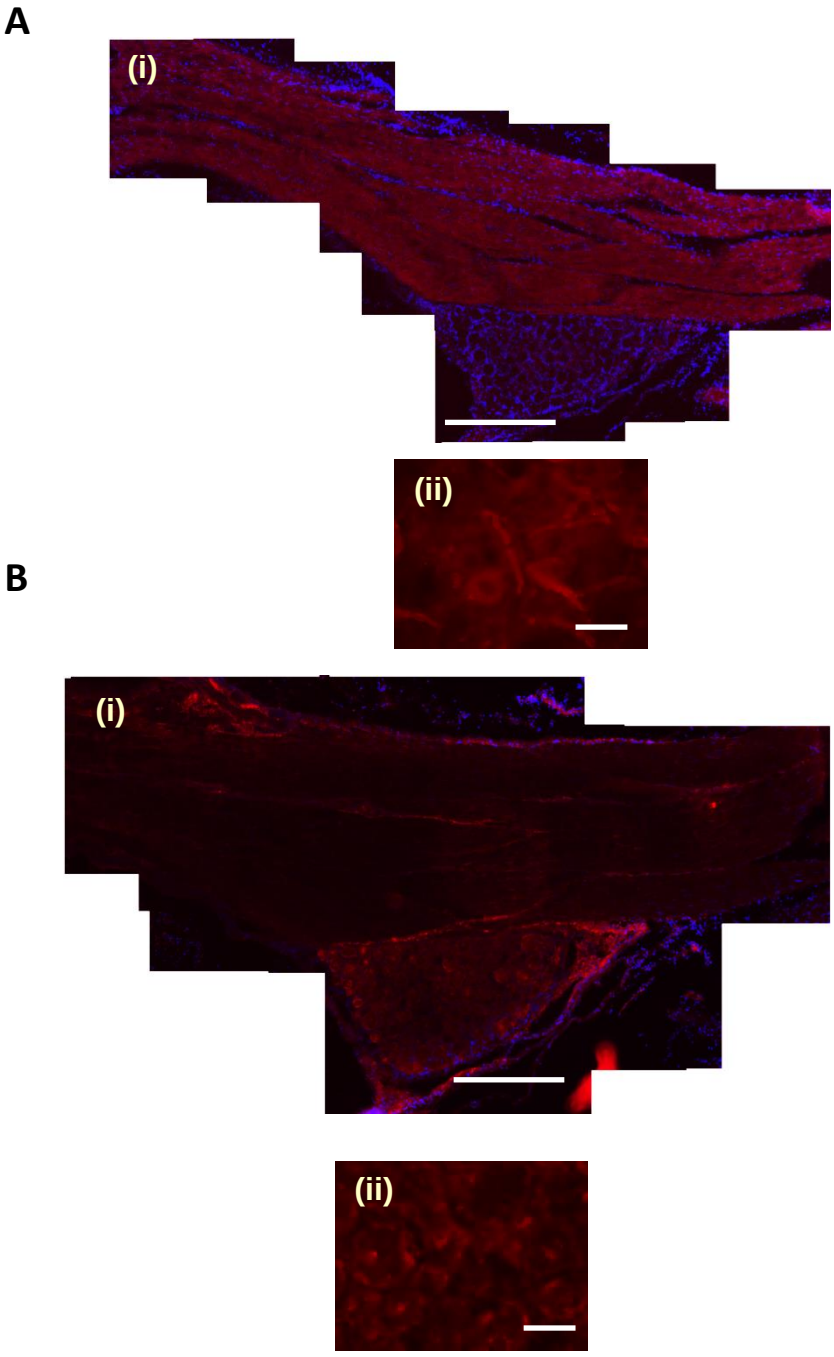

Figure 4.2: Localisation of $CD8^+$ and $CD4^+$ inflammation responses in DRGN sections.

(A) Immunohistochemistry of CD8 T cells 'cytotoxic' (RED) for intact animals. **(B)** immunoreactivity of CD4 T cells 'helper' (RED) for intact animals. Scale bar in (i)=500µm and in (ii)=50µm. (n=6)

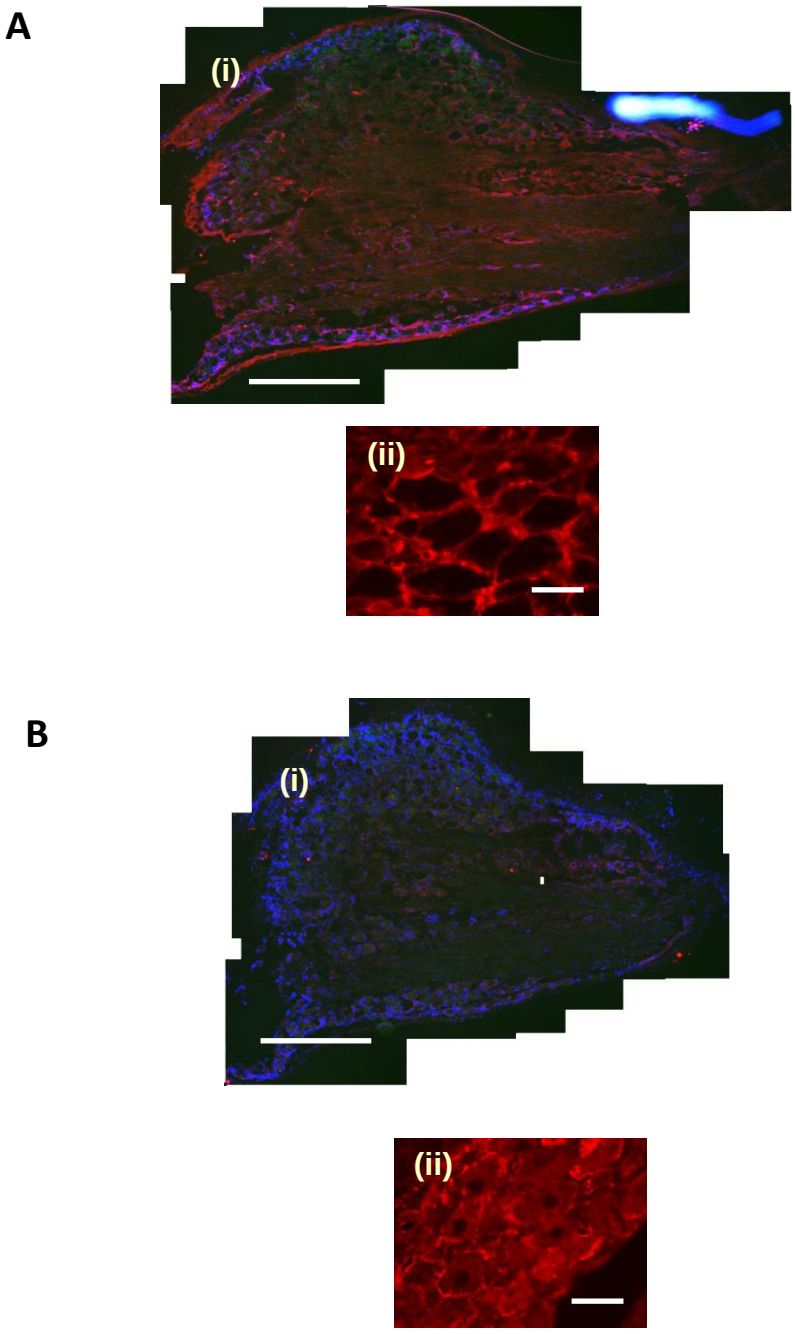

Figure 4.3: Localisation of CD68^{+} and GFAP^{+} inflammation responses in DRGN sections for animals received PBS for 29 days.

(A) Immunohistochemistry for CD68 macrophages (RED). **(B)** immunoreactivity of GFAP glial cells (RED). Scale bar in (i)=500μm and in (ii)=50μm. (n=6)

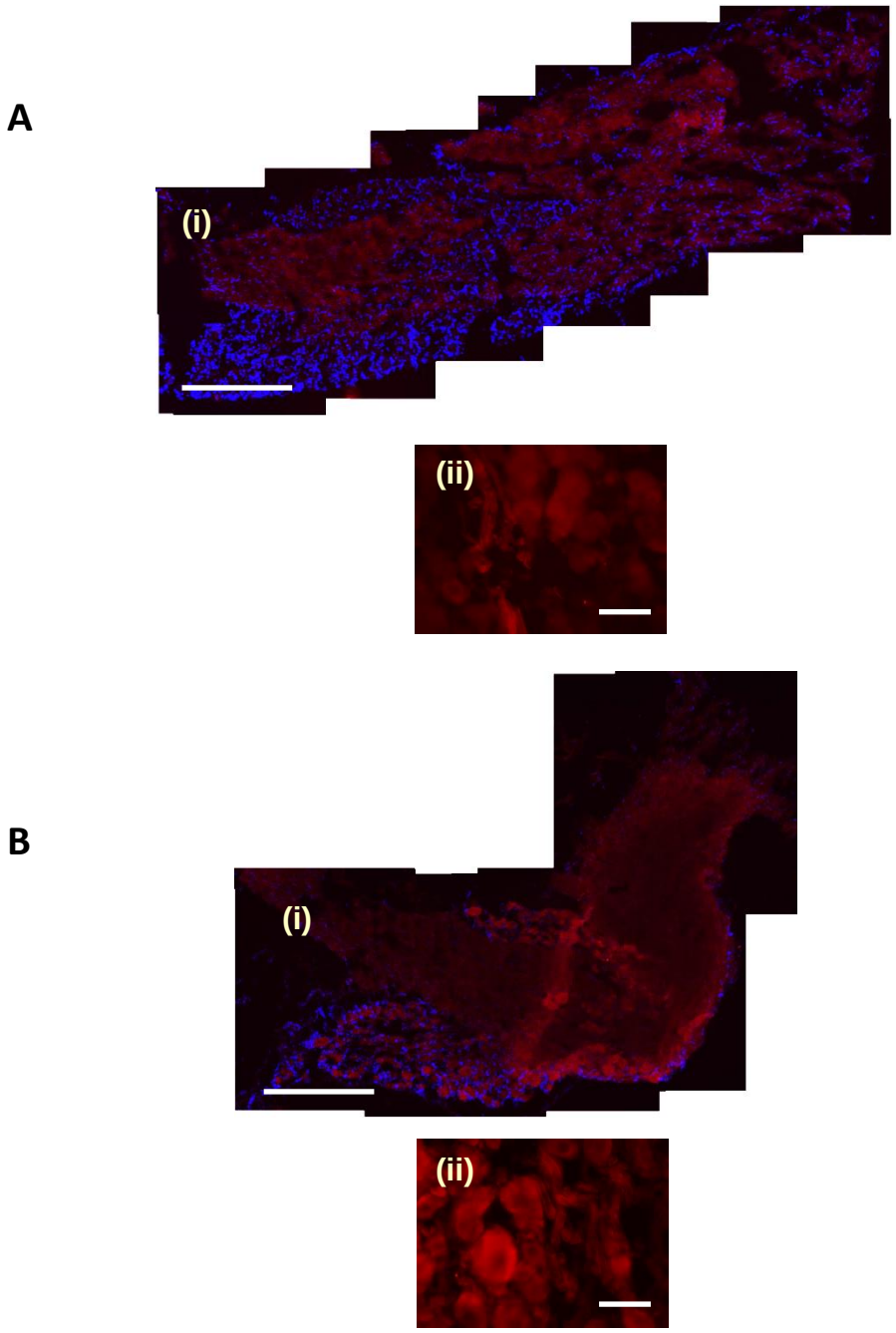

Figure 4.4: Localisation of $CD8^+$ and $CD4^+$ inflammation responses in DRGN sections for animals received PBS for 29 days.

(A) Immunohistochemistry of CD8 T cells 'cytotoxic' (RED). **(B)** immunoreactivity of CD4 T cells 'helper' (RED). Scale bar in (i)=500μm and in (ii)=50μm. (n=6)

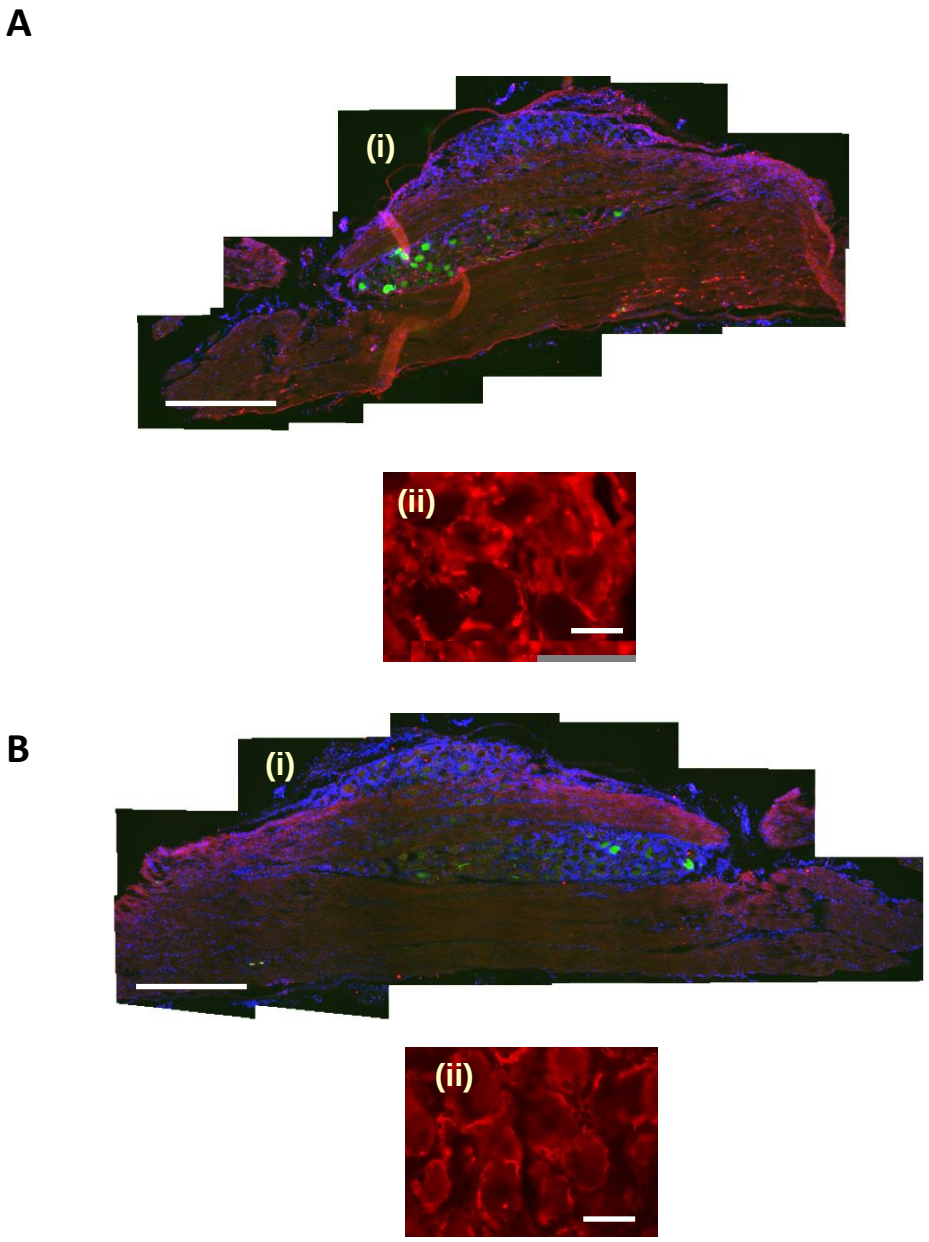

Figure 4.5: Localisation of CD68^{+} and GFAP^{+} inflammation responses in DRGN sections for animals injected with DC+PEI-gfp for 29 days.

(A) Immunohistochemistry for CD68 macrophages. **(B)** immunoreactivity of GFAP glial cells. Scale bar in (i) =500μm and in (ii) =50μm. (n=6)

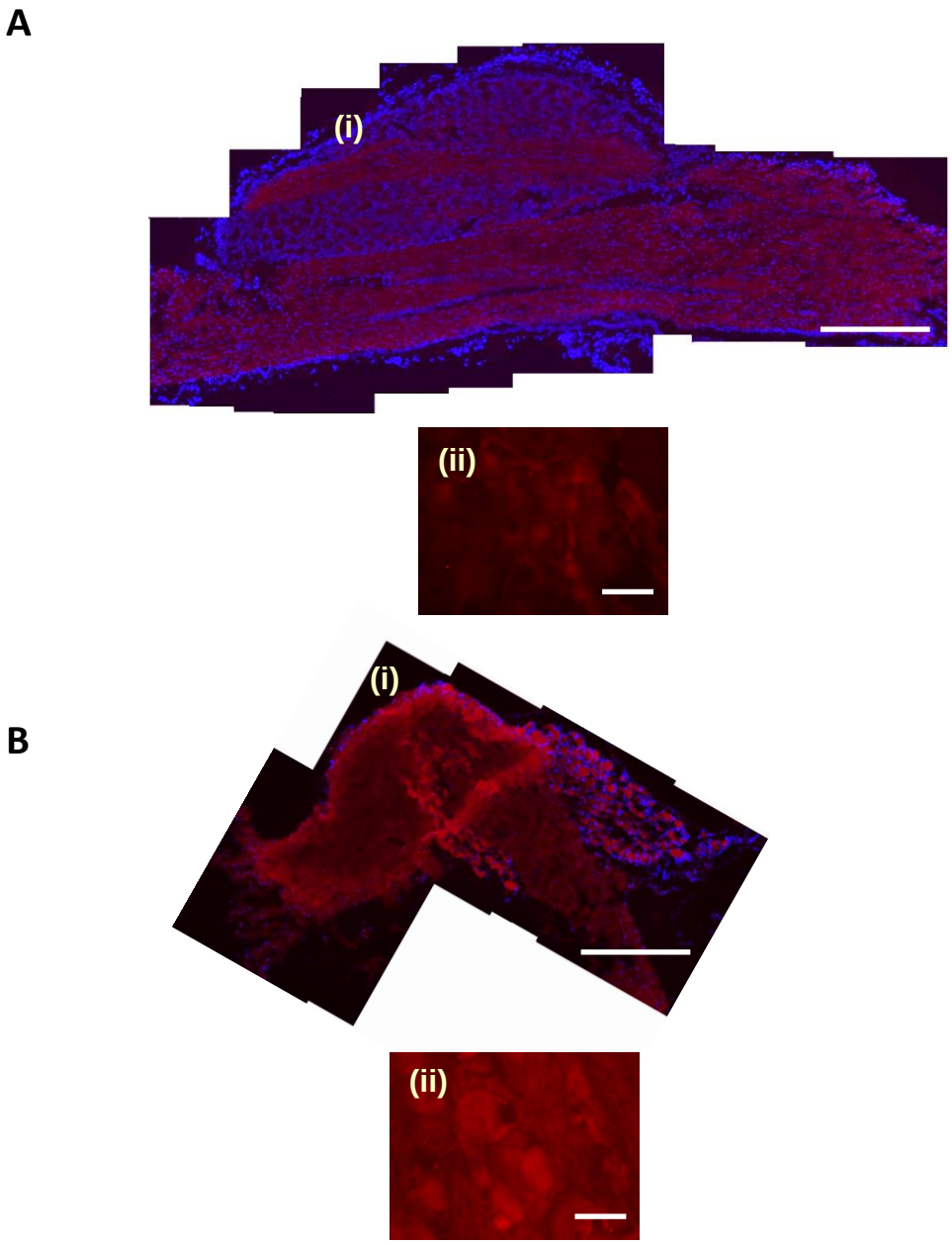

Figure 4.6 Localisation of $CD8^+$ and $CD4^+$ inflammation responses in DRGN sections for animals injected with DC+PEI-gfp for 29 days.

(A) Immunohistochemistry of CD8 T cells 'cytotoxic' (RED). **(B)** immunoreactivity of CD4 T cells 'helper' (RED). Scale bar in (i)=500μm and in (ii)=50μm. (n=6)

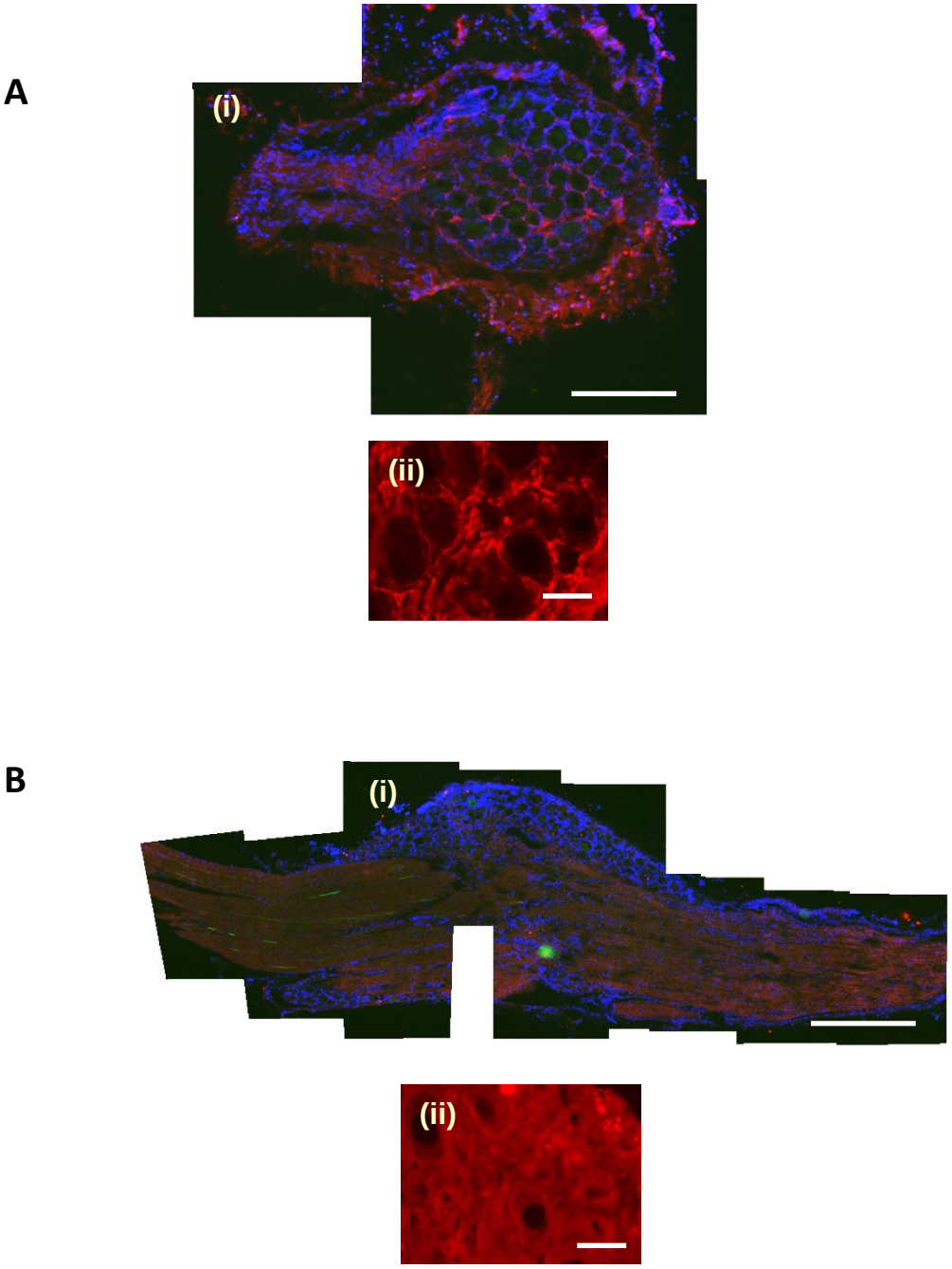

Figure 4.7 Localisation of CD68^{+} and GFAP^{+} inflammation responses in DRGN sections for animals injected with DC+PEI-nt3/gfp for 29 days.

(A) Immunohistochemistry for CD68 macrophages (RED). **(B)** immunoreactivity of GFAP glial cells (RED). Scale bar in **(i)** =500μm and in **(ii)** =50μm. (n=6)

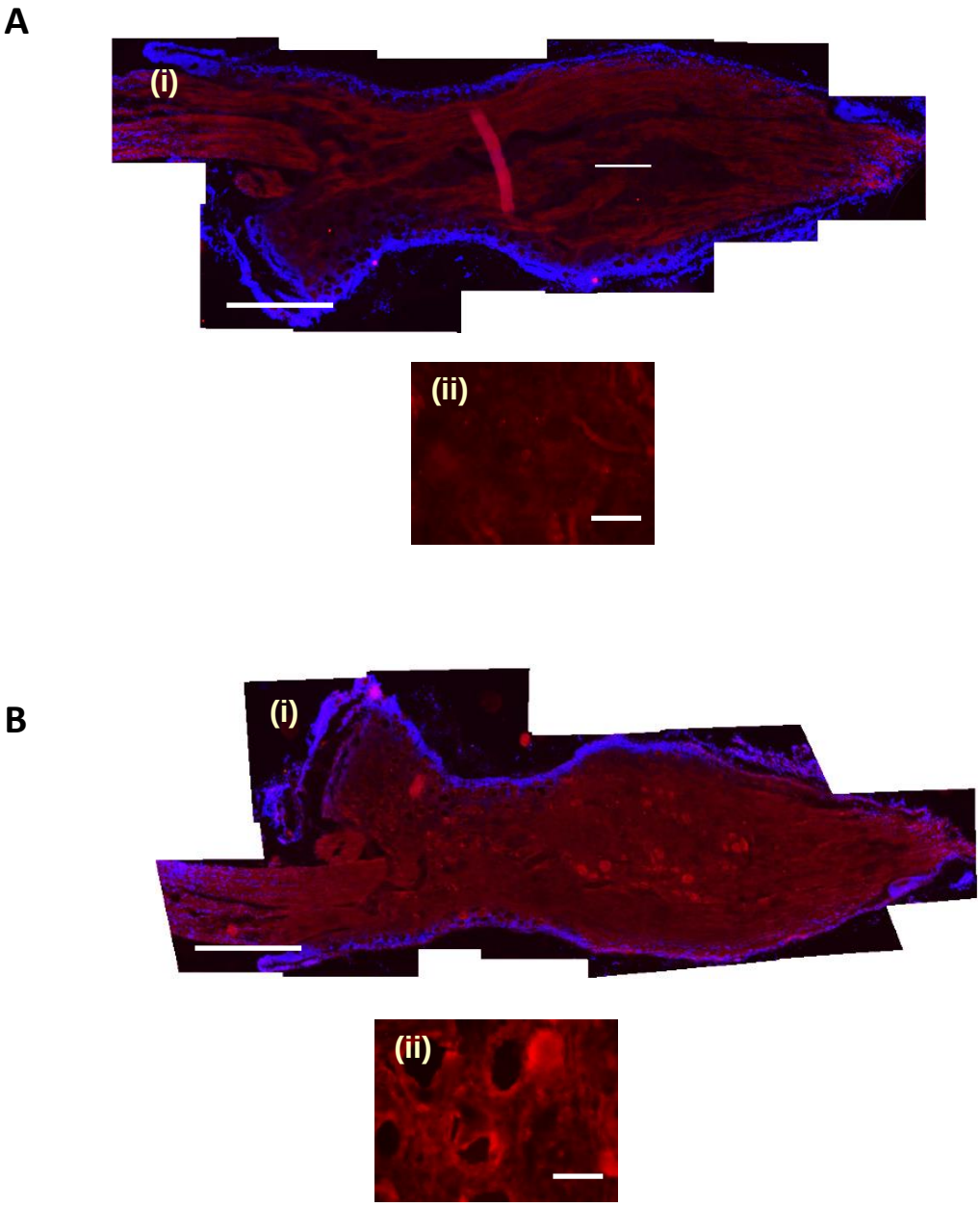

Figure 4.8: Localisation of $CD8^+$ and $CD4^+$ inflammation responses in DRGN sections for animals injected with DC+PEI-nt3/gfp for 29 days.

(A) Immunohistochemistry of CD8 T cells 'cytotoxic' (RED). **(B)** immunoreactivity of CD4 T cells 'helper' (RED). Scale bar in (i)=500μm and in (ii)=50μm. (n=6)

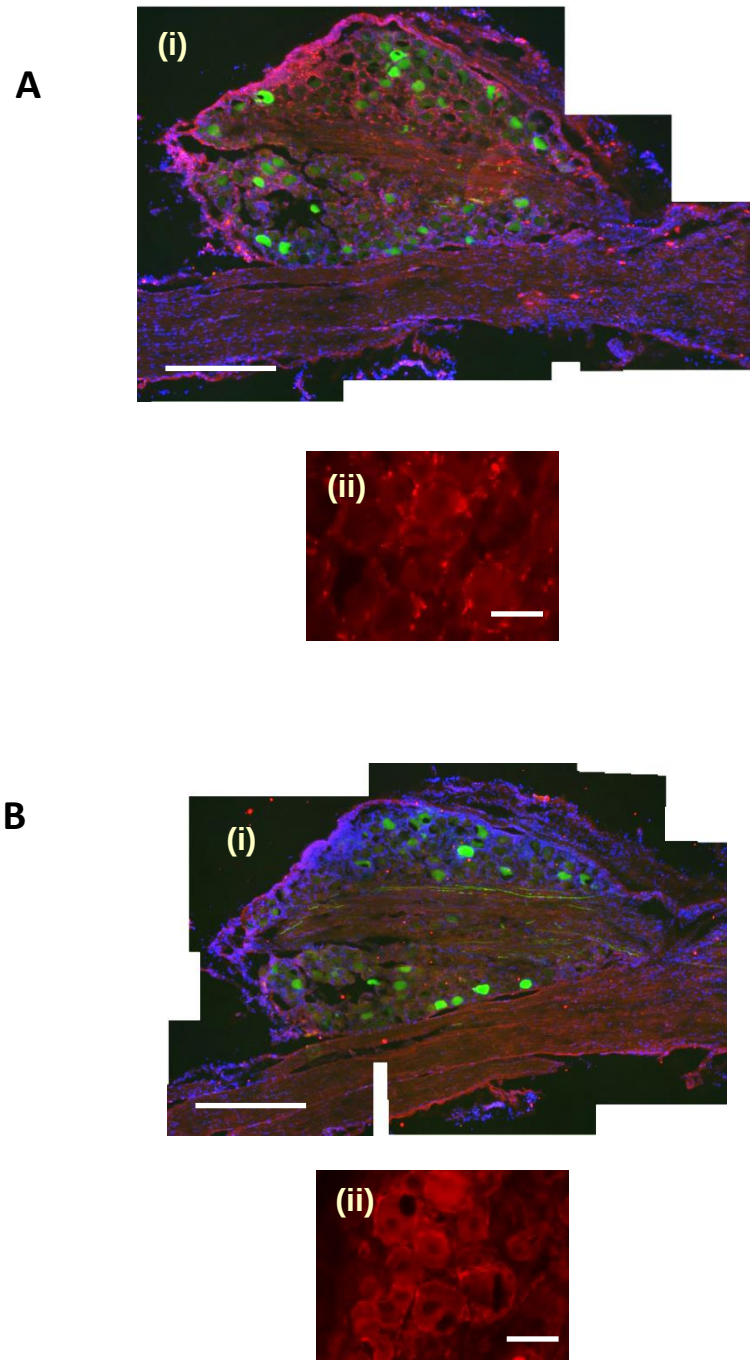

Figure 4.9: Localisation of CD68^{+} and GFAP^{+} inflammation responses in DRGN sections for animals injected with DC+PEI-shAMIGO3/gfp for 29 days.

(A) Immunohistochemistry for CD68 macrophages (RED). **(B)** immunoreactivity of GFAP glial cells (RED). Scale bar in **(i)** =500μm and in **(ii)** =50μm. (n=6)

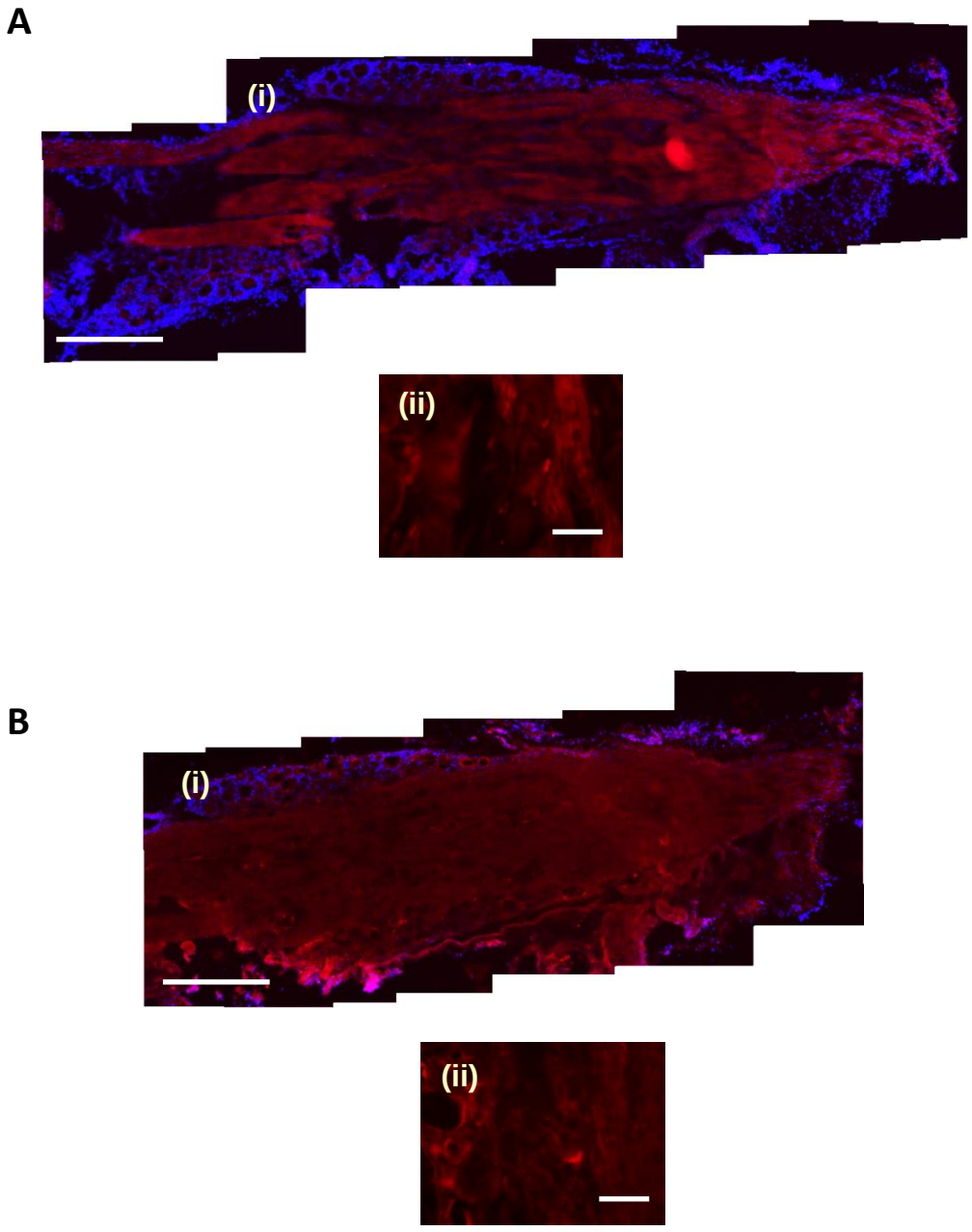

Figure 4.10 Localisation of $CD8^+$ and $CD4^+$ inflammation responses in DRGN sections for animals injected with DC+PEI-shAMIGO3/gfp for 29 days.

(A) Immunohistochemistry of CD8 T cells 'cytotoxic' (RED). **(B)** immunoreactivity of CD4 T cells 'helper' (RED). Scale bar in (i)=500μm and in (ii)=50μm. (n=6)

4.3 Discussion

In this report, I investigated the differences in the inflammatory response including glial cells, macrophages and T-cells in groups of animals after intra-DRG injection of several treatments including PBS, PEI-*gfp*, PEI-*nt3/gfp* and PEI-shAMIGO3-*nt3/gfp* which performed in chapter 3. Red colour staining was used to avoid gfp (green) expression which encode with the plasmids that been injected previously. Non-viral vector was used (*in vivo*-jetPEI) in this study to minimize immune responses after injection of plasmids, since *in vivo*-jetPEI is increasingly being used as safer alternative to viral vectors that pose safety questions, including induction of immune responses and virus-associated pathogenicity (Nayak and Herzog, 2010, Mingozzi and High, 2013, Daya and Berns, 2008). Moreover, PEI is safe and does not induce off-target immune-mediated cytokines such as TNF-α, IFN-γ, IL-6, IL-12/IL-23, IL-1β, and IFN-β (Bonnet et al., 2008). Therefore, the lack of immunogenic responses after PEI injection is to be expected and represents a further advantage over viral vectors. On the other hand, other delivery methods such as viral vectors such as (AAV) induce non-specific inflammatory responses. For example, AAV particles access the lymph nodes draining the DRG or the CSF, and lead to both local and systemic inflammatory responses (Kuhlmann et al., 2001, Weller et al., 2010).

In this study, I used anti-CD68 (ED1) antibody to detect macrophages in DRGN sections which is known to detect up to 98% of rat macrophages (Dijkstra et al., 1985). DRGN contain occasional $CD68^{+}$ macrophages (Hu and McLachlan, 2003, Hu et al., 2007a, Kim and Moalem-Taylor, 2011), which was evident in our studies (Figure **4.1**A). Macrophages are found in many tissues but the function of those

seen in intact DRG is to act as part of the initial, innate immune response to immediate infection or tissue damage. Furthermore, resident macrophages in DRG are implicated in phagocytosis of neuronal debris within the DRG (Hu and McLachlan, 2003).

Animals that received PBS showed slightly higher $CD68^+$ macrophages than that observed in intact animals, this increase of $CD68^+$ macrophages may due to direct trauma following intra-DRG injection with PBS. Since normally the insertion of glass micropipette directly to the DRG ganglia parenchyma, it is likely to result in some tissue disruption and hence may lead to $CD68^+$ macrophage activation. Interestingly, a slight increase of $CD68^+$ immunoreactivity could also be observed in DRG sections of animals injected with DC+PEI-gfp, DC+PEI-nt3/gfp and DC+PEI-shAMIGO3/gfp plasmids compared to animals which received PBS, probably as consequences of the use of *in vivo*-jetPEI vector. This suggests that *in vivo*-jetPEI may cause minimal activation of immune responses but these remains to be confirmed in further studies.

$GFAP^+$ immunoreactivity in glial cells was virtually absence in intact compared to animals receiving PBS, where $GFAP^+$ immunoreactivity was slightly increased. In addition, no apparent differences between PBS and animals injected with DC+PEI-gfp, DC+PEI-nt3/gfp and DC+PEI-shAMIGO3/gfp plasmids were observed, suggesting that the slight activation of glia could be due to the trauma to the DRG by the injection and not from the *in vivo*-jetPEI containing DNA.

Both cytotoxic and helper T cells were absent in DRGN injected with PBS and animals treated with DC+PEI-gfp, DC+PEI-nt3/gfp and DC+PEI-shAMIGO3/gfp plasmids. This was possibly due to the fact that samples were harvested at 29 days after SCI, whilst in a separate study by Surey et al. (2014) (Surey, 2014), T-cell infiltration after the same rat SCI was elevated between 3-7 days after injury and then dropped by 50% after 3 weeks (Surey, 2015).

In conclusion, the results of this chapter suggest that *in vivo*-jetPEI is safe to use as it invokes only little or no inflammatory responses after delivery of plasmid DNA. This is in contrast to viral vectors that may invoke a strong non-specific immune response.

CHAPTER 5: Overexpression of RTN3 enhances dorsal column axon regeneration after spinal cord injury

5.1 Introduction

5.1.1 A basic background of Reticulons (RTNs)

Reticulons (RTNs) are membrane-bound proteins of which four genes have been identified in mammals and termed RTN1, 2, 3 and 4/Nogo, they are called endoplasmic reticulum (ER) proteins because of their subcellular localisation where they exhibit a reticular distribution (Oertle and Schwab, 2003, Yang and Strittmatter, 2007, Senden et al., 1994). In addition, RTNs are also called neuroendocrine-specific proteins (NSP) when they were first discovered and found enriched in neuronal and neuroendocrine tissues (Roebroek et al., 1993, Hens et al., 1998). Moreover, RTNs are characterized by highly conserved reticulon homology domains (RHD), about 150-200 amino acid that are located in RTNs C-terminal which are involved in improvement of localization and function of these proteins.

RTNs are found in a variety of tissues for example, in brain, kidney, spleen and liver. Also, they play different roles such as (1) ER shaping and morphology, (2) membrane trafficking; for example, they were described to interact with Golgi and plasma membrane suggesting that they are involved in this site (3) apoptosis; as a number of evidences that overexpression of RTNs involved in ER-stress induced cell death by Ca^{2+} depletion from endoplasmic reticulum stores.

Moreover, RTNs are found to be involved in many neurodegenerative diseases such as Alzheimer's, amyotrophic lateral sclerosis and multiple sclerosis (Chiurchiu et al., 2014). However, RTN1, 2 and 4 have three splice isoforms A, B and C whilst RTN3 only has two spliced isoforms RTN3A and B **Figure 5.1**. The

human RTN1 is expressed in neurons and neuroendocrine tissues as well as in neuroblastoma cell lines where type C is the most studied and is considered being a neuronal differentiation marker (Roebroek et al., 1993, Hens et al., 1998, Chiurchiu et al., 2014).

RTN2 is found to be enriched in muscles and brain respectively, Liu et al indicates that RTN2B interact with excitatory amino acid transporter (EAAT1) which is important in learning and memory, where RTN2B has a positive regulation and enhances EAAT1 delivery from ER to cell surface (Liu et al., 2008). The fourth member of the family is known as Nogo and has been widely investigated in recent years because of it is involvement in CNS growth cone collapse after injury. RTN4/Nogo is expressed in oligodendrocytes and interacts with NgR1 receptor in neuronal membranes after spinal cord injury and inhibits axon regeneration and neurite outgrowth (Schwab, 2010, O'Neill et al., 2004).

In the pages below, I will focus on the third member of the RTN family as it is our gene of interest amongst others. However, due to lack of resources about our novel findings that up-regulation of RTN3 promotes axon regeneration after SCI, here we will indicate the other role of RTN3 to give a brief background about this gene. The background will indicate the most important findings about the role of RTN3 in neuronal tissues.

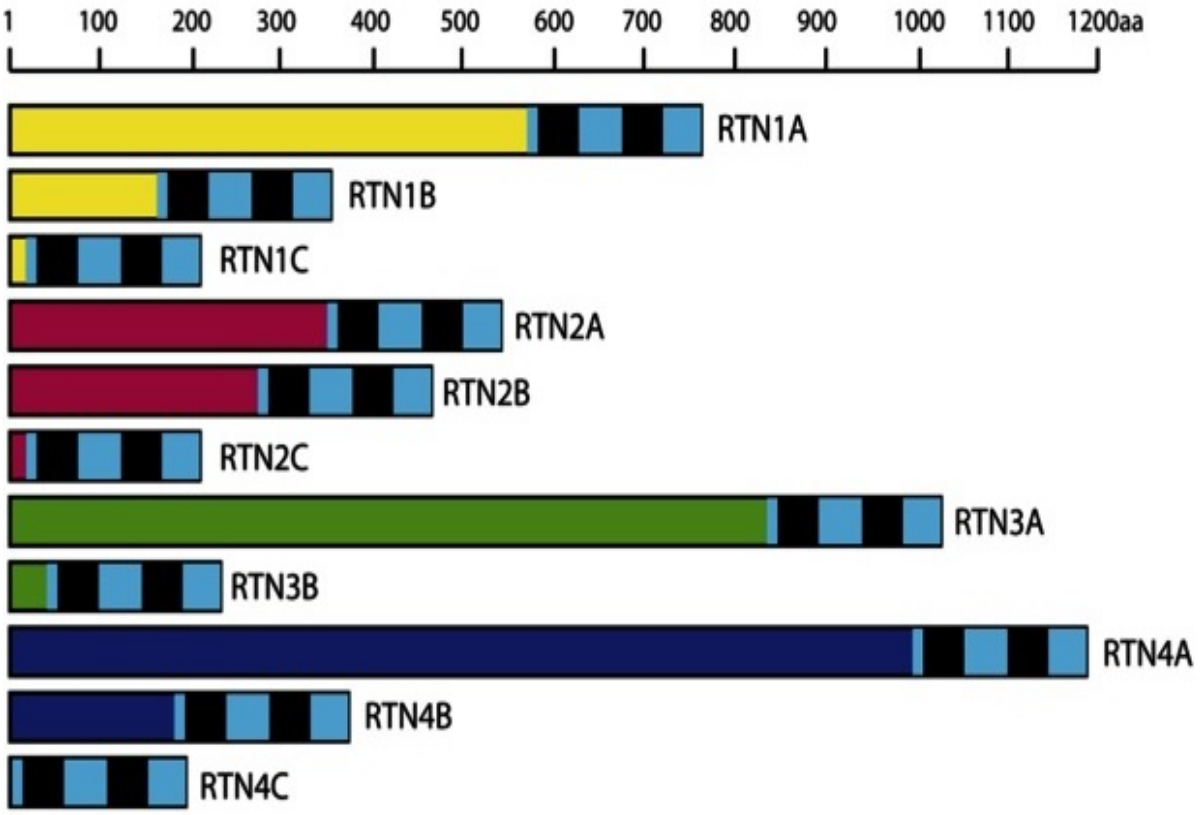

Figure 5.1: Schematic representation of mammalian reticulon family.

Topology and classification of splice isoforms of RTNs; the top scale bar is amino acid describe the length of each RTN. Light blue and black boxes represent reticulon homology proteins (RDH) that interact with C-terminal of RTNs (Adapted from (Chiurchiu et al., 2014)).

5.1.2 Reticulon 3 may play role in developing axons during embryo

RTN3 is expressed in many types of tissues but first isolated was from human retina and later shown to have the highest expression in the brain (Cai et al., 2005). The human RTN3 gene is localized in 11q13 and mutations of this gene cause dysfunction of the retina and is therefore speculated that this gene may play a role in retinal function (Kumamaru et al., 2004). Expression of RTN3 in the olfactory and optic nerve during development and adult stages was found to be important in axonal development. Kumamaru et al, (2004) showed that RTN3 is expressed highly in Muller cells in the rat retina and is also highly expressed in the optic nerve in embryo but less so in the adult. However, in the olfactory system RTN3 is found to be highly expressed in both embryo and adult stages and may therefore permit regeneration of these neurons since olfactory neurons are replaced regularly. Furthermore, RTN3 is also localised in cultured cortical neurons and concentrated in axon growth cones in the early days after culture (Kumamaru et al., 2004). RTN3 was also co-localized with synaptophysin in the developing axons of cultured cortical neurons (**Figure 5.2).** However, all these finding suggest that RTN3 may have some function in glial cells and formation of synapses as it is co-localized with synaptophysin. Moreover, RTN3 may play important role in the developing axon by the transportation of proteins and lipids through the synapses (Kumamaru et al., 2004).

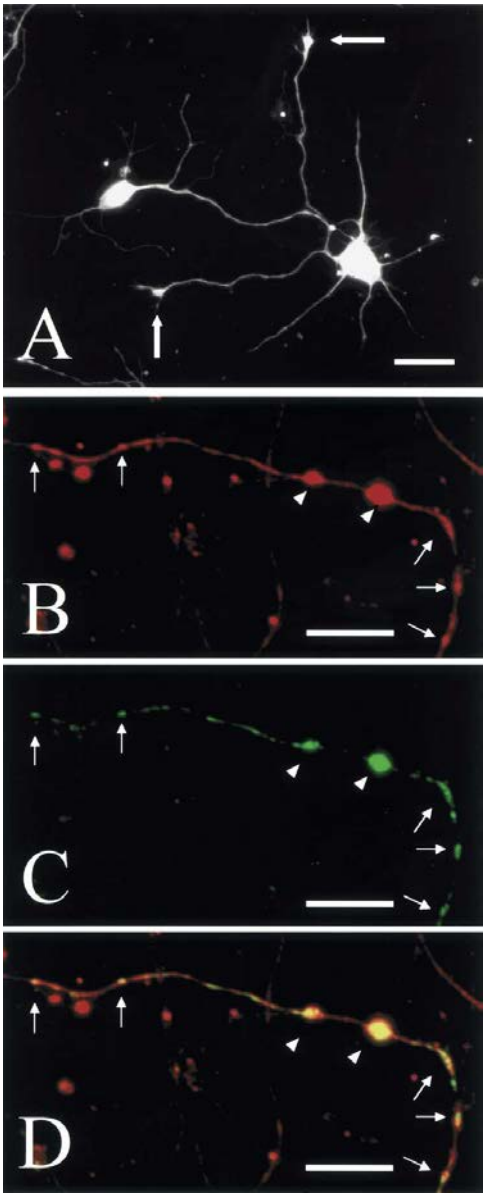

Figure 5.2: Distribution of RTN3 in cortical neurons culture and synapses.

(A) RTN3 immunostaining distribution where detected in the all over the cortical neurons. **(B)** RTN3, **(C)** synaptophysin expression in axon using confocal microscopy. **(D)** Merged image shows colocalization of RTN3 and synaptophysin. (adapted from (Kumamaru et al., 2004)).

5.1.3 Overexpression of RTN3 causes neurite dystrophy in neurodegenerative diseases

Neurite dystrophy refers to swollen dendrites or swollen axons found mainly in patient brains suffering from neurodegenerative diseases (NDD) such as Alzheimer's, Parkinson's and Lewy body diseases. For example, in patients with Alzheimer's disease (AD), neurites dystrophy is often found in the areas around neuritic amyloid plaques (Irizarry et al., 1998, Hu et al., 2007b). RTN3 immunoreactive dystrophic neurites (RIDNs) are present and extensively accumulate in neurite dystrophy of AD's brains and amyloid precursor protein of transgenic mice expressing RTN3 (Tg-RTN3). The formation of RIDNs is also accompanied by expression of high molecular weight of RTN3 in NDD patients (Hu et al., 2007b, Shi et al., 2009a). The levels RTN3 in transgenic mice Tg-RTN3 appear to govern the formation RIDNs, where the more expression of RTN3 the more RIDNs will form initially in cortical regions and hippocampal CA1 region, a critical area of memory and learning (Shi et al., 2009a).

Interestingly, the levels of RIDNs were not detectable in mice younger than 6 months, whereas a few intermittent RIDNs were detectable in mice at age of 1 year. Moreover, RIDNs are abundantly present in mouse brains at aged 2 years. However, the amount of RIDNs found in Tg-RTN3 mice at early age of 3 months resembles that in 2 years old non-transgenic mice, these finding suggested that aggregation of RTN3 is involved in dystrophic neuritis and results in Alzheimer's disease pathogenesis (Shi et al., 2009a).

5.1.4 RTN3 expression is reduced during axonal transport of BACE1 thus causing reduction of amyloid deposits

The pathological features of Alzheimer's disease are complex: one of the pathological hallmarks is the presence of neuritic amyloid plaques surrounded by dystrophic neurites, reactive astrocytes and activated microglia (Deng et al., 2013). The aggregation of β-amyloid peptides (Aβ) in the brain mostly results in accumulation of amyloid deposits and that are excised from amyloid precursor protein (APP). However, β-amyloid cleaving enzyme 1 (BACE1) is initiated as cleavage of APP at β-secretase site occurs, and this enhances the generation of Aβ (Deng et al., 2013, Shi et al., 2014). Increasing BACE1 activity was found to generate amyloid deposition and Aβ accumulation in Alzheimer's disease patients, thus reduced BACE1 activity and prevented pathological damage.

BACE1 not only resides in neuronal soma but is also found in synapses where BACE1 was shown in presynaptic terminals (Kandalepas et al., 2013). Formation of amyloid deposits is correlated with the release of Aβ from synaptic terminals and thus, BACE1, APP and Aβ release from neuronal presynaptic terminals need to be transport through the axons to allow the cleavage to occur at synaptic site. However, APP has been shown to be axonally transported (Koo et al., 1990, Lee et al., 2005a, Wang et al., 2012b).

RTN3 is among the RTNs that were expressed richly in neurons and present enriched in axons and dendrites (Deng et al., 2013). However, RTN3 negatively regulates BACE1 activity thus, overexpression of RTN3 reduces the transport of BACE1 through the axons as well as increasing the retention of BACE1 in the ER (Shi et al., 2009b). The retention of BACE1 in the ER could decrease the levels of

BACE1 exiting from late Golgi, preventing axonal transport (Deng et al., 2013). However, increased expression of RTN3 impacts the transportation of BACE1 through the axons and demonstrated reduction of amyloid deposits and reduced pathological damage in Alzheimer's disease patients.

5.1.5 Hypothesis

In the microarray data that has been collected from rat DRGN in regenerating and non-regenerating injury models, RTN3 found significantly increased in regenerating injury paradigms compared to intact and non-regenerating models. Therefore I hypothesised that up-regulation of RTN3 promotes axon regeneration after SCI.

5.1.6 Aims

- To validate our microarray data by RT-PCR and localization of RTN3 in DRG sections using immunohistochemistry.
- Determine the levels of RTN3 protein in DRG lysates in regenerating and non-regenerating injury models by western blot.
- Knock down/up-regulate RTN3 in primary DRGN cultures using siRNA to test its effects on disinhibited DRGN neurite outgrowth.
- Supress or overexpress the gene *in vivo* depending on how it regulates disinhibited DRGN neurite outgrowth and determine its effects on DC axon regeneration.

5.2 Materials and methods

Please refer to the main methods and materials chapter for standard and detailed protocols.

5.2.1 Experimental design

Preconditioned sciatic nerve injury was performed to 2 group of animals (n = 3) 7 days prior to DC crush, followed the DC crush. First group of animal received a PEI/CMV-GFP plasmid and used as a control, whereas the second group injected with CMV-RTN3/*gfp* plasmid include *in vivo*-jetPEI vector via intra-DRG rout **(Figure 5.3)**. Animals were allowed to survive for 21 days and killed by overdose of CO_2 and intracardially perfused, and L5 DRG ganglia and DC lesion site were collected for further analysis.

5.2.2 Preparation of plasmid and *in vivo*-jetPEI vector

Since the used of *in vivo*-jetPEI as a delivery vector displayed efficient transfection rates and reduced immune response seen in DRGN following injection (see chapter 3 and 4), therefore I used the same non-viral delivery vector here to overexpress RTN3 after DC injury. 0.24µl of *in vivo*-jetPEI was mixed with 5% glucose solution and then added to 2µg/µl of CMV-RTN3/*gfp* plasmid (

Figure 5.3) (as explained in section 3.2.2). Due to lack of time, optimal concentration of plasmid was not preformed; however I used the concentration as shown in (chapter 3). Finally, 2µl of the complex was loaded into glass micropipettes and injected directly into L5 DRG ganglia using intra-DRG route immediately after the DC crush at T8.

A

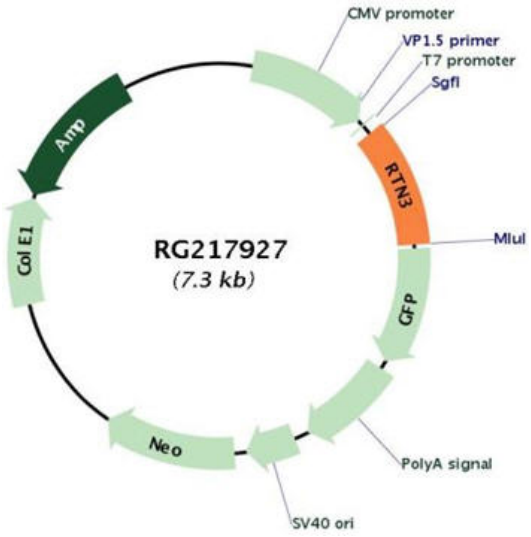

B

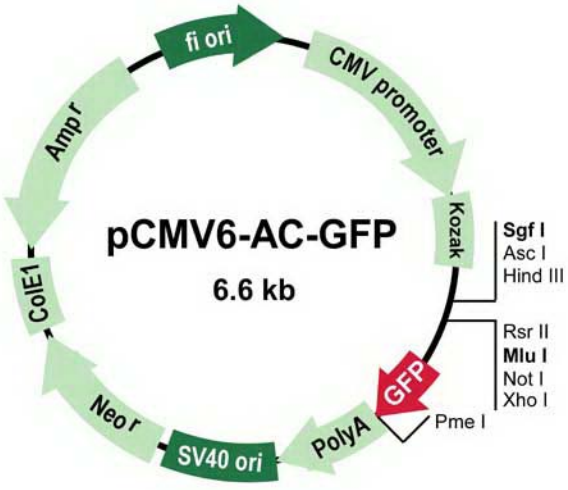

Figure 5.3: plasmids map used in this study. (A) is CMV-RTN3/*gfp* to enhance the expression of RTN3, and (B) is CMV-GFP used as a control.

5.3 Results

5.3.1 mRNA levels of RTN3 were increased in regeneration injury model.

By microarray, there was no change in RTN3 mRNA levels after DC injury compared to intact controls. However, in regenerating SN and pSN+DC models, RTN3 mRNA levels were significantly elevated by 4.11 ± 0.03 and 6.22 ± 0.04-fold ($P<0.0001$), respectively, compared to intact controls (**Table 5.1**).

These results suggested that elevated levels of RTN3 are required to promote DRGN axon regeneration.

Gene	Description	DC	SN	pSN+DC
RTN3	Reticulon3	1.01±0.01	4.11±0.03	6.22±0.04

Mean ± SEM values were shown from four different samples.

Table 5.1: Microarray data analysis of fold-change in mRNA levels of RTN3.

The fold-differences compared to control intact DRGNs 7 days in DC, SN and pSN+DC crush models. (n=6)

5.3.2 Immunohistochemistry and western blot of RNT3 levels correlated with mRNA levels

RTN3 immunostaining was absent in intact control DRG sections whereas in DRG sections taken after 7 days following DC injury, RTN3 was barley detected and slight immunoreactivity could be seen in the nucleus of DRGN **(Figure 5.4)**. However, in regeneration SN injury higher levels of RTN3 immunoreactivity were localised in DRG nucleus, whereas in pSN+DC, RTN3 was widely observed in the nucleus and the cytoplasm of DRGN **(Figure 5.4)**. Moreover, RT-PCR was used for further confirmation and results displayed mRNA of RTN3 was elevated in regeneration injury models (SN and pSN+DC) **(Figure 5.6).**

Western blot was also used to determine RTN3 levels from extracted total protein from DRG in regenerating and non-regenerating model. Our results showed low expression of RTN3 protein levels in intact and DC treated DRGNs **(Figure 5.6A)**. Interestingly, RTN3 protein levels were significantly increased in regenerating SN and pSN+DC treated DRG **(Figure 5.6A)** suggesting that up regulation of RTN3 plays role in axon regeneration. Densitometry of detected bands confirmed that RTN3 levels were 50% higher in regenerating SN and pSN+DC models compared to DC or intact controls **(Figure 5.6B)**.

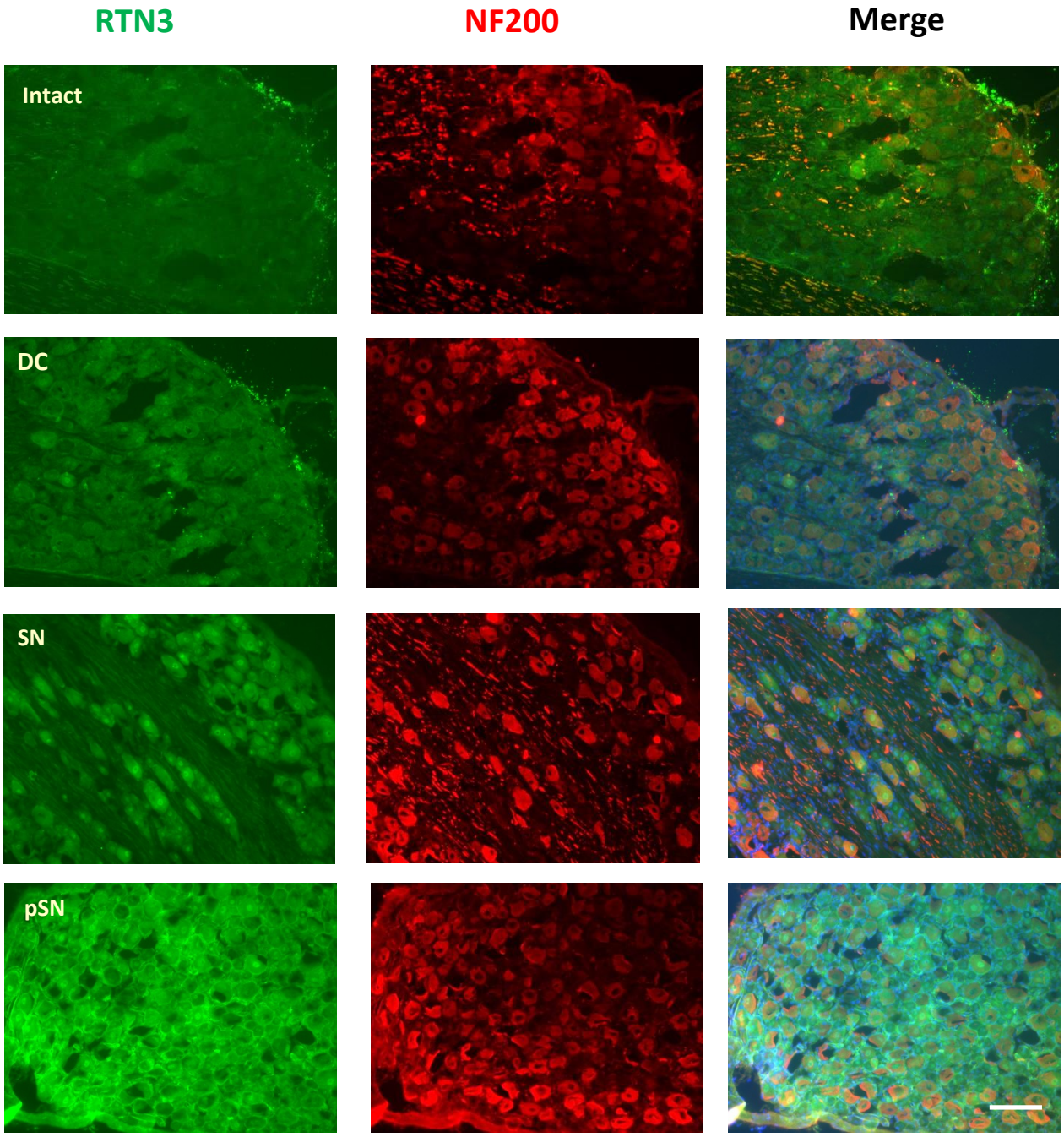

Figure 5.4: immunohistochemistry to show level of RTN3 in intact and injured rat DRG section.

RTN3 protein levels were absent in intact DRG and barley detected in non-regenerating DC models. RTN3 was localised in the nucleus in regeneration SN models, and present in the nucleus and cytoplasm in pSN+DC. All sections were double stained with Neurofilament 200. Scale bar = 500µm. (n=3)

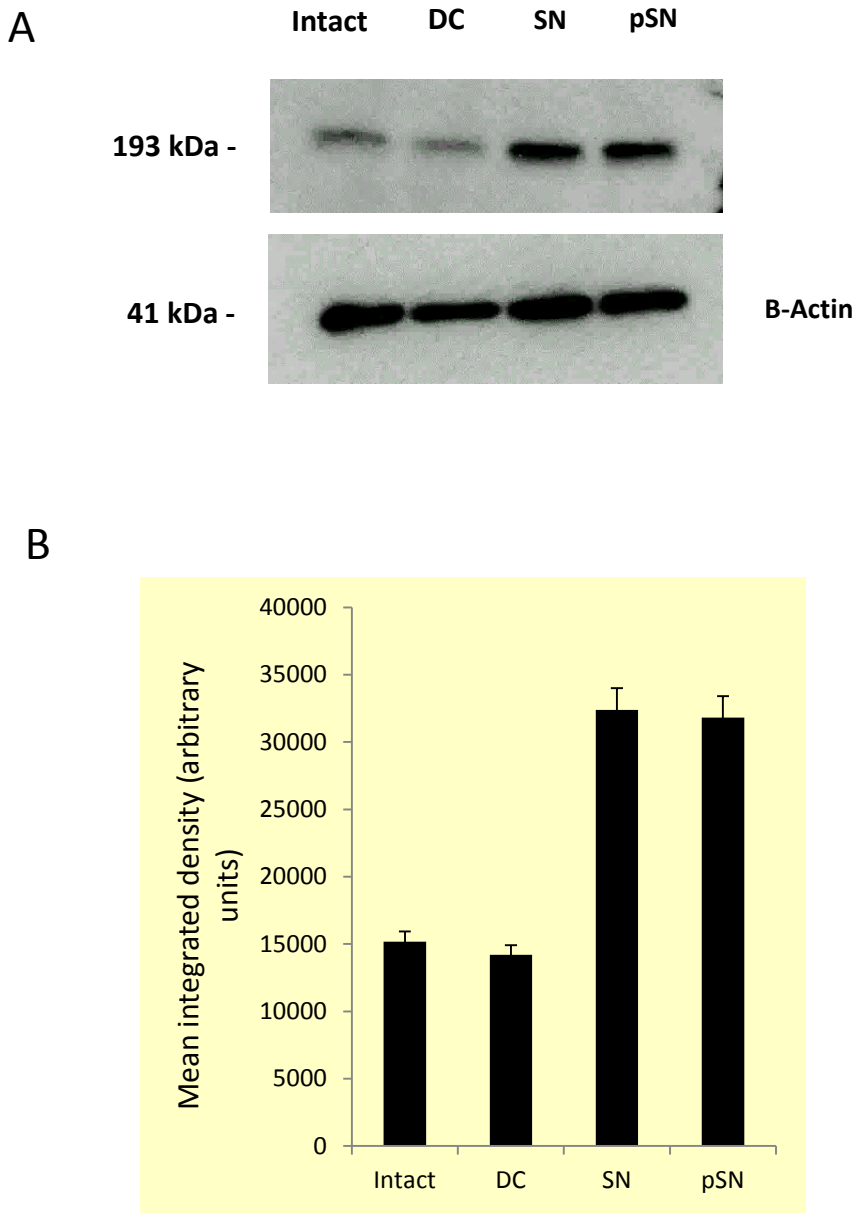

Figure 5.5: Protein levels of RTN3 at 7 days in intact, non- regeneration and regeneration models.

(A) western blot of protein lysates of DRG in different injury models showing RTN3 protein increased in regenerating models compared to intact or DC injury models. (B) densitometry was used to quantify the levels of RTN3 protein. (n=3)

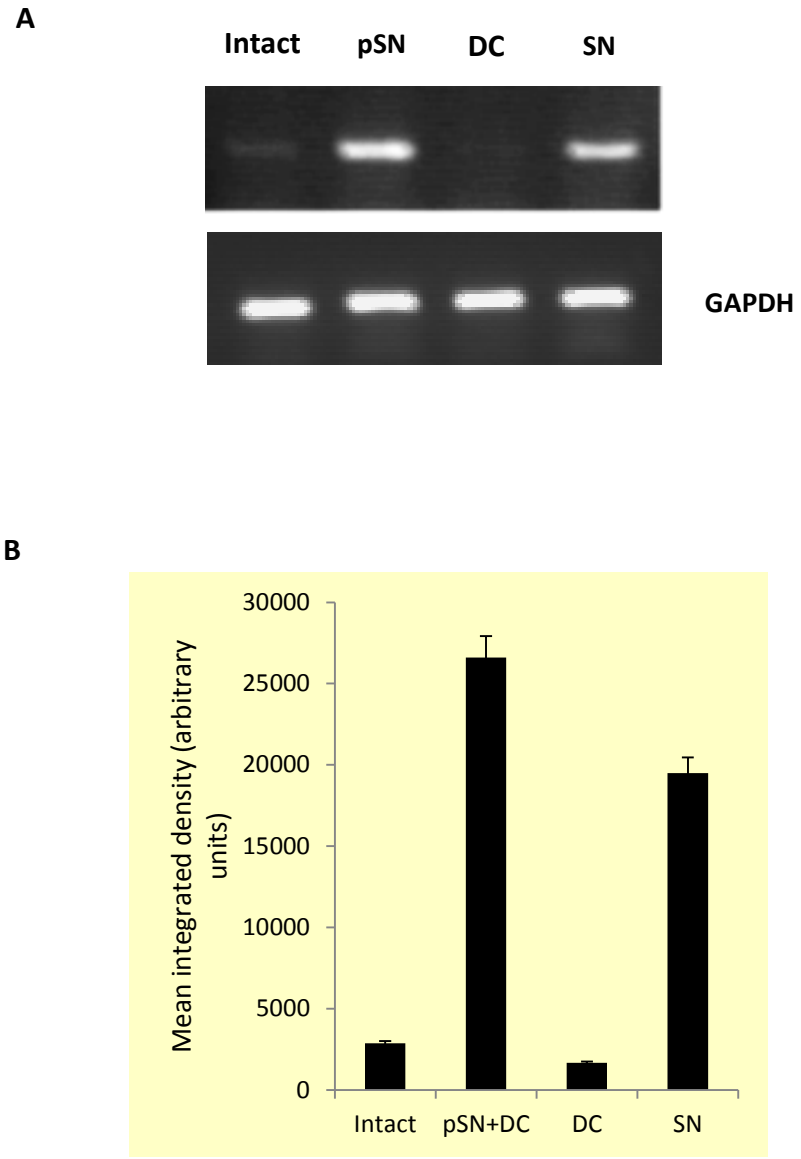

Figure 5.6: mRNA levels of RTN3 after 7days of intact, non- regeneration and regeneration injury models.

(A) RT-PCR for cDNA reversed from mRNA that extracted from DRG bundle showed RTN3 remained low in intact and DC model compared to SN and pSN+DC models where high expression of RTN3 was observed. **(B)** Densitometry was used to quantify the mRNA level of RTN3. (n=3)

5.3.3 Knockdown of RTN3 using siRNA supresses neurite outgrowth

According to the previous finding that RTN3 found unregulated in regeneration models, here i tested whether the gene is involved in axon regeneration. Firstly I used dissociated adult rat DRGN to investigate the consequence of RTN3 knockdown on disinhibited DRGN neurite outgrowth. Our prediction was that knockdown of RTN3 will reduce DRGN neurite outgrowth as upregulation of the gene correlates with axon regeneration. DRGN were treated with Lipofectamine alone, siEGFP (non-specific transfection control), FGF2, FGF2+siRTN3 and siRTN3. DRGN were grown for 3 days and then knockdown of RTN3 was analysed by western blot. We found that in **(Figure 5.7, Figure 5.9)** there were no changes in RTN3 protein level in Lipofectamine/untreated, siEGFP treated control DRGN. However, DRGN treated with siRTN3 caused a reduction of RTN3 levels by >70% to barely detectable levels. Knockdown of RTN3 correlated with significant reduction in DRGN neurite outgrowth **(Figure 5.7, Figure 5.9).**

In addition, immunocytochemistry showed 92% reduction in the number of RTN3+ DRGN after siRTN3 treatment in DRGN, demonstrating successful RTN3 knockdown **(Figure 5.9)**. After siRTN3 treatment, DRGN neurites were significantly reduced after RTN3 knockdown in terms of the mean neurite length to 24.96 ± 2.1µm after siRTN3 treatment (**Figure 5.)** whilst the number of DRGN with neurites reduced to 37 ± 4 (**Figure 5.)**. DRGN survival however, was unaffected in all treatment conditions (**Figure 5.)** showing that knockdown of RTN3 gene has no negative impacts in DRGN survival. These results suggested that RTN3 regulates neurite outgrowth and reduction of RTN3 supresses the growth of DRGN neurites and thus, RTN3 plays a role in neurite outgrowth.

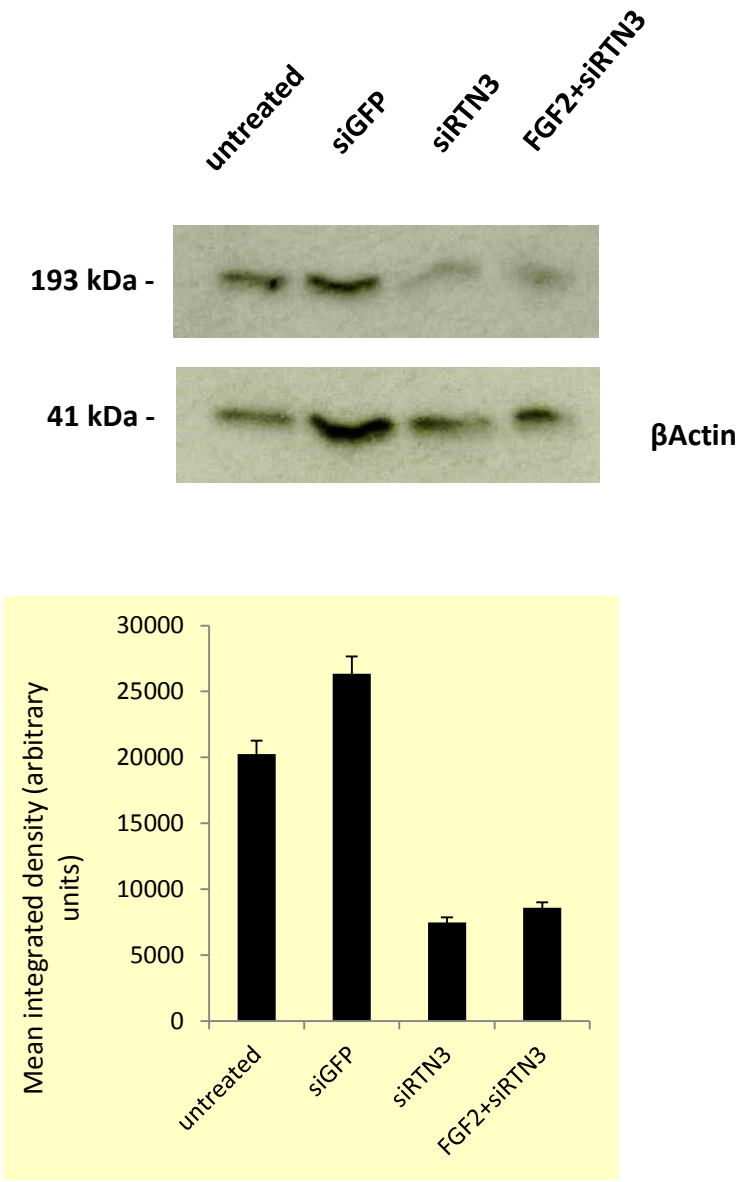

Figure 5.7: Protein level of RTN3 in DRGNs primary cultured treated with siRTN3 for 3 days.

(A) Western blot for RTN3 in untreated, siGFP, siRTN3 and FGF2+siRTN3 treated DRGNs for 3 days showed knockdown of RTN3. **(B)** Densitometry used to quantify the suppression of RTN3 after mediated by siRNA. (n=3)

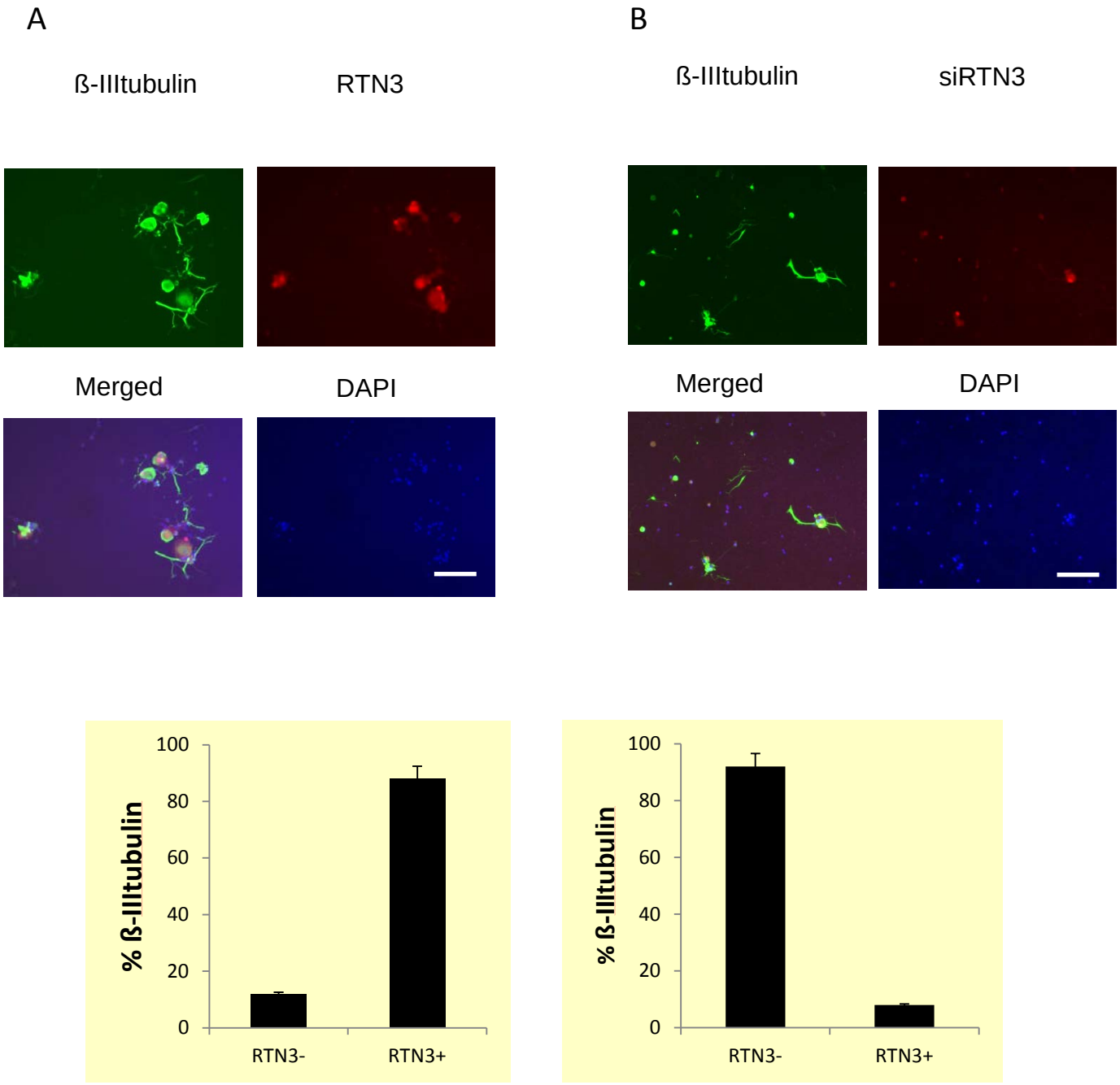

Figure 5.8: Immunocytochemistry for RTN3 in primary DRGN.

(A) Representative immunolocalization for RTN3 in untreated DRGN showing he percentage of RTN3 protein in ß-III tubulin^{+} DRGN. **(B)** DRGN transfected with siRTN3 showed reduced RTN3 protein level by 92%. Scale bar = 100µm. (n=3)

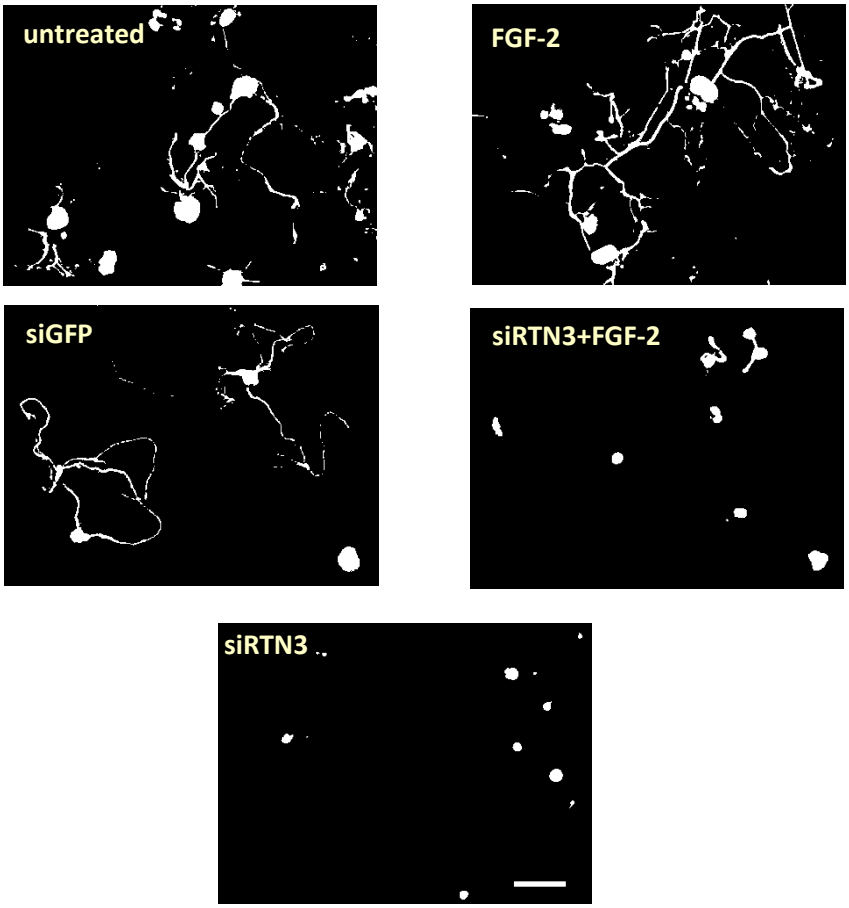

Figure 5.9: siRNA mediated RTN3 in rat primery DRGNs cultured.

Representitive photomicrographs of βIII-tubulin of DRGNs neutite outgrowth in 8 wells chamber slide transfected with siRNA and untransfected DRGNs. Photomicrographs showed inhibition of neurite outgrowth corrolated with supression of RTN3 even with growth factor. Scale bar = 100µm. (n=3)

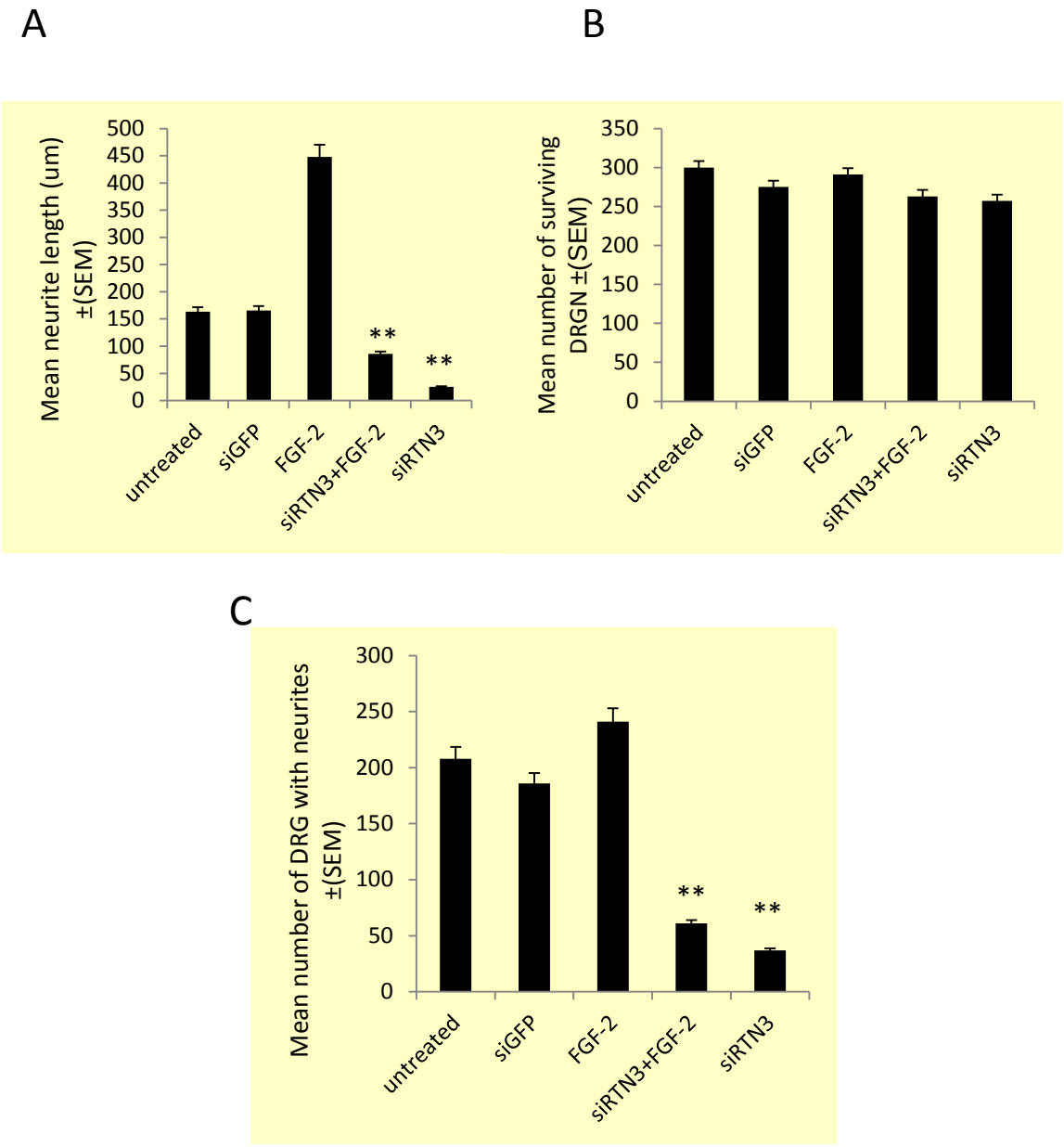

Figure 5.10: DRGN survival and neurite outgrowth after knockdown of RTN3.

(A) Mean neurite length, (B) mean number of survival DRGN and (C) mean number of DGRN with neurites. ± SEM means values shown from three different animals. ***P<0.001, Analysis of Variance. (n=3)

5.3.4 RTN3 may interact with CRELD1 after DC injury models

Since immunocytochemistry of RTN3 was localised in DRGN nucleus after SN injury and in pSN+DC, I speculated that there is an unknown gene that is up-regulated after DC injury and interacts/recruits RTN3 in DRGN membranes thus allowing the DRGN to produce RTN3 protein widely as seen in (**Figure 5.4**).

After further research I found cell adhesion molecules named cysteine rich with EGF like domains 1 (CRELD1) to interact with RTN3 and which reduced HeLa cell apoptosis (Xiang and Zhao, 2009). CRELD1 changed RTN3 localization from nucleus to cell membrane possibly via ER, where I speculated that this observation correlated with our predictions since RTN3 resides in ER after SN injury then is localized in DRGN membranes after DC injury models (**Figure 5.4**). I speculate that CRELD1 is co-expressed with RTN3 protein in non-regeneration DC injury models, however immunohistochemistry for CRELD1 showed that CRELD1 was present DRGN in all injury models including intact controls (**Figure 5.7)**. Western blot and RT-PCR confirmed that CRELD1 is expressed in DRGN in both intact and injured DRGN (**Figure 5.8).**

These primary findings suggested that CRELD1 may interact with RTN3 after DC injury, therefore further investigation and experimental work are required to confirm whether CRELD1 has a role in modulating and distributing RTN3 in DRGN as shown in pSN+DC.

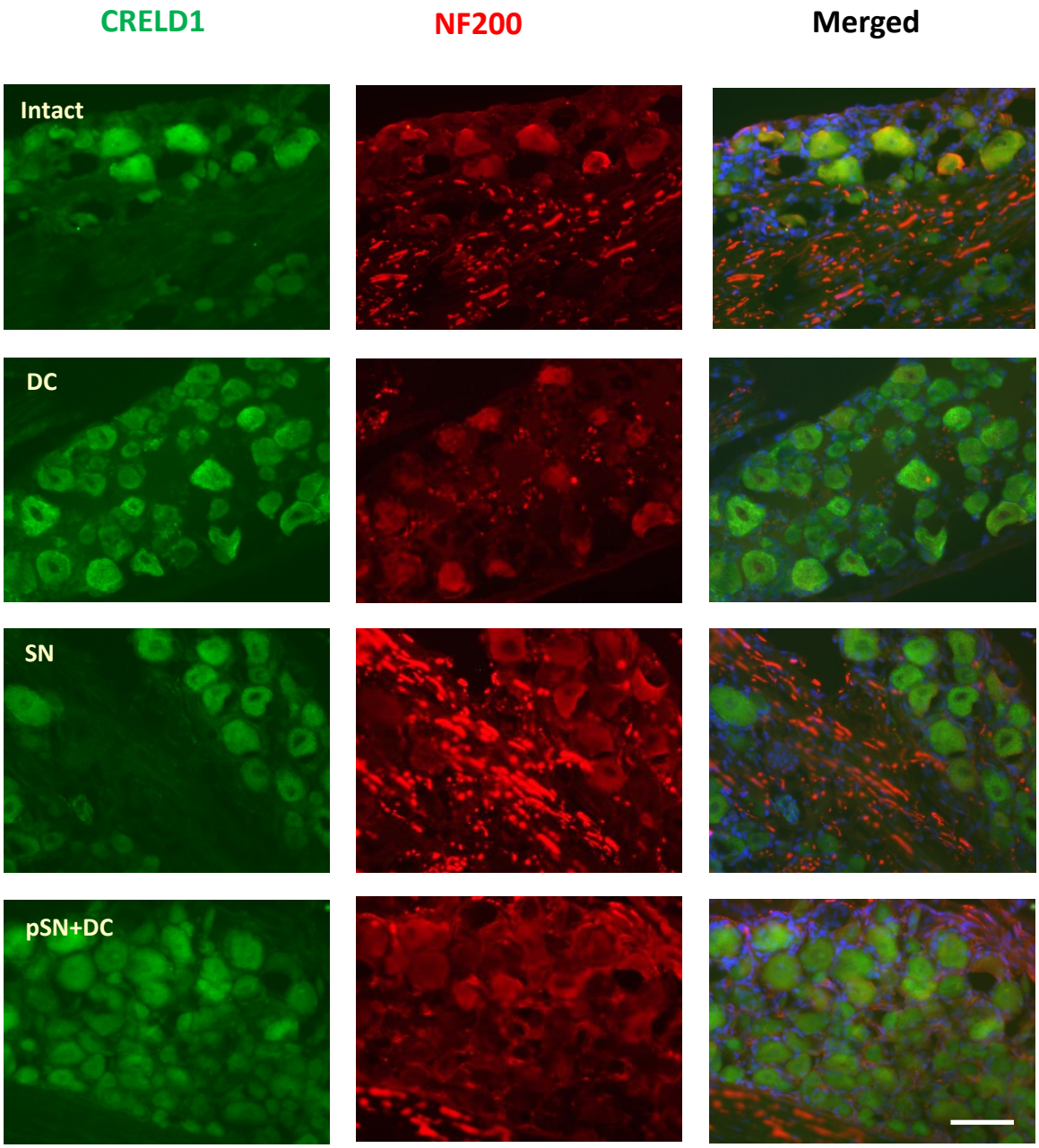

Figure 5.7: immunohistochemistry showed level of CRELD1 in intact and injured rat DRG sections.

CRELD1 protein level was expressed in all DRG sections includes intact, non-regeneration and regeneration models. All sections were double stained with Neurofilament 200. Scale bar = 500µm. (n=3)

A

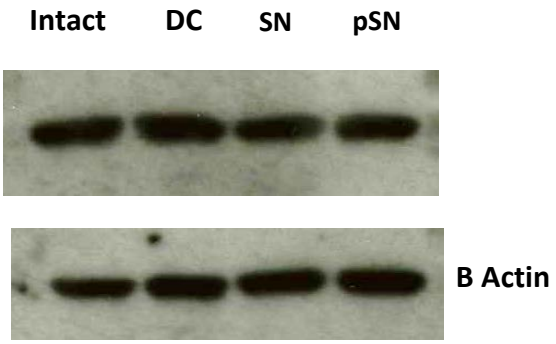

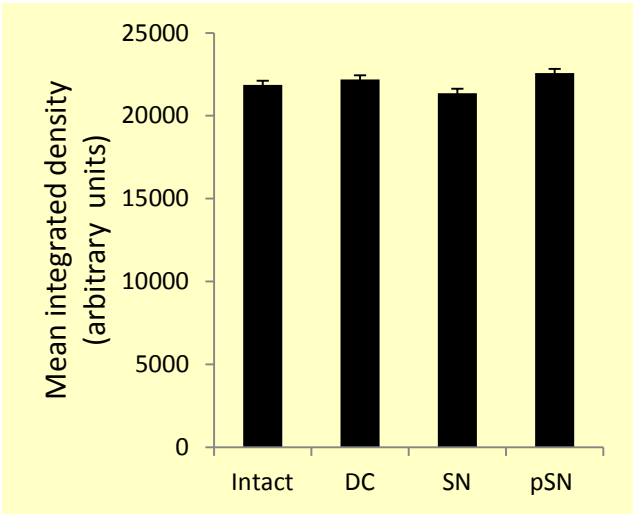

B

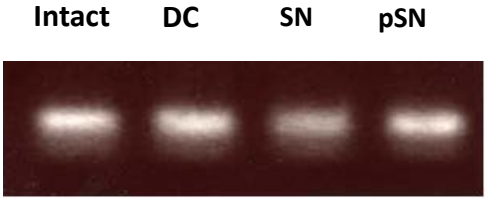

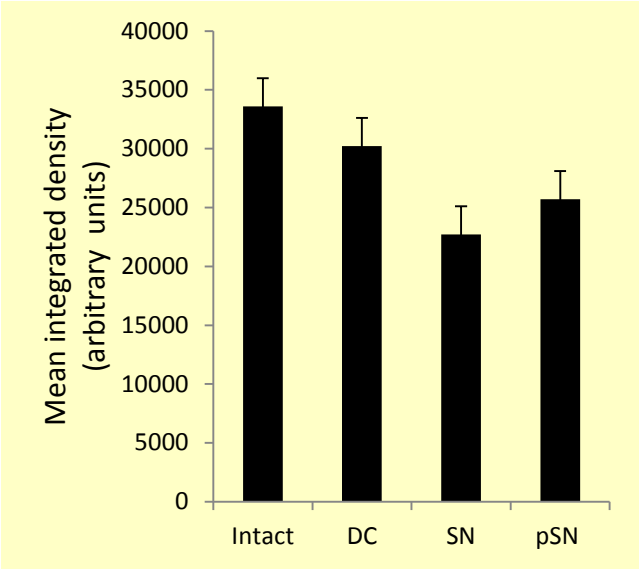

Figure 5.8: **protein and mRNA levels form DRGN ganglia for CRELD1.**

(A) Western blot and **(B)** RT-PCR showed CRELD1 protein and mRNA levels in intact, non-regeneration and regeneration models. Densitometry was used to quantify CRELD1 protein and mRNA. (n=3)

5.3.5 *In vivo* delivery of RTN by in vivo-jetPEI-RTN3/*gfp* promotes dorsal column axon regeneration

Since raised RTN3 levels correlate with DRGN axon regeneration and suppression of RTN3 reduced DRGN neurite outgrowth, I speculated that overexpression of RTN3 might promote DC axon regeneration *in vivo*. Here I tested whether overexpression of RTN3 promotes DC axon regeneration by delivery of a plasmid containing RTN3/gfp using in vivo-jetPEI to the injured DRGN. Regeneration was simultaneously stimulated with preconditioning SN lesions.

Seven days after preconditioning lesions, animals received DC injury followed by immediate injection of PEI-RTN3/*gfp* plasmid to the left L5 DRG bundle and animals were allowed to survive for 3 weeks. Double immunohistochemistry for RTN3 and GFP showed that in control pSN+DC treated rats which were injected with a control gfp containing plasmid, GFP expression was present in most DRGN but RTN3 immunoreactivity was present at low levels (**Figure 5.9A)**. However, DRGN treated with RT3/gfp plasmid demonstrated GFP expression in a similar proportion of DRGN to pSN+DC-gfp treated controls but that RTN3 immunoreactivity was over-expressed to much higher levels than the control DRGN. These results suggested successful overexpression of RTN3 in transfected DRGN (**Figure 5.9B)**.

Furthermore, Immunohistochemistry for GAP43 to detect regenerating axons at the T8 DC lesion site showed that a few axons had regenerated into the lesion site (**Figure 5.14A)** but in animals where RTN3 was overexpressed, many $GAP43^{+}$ axons had regenerated and reached to caudal segment and some axons

traversed and passed through the cavity compare to the control treated group (**Figure 5.10B)**. I conclude that over expression of RTN3 in DRGN ganglia promotes axon regeneration (**Figure 5.10)**. Nonetheless, the mechanism of how RTN3 promotes the axons to regenerate is still unknown but all these finding suggested that up-regulation of RTN3 after SCI leads to the regeneration of axons.

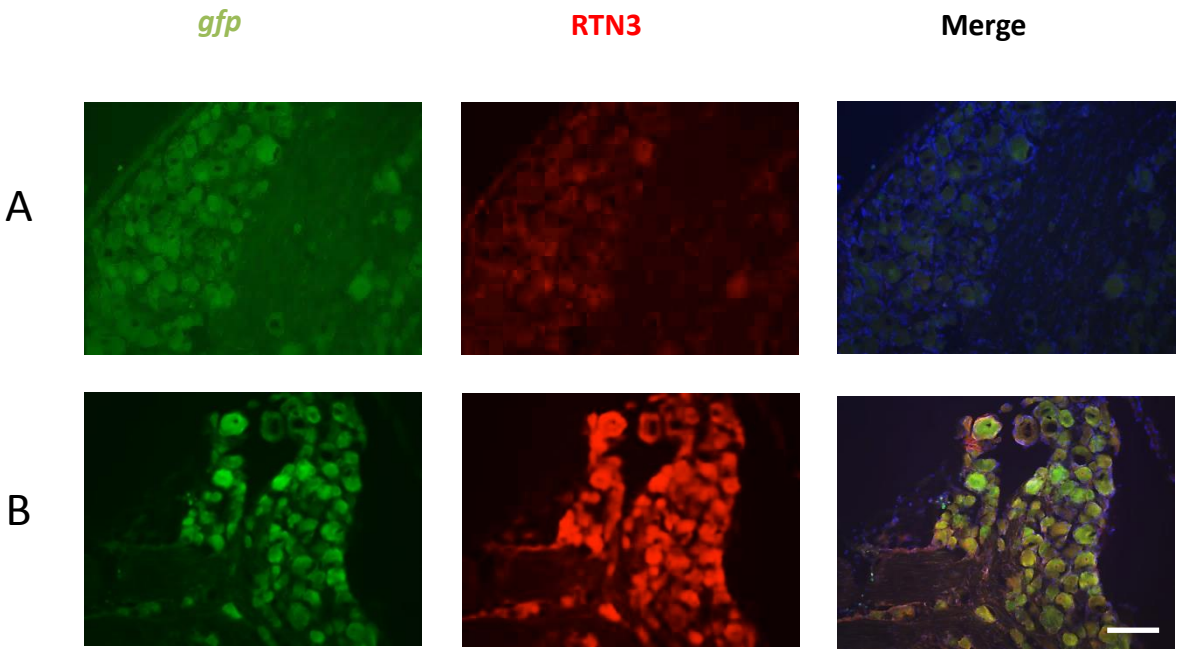

Figure 5.9: RTN3 levels are overexpression after intra-DRG injection of pSN+DC-PEI-RTN3/*gfp* plasmid in L4/5 DRGN.

(A) Immunohistochemistry showed low levels of RTN3 were detected in DRGN ganglia of a control pSN+DC animal whilst **(B)** significantly higher levels of RTN3 and GFP were detected in DRGN ganglia of animal injected with PEI-RTN3/*gfp* plasmid. Scale bar = 100µm. (n=3)

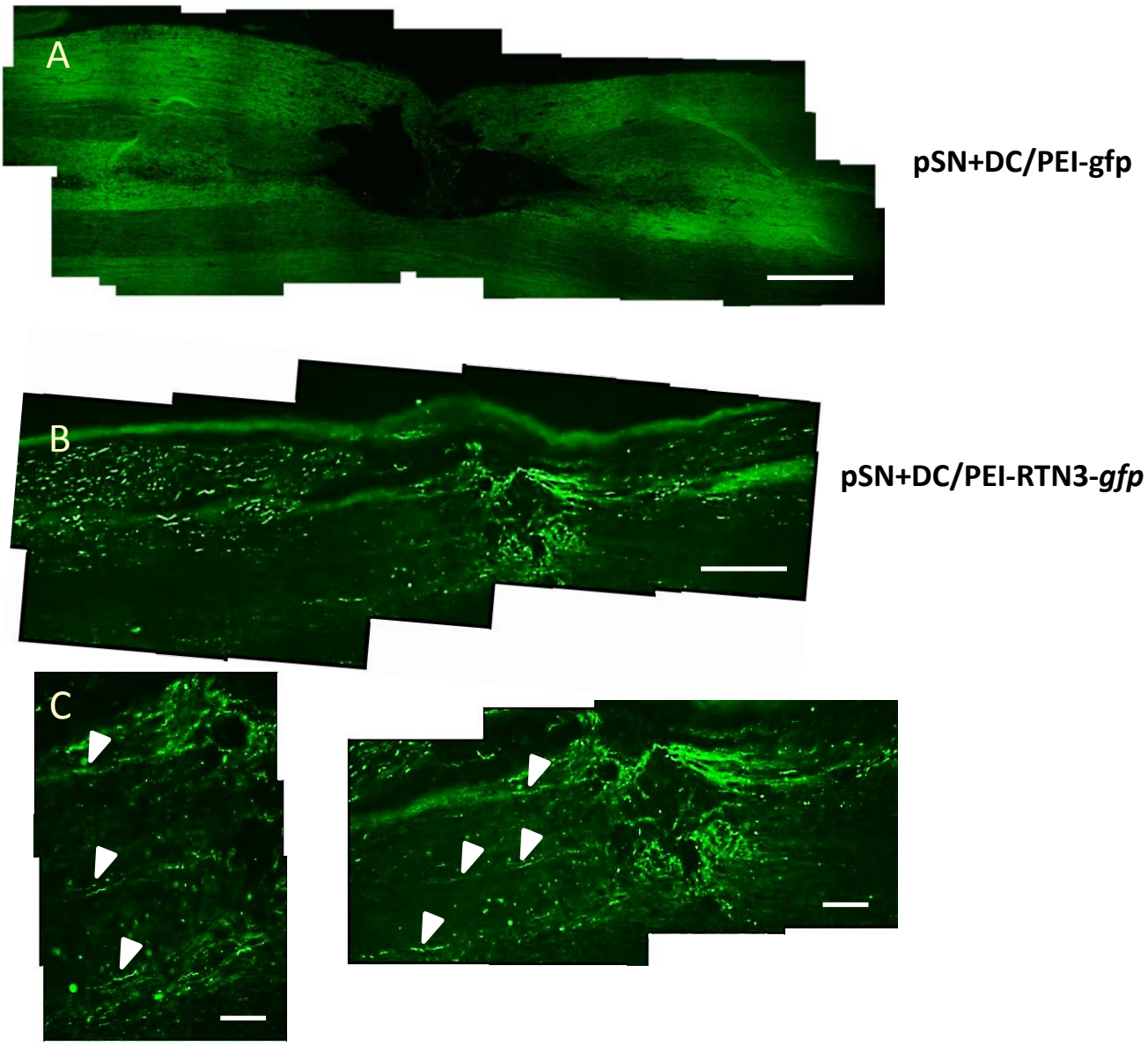

Figure 5.10: Overexpression of RTN3 in DRGN promotes DC axon regeneration.

(A) There were no GAP43^{+} axons regeneration following pSN+DC. **(B)** Overexpression of RTN3 promotes GAP43^{+} axons (arrowheads) regeneration through the DC lesion site. **(C)** High power view of axons emanating from the lesion site. Scale bar in A and B=500μm; in C = 50μm. (n=3)

5.4 Discussion

In this report, I investigated the role of RTN3 in terms of axonal regeneration. I found mRNA and protein levels of RTN3 were significantly increased in regenerating models compared to intact and non-regenerating models. I also, knocked down RTN3 using siRNA and showed that this suppressed DRGN neurite outgrowth. These results prompted us to overexpresses RTN3 *in vivo* by using non-viral vectors and I found that overexpression of RTN3 promotes the axons in the DC to regenerate.

5.4.1 RTN3 levels increase in regenerating injury models

I found that mRNA levels of RTN3 were increased in in microarrays in regenerating DRGN models. I therefore predicted that RTN3 might be positively involved in the dynamics of the axon growth cone, leading to axon regeneration. Immunohistochemistry in DRGN showed that RTN3 was localised in DRGN nuclei after SN injury and was absent in both intact and non-regenerating DC injury models, correlating with our microarray data. By western blot, I found that RTN3 protein levels were also absent in intact and non-regenerating DRGN models and significantly in regenerating models, corroborating with our other findings. The localisation of RTN3 in DRGN nuclei, however, after SN injury may be involved in different regulatory mechanisms such as shaping the ER (Wakana et al., 2005, Zurek et al., 2011) and remains to be investigated. Immunohistochemistry of RTN3 in pSN+DC injury models were present both in the nucleus but also in the cytoplasm and shows a slightly different distribution of the RTN in these models.

I'm currently unsure why this is so but this remains to be investigated. I also, confirmed that the mRNA and protein levels of RTN3 were elevated in pSN+DC by western blot and RT-PCR therefore suggest that RTN3 is required to promote CNS axon regeneration.

5.4.2 Knockdown of RTN3 using siRNA negatively affected neurite outgrowth

To confirm the role of RTN3, I used dissociated adult rat DRGN cultures to investigate the consequence of RTN3 knockdown on DRGN neurite outgrowth (Ahmed et al., 2010, Ahmed et al., 2013, Ahmed et al., 2011a). Since RTN3 was raised 6-fold in pSN+DC models I predicted that knockdown of RTN3 will suppress DRGN neurite outgrowth. I used different concentrations of siRNA to RTN3 and observed that there was a significant reduction of neurite outgrowth in DRGN treated with siRTN3 compared to control samples, even when stimulated to grow with FGF2. Knock down of RTN3 however, did not induce DRGN death and hence our results show that knocking down RTN3 has a direct effect on DRGN neurite outgrowth, confirming a role of RTN3 in DRGN neuritogensis. The mechanism by which RTN3 promotes DRGN neurite outgrowth is currently not known. However, it is likely that RTN3 modulates intracellular signaling pathways that promote DRGN neurite outgrowth. The elucidation of the mechanisms leading to enhanced DRGN neurite outgrowth will be investigated in future experiments.

5.4.3 CRELD1 is expressed after DC injury and may interact with RTN3

I have also tried to investigate the signalling mechanisms of RTN3, but without much success. However, one of the signalling molecules, CRELD1, was equally expressed in DRGN of all models and did not show any modulation and therefore our immunohistochemical findings only suggest that CRELD1 is available to interact with RTN3 but how this interaction occurs and what signalling molecules are invoked remains to be elucidated. CRELD1 does change the localisation of RTN3 from the ER to the cell membrane (Xiang and Zhao, 2009) and this is probably what happened in our pSN+DC models. Other proteins are also known to interact with RTN3 but not recruiting RTN3 from ER to the cell membrane, for example FADD, the endogenous FADD protein was found to recruited by RTN3 to the ER membrane and caused cell death (Xiang et al., 2006). CRELD1 is also a cell adhesion molecule and considered as one of the gene candidates in atrioventricular septal defects (Rupp et al., 2002, Robinson et al., 2003).

5.4.4 pSN+DC-PEI-RTN3/*gfp* promotes dorsal column axon regeneration after DC injury

After successful intra-DRG injection using *in vivo*-jetPEI vector in previous chapters (Chapter 3), I used the same experimental setup in this report to up-regulate the expression of RTN3 and determine its consequences on DC axon regeneration. Immunohistochemistry in DRGN showed abundant expression of gfp suggesting efficient transduction of DRGN after intra-DRG injection of the plasmid via the non-viral vector. Also, RTN3 was significantly overexpressed in DRGN

receiving the RTN3 vector and hence confirming the utility of *in vivo*-jetPEI for use in CNS gene delivery.

After overexpression of RTN3, many $GAP43^{+}$ axons regenerated through the crush site, with some traversing the cavity and reaching the distal segment of spinal cord. These results showed that RTN3 overexpression promotes DC axon regeneration.

Chapter 6: A novel role of AEG-1/MTDH/LYRIC in CNS axon regeneration

6.1 Introduction

6.1.1 Astrocyte Elevated Gene-1

Human immunodeficiency virus-1 (HIV-1) has a negative impact in the CNS and results in HIV-1 associated dementia (HAD) and neurodegeneration, where HAD is developed in about 20% of HIV-1 infected patients (Lipton and Gendelman, 1995, Lee et al., 2013). HIV-1 mainly infects resident macrophages (microglia) and rarely targets astrocyte but not neurons (Minagar et al., 2002). It is said that HIV-1 infects <1% of astrocyte despite their abundance in the brain, but believed that HIV-1-infected astrocytes are participants in neurodegeneration and HAD (Brack-Werner, 1999)

However, astrocyte elevated gene-1 (AEG-1) was among the 15 AEGs that was initially discovered in primary human fetal astrocytes (PHFAs) after infection by HIV-1 using rapid subtraction hypridization approaches (RaSH). In the HIV-1 infected PHFAs method, a series of HIV-1 induced genes termed (astrocyte supressed genes, ASGs) and (astrocyte elevated genes, AEGs) were identified (Su et al., 2002).

AEG-1 is sometimes loosely referred to as metadherin (MTDH) and lysine-rich CEACAM1 co-isolated (LYRIC1). AEG-1 is found highly expressed during the development period of mouse embryos and suggested to have a role in neurogenesis. Subsequent research has shown that AEG-1 is involved in many forms of cancers such as lung, prostate and renal cancer among others and implicated in HAD and glioma-associated neurdegeneration (Lee et al., 2011, Lee et al., 2013, Jeon et al., 2010). Later on, mRNA expression of AEG-1 was

detected in a various types of normal human tissues with elevated levels in the liver, heart, skeletal muscle, thyroid and adrenal glands (Su et al., 2002, Su et al., 2003, Lee et al., 2013). In CNS, AEG-1 found relatively lower levels in normal brain samples compared with glioma tissues, as detected by immunohistochemistry (He et al., 2014). In line with these results latter findings from found that AEG-1 is expressed in motor neurons of C57BL/6 mice (Yin et al., 2015).

6.1.2 Metadherin (MTDH)

MTDH (METastasis ADHEsion protein) is an AEG-1 murine ortholog and was cloned in 4T1 mouse mammary tumour cells in an attempt to identify cell surface receptors that mediate metastasis of lung cancer (Brown and Ruoslahti, 2004). A lung-homing-domain (LHD) which mediates lung metastasis was identified in ‘’MTDH’’ using *in vivo* phage screening and subsequently called metadherin (Liu et al., 2011). Brown and Ruoslahti used phage expression libraries from breast carcinoma cDNA to identify protein domains that bind to the vasculature of the lung and showed that LHD of MTDH was localised to the extracellular surface (Brown and Ruoslahti, 2004).

The authors also showed high levels of MTDH/AEG-1 in human breast cancer whilst lower levels were present in healthy breast tissue. Moreover, an LDH antibody antagonist inhibited breast cancer lung metastasis and suggested that MTDH/AEG-1 plays a significant role in this process (Brown and Ruoslahti, 2004, Lee et al., 2013). MTDH or metastasis adhesion protein was found overexpressed in human breast cancer that had predominantly metastasized to the lung, brain,

liver and bone (Hu et al., 2009). MTDH became an official nomenclature of LYRIC and AEG-1 based on the functional data of MTDH as promoting lung metastasis.

6.1.3 LYsine RIch CEACAM1 (LYRIC1)

In 2004, two researcher groups discovered a novel protein which they named LYRIC1 and 3D3/LYRIC1 derived from LYsine RIch CEACAM1 (Carcinoembryonic antigen-related cell adhesion molecule-1) co-isolated (Britt et al., 2004, Sutherland et al., 2004). LYRIC1 and 3D3/LYRIC1 were discovered in an attempt to identify the proteins that localized at nuclear sub-compartments and tight junction. Rat LYRIC1 interacted with CEACAM1 and co-localized with tight junctions in epithelial cells. LYRIC1 was expressed and localized in cytoplasm, cell perimeter and involved in perinuclear disruption (Britt et al., 2004).

On the other hand, Sutherland et al, 2004 cloned mouse 3D3/LYRIC independently from AEG-1/MTDH using gene-trap approaches in an attempt to find proteins that located at the nucleus sub-compartment. They used mouse F9/3D3 cell line for cloning and found 3D3/LYRIC1 expressed not only in ER but also in the nuclear envelop, suggesting that 3D3/LYRIC1 has a possible connection between tissue compartments and ER (Sutherland et al., 2004). Rat LYRIC1 is found expressed in different cells from the mouse 3D3/LYRIC suggesting different role in nucleus, cytoplasm and cell membrane that contribute to different cell signalling pathways (Lee et al., 2013).

6.1.4 The relative expression of AEG-1

The initial characterization of AEG-1 indicates a similar physicochemical property including molecular weight, amino acid composition and transmembrane domain. Despite the differences in their tissue disruption and number and size of transcripts, a 3.5 kb mRNA band was reported for AEG-1 in different studies (Britt et al., 2004, Brown and Ruoslahti, 2004, Kang et al., 2005, Sutherland et al., 2004). AEG-1 localization and membrane topology are important factors for their function. However, two types of membrane topology of AEG-1 were predicted in the beginning, type Ib and II. The role of type II was predicted to mediate metastases whereas, type Ib localized in nucleus/ER and supports tumour promoting activity of AEG-1 (Britt et al., 2004, Brown and Ruoslahti, 2004, Kang et al., 2005, Sutherland et al., 2004).

AEG-1 expressed in healthy human tissues with higher expression in liver, heart, skeletal muscle, thyroid and adrenal glands (Su et al., 2002, Su et al., 2003, Lee et al., 2013). AEG-1 gene is now considered a pivotal oncogene implicated in many oncogenic signalling pathways including NF-κB, MAPK, Wnt and PI3K-Akt. Moreover, AEG-1 is found highly expressed in different cancer types such as breast, brain, colorectal cancers as well as neuroblastoma, hepatocellular carcinoma and non-small cell lung cancer among others (Yoo et al., 2011, Lee et al., 2011, Lee et al., 2008). In addition to being an important oncogene, overexpression of AEG-1 promotes tumour growth, chemo-resistance, invasion and metastasis, as well as enhancing malignant aggressiveness (**Figure 6.1)** (Yoo et al., 2011, Emdad et al., 2013).

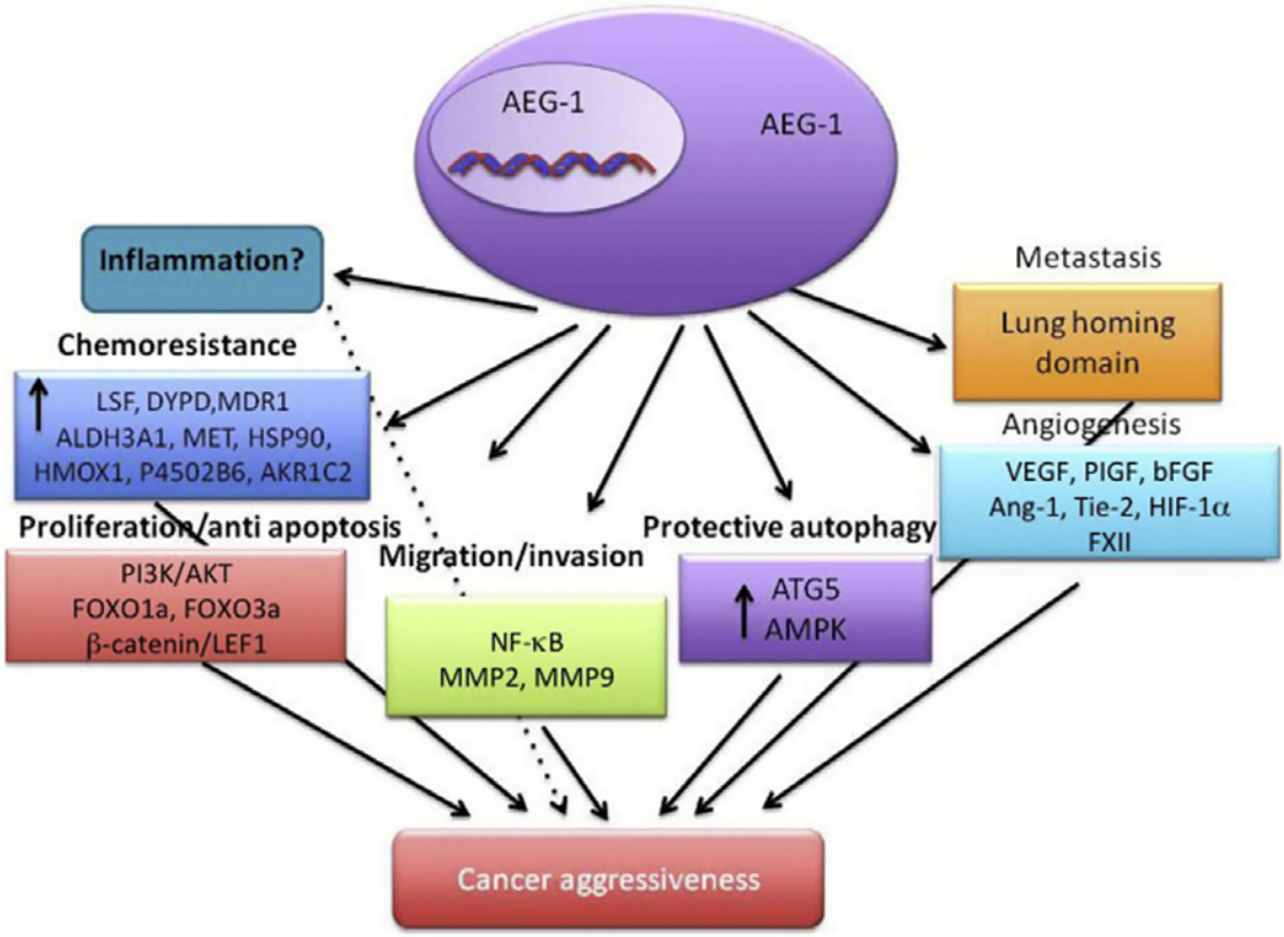

Figure 6.1 Possible effectors molecules and biological function of AEG-1 leads to cancer aggressiveness.

(adapted from (Emdad et al., 2013).

6.1.5 The role of AEG-1 in reactive astrocyte after CNS injury

Astrocytes are the most abundant cells in the brain and they provide support functions to the neurons including maintenance of extracellular ion balance, provision of nutrients to nervous tissue, and repair process after injury among others (Vartak-Sharma and Ghorpade, 2012, Bouzier-Sore et al., 2002). Since astrocytes are involved in tissue scarring and in response to CNS injury in a process called reactive astrogliosis (discussed in more details in section 1.4.4.1), induction of cancer may not be the only role of AEG-1.

Neha *et al* investigated the expression of AEG-1 in astrocytes undergoing astrogliosis in a mouse brain injury model and found that trauma to the brain induces expression of AEG-1 during astrogliosis. The movement of astrocytes to the injured site was also investigated and results showed that by knocking down AEG-1 genes, there was less movement of astrocytes to the injured site and the wound took longer to heal compared to models where the AEG-1 was present **(Figure 6.2)**.

This suggested that AEG-1 regulates migration and proliferation of astrocytes to the injury site (Vartak-Sharma and Ghorpade, 2012). Injury to the CNS will inevitably elicit astrogliosis since AEG-1 has been implicated in modulation of astrocyte response to injury.

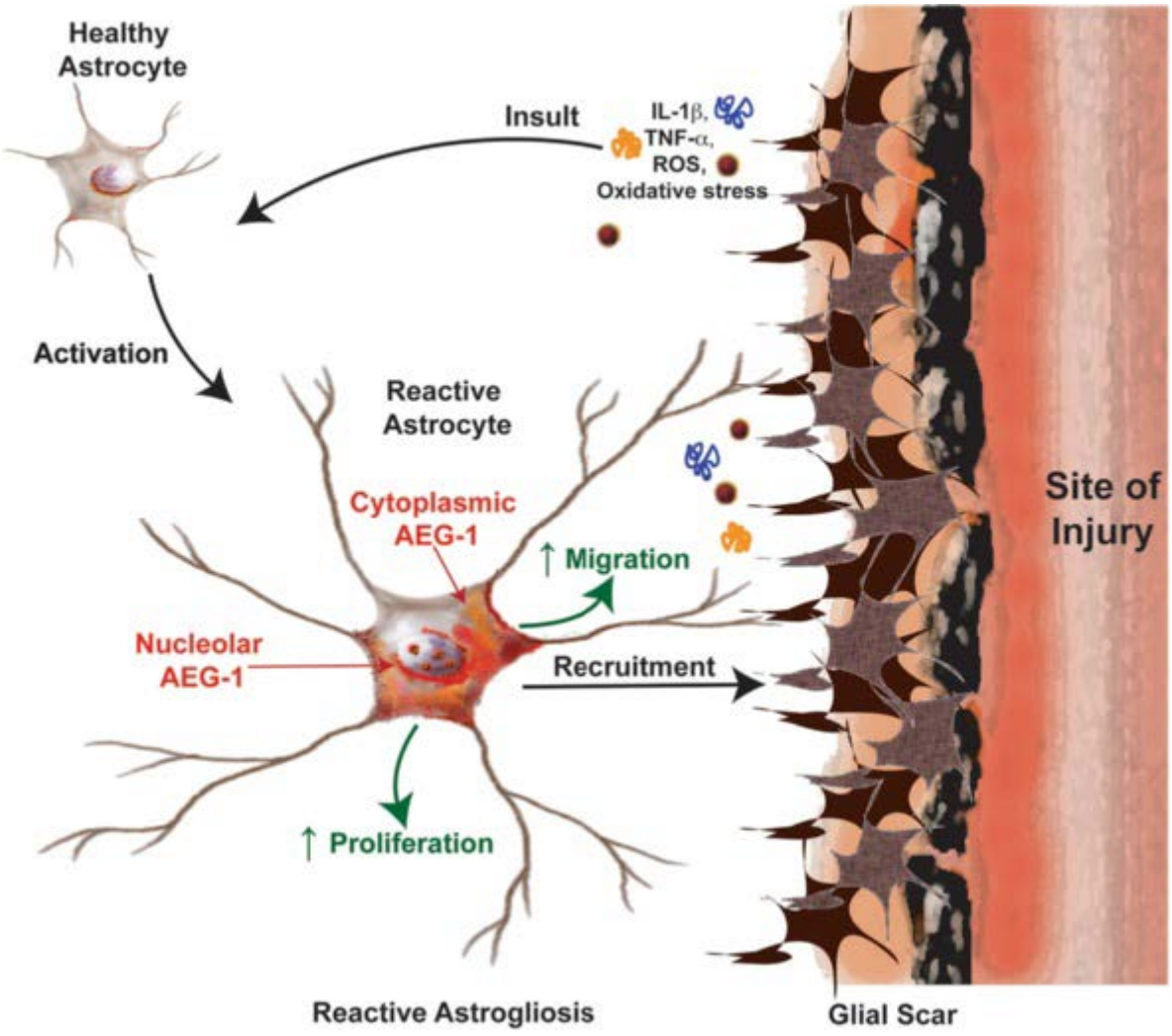

Figure 6.2: The role of AEG-1 in reactive astrogliosis.

Injury to the CNS mediates activation of many molecules such as inflammatory cytokines (e.g. interliuken-1β (IL-1β)), reactive oxygen species (ROS) and tumour necrosis factor-α (TNF-α). These molecules activate nearby healthy astrocytes and change the intracellular signalling pathways and microenvironments resulting in reactive astrogliosis. Increased expression of AEG-1 and reactive astrogliosis is a plausible mechanism for AEG-1-mediated regulation of astrocyte migration and proliferation during astrogliosis. Adapted from (Vartak-Sharma and Ghorpade, 2012).

6.1.6 AEG-1 increase glutamate excitotoxicity in glioma-induced neurodegeneration

Among CNS tumors, glioma has been identified as one of the commonest types of brain cancer in adult CNS, which originate from neuroepithelial tissues. And morphologically glioma is classified as astrocytic, oligodendroglial, choroid plexus and ependymal tumors (Nakada et al., 2007, Lee et al., 2011). Glutamate excitotoxicity plays a key role in glioma-induced neurodegeneration but the mechanisms of this phenomenon are still not fully understood. Since glutamate is an important neurotransmitter that is involved in normal brain function, high concentrations of glutamate must be removed constantly to avoid neurotoxin and neuron death. (Headley and Grillner, 1990, Sontheimer, 2008).

Astrocytes predominantly expressed excitatory amino acid transporter 1 and 2 (EAAT1, 2) that are responsible for clearing excitotoxic glutamate levels from neuronal synapses. Glioma is shown to release high levels of glutamate and a failure of astrocytes to produced EAAT2 leads to impaired glutamate regulation and widespread neuronal death (Kim et al., 2011, Ye and Sontheimer, 1999, Marcus et al., 2010).

Increased expression of AEG-1 in astrocytes after neurodegenerative diseases include glioma and HIV-1 infection which causes reduced levels of EAAT2, meaning that AEG-1 negatively affected EAAT2 to uptake the high levels of glutamate, which leads to neuronal death. In normal astrocytes, a cyclic AMP-responsive element binding protein (CREB), interacted with EAAT2 promoter and

positively regulated EAAT2 expression, whilst in glioma, AEG-1 plays a key role by inhibiting EAAT2 levels.

AEG-1 was found to work as a bridge between CBP and a transcription factor called Ying Yang-1 (YY1) interaction in EAAT2 promoter in reactive astrocyte. This interaction caused YY1 to function negatively on EAAT2 by supressing CBP, which leads to disable abolishing glutamate from neurons synapses (**Figure 6.3)** (Lee et al., 2011).

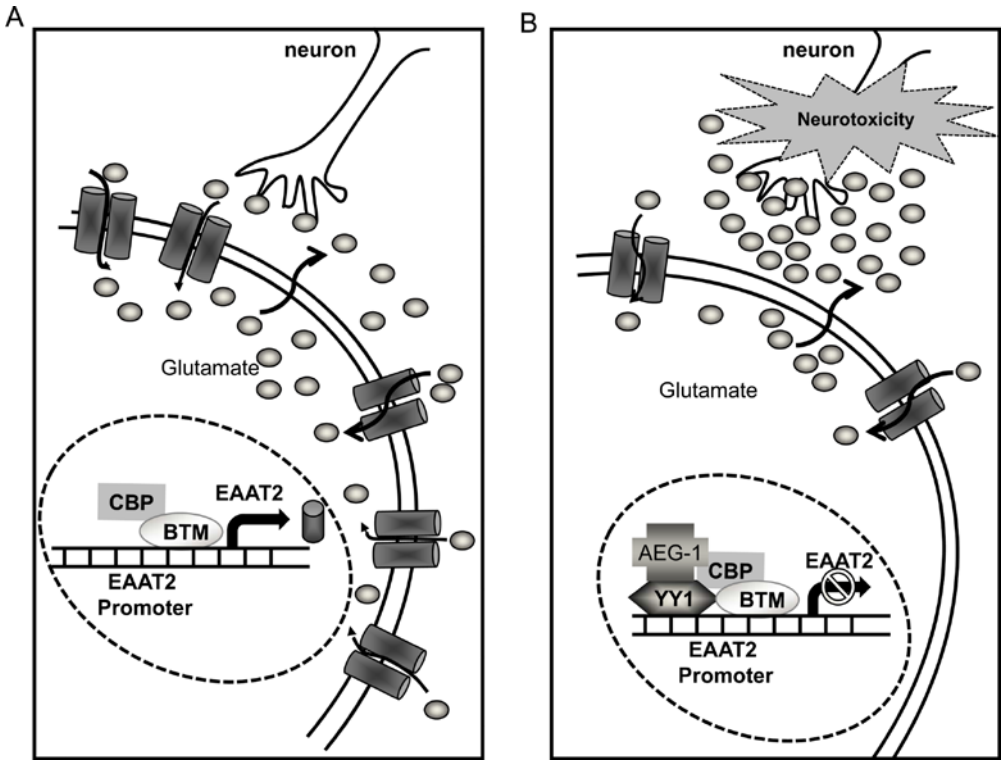

Figure 6.3: A schematic mechanism of AEG-1 supressed EAAT2 expression in human glioma. (A) Normal expression of EAAT2 in intact astrocyte. (B) In glioma, expression of AEG-1 negatively affects EAAT2 regulation leads to neuronal death. (Adapted from (Lee et al., 2011).

6.1.7 Hypothesis

We showed by microarrays that AEG-1 is extremely elevated in regenerating DRGN injury models compared to non-regenerating injury models. I therefore speculated whether high levels of AEG-1 are required to promote axon regeneration after SCI.

6.1.8 Aims

- Validate our microarray data by extracting mRNA from regenerating and non-regenerating DRGN injury models using RT-PCR.
- To determine AEG-1 protein levels using western blot from DRGN protein lysates.
- Localize AEG-1 protein in DRGN injury models by immunohistochemistry.
- Knock down AEG-1 using specific siRNA in primary DRGN to determine a role for AEG-1 in DRGN neurite outgrowth.

6.2 Results

6.2.1 AEG-1 mRNA levels increase in SN and pSN+DC injury models by microarray analysis.

As it is been described in the previous chapter, microarray data was scanned in non-regenerating DC and regenerating SN and pSN+DC models to identify genes that correlated with DC axon regeneration. One of these identified was AEG-1, whose mRNA levels were increased by 65- and 116-fold in SN and pSN+DC models, respectively (**Figure 6.4).** These results suggested that AEG-1 levels correlated with axon regeneration.

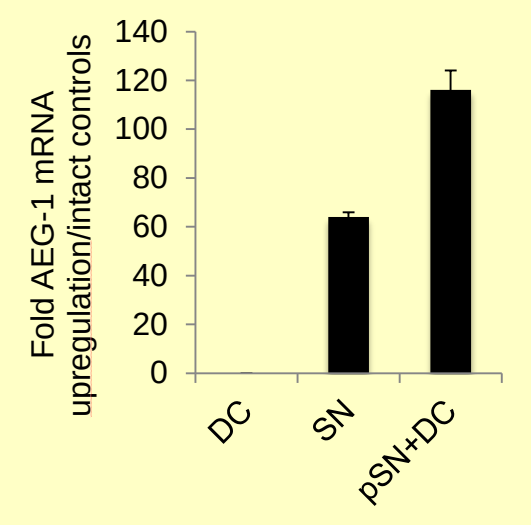

Figure 6.4: Levels of AEG-1 expression in regenerating and non-regenerating SCI models at 10 days after injury. Microarray data shows fold-change of AEG-1 mRNA in different models compared with intact controls. (n=6)

6.2.2 Confirmation of AEG-1 expression in pSN+DC

For further confirmation that the levels of AEG-1 were elevated in regenerating DRGN models, semi-quantitative RT-PCR in different injury models was used (**Figure 6.5A).** The results showed that high levels of AEG-1 mRNA expression was present in regenerating SN and pSN+DC compared with non-regenerating DC or intact controls, with pSN+DC model showing the greatest levels of AEG-1 mRNA.

Western blot of protein lysates also confirmed high levels of AEG-1 in regenerating SN and pSN+DC models (**Figure 6.5C),** with the greatest levels of AEG-1 protein being detected in pSN+DC models. Immunohistochemistry also corroborated these observations, showing that high levels of AEG-1 immunoreactivity was present in DRGN in SN and pSN+DC models, whilst low levels were detected in both intact and non-regenerating DC models (**Figure 6.6).** Taken together, these results suggested significant upregulation of AEG-1 in regenerating SN and pSN+DC, with the highest levels localised in DRGN after pSN+DC.

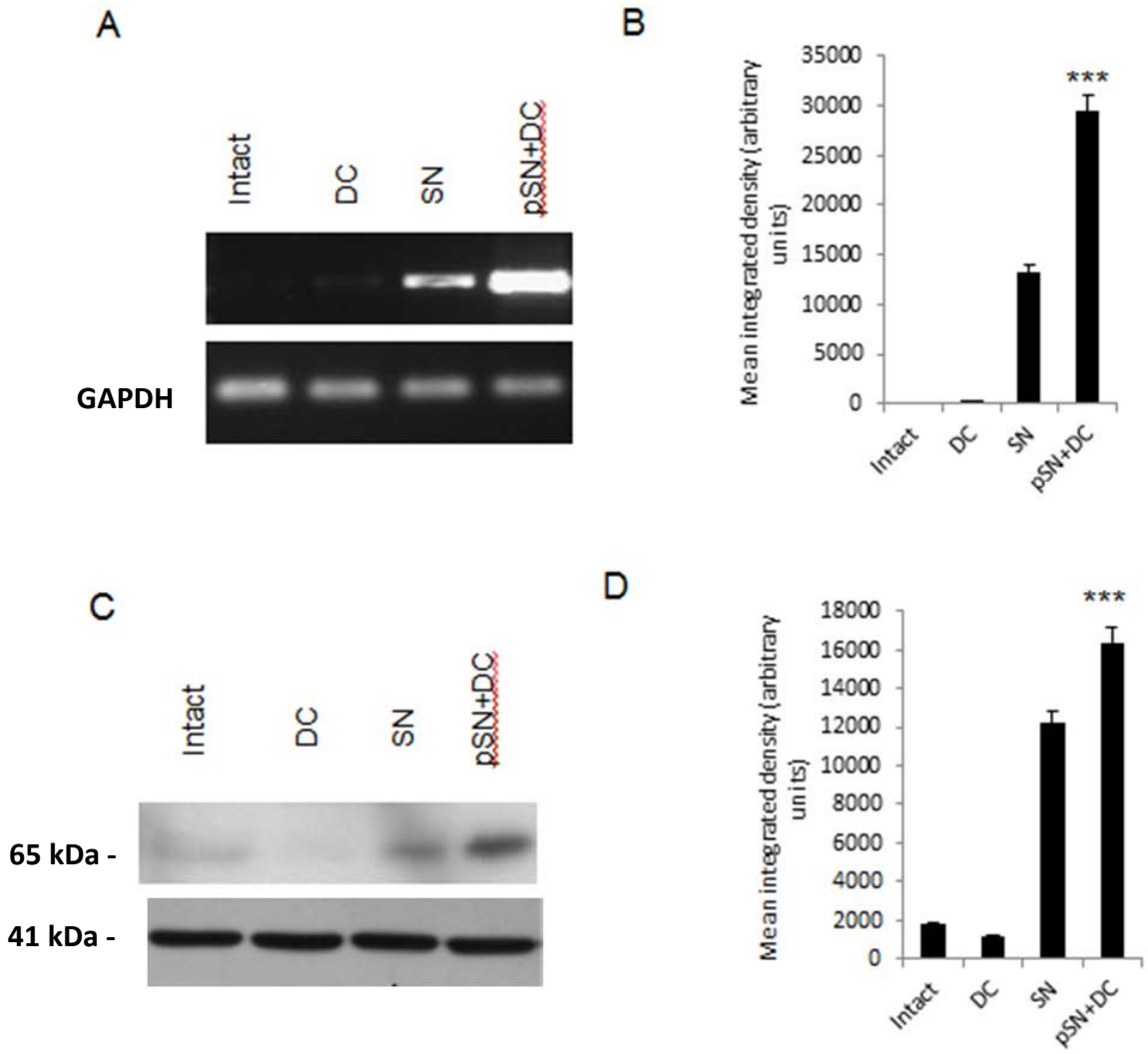

Figure 6.5: Levels of AEG-1 expression in regenerating and non-regenerating DRGN models at 7 days after injury.

(A) Semi-quantitative of RT-PCR from DRGN ganglia after SCI injury models showed increase expression of AEG-1 mRNA after pSN+DC. **(B)** Densitometry used to quantify the expression. **(C)** Western blotting from DRGN ganglia protein lysate corroborated RT-PCR results where **(D)** is densitometry of protein expression used in western blot. ***P<0.0001, Analysis of Variance. (n=3)

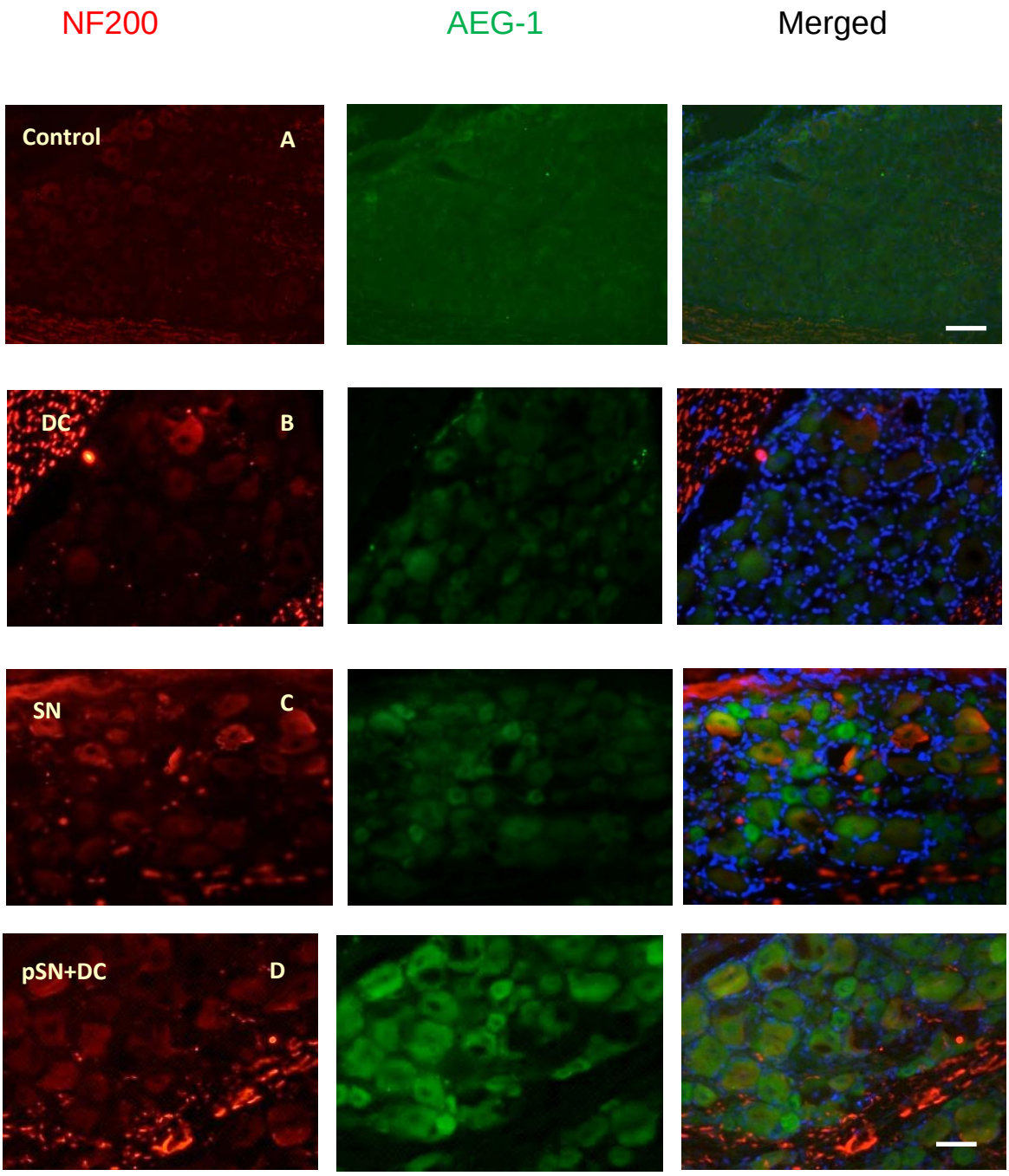

Figure 6.6: Levels of AEG-1 expression in regenerating and non-regenerating SCI models at 7 days after injury.

Immunohistochemistry shows low levels of AEG-1 protein in sections of intact control and after DC injury whilst increased AEG-1 immunohistochemistry levels were detected in sections of DRG from regenerating SN and pSN+DC models. Scale bar A= 500µm; B, C and D=50 µm. (n=3).

6.2.3 Knockdown of AEG-1 suppresses DRGN neurite outgrowth

Dissociated adult rat DRGN were used to investigate the consequence of AEG-1 knockdown on DRGN neurite outgrowth. Since high levels of AEG-1 correlate with DRGN axon regeneration, I predicted that knockdown of AEG-1 will reduce DRGN neurite outgrowth. DRGN were treated with Lipofectamine 2000 alone, siEGFP (non-specific transfection control), Scr-siAEG-11 (scrambled siRNA to AEG-1) and siAEG-1. DRGN were grown for 3 days and then knock down of AEG-1 was analysed by western blot, and found that (**Figure 6.7A)** there were no changes in AEG-1 protein level in Lipofectamine/untreated, siEGFP or Scr-siAEG-1-treated DRGN. However, DRGN treated with siAEG-1 showed reduced AEG-1 protein to barely detectable levels (**Figure 6.7B).** Densitometry to quantify the levels of AEG-1 protein showed 95% AEG-1 knockdown efficiency with siAEG-1 in DRGN cultures.

Immunohistochemistry for βIII-tubulin to measure DRGN survival and neurite outgrowth in FGF2, FGF2+siEGFP, FGF2+Scr-siAEG-1 and FGF2+siAEG-1 treated DRGN, showed that DRGN neurite outgrowth was significantly reduced after AEG-1 knockdown (**Figure 6.8A),** and in terms of the mean neurite length (**Figure 6.8B)** as well as, the number of DRGN with neurites (**Figure 6.8C).** DRGN survival however, was unaffected in all treated conditions (**Figure 6.8D)** showing that knockdown of AEG-1 gene has no toxicity in DRGN. These results demonstrate that AEG-1 knockdown suppresses DRGN neurite outgrowth, therefore it can be argued that AEG-1 is required for DRGN axon regeneration.

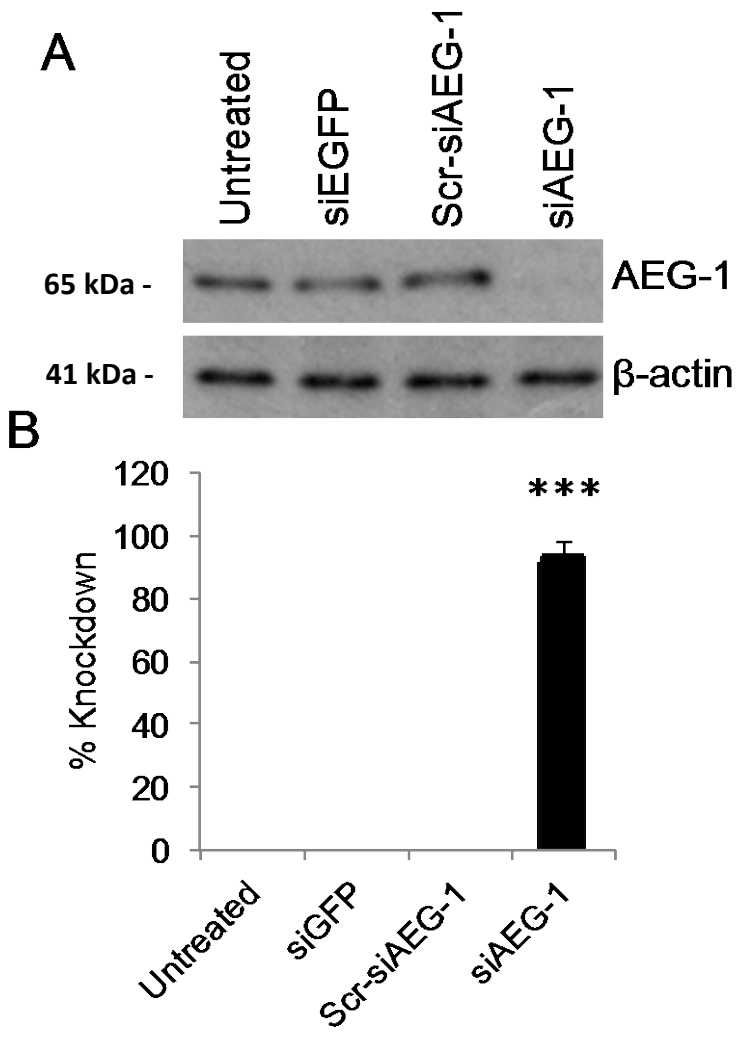

Figure 6.7: siRNA mediated knockdown of AEG-1.

(A) In Lipofectamine, siEGFP and Scr-siAEG-1-treated cultures, no changes in AEG-1 protein levels were observed. However, treatment siAEG-1 reduced AEG-1 protein to barely detectable levels. **(B)** Densitometry to quantify the levels of AEG-1 protein showed 95% AEG-1 knockdown efficiency with siAEG-1 in DRGN cultures. ***P<0.0001, Analysis of Variance. (n=3)

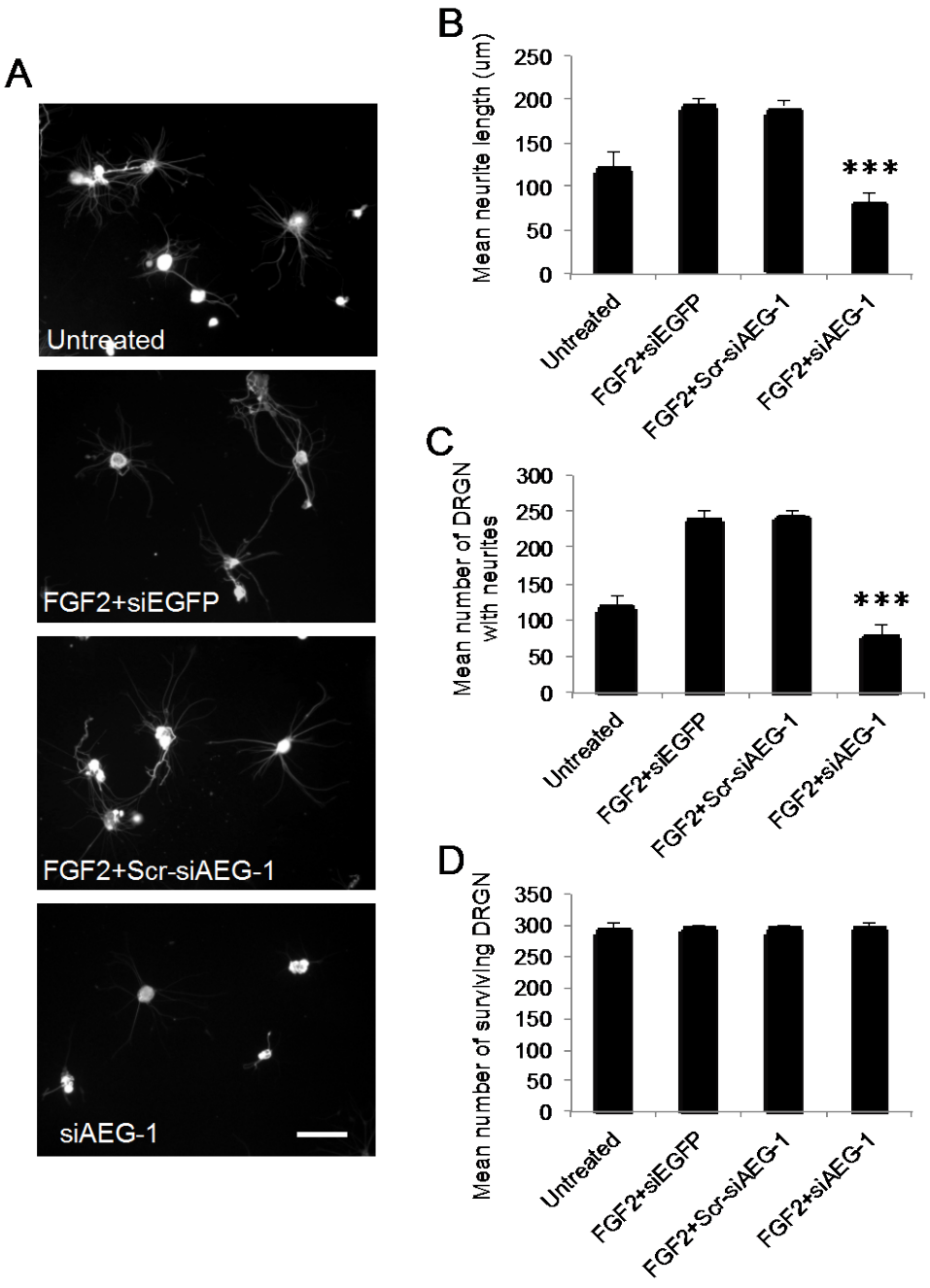

Figure 6.8: Knockdown of AEG-1 suppresses DRGN neurite outgrowth.

(A) photomicrographs of bIII-tubulin^{+} DRGN neurite outgrowth in untreated, FGF+siEGFP, FGF2+Scr-siAEG-1 and FGF2+siAEG-1 transfected DRGN for 3 days, **(B)** Mean neurite length (µm), **(C)** Mean number of DRGN with neurites and **(D)** Mean number of surviving DRGN. ***P<0.0001, Analysis of Variance. (n=3)

6.2.4 Knockdown of AEG-1 in DRGN cultures at 7 days after pre conditioning dorsal colum (pSN+DC) lesions

Since pre-conditioning SN lesions increase the levels of AEG-1 protein, I investigated if AEG-1 knockdown will also reduce DRGN neurite outgrowth in dissociated DRGN after pre-conditioning lesions. Firstly, knockdown of AEG-1 in pre-conditioning DRGN cultures were analysed by western blot and we found in (**Figure 6.A)** that DRGN treated with siAEG-1 showed reduction of protein levels compare to Lipofectamine/untreated, siEGFP and Scr-siAEG-1-treated DRGN. Densitometry to quantify the levels of AEG-1 protein showed 90% AEG-1 knockdown efficiency with siAEG-1 in DRGN cultures (**Figure 6.B)**.

After 7 days pre-conditioning, dissociated DRGN displayed greater than 4-fold more neurite lengths than dissociated DRGN that had not received pre-conditioning lesions (Compare **Figure 6.8B** to **Figure 6.B**). Treatment of dissociated pre-conditioned DRGN with siGFP or Scr-siAEG-1 did not reduce the number of DRGN with neurites (**Figure 6.B)** nor the mean neurite length (**Figure 6.C)**. However, knockdown of AEG-1 in pre-conditioned DRGN significantly reduced the number of DRGN with neurites **(Figure 6.C)** and the mean neurite length (**Figure 6.B)**. These results suggest that AEG-1 regulates DRGN neurite outgrowth even in pre-conditioned DRGN.

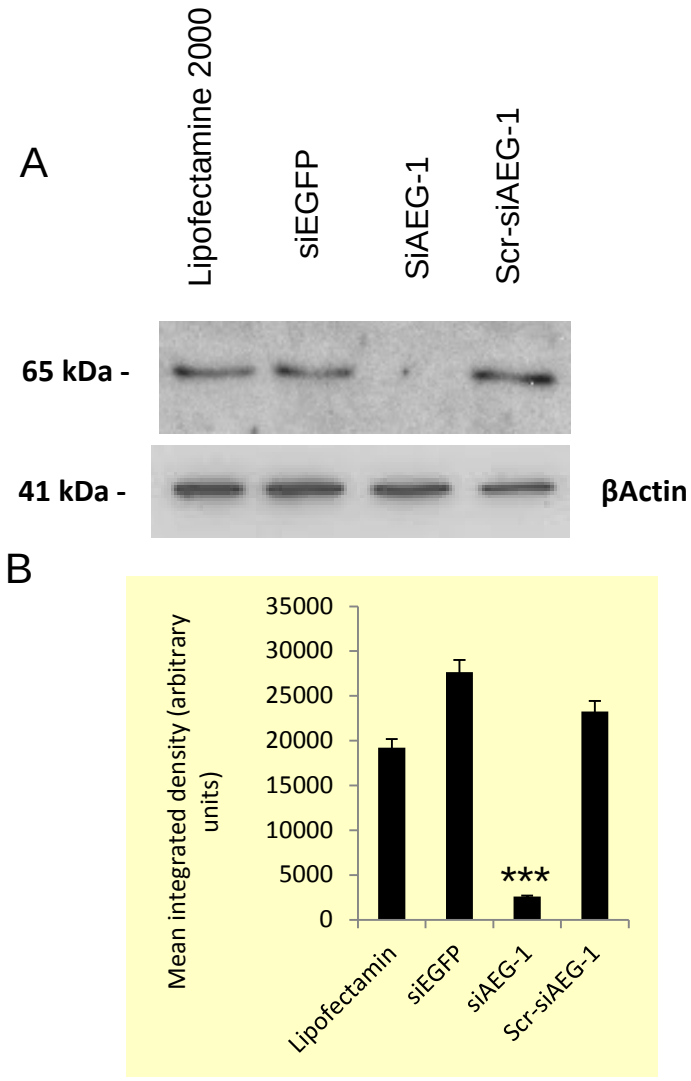

Figure 6.9: siAEG-1 also knocks down AEG-1 protein in pre-conditioned DRGN

(**A**) no change of AEG-1 protein levels was obsereved in untreated and treated pre-conditoned DRGN with no treatment, siEGFP and Scr-siAEG-1. DRGN treated with siAEG-1 showed significatnt reduction of AEG-1 protein levels. (**B**) Densitometry to quantify the suppression of AEG-1 protein levels. ***P<0.0001, Analysis of Variance. (n=3)

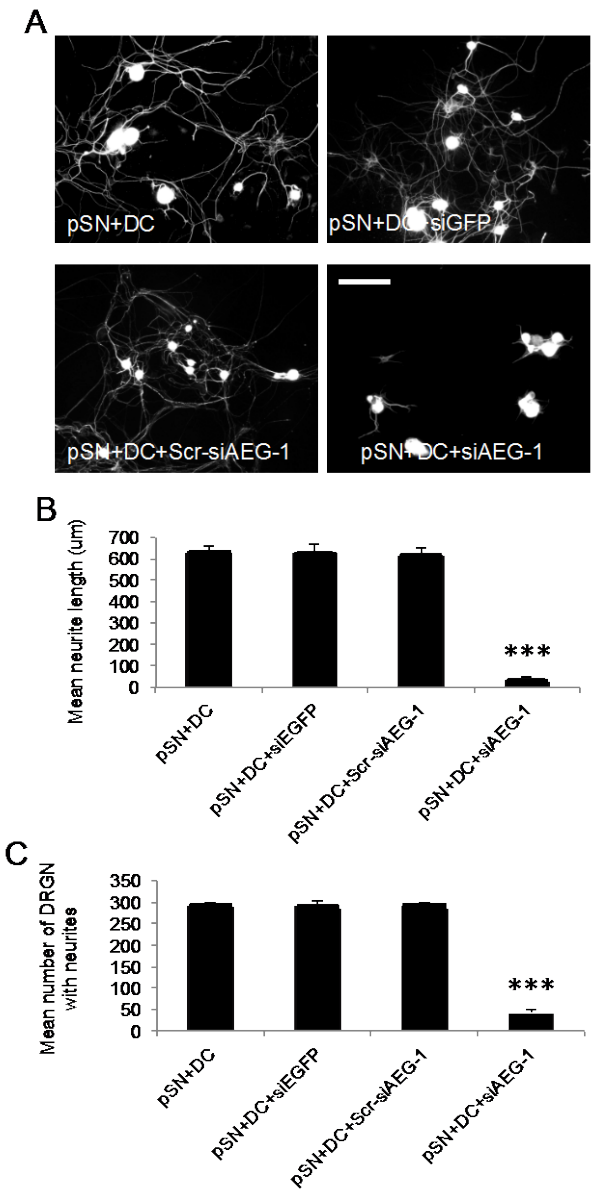

Figure 6.10: Knockdown of AEG-1 in DRGN cultures at 7 days after pSN+DC lesions.

(A) photomicrographs of βIII-tubulin+ DRGN neurite outgrowth in pSN+DC, pSN+DC+siEGFP, pSN+DC+Scr-siAEG-1 and pSN+DC+siAEG-1 transfected cells showing that AEG-1 significantly suppressed the growth of DRGN provided by pre-conditioning SN lesions. Quantification of the data showed that AEG-1 knockdown suppressed the **(B)** Mean number of DRGN with neurites and **(C)** Mean neurite length (um). ***P<0.0001, Analysis of Variance. (n=3)

6.3 Discussion

In this study I have investigated the role of AEG-1 in axonal regeneration. This was done by evaluating expression of AEG-1 in regenerating and non-regenerating DC injury models. I found that AEG-1 was highly elevated in regenerating injury models compared to intact and non-regenerating models. I also showed by siRNA-mediated knockdown in DRGN cultures that knockdown of AEG-1 suppressed DRGN neurite outgrowth. These results suggest that AEG-1 is required for axonal regeneration after CNS injury.

6.3.1 AEG-1 is may require for CNS axon regeneration

AEG-1 is said to modulate the response of astrocytes to injury and help in the formation of scar tissue or repair. The mechanism by which AEG-1 does this may not be known but there is evidence of increased levels of AEG-1 during astrogliosis and this expression helps migration and proliferation of astrocytes during CNS injury (Vartak-Sharma and Ghorpade, 2012). Besides its role in astrocyte, AEG-1 detected in highly in mouse brain embryos, demonstrating that AEG-1 may play an important role in development of the mouse brain (Jeon et al., 2010). Moreover, a recent study invstgated the role of AEG-1 after peripheral nerve injury and found that AEG-1 regulated migration and proliferation of Schwann cells after SN injury (Wang et al., 2016).

In fact, the role of AEG-1 in cancer was widely investigated as a crucial factor of proliferation and tumour progression. On the other hand, AEG-1 has been shown to have positive regulatory effects after nervous system injuries orchestrating migration and proliferation of glial cells and implicated in CNS scar healing (Vartak-Sharma and Ghorpade, 2012, Wang et al., 2016).

Our microarray data suggested that AEG-1 has a potential role in CNS axon regeneration. I found that AEG-1 was significantly up-regulated in regenerating SN and pSN+DC lesions compared with intact control and non-regenerating DC lesion models and thus correlated positively with axon regeneration.

6.3.2 Knockdown of AEG-1 supresses DRGN neurite outgrowth

Knockdown of AEG-1 in dissociated adult rat DRGN cultures showed that neurite outgrowth was significantly attenuated, without affecting DRGN survival. Even in pre-conditioned DRGN, knockdown of AEG-1 had the same effect of suppressing DRGN neurite outgrowth. These results confirm our predictions that knocking down AEG-1 negatively affects axon regeneration but has no significant effects on DRGN survival. The mechanisms by which AEG-1 promotes DRGN neurite outgrowth is not known, however, it is likely that AEG-1 modulates intracellular signaling pathways that promote DRGN neurite outgrowth. The elucidation of the mechanisms leading to enhanced DRGN neurite outgrowth will be investigated in future experiments.

CHAPTER 7: General Discussion

7.1 Summary findings

The main objective of this work is to promote CNS axon regeneration following CNS injury by manipulating some of the most highly regulated genes (i.e. AMIGO3, RTN3 and AEG-1) that obtained after microarrays screening of L4/5 DRGN that received regenerating and non-regenerating injury models. Since the main hypothesis of the thesis was to whether up/down-regulation of these genes would primary promote spinal cord axon regeneration.

I found in chapter 3 that AMIGO3 raised in DRGN after non-regenerating (DC) injury models compare to intact and regenerating models, as well as suppression of AMIGO3 combined with NT3 in presence of CME led to promote dissected DRGN neurite outgrowth, which suggested knockdown AMIGO3 enhance CNS axon growth after injury. However, based on *in vitro* outcomes; non-viral vector mediated shAMIGO3/NT3 plasmid was injected *in vivo* for 29 days after DC injury model aiming to disinhibit dorsal column axons from L4/5 DRGN. The results showed the plasmid encoding shAMIGO3/*nt3-gfp* targeted large DRGNs diameter compare to medium and small diameter and promotes axon regeneration since number of $GAP43^{+}$ (up to 4-6 mm) were observed passing through the lesion site and entering into the distal segment of the spinal cord. These results suggested that suppression of AMIGO3 combined with expression of NT3 simultaneous stimulation of DC axon regeneration and promotes functional recovery

Furthermore, inflammatory responses include macrophages, glial cells and T cells were also observed in animals groups injected with *in vivo*-jetPEI vector mediating DC+PEI-gfp, DC+PEI-nt3/gfp and DC+PEI-shAMIGO3/gfp plasmids. A slight increase of macrophages was seen in animals received *in vivo*-jetPEI/plasmids

compared to intact and PBS groups. However, $GFAP^+$ levels were virtually absence in intact animals and slightly increased in animals injected with PBS and *in vivo*-jetPEI/plasmids, the similar pattern between PBS and *in vivo*-jetPEI/plasmids groups may due to the mechanical breakthrough of the injection in DRGN bundle. On the other hand, no significant increase was observed in DRGN section of either CD8 or CD4 inflammatory markers following PBS or *in vivo*-jetPEI/plasmids. These outcomes conclude that *in vivo*-jetPEI is safe and does not induce inflammatory responses.

In chapter 5 and 6, mRNA levels of RTN3 and AEG-1 were elevated after pre-conditional lesions by 6 and 116-fold, respectively compared to intact and non-regenerating injury models. Immunohistochemistry and western blot results of both genes were correlated with microarrays data, suggested overexpression of both genes enhance CNS axon growth. By knocking down RTN3 and AEG-1 in primary DRGN culture using siRNA, results were showed the suppression of neurite outgrowth was correlated with knockdown of both genes, demonstrated that RTN3 and AEG-1 are required for CNS axon regeneration. However, overexpress of RTN3 *in vivo* using *in vivo*-jetPEI vector delivering plasmid encoding RTN3 resulted a number of $GAP43^+$ axons reached the lesion site and passed into the distal segment of the spinal cord.

The data presented in this thesis demonstrated that these genes identified by microarray screening play a part in the axon regeneration after SCI, and could be used to establish possible mechanisms to promote CNS axon growth in the human.

7.2 Combinatorial therapeutic strategies for SCI treatment hold much promise for the future

The majority of SCI experimental was to investigate the consequences of single treatment, but however recently combining treatments have a growing interest since they are likely to have much better outcomes than single treatment (Tsai et al., 2005, Wang et al., 2012a, Tom et al., 2013, Olson, 2013). A combinatorial strategy is required to promote optimal CNS axon regeneration due to the complexity of the injury. For example, Ahmed and others have shown that suppression of axon growth inhibitory molecules combined with neurotrophic factor stimulation promotes significant disinhibited DRGN neurite outgrowth in the presence of CME (Ahmed et al., 2005, Ahmed et al., 2006, Ahmed et al., 2009, Ahmed et al., 2011b).

However, shAMIGO3 combined with NT-3 (showed in Chapter 3) and overexpression of RTN3 (showed in Chapter 5) enhanced disinhibited DC axon regeneration after DC injury as well as up-regulation of AEG-1 (showed in Chapter 6). All of these treatments required an axon growth stimulus such as Nt3 or pre-conditioning lesions to effect better regeneration. Disappointingly due to lack of time, a combinatorial treatment of all of these genes could not be preform. Whilst, individual treatment for above genes showed a number of promising featured of DC axon regeneration combining these genes seems highly likely to prove to be more useful.

7.3 Advantages / disadvantages of *in vivo*-jetPEI

A polycation such as Polyethylenimine (PEI) is one of most highly used non-viral vectors to transfect DNA/RNA both *in vitro* and *in vivo* (Wu et al., 2004). One of the features of PEI is that it carries high concentration of positive charged nitrogen atoms allowing it to condense negative charges molecules such as DNA and form PEI/DNA complex that capable to enter the cell via endocytosis (Benjaminsen et al., 2013). In the *in vivo* study, PEI gives immediate therapeutic benefit once transfected compared to viral vectors that requires 7-14 days to reach maximum transgene expression (Lungwitz et al., 2005). PEI is therefore beneficial for acute condition such as SCI that requires immediate therapy. PEI tends to have a higher transfection efficiencies, up to 4X higher, than naked DNA, a higher biosafety, easy to prepare and highly stable in nature (Wiseman et al., 2003). PEI mediated nerve growth factor (NGF) has been used to protect axotomized septal cholinergic neurons (which is important for memory and learning) in the brain. Results showed 72% of these neurons survived in injured animals after PEI/pNGF injection (Wu et al., 2004). Moreover, PEI is safe and does not induce off-target immune-mediated cytokines such as TNF-α, IFN-γ, IL-6, IL-12/IL-23, IL-1β, and IFN-β (Bonnet et al., 2008). Therefore, the lack of immunogenic responses after PEI injection is to be expected and represents a further advantage over viral vectors. The disadvantage of non-viral carriers including PEI is that they have a lower transection efficiency compared to delivery efficiency of viral vectors (Yang, 2015), however, in DRGN this was not evident as we were able to transduce as many DRGN as viral vectors previously tested (Jacques et al., 2012).

7.4 Clinical trials in SCI

Whilst many SCI experimental therapeutics displayed promising results in laboratories and pre-clinical settings; only a few of these treatments have undergone testing in human clinical trials. There are three main categories of treatments that have reached clinical trials; regeneration promoting therapies, neuroprotective therapies and cell transplant strategies (Gensel et al., 2011, Varma et al., 2013). In regeneration promoting therapies, there are a few experimental treatments that have reached human testing. One of these is the humanised anti Nogo-A antibody, which thus far has completed the first phase of safety trials. Fifty two patients were recruited in this trial with different levels of spinal cord injuries and different severities, the anti-Nogo-A antibodies displayed no adverse effects after intrathecal administration, but disappointingly no positive findings were observed in terms of neurological changes (Zorner and Schwab, 2010). Moreover, Cethrin (a bacterial enzyme derived from C3 transferase lead to disrupt Rho-A signalling pathway by blocking Rho-A activity) has undergone phase I/IIa clinical trials, following completion of both phases the outcomes indicated no serious adverse effects upon extradural administration, but the treatments do result in enhanced motor recovery (Fehlings and Baptiste, 2005, Fehlings et al., 2011).

In addition, Ganglioside GM-1 is another therapeutic targeting regeneration, which is one of the largest SCI clinical trials in terms of the number of patients involved to assess the efficacy of this drug. GM-1 is derived from Gangliosides (complex glycolipids reside in cell membrane at high concentration found in CNS) and shown to promote axonal sprouting *in vitro* and enhanced regeneration in several

CNS injury models *in vivo* (Ferrari et al., 1983, Sabel et al., 1987). After safety trials in humans, intravenous dosing of GM-1 underwent phase 2 clinical trials but disappointingly no significant improvements in the primary outcomes were observed in SCI patients, except enhancement of bowel/bladder and sensory function (Geisler et al., 2001). Finally, oral administration of lithium was undertaken in clinical trials as potential treatment for SCI, in which lithium was found to block the actions of glycogen synthase kinase 3β (GSK-3β). This kinase was shown to inhibit axonal growth, however following intake of lithium no significant adverse effects or neurological outcomes were reported in either phase I or II trials (Dill et al., 2008, Yang et al., 2012).

In terms of neuroprotective therapies, the only treatment that has undergone numerous clinical tests and have been recommended to use in number of countries for clinical treatment of acute SCI is methylprednisolone (Bracken et al., 1997). Methylprednisolone is steroidal anti-inflammatory treatment that is recommended for patients that helps to attenuate secondary damage after SCI and shown to improve functional recovery if taken within eight hours of the injury (Bracken et al., 1990, Bracken et al., 1997). However, high doses of this drug have led to increased infection and respiratory complications therefore, as a standard of care it is no longer a treatment in the majority of the countries for acute SCI (Felleiter et al., 2012, Breslin and Agrawal, 2012). In contrast, other neuroprotective therapies that completed clinical trials have shown no significant benefit; one of these is Nimidopine (enhances cerebral blood flow to the cord by blocking calcium channels and decrease apoptosis in pre-clinical models) which increases risk of infection and has failed to display any significant neurobiological benefits in a 106 random control trials (Fehlings and Baptiste, 2005). Gacyclidine-

GK 11 (an N-methyl-D-aspartate (NMDA) receptor antagonist reduces glutamate excitotoxicity levels) is other neuroprotective agent demonstrated to have remarkable results in animal models after CNS trauma with fewer adverse effects compared to other NMDA receptor blockers. However, GK-11 showed no improvements in either sensory or motor function in clinical trials during one year of follow up (Fehlings and Baptiste, 2005, Tator, 2006).

Whilst, there has not been much success in various clinical trials of regenerative-promoting therapies and neuroprotective treatments, cell transplant strategies for SCI have also met with limited success. In cell-based strategies, stem cells among the number of cell types have been the most common cells used in clinical studies (Gensel et al., 2011, Varma et al., 2013). For example, mesenchymal stem cells (MSC) showed no adverse effects after intrathecal infusion, although in one trial neuropathic pain with spasticity was reported in some patients, however, modest improvements were reported in motor and/or sensory functions in many of these trials (Sykova et al., 2006) (Kumar et al., 2009, Kishk et al., 2010). Olfactory ensheathing cells (OECs) are another cell type that have been used in SCI clinical trials, based on promising results seen after OEC transplantation in experimental SCI models (Ramón-Cueto et al., 2000, Li et al., 2003). Following transplantation of OEC into human patients, one group have reported improvements in both motor and sensory functions (Lima et al., 2006, Lima et al., 2010) whilst no improvements have been noticed in other groups (Feron et al., 2005) with no serious remarkable adverse effects reported in both groups.

Finally, epidural stimulation enabled a twenty three years old man who had paraplegia from a C7–T1 subluxation as a result of a motor vehicle accident to achieve full weight-bearing standing with assistance provided only for balance for about 4 minutes as well as 7 months after implantation, the patient recovered supraspinal control of some leg movements, but only during epidural stimulation (Harkema et al., 2011).

All in all, there is yet to be a major success in SCI therapeutics from pre-clinical experimental to clinical efficacy in human patients. Whilst the failure of many trails is continuing, perhaps more caution should be taken into consideration before translating the treatment forward to the clinical test stage. Before any clinical trials of an experimental treatment, the therapeutics should be assessed in pre-clinical settings such as using the most common injury models (contusion or compression models) and assessed in small common animals e.g. rodents, and then progress to large clinically relevant animals such as porcine and non-human primates before being applied human patients.

7.5 Conclusions

In conclusion, this study was based on genes that were induced and modified after DC injury detected using microarray screening in non-regenerating and regenerating DRGN injury models. Over 300 genes were identified and speculated that regulation of these genes may play important roles in CNS axon regeneration. In this thesis, three genes (AMIGO3, RTN3 and AEG-1) were studied along with their manipulation in SCI models both *in vitro* and *in vivo*.

AMIGO3: *In vivo*-jetPEI vector mediated suppression of AMIGO3 combined with NT-3 *in vivo* enhanced DC axon regeneration. PEI/shAMIGO3-nt-gfp plasmid injected via intra-DRG route in L5 DRGN for 29 days was able to disinhibit axon regeneration, $GAP43^+$ fibres were observed crossing the DC lesion site and entering the distal segment of the spinal cord.

RTN3: since mRNA levels were up-regulated in regenerating injury models, we confirmed *in vitro* that overexpression of RTN3 promotes axon regeneration. Using *in vivo*-jetPEI transduced plasmids encoding RTN3 along with pre-conditioning lesions, we were subsequently able to enhance the number of $GAP43^+$ axon fibres crossing the lesion site and reaching into the distal cord.

AEG-1: mRNA levels of AEG-1 were found highly elevated (by 116-fold) in regenerating pSN+DC injury models after 7 days of injury. Our results showed AEG-1 protein levels were also enhanced in regenerating DRGN models and siRNA-mediated knockdown of AEG-1 in DRGN cultures suppressed DRGN neurite outgrowth, suggesting that AEG-1 is required for DRGN axon

regeneration. Disappointingly due to lack of time, I was unable to overexpress AEG-1 *in vivo* to confirm its role SCI.

7.6 Future work

There is much more further experimental work required and all work stated below for each chapter of the results was not completed due to lack of time within the project period. The author would be extremely interested in perform the following additional work with at least three experimental replicates for results assurance. The evidences resulting from the additional work would strongly support this study and hoping to participate in the future of SCI treatments.

Chapter 3: in-vivo suppression of AMIGO3 combined with overexpression of NT-3 disinhibited DC axon regeneration.

Suppression of AMIGO3 combined with overexpression of NT-3 using non-viral vector displayed promising results where axons regenerated from lumber region of rat spinal cord along to injury site at T8 after 29 days. It would be worth using further time point such as 6, 8 and 12 weeks to assess the efficacy of suppression of AMIGO3. Since my supervisor and I used partial laminectomy in this study, complete transection model of the spin could be used to assess knockdown of AMIGO3, and the complete cut area of the spinal cord could be supported by peripheral nerve graft (Cote et al., 2011) or collagen based gels loaded with Decorin and anti-scarring proteoglycans (Ahmed et al., 2014). Functional recovery

tests such as horizontal ladder or thermal stimuli following the above work should be used as further assessment of this study.

Chapter 4: Inflammatory-induced responses after non-viral mediated suppression of AMIGO3.

It would be better to determine the inflammatory response by fluorescence activity and looking at the DRGN for invasion of other cells of the immune system such as B cells and dendritic cells. As well as, identify the presence of other immune molecules such as chemokines and cytokines and quantify their levels following injection with *in vivo*-jetPEI/plasmids. However, it would be also worth to investigate endogenous immune response following shRNA/plasmids injection such as interferon/PKR. On the other hand, the use of naïve animals would be much more useful to determine the estimate levels of inflammation response cells that contributed to the procedure, this done by undergo the animals with the entire injection procedure without injection e.g. inserting the needle without releasing any fluids. This would clearly and facilitate the inflammation response involved in this procedure.

Chapter 5: overexpression of RTN3 enhances DC axon regeneration following SCI.

In this chapter, more *in vitro* and *in vivo* experimental works are required since a few preliminary *in vivo* data was done due to time constraint. The further works can fall into the following points:

- Scramble version of siRTN3 into primary DRGN culture. *In vivo* transection of Scr-siRTN3 will increase the fact that siRTN3 was specific to RTN3 and suppression of neurite outgrowth was due to knockdown of RTN3 not from siRNA.
- Examine the effect of overexpression of RTN3 on rat RohA levels. This can be done by transfecting COS-1 cell with full length of NgR1, p75 and AMIGO3 in presence of myelin substrate. Full length of RTN3 can be transfected upon transfection of these molecules and RohA level could be determine by western blot.
- Preform optimal concentration of RTN3/gfp plasmid that used in this study. It would be better to investigate the optimal concentration of RTN3 plasmid by transecting primary cultured DRGN with different concentrations starting from 0.5-4 µg of DNA plasmid likewise seen in chapter 3.

- Further *in vivo* experimental groups should be involved in future work. A number of additional groups should be added that include sham and PBS injection. This will ascertain the results showed after up-regulation of RTN3 was from the therapeutic plasmid not from other factors.

- More number of animals in each group should be added. I have used 3 animals in this study due the reason state above but it would be much better to employ at least 6 animals in each group for future work.
- Primarily using further time points starting from 3, 6, 8 and 12 weeks to determine the effect of RTN3 following DC injury, if the results are promising further time points could be used lasts up months.
- Preform quantification of axon fibres in DC lesion site as shown in section 3.3.8. Since the study was done on only 3 animals, the other strongly suggested to increase the number of animals that received PEI-RTN3/gfp and all animals will be subjected to count the $GAP43^{+}$ fibres from 4mm caudal and restoral of epicentre lesion.
- Up-regulation of RTN3 following complete transection of the spinal cord as described above, and support the lesion with peripheral graft or collagen based gel.

Chapter 6: novel role of AEG-1/MTDH/LYRIC in CNS axon regeneration.

Since up-regulation of AEG-1 has primarily shown to enhance CNS axon regeneration, it is necessary to assess the gene *in vivo* by plasmid injection as stated above. Most likely the further work of this chapter would be similar to chapter 5 future works since over expression of both genes would show similar results.

References

ACOSTA, C., DJOUHRI, L., WATKINS, R., BERRY, C., BROMAGE, K. & LAWSON, S. N. 2014. TREK2 expressed selectively in IB4-binding C-fiber nociceptors hyperpolarizes their membrane potentials and limits spontaneous pain. *J Neurosci,* 34**,** 1494-509.

AGUIRRE, A. & GALLO, V. 2007. Reduced EGFR signaling in progenitor cells of the adult subventricular zone attenuates oligodendrogenesis after demyelination. *Neuron Glia Biol,* 3**,** 209-20.

AGUZZI, A., BARRES, B. A. & BENNETT, M. L. 2013. Microglia: scapegoat, saboteur, or something else? *Science,* 339**,** 156-61.

AHMED, Z., DENT, R. G., SUGGATE, E. L., BARRETT, L. B., SEABRIGHT, R. J., BERRY, M. & LOGAN, A. 2005. Disinhibition of neurotrophin-induced dorsal root ganglion cell neurite outgrowth on CNS myelin by siRNA-mediated knockdown of NgR, p75NTR and Rho-A. *Molecular and cellular neurosciences,* 28**,** 509-23.

AHMED, Z., DOUGLAS, M. R., JOHN, G., BERRY, M. & LOGAN, A. 2013. AMIGO3 is an NgR1/p75 co-receptor signalling axon growth inhibition in the acute phase of adult central nervous system injury. *PLoS One,* 8**,** e61878.

AHMED, Z., DOUGLAS, M. R., READ, M. L., BERRY, M. & LOGAN, A. 2011a. Citron kinase regulates axon growth through a pathway that converges on cofilin downstream of RhoA. *Neurobiol Dis,* 41**,** 421-9.

AHMED, Z., DOUGLAS, M. R., READ, M. L., BERRY, M. & LOGAN, A. 2011b. Citron kinase regulates axon growth through a pathway that converges on cofilin downstream of RhoA. *Neurobiology of disease,* 41**,** 421-9.

AHMED, Z., JACQUES, S. J., BERRY, M. & LOGAN, A. 2009. Epidermal growth factor receptor inhibitors promote CNS axon growth through off-target effects on glia. *Neurobiology of disease,* 36**,** 142-50.

AHMED, Z., READ, M. L., BERRY, M. & LOGAN, A. 2010. Satellite glia not DRG neurons constitutively activate EGFR but EGFR inactivation is not correlated with axon regeneration. *Neurobiol Dis,* 39**,** 292-300.

AHMED, Z., SUGGATE, E. L., BROWN, E. R., DENT, R. G., ARMSTRONG, S. J., BARRETT, L. B., BERRY, M. & LOGAN, A. 2006. Schwann cell-derived factor-induced modulation of the NgR/p75NTR/EGFR axis disinhibits axon growth through CNS myelin in vivo and in vitro. *Brain : a journal of neurology,* 129**,** 1517-33.

AKHTAR, A. Z., PIPPIN, J. J. & SANDUSKY, C. B. 2008. Animal models in spinal cord injury: a review. *Rev Neurosci,* 19**,** 47-60.

ALBERTS, B., JOHNSON, A., LEWIS, J., RAFF, M., ROBERTS, K. & WALTER, P. 2002. Helper T cells and Lymphocyte activation.

ALLEN, A. R. 1911. Surgery of experimental lesion of spinal cord equivalent to crush injury of fracture dislocation of spinal column: a preliminary report. *Journal of the American Medical Association,* 57**,** 878-880.

ANKENY, D. P. & POPOVICH, P. G. 2009. Mechanisms and implications of adaptive immune responses after traumatic spinal cord injury. *Neuroscience,* 158**,** 1112-21.

ATWAL, J. K., PINKSTON-GOSSE, J., SYKEN, J., STAWICKI, S., WU, Y., SHATZ, C. & TESSIER-LAVIGNE, M. 2008. PirB is a functional receptor for myelin inhibitors of axonal regeneration. *Science,* 322**,** 967-970.

BARROS FILHO, T. E. & MOLINA, A. E. 2008. Analysis of the sensitivity and reproducibility of the Basso, Beattie, Bresnahan (BBB) scale in Wistar rats. *Clinics (Sao Paulo),* 63**,** 103-8.

BARTUS, K., GALINO, J., JAMES, N. D., HERNANDEZ-MIRANDA, L. R., DAWES, J. M., FRICKER, F. R., GARRATT, A. N., MCMAHON, S. B., RAMER, M. S., BIRCHMEIER, C., BENNETT, D. L. & BRADBURY, E. J. 2016. Neuregulin-1 controls an endogenous repair mechanism after spinal cord injury. *Brain,* 139**,** 1394-416.

BARTUS, K., JAMES, N. D., DIDANGELOS, A., BOSCH, K. D., VERHAAGEN, J., YANEZ-MUNOZ, R. J., ROGERS, J. H., SCHNEIDER, B. L., MUIR, E. M. & BRADBURY, E. J. 2014. Large-scale chondroitin sulfate proteoglycan digestion with chondroitinase gene therapy leads to reduced pathology and modulates macrophage phenotype following spinal cord contusion injury. *J Neurosci,* 34**,** 4822-36.

BASSO, D. M., BEATTIE, M. S. & BRESNAHAN, J. C. 1995. A sensitive and reliable locomotor rating scale for open field testing in rats. *J Neurotrauma,* 12**,** 1-21.

BASSO, D. M., BEATTIE, M. S., BRESNAHAN, J. C., ANDERSON, D. K., FADEN, A. I., GRUNER, J. A., HOLFORD, T. R., HSU, C. Y., NOBLE, L. J., NOCKELS, R., PEROT, P. L., SALZMAN, S. K. & YOUNG, W. 1996. MASCIS evaluation of open field locomotor scores: effects of experience and teamwork on reliability. Multicenter Animal Spinal Cord Injury Study. *J Neurotrauma,* 13**,** 343-59.

BEHAR, O., GOLDEN, J. A., MASHIMO, H., SCHOEN, F. J. & FISHMAN, M. C. 1996. Semaphorin III is needed for normal patterning and growth of nerves, bones and heart. *Nature,* 383**,** 525.

BENJAMINSEN, R. V., MATTEBJERG, M. A., HENRIKSEN, J. R., MOGHIMI, S. M. & ANDRESEN, T. L. 2013. The possible "proton sponge" effect of polyethylenimine (PEI) does not include change in lysosomal pH. *Molecular Therapy,* 21**,** 149-157.

BERANEK, J. 2005. CD68 is not a macrophage-specific antigen. *Annals of the rheumatic diseases,* 64**,** 342-344.

BERRY, M. 1982. Post-injury myelin-breakdown products inhibit axonal growth: an hypothesis to explain the failure of axonal regeneration in the mammalian central nervous system. *Bibl Anat***,** 1-11.

BERRY, M., CARLILE, J. & HUNTER, A. 1996. Peripheral nerve explants grafted into the vitreous body of the eye promote the regeneration of retinal ganglion cell axons severed in the optic nerve. *J Neurocytol,* 25**,** 147-70.

BERTRAM, C. D. & HEIL, M. 2017. A Poroelastic Fluid/Structure-Interaction Model of Cerebrospinal Fluid Dynamics in the Cord With Syringomyelia and Adjacent Subarachnoid-Space Stenosis. *J Biomech Eng,* 139.

BIVAS-BENITA, M., GILLARD, G. O., BAR, L., WHITE, K. A., WEBBY, R. J., HOVAV, A. H. & LETVIN, N. L. 2013. Airway CD8(+) T cells induced by pulmonary DNA immunization mediate protective anti-viral immunity. *Mucosal Immunol,* 6**,** 156-66.

BLAIN, A. M. 2009. *Investigating molecular mechanisms of neuronal regeneration: a microarray approach.* University of Glasgow.

BLAKEMORE, W. F. & KEIRSTEAD, H. S. 1999. The origin of remyelinating cells in the central nervous system. *J Neuroimmunol,* 98**,** 69-76.

BLIGHT, A. 2000. Animal models of spinal cord injury. *Topics in Spinal Cord Injury Rehabilitation,* 6**,** 1-13.

BLIGHT, A. R. 1985. Delayed demyelination and macrophage invasion: a candidate for secondary cell damage in spinal cord injury. *Cent Nerv Syst Trauma,* 2**,** 299-315.

BLIGHT, A. R. 1992. Macrophages and inflammatory damage in spinal cord injury. *J Neurotrauma,* 9 Suppl 1**,** S83-91.

BLIGHT, A. R., COHEN, T. I., SAITO, K. & HEYES, M. P. 1995. Quinolinic acid accumulation and functional deficits following experimental spinal cord injury. *Brain,* 118 (Pt 3)**,** 735-52.

BONNET, M.-E., ERBACHER, P. & BOLCATO-BELLEMIN, A.-L. 2008. Systemic delivery of DNA or siRNA mediated by linear polyethylenimine (L-PEI) does not induce an inflammatory response. *Pharmaceutical research,* 25**,** 2972.

BOUSSIF, O., LEZOUALC'H, F., ZANTA, M. A., MERGNY, M. D., SCHERMAN, D., DEMENEIX, B. & BEHR, J. P. 1995. A versatile vector for gene and oligonucleotide transfer into cells in culture and in vivo: polyethylenimine. *Proc Natl Acad Sci U S A,* 92**,** 7297-301.

BOUZIER-SORE, A. K., MERLE, M., MAGISTRETTI, P. J. & PELLERIN, L. 2002. Feeding active neurons: (re)emergence of a nursing role for astrocytes. *J Physiol Paris,* 96**,** 273-82.

BRACK-WERNER, R. 1999. Astrocytes: HIV cellular reservoirs and important participants in neuropathogenesis. *AIDS,* 13**,** 1-22.

BRACKEN, M. B., SHEPARD, M. J., COLLINS, W. F., HOLFORD, T. R., YOUNG, W., BASKIN, D. S., EISENBERG, H. M., FLAMM, E., LEO-SUMMERS, L., MAROON, J. & ET AL. 1990. A randomized, controlled trial of methylprednisolone or naloxone in the treatment of acute spinal-cord injury. Results of the Second National Acute Spinal Cord Injury Study. *N Engl J Med,* 322**,** 1405-11.

BRACKEN, M. B., SHEPARD, M. J., HOLFORD, T. R., LEO-SUMMERS, L., ALDRICH, E. F., FAZL, M., FEHLINGS, M., HERR, D. L., HITCHON, P. W., MARSHALL, L. F., NOCKELS, R. P., PASCALE, V., PEROT, P. L., JR., PIEPMEIER, J., SONNTAG, V. K., WAGNER, F., WILBERGER, J. E., WINN, H. R. & YOUNG, W. 1997. Administration of methylprednisolone for 24 or 48 hours or tirilazad mesylate for 48 hours in the treatment of acute spinal cord injury. Results of the Third National Acute Spinal Cord Injury Randomized Controlled Trial. National Acute Spinal Cord Injury Study. *JAMA,* 277**,** 1597-604.

BRADBURY, E. J., MOON, L. D., POPAT, R. J., KING, V. R., BENNETT, G. S., PATEL, P. N., FAWCETT, J. W. & MCMAHON, S. B. 2002. Chondroitinase ABC promotes functional recovery after spinal cord injury. *Nature,* 416**,** 636-40.

BRAHMACHARI, S., FUNG, Y. K. & PAHAN, K. 2006. Induction of glial fibrillary acidic protein expression in astrocytes by nitric oxide. *J Neurosci,* 26**,** 4930-9.

BREDESEN, D. E. 1995. Neural apoptosis. *Annals of neurology,* 38**,** 839-851.

BRESLIN, K. & AGRAWAL, D. 2012. The use of methylprednisolone in acute spinal cord injury: a review of the evidence, controversies, and recommendations. *Pediatric emergency care,* 28**,** 1238-1245.

BRITT, D. E., YANG, D. F., YANG, D. Q., FLANAGAN, D., CALLANAN, H., LIM, Y. P., LIN, S. H. & HIXSON, D. C. 2004. Identification of a novel protein, LYRIC, localized to tight junctions of polarized epithelial cells. *Exp Cell Res,* 300**,** 134-48.

BROWN, D. M. & RUOSLAHTI, E. 2004. Metadherin, a cell surface protein in breast tumors that mediates lung metastasis. *Cancer Cell,* 5**,** 365-74.

BULSARA, K. R., ISKANDAR, B. J., VILLAVICENCIO, A. T. & SKENE, J. H. 2002. A new millenium for spinal cord regeneration: growth-associated genes. *Spine (Phila Pa 1976),* 27**,** 1946-9.

BUNDESEN, L. Q., SCHEEL, T. A., BREGMAN, B. S. & KROMER, L. F. 2003. Ephrin-B2 and EphB2 regulation of astrocyte-meningeal fibroblast interactions in response to spinal cord lesions in adult rats. *J Neurosci,* 23**,** 7789-800.

BUNGE, R. G. 1960. NEW FACES FOR A NEW ERA IN MEDICINE. *JAMA,* 173**,** 1438-1441.

BUNGE, R. G. & BRADBURY, J. T. 1961. Intratubular bodies of the human testis. *J Urol,* 85**,** 306-10.

CAI, Y., SAIYIN, H., LIN, Q., ZHANG, P., TANG, L., PAN, X. & YU, L. 2005. Identification of a new RTN3 transcript, RTN3-A1, and its distribution in adult mouse brain. *Brain Res Mol Brain Res,* 138**,** 236-43.

CAO, L. & HE, C. 2013. Polarization of macrophages and microglia in inflammatory demyelination. *Neurosci Bull,* 29**,** 189-98.

CARIM-TODD, L., ESCARCELLER, M., ESTIVILL, X. & SUMOY, L. 2003. LRRN6A/LERN1 (leucine-rich repeat neuronal protein 1), a novel gene with enriched expression in limbic system and neocortex. *Eur J Neurosci,* 18**,** 3167-82.

CASE, L. C. & TESSIER-LAVIGNE, M. 2005. Regeneration of the adult central nervous system. *Current biology,* 15**,** R749-R753.

CASHA, S., YU, W. & FEHLINGS, M. 2001. Oligodendroglial apoptosis occurs along degenerating axons and is associated with FAS and p75 expression following spinal cord injury in the rat. *Neuroscience,* 103**,** 203-218.

CHEN, Y., AULIA, S., LI, L. & TANG, B. L. 2006. AMIGO and friends: an emerging family of brain-enriched, neuronal growth modulating, type I transmembrane proteins with leucine-rich repeats (LRR) and cell adhesion molecule motifs. *Brain Res Rev,* 51**,** 265-74.

CHEN, Y., HOR, H. H. & TANG, B. L. 2012. AMIGO is expressed in multiple brain cell types and may regulate dendritic growth and neuronal survival. *Journal of cellular physiology,* 227**,** 2217-2229.

CHERIYAN, T., RYAN, D. J., WEINREB, J. H., CHERIYAN, J., PAUL, J. C., LAFAGE, V., KIRSCH, T. & ERRICO, T. J. 2014. Spinal cord injury models: a review. *Spinal Cord,* 52**,** 588-95.

CHIURCHIU, V., MACCARRONE, M. & ORLACCHIO, A. 2014. The role of reticulons in neurodegenerative diseases. *Neuromolecular Med,* 16**,** 3-15.

CHO, J. H., LEPINE, M., ANDREWS, W., PARNAVELAS, J. & CLOUTIER, J. F. 2007. Requirement for Slit-1 and Robo-2 in zonal segregation of olfactory sensory neuron axons in the main olfactory bulb. *J Neurosci,* 27**,** 9094-104.

CHONG, M., WOOLF, C., HAQUE, N. & ANDERSON, P. 1999. Axonal regeneration from injured dorsal roots into the spinal cord of adult rats. *Journal of Comparative Neurology,* 410**,** 42-54.

CHRISTENSEN, M. D., EVERHART, A. W., PICKELMAN, J. T. & HULSEBOSCH, C. E. 1996. Mechanical and thermal allodynia in chronic central pain following spinal cord injury. *Pain,* 68**,** 97-107.

CHRISTENSEN, M. D. & HULSEBOSCH, C. E. 1997. Chronic central pain after spinal cord injury. *J Neurotrauma,* 14**,** 517-37.

CHUNG, K., LANGFORD, L. A. & COGGESHALL, R. E. 1987. Primary afferent and propriospinal fibers in the rat dorsal and dorsolateral funiculi. *J Comp Neurol,* 263**,** 68-75.

CODELUPPI, S., SVENSSON, C. I., HEFFERAN, M. P., VALENCIA, F., SILLDORFF, M. D., OSHIRO, M., MARSALA, M. & PASQUALE, E. B. 2009. The Rheb–mTOR pathway is upregulated in reactive astrocytes of the injured spinal cord. *Journal of Neuroscience,* 29**,** 1093-1104.

COTE, M. P., AMIN, A. A., TOM, V. J. & HOULE, J. D. 2011. Peripheral nerve grafts support regeneration after spinal cord injury. *Neurotherapeutics,* 8**,** 294-303.

DAVID, S. & AGUAYO, A. J. 1981. Axonal elongation into peripheral nervous system "bridges" after central nervous system injury in adult rats. *Science,* 214**,** 931-933.

DAVID, S. & KRONER, A. 2011. Repertoire of microglial and macrophage responses after spinal cord injury. *Nat Rev Neurosci,* 12**,** 388-99.

DAVIDSON, B. L. & BREAKEFIELD, X. O. 2003. Viral vectors for gene delivery to the nervous system. *Nat Rev Neurosci,* 4**,** 353-64.

DAVOODY, L., QUITON, R. L., LUCAS, J. M., JI, Y., KELLER, A. & MASRI, R. 2011. Conditioned place preference reveals tonic pain in an animal model of central pain. *J Pain,* 12**,** 868-74.

DAYA, S. & BERNS, K. I. 2008. Gene therapy using adeno-associated virus vectors. *Clin Microbiol Rev,* 21**,** 583-93.

DE POMMERY, J., ROUDIER, F. & MENETREY, D. 1984. Postsynaptic fibers reaching the dorsal column nuclei in the rat. *Neurosci Lett,* 50**,** 319-23.

DE WINTER, F., OUDEGA, M., LANKHORST, A. J., HAMERS, F. P., BLITS, B., RUITENBERG, M. J., PASTERKAMP, R. J., GISPEN, W. H. & VERHAAGEN, J. 2002. Injury-induced class 3 semaphorin expression in the rat spinal cord. *Exp Neurol,* 175**,** 61-75.

DE WIT, J. & GHOSH, A. 2014. Control of neural circuit formation by leucine-rich repeat proteins. *Trends Neurosci,* 37**,** 539-50.

DE WIT, J., HONG, W., LUO, L. & GHOSH, A. 2011. Role of leucine-rich repeat proteins in the development and function of neural circuits. *Annu Rev Cell Dev Biol,* 27**,** 697-729.

DEMENEIX, B., BEHR, J., BOUSSIF, O., ZANTA, M. A., ABDALLAH, B. & REMY, J. 1998. Gene transfer with lipospermines and polyethylenimines. *Adv Drug Deliv Rev,* 30**,** 85-95.

DENG, M. Z., HE, W. X., TAN, Y., HAN, H. L., HU, X. Y., XIA, K., ZHANG, Z. H. & YAN, R. Q. 2013. Increased Expression of Reticulon 3 in Neurons Leads to Reduced Axonal Transport of beta Site Amyloid Precursor Protein-cleaving Enzyme 1. *Journal of Biological Chemistry,* 288**,** 30236-30245.

DEVIVO, M. J. 2012. Epidemiology of traumatic spinal cord injury: trends and future implications. *Spinal Cord,* 50**,** 365-72.

DI GIOVANNI, S. 2006. Regeneration following spinal cord injury, from experimental models to humans: where are we? *Expert Opin Ther Targets,* 10**,** 363-76.

DIJKSTRA, C. D., DOPP, E. A., JOLING, P. & KRAAL, G. 1985. The heterogeneity of mononuclear phagocytes in lymphoid organs: distinct macrophage subpopulations in the rat recognized by monoclonal antibodies ED1, ED2 and ED3. *Immunology,* 54**,** 589-99.

DILL, J., WANG, H., ZHOU, F. & LI, S. 2008. Inactivation of glycogen synthase kinase 3 promotes axonal growth and recovery in the CNS. *J Neurosci,* 28**,** 8914-28.

DOMENICONI, M., CAO, Z., SPENCER, T., SIVASANKARAN, R., WANG, K., NIKULINA, E., KIMURA, N., CAI, H., DENG, K., GAO, Y., HE, Z. & FILBIN, M. 2002. Myelin-associated glycoprotein interacts with the Nogo66 receptor to inhibit neurite outgrowth. *Neuron,* 35**,** 283-90.

DUFFY, P., WANG, X., SIEGEL, C. S., TU, N., HENKEMEYER, M., CAFFERTY, W. B. & STRITTMATTER, S. M. 2012. Myelin-derived ephrinB3 restricts axonal regeneration and recovery after adult CNS injury. *Proc Natl Acad Sci U S A,* 109**,** 5063-8.

ELLERMEIER, J., WEI, J., DUEWELL, P., HOVES, S., STIEG, M. R., ADUNKA, T., NOERENBERG, D., ANDERS, H. J., MAYR, D., POECK, H., HARTMANN, G., ENDRES, S. & SCHNURR, M. 2013. Therapeutic efficacy of bifunctional siRNA combining TGF-beta1 silencing with RIG-I activation in pancreatic cancer. *Cancer Res,* 73**,** 1709-20.

EMDAD, L., DAS, S. K., DASGUPTA, S., HU, B., SARKAR, D. & FISHER, P. B. 2013. AEG-1/MTDH/LYRIC: signaling pathways, downstream genes, interacting proteins, and regulation of tumor angiogenesis. *Adv Cancer Res,* 120**,** 75-111.

ERTURK, A., HELLAL, F., ENES, J. & BRADKE, F. 2007. Disorganized microtubules underlie the formation of retraction bulbs and the failure of axonal regeneration. *J Neurosci,* 27**,** 9169-80.

ESKANDER, M. A., RUPAREL, S., GREEN, D. P., CHEN, P. B., POR, E. D., JESKE, N. A., GAO, X., FLORES, E. R. & HARGREAVES, K. M. 2015. Persistent Nociception Triggered by Nerve Growth Factor (NGF) Is Mediated by TRPV1 and Oxidative Mechanisms. *J Neurosci,* 35**,** 8593-603.

EVA, R., ANDREWS, M. R., FRANSSEN, E. H. & FAWCETT, J. W. 2012. Intrinsic mechanisms regulating axon regeneration: an integrin perspective. *Int Rev Neurobiol,* 106**,** 75-104.

FABES, J., ANDERSON, P., BRENNAN, C. & BOLSOVER, S. 2007. Regeneration-enhancing effects of EphA4 blocking peptide following corticospinal tract injury in adult rat spinal cord. *Eur J Neurosci,* 26**,** 2496-505.

FAGOE, N. D., ATTWELL, C. L., KOUWENHOVEN, D., VERHAAGEN, J. & MASON, M. R. 2015. Overexpression of ATF3 or the combination of ATF3, c-Jun, STAT3 and Smad1 promotes regeneration of the central axon branch of sensory neurons but without synergistic effects. *Human molecular genetics,* 24**,** 6788-6800.

FAULKNER, J. & KEIRSTEAD, H. S. 2005. Human embryonic stem cell-derived oligodendrocyte progenitors for the treatment of spinal cord injury. *Transpl Immunol,* 15**,** 131-42.

FAULKNER, J. R., HERRMANN, J. E., WOO, M. J., TANSEY, K. E., DOAN, N. B. & SOFRONIEW, M. V. 2004. Reactive astrocytes protect tissue and preserve function after spinal cord injury. *J Neurosci,* 24**,** 2143-55.

FAWCETT, J. W. & ASHER, R. A. 1999. The glial scar and central nervous system repair. *Brain Res Bull,* 49**,** 377-91.

FEHLINGS, M. G. & BAPTISTE, D. C. 2005. Current status of clinical trials for acute spinal cord injury. *Injury,* 36 Suppl 2**,** B113-22.

FEHLINGS, M. G., THEODORE, N., HARROP, J., MAURAIS, G., KUNTZ, C., SHAFFREY, C. I., KWON, B. K., CHAPMAN, J., YEE, A., TIGHE, A. & MCKERRACHER, L. 2011. A phase I/IIa clinical trial of a recombinant Rho protein antagonist in acute spinal cord injury. *J Neurotrauma,* 28**,** 787-96.

FELLEITER, P., MÜLLER, N., SCHUMANN, F., FELIX, O. & LIERZ, P. 2012. Changes in the use of the methylprednisolone protocol for traumatic spinal cord injury in Switzerland. *Spine,* 37**,** 953-956.

FENG, L., LI, F., LIU, Y., ZHENG, X., ZHANG, B. & CHEN, L. 2009. A convenient plasmid-based system containing three reporter genes for real-time and quantitative analysis of messenger RNA silencing. *Anal Biochem,* 394**,** 284-6.

FERNANDES, K. J., FAN, D. P., TSUI, B. J., CASSAR, S. L. & TETZLAFF, W. 1999. Influence of the axotomy to cell body distance in rat rubrospinal and spinal motoneurons: differential regulation of GAP-43, tubulins, and neurofilament-M. *J Comp Neurol,* 414**,** 495-510.

FERON, F., PERRY, C., COCHRANE, J., LICINA, P., NOWITZKE, A., URQUHART, S., GERAGHTY, T. & MACKAY-SIM, A. 2005. Autologous olfactory ensheathing cell transplantation in human spinal cord injury. *Brain,* 128**,** 2951-60.

FERRARI, G., FABRIS, M. & GORIO, A. 1983. Gangliosides enhance neurite outgrowth in PC12 cells. *Brain Res,* 284**,** 215-21.

FIDLER, P. S., SCHUETTE, K., ASHER, R. A., DOBBERTIN, A., THORNTON, S. R., CALLE-PATINO, Y., MUIR, E., LEVINE, J. M., GELLER, H. M. & ROGERS, J. H. 1999. Comparing astrocytic cell lines that are inhibitory or permissive for axon growth: the major axon-inhibitory proteoglycan is NG2. *Journal of Neuroscience,* 19**,** 8778-8788.

FILBIN, M. T. 2003. Myelin-associated inhibitors of axonal regeneration in the adult mammalian CNS. *Nat Rev Neurosci,* 4**,** 703-13.

FISHER, D., XING, B., DILL, J., LI, H., HOANG, H. H., ZHAO, Z., YANG, X.-L., BACHOO, R., CANNON, S. & LONGO, F. M. 2011. Leukocyte common antigen-related phosphatase is a functional receptor for chondroitin sulfate proteoglycan axon growth inhibitors. *Journal of Neuroscience,* 31**,** 14051-14066.

FITCH, M. T., DOLLER, C., COMBS, C. K., LANDRETH, G. E. & SILVER, J. 1999. Cellular and molecular mechanisms of glial scarring and progressive cavitation: in vivo and in vitro analysis of inflammation-induced secondary injury after CNS trauma. *J Neurosci,* 19**,** 8182-98.

FITCH, M. T. & SILVER, J. 2008. CNS injury, glial scars, and inflammation: Inhibitory extracellular matrices and regeneration failure. *Exp Neurol,* 209**,** 294-301.

FLEMING, J. C., NORENBERG, M. D., RAMSAY, D. A., DEKABAN, G. A., MARCILLO, A. E., SAENZ, A. D., PASQUALE-STYLES, M., DIETRICH, W. D. & WEAVER, L. C. 2006. The cellular inflammatory response in human spinal cords after injury. *Brain,* 129**,** 3249-69.

FOROSTYAK, S., JENDELOVA, P. & SYKOVA, E. 2013. The role of mesenchymal stromal cells in spinal cord injury, regenerative medicine and possible clinical applications. *Biochimie,* 95**,** 2257-70.

FOURNIER, A. E., GRANDPRE, T. & STRITTMATTER, S. M. 2001. Identification of a receptor mediating Nogo-66 inhibition of axonal regeneration. *Nature,* 409**,** 341-6.

GAGE, F. H. 2000. Mammalian neural stem cells. *Science,* 287**,** 1433-8.

GAO, Y., NIKULINA, E., MELLADO, W. & FILBIN, M. T. 2003. Neurotrophins elevate cAMP to reach a threshold required to overcome inhibition by MAG through extracellular signal-regulated kinase-dependent inhibition of phosphodiesterase. *Journal of Neuroscience,* 23**,** 11770-11777.

GEISLER, F. H., COLEMAN, W. P., GRIECO, G., POONIAN, D. & SYGEN STUDY, G. 2001. Measurements and recovery patterns in a multicenter study of acute spinal cord injury. *Spine (Phila Pa 1976),* 26**,** S68-86.

GENSEL, J. C., DONNELLY, D. J. & POPOVICH, P. G. 2011. Spinal cord injury therapies in humans: an overview of current clinical trials and their potential effects on intrinsic CNS macrophages. *Expert opinion on therapeutic targets,* 15**,** 505-518.

GIESLER, G. J., JR. & CLIFFER, K. D. 1985. Postsynaptic dorsal column pathway of the rat. II. Evidence against an important role in nociception. *Brain Res,* 326**,** 347-56.

GIESLER, G. J., JR., NAHIN, R. L. & MADSEN, A. M. 1984. Postsynaptic dorsal column pathway of the rat. I. Anatomical studies. *J Neurophysiol,* 51**,** 260-75.

GIGER, R. J., HOLLIS, E. R., 2ND & TUSZYNSKI, M. H. 2010. Guidance molecules in axon regeneration. *Cold Spring Harb Perspect Biol,* 2**,** a001867.

GIL, V., BICHLER, Z., LEE, J. K., SEIRA, O., LLORENS, F., BRIBIAN, A., MORALES, R., CLAVEROL-TINTURE, E., SORIANO, E., SUMOY, L., ZHENG, B. & DEL RIO, J. A. 2010. Developmental expression of the oligodendrocyte myelin glycoprotein in the mouse telencephalon. *Cereb Cortex,* 20**,** 1769-79.

GIUFFRIDA, R. & RUSTIONI, A. 1992. Dorsal root ganglion neurons projecting to the dorsal column nuclei of rats. *J Comp Neurol,* 316**,** 206-20.

GLEDHILL, R. F., HARRISON, B. M. & MCDONALD, W. I. 1973. Demyelination and remyelination after acute spinal cord compression. *Exp Neurol,* 38**,** 472-87.

GOLDSHMIT, Y., GALEA, M. P., WISE, G., BARTLETT, P. F. & TURNLEY, A. M. 2004. Axonal regeneration and lack of astrocytic gliosis in EphA4-deficient mice. *J Neurosci,* 24**,** 10064-73.

GORITZ, C., DIAS, D. O., TOMILIN, N., BARBACID, M., SHUPLIAKOV, O. & FRISEN, J. 2011. A pericyte origin of spinal cord scar tissue. *Science,* 333**,** 238-42.

GRILL, R. J., BLESCH, A. & TUSZYNSKI, M. H. 1997. Robust growth of chronically injured spinal cord axons induced by grafts of genetically modified NGF-secreting cells. *Exp Neurol,* 148**,** 444-52.

GRIMPE, B. & SILVER, J. 2004. A novel DNA enzyme reduces glycosaminoglycan chains in the glial scar and allows microtransplanted dorsal root ganglia axons to regenerate beyond lesions in the spinal cord. *J Neurosci,* 24**,** 1393-7.

GUEST, J. D., HIESTER, E. D. & BUNGE, R. P. 2005. Demyelination and Schwann cell responses adjacent to injury epicenter cavities following chronic human spinal cord injury. *Exp Neurol,* 192**,** 384-93.

HABIB, A. A., MARTON, L. S., ALLWARDT, B., GULCHER, J. R., MIKOL, D. D., HOGNASON, T., CHATTOPADHYAY, N. & STEFANSSON, K. 1998. Expression of the oligodendrocyte-myelin glycoprotein by neurons in the mouse central nervous system. *J Neurochem,* 70**,** 1704-11.

HAINES, B. P. & RIGBY, P. W. 2008. Expression of the Lingo/LERN gene family during mouse embryogenesis. *Gene Expr Patterns,* 8**,** 79-86.

HAMMOND, T. R., GADEA, A., DUPREE, J., KERNINON, C., NAIT-OUMESMAR, B., AGUIRRE, A. & GALLO, V. 2014. Astrocyte-derived endothelin-1 inhibits remyelination through notch activation. *Neuron,* 81**,** 588-602.

HARKEMA, S., GERASIMENKO, Y., HODES, J., BURDICK, J., ANGELI, C., CHEN, Y., FERREIRA, C., WILLHITE, A., REJC, E., GROSSMAN, R. G. & EDGERTON, V. R. 2011. Effect of epidural stimulation of the lumbosacral spinal cord on voluntary movement, standing, and assisted stepping after motor complete paraplegia: a case study. *Lancet,* 377**,** 1938-47.

HATA, K., FUJITANI, M., YASUDA, Y., DOYA, H., SAITO, T., YAMAGISHI, S., MUELLER, B. K. & YAMASHITA, T. 2006. RGMa inhibition promotes axonal growth and recovery after spinal cord injury. *J Cell Biol,* 173**,** 47-58.

HAWTHORNE, A. L. & POPOVICH, P. G. 2011. Emerging concepts in myeloid cell biology after spinal cord injury. *Neurotherapeutics,* 8**,** 252-261.

HE, Z., HE, M., WANG, C., XU, B., TONG, L., HE, J., SUN, B., WEI, L. & CHU, M. 2014. Prognostic significance of astrocyte elevated gene-1 in human astrocytomas. *Int J Clin Exp Pathol,* 7**,** 5038-44.

HEADLEY, P. M. & GRILLNER, S. 1990. Excitatory amino acids and synaptic transmission: the evidence for a physiological function. *Trends Pharmacol Sci,* 11**,** 205-11.

HELLAL, F., HURTADO, A., RUSCHEL, J., FLYNN, K. C., LASKOWSKI, C. J., UMLAUF, M., KAPITEIN, L. C., STRIKIS, D., LEMMON, V., BIXBY, J., HOOGENRAAD, C. C. & BRADKE, F. 2011. Microtubule stabilization reduces scarring and causes axon regeneration after spinal cord injury. *Science,* 331**,** 928-31.

HENS, J., NUYDENS, R., GEERTS, H., SENDEN, N. H. M., VAN DE VEN, W. J. M., ROEBROEK, A. J. M., VAN DE VELDE, H. J. K., RAMAEKERS, F. C. S. & BROERS, J. L. V. 1998. Neuronal differentiation is accompanied by NSP-C expression. *Cell and Tissue Research,* 292**,** 229-237.

HOLLIS, E. R., 2ND & ZOU, Y. 2012. Reinduced Wnt signaling limits regenerative potential of sensory axons in the spinal cord following conditioning lesion. *Proc Natl Acad Sci U S A,* 109**,** 14663-8.

HOLNESS, C. L. & SIMMONS, D. L. 1993. Molecular cloning of CD68, a human macrophage marker related to lysosomal glycoproteins. *Blood,* 81**,** 1607-13.

HOMMA, S., SHIMADA, T., HIKAKE, T. & YAGINUMA, H. 2009. Expression pattern of LRR and Ig domain-containing protein (LRRIG protein) in the early mouse embryo. *Gene Expr Patterns,* 9**,** 1-26.

HORNER, P. J. & GAGE, F. H. 2000. Regenerating the damaged central nervous system. *Nature,* 407**,** 963-70.

HOULE, J. D., TOM, V. J., MAYES, D., WAGONER, G., PHILLIPS, N. & SILVER, J. 2006. Combining an autologous peripheral nervous system "bridge" and matrix modification by chondroitinase allows robust, functional regeneration beyond a hemisection lesion of the adult rat spinal cord. *Journal of Neuroscience,* 26**,** 7405-7415.

HSU, J. Y., BOURGUIGNON, L. Y., ADAMS, C. M., PEYROLLIER, K., ZHANG, H., FANDEL, T., CUN, C. L., WERB, Z. & NOBLE-HAEUSSLEIN, L. J. 2008. Matrix metalloproteinase-9 facilitates glial scar formation in the injured spinal cord. *J Neurosci,* 28**,** 13467-77.

HU, F. & STRITTMATTER, S. M. 2008. The N-terminal domain of Nogo-A inhibits cell adhesion and axonal outgrowth by an integrin-specific mechanism. *J Neurosci,* 28**,** 1262-9.

HU, G., CHONG, R. A., YANG, Q., WEI, Y., BLANCO, M. A., LI, F., REISS, M., AU, J. L., HAFFTY, B. G. & KANG, Y. 2009. MTDH activation by 8q22 genomic gain promotes chemoresistance and metastasis of poor-prognosis breast cancer. *Cancer Cell,* 15**,** 9-20.

HU, P., BEMBRICK, A. L., KEAY, K. A. & MCLACHLAN, E. M. 2007a. Immune cell involvement in dorsal root ganglia and spinal cord after chronic constriction or transection of the rat sciatic nerve. *Brain Behav Immun,* 21**,** 599-616.

HU, P. & MCLACHLAN, E. M. 2003. Distinct functional types of macrophage in dorsal root ganglia and spinal nerves proximal to sciatic and spinal nerve transections in the rat. *Exp Neurol,* 184**,** 590-605.

HU, X., SHI, Q., ZHOU, X., HE, W., YI, H., YIN, X., GEARING, M., LEVEY, A. & YAN, R. 2007b. Transgenic mice overexpressing reticulon 3 develop neuritic abnormalities. *EMBO J,* 26**,** 2755-67.

HUEBNER, E. A. & STRITTMATTER, S. M. 2009. Axon regeneration in the peripheral and central nervous systems. *Results Probl Cell Differ,* 48**,** 339-51.

HULSEBOSCH, C. E. 2002. Recent advances in pathophysiology and treatment of spinal cord injury. *Adv Physiol Educ,* 26**,** 238-55.

HUNT, D., COFFIN, R. S. & ANDERSON, P. N. 2002. The Nogo receptor, its ligands and axonal regeneration in the spinal cord; a review. *J Neurocytol,* 31**,** 93-120.

HUTSON, T. H., FOSTER, E., DAWES, J. M., HINDGES, R., YANEZ-MUNOZ, R. J. & MOON, L. D. 2012. Lentiviral vectors encoding short hairpin RNAs efficiently transduce and knockdown LINGO-1 but induce an interferon response and cytotoxicity in central nervous system neurones. *J Gene Med,* 14**,** 299-315.

HUTSON, T. H., FOSTER, E., MOON, L. D. & YANEZ-MUNOZ, R. J. 2014. Lentiviral vector-mediated RNA silencing in the central nervous system. *Hum Gene Ther Methods,* 25**,** 14-32.

ILLES, J., REIMER, J. C. & KWON, B. K. 2011. Stem cell clinical trials for spinal cord injury: readiness, reluctance, redefinition. *Stem Cell Rev,* 7**,** 997-1005.

IRIZARRY, M. C., GROWDON, W., GOMEZ-ISLA, T., NEWELL, K., GEORGE, J. M., CLAYTON, D. F. & HYMAN, B. T. 1998. Nigral and cortical Lewy bodies and dystrophic nigral neurites in Parkinson's disease and cortical Lewy body disease contain alpha-synuclein immunoreactivity. *J Neuropathol Exp Neurol,* 57**,** 334-7.

JACQUE, C. M., VINNER, C., KUJAS, M., RAOUL, M., RACADOT, J. & BAUMANN, N. A. 1978. Determination of glial fibrillary acidic protein (GFAP) in human brain tumors. *J Neurol Sci,* 35**,** 147-55.

JACQUES, S. J., AHMED, Z., FORBES, A., DOUGLAS, M. R., VIGENSWARA, V., BERRY, M. & LOGAN, A. 2012a. AAV8 gfp preferentially targets large diameter dorsal root ganglion neurones after both intra-dorsal root ganglion and intrathecal injection. *Molecular and Cellular Neuroscience,* 49**,** 464-474.

JACQUES, S. J., AHMED, Z., FORBES, A., DOUGLAS, M. R., VIGENSWARA, V., BERRY, M. & LOGAN, A. 2012b. AAV8(gfp) preferentially targets large diameter dorsal root ganglion neurones after both intra-dorsal root ganglion and intrathecal injection. *Mol Cell Neurosci,* 49**,** 464-74.

JAKEMAN, L. B., GUAN, Z., WEI, P., PONNAPPAN, R., DZWONCZYK, R., POPOVICH, P. G. & STOKES, B. T. 2000. Traumatic spinal cord injury produced by controlled contusion in mouse. *J Neurotrauma,* 17**,** 299-319.

JAMES, N. D. 2013. *Characterising changes in pathology and function in clinically relevant models of spinal cord injury and using chondroitinase ABC gene therapy to promote repair.* King's College London (University of London).

JEON, H. Y., CHOI, M., HOWLETT, E. L., VOZHILLA, N., YOO, B. K., LLOYD, J. A., SARKAR, D., LEE, S. G. & FISHER, P. B. 2010. Expression patterns of astrocyte elevated gene-1 (AEG-1) during development of the mouse embryo. *Gene Expr Patterns,* 10**,** 361-7.

JONES, L. L., MARGOLIS, R. U. & TUSZYNSKI, M. H. 2003. The chondroitin sulfate proteoglycans neurocan, brevican, phosphacan, and versican are differentially regulated following spinal cord injury. *Exp Neurol,* 182**,** 399-411.

JONES, L. L. & TUSZYNSKI, M. H. 2002. Spinal cord injury elicits expression of keratan sulfate proteoglycans by macrophages, reactive microglia, and oligodendrocyte progenitors. *J Neurosci,* 22**,** 4611-24.

JONES, L. S. 1996. Integrins: possible functions in the adult CNS. *Trends Neurosci,* 19**,** 68-72.

JU, G., WANG, J., WANG, Y. & ZHAO, X. 2014. Spinal cord contusion. *Neural Regen Res,* 9**,** 789-94.

KAJANDER, T., KUJA-PANULA, J., RAUVALA, H. & GOLDMAN, A. 2011. Crystal structure and role of glycans and dimerization in folding of neuronal leucine-rich repeat protein AMIGO-1. *J Mol Biol,* 413**,** 1001-15.

KANAGAL, S. G. & MUIR, G. D. 2008. The differential effects of cervical and thoracic dorsal funiculus lesions in rats. *Behav Brain Res,* 187**,** 379-86.

KANDALEPAS, P. C., SADLEIR, K. R., EIMER, W. A., ZHAO, J., NICHOLSON, D. A. & VASSAR, R. 2013. The Alzheimer's beta-secretase BACE1 localizes to normal presynaptic terminals and to dystrophic presynaptic terminals surrounding amyloid plaques. *Acta Neuropathol,* 126**,** 329-52.

KANG, D. C., SU, Z. Z., SARKAR, D., EMDAD, L., VOLSKY, D. J. & FISHER, P. B. 2005. Cloning and characterization of HIV-1-inducible astrocyte elevated gene-1, AEG-1. *Gene,* 353**,** 8-15.

KARIMI-ABDOLREZAEE, S. & BILLAKANTI, R. 2012. Reactive astrogliosis after spinal cord injury-beneficial and detrimental effects. *Mol Neurobiol,* 46**,** 251-64.

KEIRSTEAD, H. S. & BLAKEMORE, W. F. 1999. The role of oligodendrocytes and oligodendrocyte progenitors in CNS remyelination. *Adv Exp Med Biol,* 468**,** 183-97.

KEIRSTEAD, H. S., NISTOR, G., BERNAL, G., TOTOIU, M., CLOUTIER, F., SHARP, K. & STEWARD, O. 2005. Human embryonic stem cell-derived oligodendrocyte progenitor cell transplants remyelinate and restore locomotion after spinal cord injury. *J Neurosci,* 25**,** 4694-705.

KEMPF, A., MONTANI, L., PETRINOVIC, M. M., SCHROETER, A., WEINMANN, O., PATRIGNANI, A. & SCHWAB, M. E. 2013. Upregulation of axon guidance molecules in the adult central nervous system of Nogo-A knockout mice restricts neuronal growth and regeneration. *Eur J Neurosci,* 38**,** 3567-79.

KIGERL, K. A., GENSEL, J. C., ANKENY, D. P., ALEXANDER, J. K., DONNELLY, D. J. & POPOVICH, P. G. 2009. Identification of two distinct macrophage subsets with divergent effects causing either neurotoxicity or regeneration in the injured mouse spinal cord. *Journal of Neuroscience,* 29**,** 13435-13444.

KIKUCHI, K., KISHINO, A., KONISHI, O., KUMAGAI, K., HOSOTANI, N., SAJI, I., NAKAYAMA, C. & KIMURA, T. 2003. In vitro and in vivo characterization of a novel semaphorin 3A inhibitor, SM-216289 or xanthofulvin. *J Biol Chem,* 278**,** 42985-91.

KIM, C. F. & MOALEM-TAYLOR, G. 2011. Detailed characterization of neuro-immune responses following neuropathic injury in mice. *Brain Res,* 1405**,** 95-108.

KIM, J. Y., SUN, Q., OGLESBEE, M. & YOON, S. O. 2003. The role of ErbB2 signaling in the onset of terminal differentiation of oligodendrocytes in vivo. *J Neurosci,* 23**,** 5561-71.

KIM, K., LEE, S. G., KEGELMAN, T. P., SU, Z. Z., DAS, S. K., DASH, R., DASGUPTA, S., BARRAL, P. M., HEDVAT, M., DIAZ, P., REED, J. C., STEBBINS, J. L., PELLECCHIA, M., SARKAR, D. & FISHER, P. B. 2011. Role of excitatory amino acid transporter-2 (EAAT2) and glutamate in neurodegeneration: opportunities for developing novel therapeutics. *J Cell Physiol,* 226**,** 2484-93.

KING, V. R., BRADBURY, E. J., MCMAHON, S. B. & PRIESTLEY, J. V. 2000. Changes in truncated trkB and p75 receptor expression in the rat spinal cord following spinal cord hemisection and spinal cord hemisection plus neurotrophin treatment. *Exp Neurol,* 165**,** 327-41.

KISHK, N. A., GABR, H., HAMDY, S., AFIFI, L., ABOKRESHA, N., MAHMOUD, H., WAFAIE, A. & BILAL, D. 2010. Case control series of intrathecal autologous bone marrow mesenchymal stem cell therapy for chronic spinal cord injury. *Neurorehabil Neural Repair,* 24**,** 702-8.

KOO, E. H., SISODIA, S. S., ARCHER, D. R., MARTIN, L. J., WEIDEMANN, A., BEYREUTHER, K., FISCHER, P., MASTERS, C. L. & PRICE, D. L. 1990. Precursor of amyloid protein in Alzheimer disease undergoes fast anterograde axonal transport. *Proc Natl Acad Sci U S A,* 87**,** 1561-5.

KUHLMANN, T., BITSCH, A., STADELMANN, C., SIEBERT, H. & BRUCK, W. 2001. Macrophages are eliminated from the injured peripheral nerve via local apoptosis and circulation to regional lymph nodes and the spleen. *J Neurosci,* 21**,** 3401-8.

KUJA-PANULA, J., KIILTOMAKI, M., YAMASHIRO, T., ROUHIAINEN, A. & RAUVALA, H. 2003. AMIGO, a transmembrane protein implicated in axon tract development, defines a novel protein family with leucine-rich repeats. *J Cell Biol,* 160**,** 963-73.

KUMAMARU, E., KUO, C. H., FUJIMOTO, T., KOHAMA, K., ZENG, L. H., TAIRA, E., TANAKA, H., TOYODA, T. & MIKI, N. 2004. Reticulon3 expression in rat optic and olfactory systems. *Neurosci Lett,* 356**,** 17-20.

KUMAR, A. A., KUMAR, S. R., NARAYANAN, R., ARUL, K. & BASKARAN, M. 2009. Autologous bone marrow derived mononuclear cell therapy for spinal cord injury: A phase I/II clinical safety and primary efficacy data. *Exp Clin Transplant,* 7**,** 241-8.

KUNDI, S., BICKNELL, R. & AHMED, Z. 2013. The role of angiogenic and wound-healing factors after spinal cord injury in mammals. *Neurosci Res,* 76**,** 1-9.

KUNZ-SCHUGHART, L., WEBER, A., REHLI, M., GOTTFRIED, E., BROCKHOFF, G., KRAUSE, S., ANDREESEN, R. & KREUTZ, M. 2002. [The" classical" macrophage marker CD68 is strongly expressed in primary human fibroblasts]. *Verhandlungen der Deutschen Gesellschaft fur Pathologie,* 87**,** 215-223.

LAEREMANS, A., NYS, J., LUYTEN, W., D'HOOGE, R., PAULUSSEN, M. & ARCKENS, L. 2013. AMIGO2 mRNA expression in hippocampal CA2 and CA3a. *Brain Struct Funct,* 218**,** 123-30.

LAGORD, C., BERRY, M. & LOGAN, A. 2002. Expression of TGFβ2 but not TGFβ1 correlates with the deposition of scar tissue in the lesioned spinal cord. *Molecular and Cellular Neuroscience,* 20**,** 69-92.

LANG, B., LIU, H., LIU, R., FENG, G., JIAO, X. & JU, G. 2004. Astrocytes in injured adult rat spinal cord may acquire the potential of neural stem cells. *Neuroscience,* 128**,** 775-783.

LAWRENCE, T. & NATOLI, G. 2011. Transcriptional regulation of macrophage polarization: enabling diversity with identity. *Nat Rev Immunol,* 11**,** 750-61.

LEE, D. H. & LEE, J. K. 2013. Animal models of axon regeneration after spinal cord injury. *Neurosci Bull,* 29**,** 436-44.

LEE, E. B., ZHANG, B., LIU, K., GREENBAUM, E. A., DOMS, R. W., TROJANOWSKI, J. Q. & LEE, V. M. 2005a. BACE overexpression alters the subcellular processing of APP and inhibits Abeta deposition in vivo. *J Cell Biol,* 168**,** 291-302.

LEE, K. H., YOON, D. H., PARK, Y. G. & LEE, B. H. 2005b. Effects of glial transplantation on functional recovery following acute spinal cord injury. *J Neurotrauma,* 22**,** 575-89.

LEE, S. G., KANG, D. C., DESALLE, R., SARKAR, D. & FISHER, P. B. 2013. AEG-1/MTDH/LYRIC, the beginning: initial cloning, structure, expression profile, and regulation of expression. *Adv Cancer Res,* 120**,** 1-38.

LEE, S. G., KIM, K., KEGELMAN, T. P., DASH, R., DAS, S. K., CHOI, J. K., EMDAD, L., HOWLETT, E. L., JEON, H. Y., SU, Z. Z., YOO, B. K., SARKAR, D., KIM, S. H., KANG, D. C. & FISHER, P. B. 2011. Oncogene AEG-1 promotes glioma-induced neurodegeneration by increasing glutamate excitotoxicity. *Cancer Res,* 71**,** 6514-23.

LEE, S. G., SU, Z. Z., EMDAD, L., SARKAR, D., FRANKE, T. F. & FISHER, P. B. 2008. Astrocyte elevated gene-1 activates cell survival pathways through PI3K-Akt signaling. *Oncogene,* 27**,** 1114-21.

LEWIN, G. R., RITTER, A. M. & MENDELL, L. M. 1993. Nerve growth factor-induced hyperalgesia in the neonatal and adult rat. *J Neurosci,* 13**,** 2136-48.

LI, Y., DECHERCHI, P. & RAISMAN, G. 2003. Transplantation of olfactory ensheathing cells into spinal cord lesions restores breathing and climbing. *Journal of Neuroscience,* 23**,** 727-731.

LI, Y., FIELD, P. M. & RAISMAN, G. 1997. Repair of adult rat corticospinal tract by transplants of olfactory ensheathing cells. *Science,* 277**,** 2000-2.

LIAO, H. W. & YAU, K. W. 2007. In vivo gene delivery in the retina using polyethylenimine. *Biotechniques,* 42**,** 285-6, 288.

LIEBL, D. J., HUANG, W., YOUNG, W. & PARADA, L. F. 2001. Regulation of Trk receptors following contusion of the rat spinal cord. *Exp Neurol,* 167**,** 15-26.

LIMA, C., ESCADA, P., PRATAS-VITAL, J., BRANCO, C., ARCANGELI, C. A., LAZZERI, G., MAIA, C. A., CAPUCHO, C., HASSE-FERREIRA, A. & PEDUZZI, J. D. 2010. Olfactory mucosal autografts and rehabilitation for chronic traumatic spinal cord injury. *Neurorehabil Neural Repair,* 24**,** 10-22.

LIMA, C., PRATAS-VITAL, J., ESCADA, P., HASSE-FERREIRA, A., CAPUCHO, C. & PEDUZZI, J. D. 2006. Olfactory mucosa autografts in human spinal cord injury: a pilot clinical study. *J Spinal Cord Med,* 29**,** 191-203; discussion 204-6.

LINGOR, P., TEUSCH, N., SCHWARZ, K., MUELLER, R., MACK, H., BAHR, M. & MUELLER, B. K. 2007. Inhibition of Rho kinase (ROCK) increases neurite outgrowth on chondroitin sulphate proteoglycan in vitro and axonal regeneration in the adult optic nerve in vivo. *J Neurochem,* 103**,** 181-9.

LIPTON, S. A. & GENDELMAN, H. E. 1995. Seminars in medicine of the Beth Israel Hospital, Boston. Dementia associated with the acquired immunodeficiency syndrome. *N Engl J Med,* 332**,** 934-40.

LISZIEWICZ, J., GABRILOVICH, D. I., VARGA, G., XU, J., GREENBERG, P. D., ARYA, S. K., BOSCH, M., BEHR, J. P. & LORI, F. 2001. Induction of potent human immunodeficiency virus type 1-specific T-cell-restricted immunity by genetically modified dendritic cells. *J Virol,* 75**,** 7621-8.

LIU, K., LU, Y., LEE, J. K., SAMARA, R., WILLENBERG, R., SEARS-KRAXBERGER, I., TEDESCHI, A., PARK, K. K., JIN, D., CAI, B., XU, B., CONNOLLY, L., STEWARD, O., ZHENG, B. & HE, Z. 2010. PTEN deletion enhances the regenerative ability of adult corticospinal neurons. *Nat Neurosci,* 13**,** 1075-81.

LIU, X., ZHANG, N., LI, X., MORAN, M. S., YUAN, C., YAN, S., JIANG, L., MA, T., HAFFTY, B. G. & YANG, Q. 2011. Identification of novel variants of metadherin in breast cancer. *PLoS One,* 6**,** e17582.

LIU, X. Z., XU, X. M., HU, R., DU, C., ZHANG, S. X., MCDONALD, J. W., DONG, H. X., WU, Y. J., FAN, G. S., JACQUIN, M. F., HSU, C. Y. & CHOI, D. W. 1997. Neuronal and glial apoptosis after traumatic spinal cord injury. *J Neurosci,* 17**,** 5395-406.

LIU, Y., VIDENSKY, S., RUGGIERO, A. M., MAIER, S., SITTE, H. H. & ROTHSTEIN, J. D. 2008. Reticulon RTN2B regulates trafficking and function of neuronal glutamate transporter EAAC1. *Journal of Biological Chemistry,* 283**,** 6561-6571.

LLORENS, F., GIL, V., IRAOLA, S., CARIM-TODD, L., MARTI, E., ESTIVILL, X., SORIANO, E., DEL RIO, J. A. & SUMOY, L. 2008. Developmental analysis of Lingo-1/Lern1 protein expression in the mouse brain: interaction of its intracellular domain with Myt1l. *Dev Neurobiol,* 68**,** 521-41.

LU, J., ASHWELL, K. W. & WAITE, P. 2000. Advances in secondary spinal cord injury: role of apoptosis. *Spine (Phila Pa 1976),* 25**,** 1859-66.

LUNGWITZ, U., BREUNIG, M., BLUNK, T. & GOPFERICH, A. 2005. Polyethylenimine-based non-viral gene delivery systems. *Eur J Pharm Biopharm,* 60**,** 247-66.

LUO, J., ZHANG, H. T., JIANG, X. D., XUE, S. & KE, Y. Q. 2009. Combination of bone marrow stromal cell transplantation with mobilization by granulocyte-colony stimulating factor promotes functional recovery after spinal cord transection. *Acta Neurochir (Wien),* 151**,** 1483-92.

LUO, L. & FLANAGAN, J. G. 2007. Development of continuous and discrete neural maps. *Neuron,* 56**,** 284-300.

MA, M., BASSO, D. M., WALTERS, P., STOKES, B. T. & JAKEMAN, L. B. 2001. Behavioral and histological outcomes following graded spinal cord contusion injury in the C57Bl/6 mouse. *Exp Neurol,* 169**,** 239-54.

MAEKAWA, M., ISHIZAKI, T., BOKU, S., WATANABE, N., FUJITA, A., IWAMATSU, A., OBINATA, T., OHASHI, K., MIZUNO, K. & NARUMIYA, S. 1999. Signaling from Rho to the actin cytoskeleton through protein kinases ROCK and LIM-kinase. *Science,* 285**,** 895-898.

MANDAI, K., GUO, T., ST HILLAIRE, C., MEABON, J. S., KANNING, K. C., BOTHWELL, M. & GINTY, D. D. 2009. LIG family receptor tyrosine kinase-associated proteins modulate growth factor signals during neural development. *Neuron,* 63**,** 614-27.

MARCUS, H. J., CARPENTER, K. L., PRICE, S. J. & HUTCHINSON, P. J. 2010. In vivo assessment of high-grade glioma biochemistry using microdialysis: a study of energy-related molecules, growth factors and cytokines. *J Neurooncol,* 97**,** 11-23.

MASON, M. R., EHLERT, E. M., EGGERS, R., POOL, C. W., HERMENING, S., HUSEINOVIC, A., TIMMERMANS, E., BLITS, B. & VERHAAGEN, J. 2010. Comparison of AAV serotypes for gene delivery to dorsal root ganglion neurons. *Mol Ther,* 18**,** 715-24.

MCCARTY, D. M., MONAHAN, P. E. & SAMULSKI, R. J. 2001. Self-complementary recombinant adeno-associated virus (scAAV) vectors promote efficient transduction independently of DNA synthesis. *Gene Ther,* 8**,** 1248-54.

MCDONALD, J. W. & BELEGU, V. 2006. Demyelination and remyelination after spinal cord injury. *J Neurotrauma,* 23**,** 345-59.

MCKERRACHER, L. & WINTON, M. J. 2002. Nogo on the go. *Neuron,* 36**,** 345-8.

MCKERRACHER, L. D., DAVID, S., JACKSON, D., KOTTIS, V., DUNN, R. & BRAUN, P. 1994. Identification of myelin-associated glycoprotein as a major myelin-derived inhibitor of neurite growth. *Neuron,* 13**,** 805-811.

MCNEILL, D. L., CHUNG, K., CARLTON, S. M. & COGGESHALL, R. E. 1988. Calcitonin gene-related peptide immunostained axons provide evidence for fine primary afferent fibers in the dorsal and dorsolateral funiculi of the rat spinal cord. *J Comp Neurol,* 272**,** 303-8.

MEABON, J. S., DE LAAT, R., IEGUCHI, K., SERBZHINSKY, D., HUDSON, M. P., HUBER, B. R., WILEY, J. C. & BOTHWELL, M. 2016. Intracellular LINGO-1 negatively regulates Trk neurotrophin receptor signaling. *Mol Cell Neurosci,* 70**,** 1-10.

MENET, V., PRIETO, M., PRIVAT, A. & Y RIBOTTA, M. G. 2003. Axonal plasticity and functional recovery after spinal cord injury in mice deficient in both glial fibrillary acidic protein and vimentin genes. *Proceedings of the National Academy of Sciences,* 100**,** 8999-9004.

MERENMIES, J., PIHLASKARI, R., LAITINEN, J., WARTIOVAARA, J. & RAUVALA, H. 1991. 30-kDa heparin-binding protein of brain (amphoterin) involved in neurite outgrowth. Amino acid sequence and localization in the filopodia of the advancing plasma membrane. *J Biol Chem,* 266**,** 16722-9.

MESSERSMITH, E. K., LEONARDO, E. D., SHATZ, C. J., TESSIER-LAVIGNE, M., GOODMAN, C. S. & KOLODKIN, A. L. 1995. Sernaphorin III can function as a selective chemorepellent to pattern sensory projections in the spinal cord. *Neuron,* 14**,** 949-959.

METZ, G. A., CURT, A., VAN DE MEENT, H., KLUSMAN, I., SCHWAB, M. E. & DIETZ, V. 2000. Validation of the weight-drop contusion model in rats: a comparative study of human spinal cord injury. *J Neurotrauma,* 17**,** 1-17.

MI, S., HU, B., HAHM, K., LUO, Y., KAM HUI, E. S., YUAN, Q., WONG, W. M., WANG, L., SU, H., CHU, T. H., GUO, J., ZHANG, W., SO, K. F., PEPINSKY, B., SHAO, Z., GRAFF, C., GARBER, E., JUNG, V., WU, E. X. & WU, W. 2007. LINGO-1 antagonist promotes spinal cord remyelination and axonal integrity in MOG-induced experimental autoimmune encephalomyelitis. *Nat Med,* 13**,** 1228-33.

MI, S., HUANG, G., LEE, X. & SHAO, Z. 2016. LINGO-1 Negatively Regulates Oligodendrocyte Differentiation by Blocking the β-integrin Signaling Pathway (I10. 002). *Neurology,* 86**,** I10. 002.

MI, S., LEE, X., SHAO, Z., THILL, G., JI, B., RELTON, J., LEVESQUE, M., ALLAIRE, N., PERRIN, S., SANDS, B., CROWELL, T., CATE, R. L., MCCOY, J. M. & PEPINSKY, R. B. 2004. LINGO-1 is a component of the Nogo-66 receptor/p75 signaling complex. *Nat Neurosci,* 7**,** 221-8.

MI, S., MILLER, R. H., LEE, X., SCOTT, M. L., SHULAG-MORSKAYA, S., SHAO, Z., CHANG, J., THILL, G., LEVESQUE, M., ZHANG, M., HESSION, C., SAH, D., TRAPP, B., HE, Z., JUNG, V., MCCOY, J. M. & PEPINSKY, R. B. 2005. LINGO-1 negatively regulates myelination by oligodendrocytes. *Nat Neurosci,* 8**,** 745-51.

MI, S., SANDROCK, A. & MILLER, R. H. 2008. LINGO-1 and its role in CNS repair. *Int J Biochem Cell Biol,* 40**,** 1971-8.

MIELE, V. J., PANJABI, M. M. & BENZEL, E. C. 2012. Anatomy and biomechanics of the spinal column and cord. *Handb Clin Neurol,* 109**,** 31-43.

MIKOL, D. D., SZUCHET, S. & STEFANSSON, K. 1988. A peanut agglutinin binding glycoprotein in CNS myelin and oligodendrocytes. *Ann N Y Acad Sci,* 540**,** 409-12.

MINAGAR, A., SHAPSHAK, P., FUJIMURA, R., OWNBY, R., HEYES, M. & EISDORFER, C. 2002. The role of macrophage/microglia and astrocytes in the pathogenesis of three neurologic disorders: HIV-associated dementia, Alzheimer disease, and multiple sclerosis. *J Neurol Sci,* 202**,** 13-23.

MINGOZZI, F. & HIGH, K. A. 2013. Immune responses to AAV vectors: overcoming barriers to successful gene therapy. *Blood,* 122**,** 23-36.

MIYAGOE-SUZUKI, Y. & TAKEDA, S. 2010. Gene therapy for muscle disease. *Exp Cell Res,* 316**,** 3087-92.

MIZUNO, K. 2013. Signaling mechanisms and functional roles of cofilin phosphorylation and dephosphorylation. *Cell Signal,* 25**,** 457-69.

MOHAMAD, C. & ANUAR, C. 2014. *Human embryonic stem cell-derived mesenchymal stem cells as a therapy for spinal cord injury.* University of Glasgow.

NAKADA, M., NAKADA, S., DEMUTH, T., TRAN, N. L., HOELZINGER, D. B. & BERENS, M. E. 2007. Molecular targets of glioma invasion. *Cell Mol Life Sci,* 64**,** 458-78.

NAKAE, A., NAKAI, K., YANO, K., HOSOKAWA, K., SHIBATA, M. & MASHIMO, T. 2011. The animal model of spinal cord injury as an experimental pain model. *BioMed Research International,* 2011.

NATHAN, C. 2002. Points of control in inflammation. *Nature,* 420**,** 846-52.

NAYAK, S. & HERZOG, R. W. 2010. Progress and prospects: immune responses to viral vectors. *Gene Ther,* 17**,** 295-304.

NGUYEN, T., MEHTA, N. R., CONANT, K., KIM, K. J., JONES, M., CALABRESI, P. A., MELLI, G., HOKE, A., SCHNAAR, R. L., MING, G. L., SONG, H., KESWANI, S. C. & GRIFFIN, J. W. 2009. Axonal protective effects of the myelin-associated glycoprotein. *J Neurosci,* 29**,** 630-7.

NISHIYAMA, A., KOMITOVA, M., SUZUKI, R. & ZHU, X. 2009. Polydendrocytes (NG2 cells): multifunctional cells with lineage plasticity. *Nat Rev Neurosci,* 10**,** 9-22.

NISTOR, G. I., TOTOIU, M. O., HAQUE, N., CARPENTER, M. K. & KEIRSTEAD, H. S. 2005. Human embryonic stem cells differentiate into oligodendrocytes in high purity and myelinate after spinal cord transplantation. *Glia,* 49**,** 385-396.

NÓGRÁDI, A. & VRBOVÁ, G. 2006. Anatomy and physiology of the spinal cord. *Transplantation of Neural Tissue into the Spinal Cord.* Springer.

O'NEILL, P., WHALLEY, K. & FERRETTI, P. 2004. Nogo and Nogo-66 receptor in human and chick: Implications for development and regeneration. *Developmental Dynamics,* 231**,** 109-121.

OERTLE, T. & SCHWAB, M. E. 2003. Nogo and its paRTNers. *Trends Cell Biol,* 13**,** 187-94.

OHORI, Y., YAMAMOTO, S., NAGAO, M., SUGIMORI, M., YAMAMOTO, N., NAKAMURA, K. & NAKAFUKU, M. 2006. Growth factor treatment and genetic manipulation stimulate neurogenesis and oligodendrogenesis by endogenous neural progenitors in the injured adult spinal cord. *J Neurosci,* 26**,** 11948-60.

OKE, W. S. 1844. Sketch of the Relative Anatomy of the Spinal Column. *Prov Med Surg J,* 7**,** 367-70.

OKOYE, I. S. & WILSON, M. S. 2011. CD4+ T helper 2 cells--microbial triggers, differentiation requirements and effector functions. *Immunology,* 134**,** 368-77.

OLSON, L. 2013. Combinatory treatments needed for spinal cord injury. *Exp Neurol,* 248**,** 309-15.

ONO, T., SEKINO-SUZUKI, N., KIKKAWA, Y., YONEKAWA, H. & KAWASHIMA, S. 2003. Alivin 1, a novel neuronal activity-dependent gene, inhibits apoptosis and promotes survival of cerebellar granule neurons. *J Neurosci,* 23**,** 5887-96.

OVERBECK, A. F., BRTVA, T. R., COX, A. D., GRAHAM, S. M., HUFF, S. Y., KHOSRAVI-FAR, R., QUILLIAM, L. A., SOLSKI, P. A. & DER, C. J. 1995. Guanine nucleotide exchange factors: activators of Ras superfamily proteins. *Mol Reprod Dev,* 42**,** 468-76.

PARK, J. B., YIU, G., KANEKO, S., WANG, J., CHANG, J. & HE, Z. 2005. A TNF receptor family member, TROY, is a coreceptor with Nogo receptor in mediating the inhibitory activity of myelin inhibitors. *Neuron,* 45**,** 345-351.

PASTERKAMP, R. J. & VERHAAGEN, J. 2001. Emerging roles for semaphorins in neural regeneration. *Brain Res Brain Res Rev,* 35**,** 36-54.

PATTERSON, J. T., COGGESHALL, R. E., LEE, W. T. & CHUNG, K. 1990. Long ascending unmyelinated primary afferent axons in the rat dorsal column: immunohistochemical localizations. *Neurosci Lett,* 108**,** 6-10.

PEKNY, M. & NILSSON, M. 2005. Astrocyte activation and reactive gliosis. *Glia,* 50**,** 427-34.

PEKNY, M., WILHELMSSON, U. & PEKNA, M. 2014. The dual role of astrocyte activation and reactive gliosis. *Neurosci Lett,* 565**,** 30-8.

PELTOLA, M. A., KUJA-PANULA, J., LIUHANEN, J., VÕIKAR, V., PIEPPONEN, P., HIEKKALINNA, T., TAIRA, T., LAURI, S. E., SUVISAARI, J. & KULESSKAYA, N. 2016. AMIGO-Kv2. 1 Potassium Channel Complex Is Associated With Schizophrenia-Related Phenotypes. *Schizophrenia bulletin,* 42**,** 191-201.

PELTOLA, M. A., KUJA‐PANULA, J., LAURI, S. E., TAIRA, T. & RAUVALA, H. 2011. AMIGO is an auxiliary subunit of the Kv2. 1 potassium channel. *EMBO reports,* 12**,** 1293-1299.

PEREGO, C., FUMAGALLI, S. & DE SIMONI, M. G. 2011. Temporal pattern of expression and colocalization of microglia/macrophage phenotype markers following brain ischemic injury in mice. *J Neuroinflammation,* 8**,** 174.

PETERS, C. M., JIMENEZ-ANDRADE, J. M., JONAS, B. M., SEVCIK, M. A., KOEWLER, N. J., GHILARDI, J. R., WONG, G. Y. & MANTYH, P. W. 2007. Intravenous paclitaxel administration in the rat induces a peripheral sensory neuropathy characterized by macrophage infiltration and injury to sensory neurons and their supporting cells. *Experimental neurology,* 203**,** 42-54.

QUARLES, R. 2002. Myelin sheaths: glycoproteins involved in their formation, maintenance and degeneration. *Cellular and Molecular Life Sciences CMLS,* 59**,** 1851-1871.

RABENAU, K. E., O'TOOLE, J. M., BASSI, R., KOTANIDES, H., WITTE, L., LUDWIG, D. L. & PEREIRA, D. S. 2004. DEGA/AMIGO-2, a leucine-rich repeat family member, differentially expressed in human gastric adenocarcinoma: effects on ploidy, chromosomal stability, cell adhesion/migration and tumorigenicity. *Oncogene,* 23**,** 5056-67.

RAMER, L. M., RAMER, M. S. & STEEVES, J. D. 2005. Setting the stage for functional repair of spinal cord injuries: a cast of thousands. *Spinal Cord,* 43**,** 134-61.

RAMÓN-CUETO, A., CORDERO, M. I., SANTOS-BENITO, F. F. & AVILA, J. 2000. Functional recovery of paraplegic rats and motor axon regeneration in their spinal cords by olfactory ensheathing glia. *Neuron,* 25**,** 425-435.

RAMÓN Y CAJAL, S., DEFELIPE, J. & JONES, E. G. 1991. Cajal's degeneration and regeneration of the nervous system. *History of neuroscience no 5.* New York: Oxford University Press,.

RANSOHOFF, R. M. & CARDONA, A. E. 2010. The myeloid cells of the central nervous system parenchyma. *Nature,* 468**,** 253-62.

RAOUL, C., BARKER, S. D. & AEBISCHER, P. 2006. Viral-based modelling and correction of neurodegenerative diseases by RNA interference. *Gene Ther,* 13**,** 487-95.

RAUVALA, H. & PIHLASKARI, R. 1987. Isolation and some characteristics of an adhesive factor of brain that enhances neurite outgrowth in central neurons. *J Biol Chem,* 262**,** 16625-35.

REYNOLDS, A., LEAKE, D., BOESE, Q., SCARINGE, S., MARSHALL, W. S. & KHVOROVA, A. 2004. Rational siRNA design for RNA interference. *Nat Biotechnol,* 22**,** 326-30.

RICCIOTTI, E. & FITZGERALD, G. A. 2011. Prostaglandins and inflammation. *Arterioscler Thromb Vasc Biol,* 31**,** 986-1000.

RICHARDSON, P., MCGUINNESS, U. & AGUAYO, A. 1980. Axons from CNS neurones regenerate into PNS grafts.

RICHARDSON, P. M. & ISSA, V. M. 1984. Peripheral injury enhances central regeneration of primary sensory neurones. *Nature,* 309**,** 791-3.

RICHFIELD, E. K. 2000. Cns Regeneration: Basic Science and Clinical Advances. *Neurology,* 55**,** 1763.

RIDET, J. L., MALHOTRA, S. K., PRIVAT, A. & GAGE, F. H. 1997. Reactive astrocytes: cellular and molecular cues to biological function. *Trends Neurosci,* 20**,** 570-7.

ROBEL, S., BARDEHLE, S., LEPIER, A., BRAKEBUSCH, C. & GOTZ, M. 2011. Genetic deletion of cdc42 reveals a crucial role for astrocyte recruitment to the injury site in vitro and in vivo. *J Neurosci,* 31**,** 12471-82.

ROBINSON, S. W., MORRIS, C. D., GOLDMUNTZ, E., RELLER, M. D., JONES, M. A., STEINER, R. D. & MASLEN, C. L. 2003. Missense mutations in CRELD1 are associated with cardiac atrioventricular septal defects. *Am J Hum Genet,* 72**,** 1047-52.

ROEBROEK, A. J., VAN DE VELDE, H. J., VAN BOKHOVEN, A., BROERS, J. L., RAMAEKERS, F. C. & VAN DE VEN, W. J. 1993. Cloning and expression of alternative transcripts of a novel neuroendocrine-specific gene and identification of its 135-kDa translational product. *J Biol Chem,* 268**,** 13439-47.

ROESSMANN, U., VELASCO, M. E., SINDELY, S. D. & GAMBETTI, P. 1980. Glial fibrillary acidic protein (GFAP) in ependymal cells during development. An immunocytochemical study. *Brain Res,* 200**,** 13-21.

ROLLS, A., SHECHTER, R. & SCHWARTZ, M. 2009. The bright side of the glial scar in CNS repair. *Nat Rev Neurosci,* 10**,** 235-41.

RUPP, P. A., FOUAD, G. T., EGELSTON, C. A., REIFSTECK, C. A., OLSON, S. B., KNOSP, W. M., GLANVILLE, R. W., THORNBURG, K. L., ROBINSON, S. W. & MASLEN, C. L. 2002. Identification, genomic organization and mRNA expression of CRELD1, the founding member of a unique family of matricellular proteins. *Gene,* 293**,** 47-57.

RUSCHEL, J., HELLAL, F., FLYNN, K. C., DUPRAZ, S., ELLIOTT, D. A., TEDESCHI, A., BATES, M., SLIWINSKI, C., BROOK, G., DOBRINDT, K., PEITZ, M., BRUSTLE, O., NORENBERG, M. D., BLESCH, A., WEIDNER, N., BUNGE, M. B., BIXBY, J. L. & BRADKE, F. 2015. Axonal regeneration. Systemic administration of epothilone B promotes axon regeneration after spinal cord injury. *Science,* 348**,** 347-52.

SABEL, B. A., DELMASTRO, R., DUNBAR, G. L. & STEIN, D. G. 1987. Reduction of anterograde degeneration in brain damaged rats by GM1-gangliosides. *Neurosci Lett,* 77**,** 360-6.

SAHNI, V. & KESSLER, J. A. 2010. Stem cell therapies for spinal cord injury. *Nat Rev Neurol,* 6**,** 363-72.

SAHNI, V., MUKHOPADHYAY, A., TYSSELING, V., HEBERT, A., BIRCH, D., MCGUIRE, T. L., STUPP, S. I. & KESSLER, J. A. 2010. BMPR1a and BMPR1b signaling exert opposing effects on gliosis after spinal cord injury. *J Neurosci,* 30**,** 1839-55.

SAIJILAFU & ZHOU, F. Q. 2012. Genetic study of axon regeneration with cultured adult dorsal root ganglion neurons. *J Vis Exp*.

SANDVIG, A., BERRY, M., BARRETT, L. B., BUTT, A. & LOGAN, A. 2004. Myelin-, reactive glia-, and scar-derived CNS axon growth inhibitors: expression, receptor signaling, and correlation with axon regeneration. *Glia,* 46**,** 225-51.

SCHACHTRUP, C., RYU, J. K., HELMRICK, M. J., VAGENA, E., GALANAKIS, D. K., DEGEN, J. L., MARGOLIS, R. U. & AKASSOGLOU, K. 2010. Fibrinogen triggers astrocyte scar formation by

promoting the availability of active TGF-beta after vascular damage. *J Neurosci,* 30**,** 5843-54.

SCHMALBRUCH, H. 1987. The number of neurons in dorsal root ganglia L4-L6 of the rat. *Anat Rec,* 219**,** 315-22.

SCHMANDKE, A., SCHMANDKE, A. & STRITTMATTER, S. M. 2007. ROCK and Rho: biochemistry and neuronal functions of Rho-associated protein kinases. *Neuroscientist,* 13**,** 454-69.

SCHMIDT, A. & HALL, A. 2002. Guanine nucleotide exchange factors for Rho GTPases: turning on the switch. *Genes Dev,* 16**,** 1587-609.

SCHNAAR, R. L. 2010. Brain gangliosides in axon-myelin stability and axon regeneration. *FEBS Lett,* 584**,** 1741-7.

SCHWAB, M. E. 2010. Functions of Nogo proteins and their receptors in the nervous system. *Nature Reviews Neuroscience,* 11**,** 799-811.

SEEGER, M., TEAR, G., FERRES-MARCO, D. & GOODMAN, C. S. 1993. Mutations affecting growth cone guidance in Drosophila: genes necessary for guidance toward or away from the midline. *Neuron,* 10**,** 409-26.

SENDEN, N. H., VAN DE VELDE, H. J., BROERS, J. L., TIMMER, E. D., KUIJPERS, H. J., ROEBROEK, A. J., VAN DE VEN, W. J. & RAMAEKERS, F. C. 1994. Subcellular localization and supramolecular organization of neuroendocrine-specific protein B (NSP-B) in small cell lung cancer. *Eur J Cell Biol,* 65**,** 341-53.

SHARMA, K., SELZER, M. E. & LI, S. 2012. Scar-mediated inhibition and CSPG receptors in the CNS. *Exp Neurol,* 237**,** 370-8.

SHARP, J., FRAME, J., SIEGENTHALER, M., NISTOR, G. & KEIRSTEAD, H. S. 2010. Human embryonic stem cell-derived oligodendrocyte progenitor cell transplants improve recovery after cervical spinal cord injury. *Stem Cells,* 28**,** 152-63.

SHEN, Y., TENNEY, A. P., BUSCH, S. A., HORN, K. P., CUASCUT, F. X., LIU, K., HE, Z., SILVER, J. & FLANAGAN, J. G. 2009. PTPσ is a receptor for chondroitin sulfate proteoglycan, an inhibitor of neural regeneration. *Science,* 326**,** 592-596.

SHI, Q., GE, Y. Y., SHAROAR, M. G., HE, W. X., XIANG, R., ZHANG, Z. H., HU, X. Y. & YAN, R. Q. 2014. Impact of RTN3 Deficiency on Expression of BACE1 and Amyloid Deposition. *Journal of Neuroscience,* 34**,** 13954-13962.

SHI, Q., HU, X., PRIOR, M. & YAN, R. 2009a. The occurrence of aging-dependent reticulon 3 immunoreactive dystrophic neurites decreases cognitive function. *J Neurosci,* 29**,** 5108-15.

SHI, Q., PRIOR, M., HE, W., TANG, X., HU, X. & YAN, R. 2009b. Reduced amyloid deposition in mice overexpressing RTN3 is adversely affected by preformed dystrophic neurites. *J Neurosci,* 29**,** 9163-73.

SHOICHET, M. S., TATE, C. C., BAUMANN, M. D. & LAPLACA, M. C. 2008. Strategies for Regeneration and Repair in the Injured Central Nervous System. *In:* REICHERT, W. M. (ed.) *Indwelling Neural Implants: Strategies for Contending with the In Vivo Environment.* Boca Raton (FL).

SILVA, G. A., SANADA, L., MACHADO, N. L., CARMO, E., OLIVEIRA, A. & FAZAN, V. P. 2015. Immunohistochemical Protocol to Identify Glial Fibrillary Acid Protein (GFAP) in the Dorsal Horn of the Spinal Cord. *The FASEB Journal,* 29**,** 704.3.

SILVER, J. & MILLER, J. H. 2004. Regeneration beyond the glial scar. *Nat Rev Neurosci,* 5**,** 146-56.

SMITH, K. J. & BENNETT, B. J. 1987. Topographic and quantitative description of rat dorsal column fibres arising from the lumbar dorsal roots. *J Anat,* 153**,** 203-15.

SNOW, D. M., LEMMON, V., CARRINO, D. A., CAPLAN, A. I. & SILVER, J. 1990. Sulfated proteoglycans in astroglial barriers inhibit neurite outgrowth in vitro. *Exp Neurol,* 109**,** 111-30.

SOFRONIEW, M. V. 2009. Molecular dissection of reactive astrogliosis and glial scar formation. *Trends Neurosci,* 32**,** 638-47.

SONTHEIMER, H. 2008. A role for glutamate in growth and invasion of primary brain tumors. *J Neurochem,* 105**,** 287-95.

SU, Z. Z., CHEN, Y., KANG, D. C., CHAO, W., SIMM, M., VOLSKY, D. J. & FISHER, P. B. 2003. Customized rapid subtraction hybridization (RaSH) gene microarrays identify overlapping expression changes in human fetal astrocytes resulting from human immunodeficiency virus-1 infection or tumor necrosis factor-alpha treatment. *Gene,* 306**,** 67-78.

SU, Z. Z., KANG, D. C., CHEN, Y., PEKARSKAYA, O., CHAO, W., VOLSKY, D. J. & FISHER, P. B. 2002. Identification and cloning of human astrocyte genes displaying elevated expression after infection with HIV-1 or exposure to HIV-1 envelope glycoprotein by rapid subtraction hybridization, RaSH. *Oncogene,* 21**,** 3592-602.

SUREY, S. 2015. *Understanding the molecular mechanisms of spinal cord cavitation after spinal cord injury.* University of Birmingham.

SUREY, S., BERRY, M., LOGAN, A., BICKNELL, R. & AHMED, Z. 2014. Differential cavitation, angiogenesis and wound-healing responses in injured mouse and rat spinal cords. *Neuroscience,* 275**,** 62-80.

SUTHERLAND, H. G., LAM, Y. W., BRIERS, S., LAMOND, A. I. & BICKMORE, W. A. 2004. 3D3/lyric: a novel transmembrane protein of the endoplasmic reticulum and nuclear envelope, which is also present in the nucleolus. *Exp Cell Res,* 294**,** 94-105.

SUZUKI, R. & NISHIYAMA, A. 2009. Polydendrocytes--their roles in development and glial tumor formation. *Brain and nerve= Shinkei kenkyu no shinpo,* 61**,** 733-739.

SYKOVA, E., HOMOLA, A., MAZANEC, R., LACHMANN, H., KONRADOVA, S. L., KOBYLKA, P., PADR, R., NEUWIRTH, J., KOMRSKA, V., VAVRA, V., STULIK, J. & BOJAR, M. 2006. Autologous bone marrow transplantation in patients with subacute and chronic spinal cord injury. *Cell Transplant,* 15**,** 675-87.

SYPECKA, J. 2011. Searching for oligodendrocyte precursors for cell replacement therapies. *Acta Neurobiol Exp (Wars),* 71**,** 94-102.

TALAC, R., FRIEDMAN, J. A., MOORE, M. J., LU, L., JABBARI, E., WINDEBANK, A. J., CURRIER, B. L. & YASZEMSKI, M. J. 2004. Animal models of spinal cord injury for evaluation of tissue engineering treatment strategies. *Biomaterials,* 25**,** 1505-10.

TAMATANI, M., SENBA, E. & TOHYAMA, M. 1989. Calcitonin gene-related peptide-and substance P-containing primary afferent fibers in the dorsal column of the rat. *Brain research,* 495**,** 122-130.

TAN, C. L., KWOK, J. C., PATANI, R., FFRENCH-CONSTANT, C., CHANDRAN, S. & FAWCETT, J. W. 2011. Integrin activation promotes axon growth on inhibitory chondroitin sulfate proteoglycans by enhancing integrin signaling. *J Neurosci,* 31**,** 6289-95.

TANG, X., DAVIES, J. E. & DAVIES, S. J. 2003. Changes in distribution, cell associations, and protein expression levels of NG2, neurocan, phosphacan, brevican, versican V2, and tenascin-C during acute to chronic maturation of spinal cord scar tissue. *J Neurosci Res,* 71**,** 427-44.

TATOR, C. H. 2006. Review of treatment trials in human spinal cord injury: issues, difficulties, and recommendations. *Neurosurgery,* 59**,** 957-82; discussion 982-7.

TOM, V. J., SANDROW-FEINBERG, H. R., MILLER, K., DOMITROVICH, C., BOUYER, J., ZHUKAREVA, V., KLAW, M. C., LEMAY, M. A. & HOULÉ, J. D. 2013. Exogenous BDNF enhances the integration of chronically injured axons that regenerate through a peripheral nerve grafted into a chondroitinase-treated spinal cord injury site. *Experimental neurology,* 239**,** 91-100.

TSAI, E. C., KRASSIOUKOV, A. V. & TATOR, C. H. 2005. Corticospinal regeneration into lumbar grey matter correlates with locomotor recovery after complete spinal cord transection and repair with peripheral nerve grafts, fibroblast growth factor 1, fibrin glue, and spinal fusion. *Journal of Neuropathology & Experimental Neurology,* 64**,** 230-244.

VARMA, A. K., DAS, A., WALLACE, G. T., BARRY, J., VERTEGEL, A. A., RAY, S. K. & BANIK, N. L. 2013. Spinal cord injury: a review of current therapy, future treatments, and basic science frontiers. *Neurochem Res,* 38**,** 895-905.

VARTAK-SHARMA, N. & GHORPADE, A. 2012. Astrocyte elevated gene-1 regulates astrocyte responses to neural injury: implications for reactive astrogliosis and neurodegeneration. *J Neuroinflammation,* 9**,** 195.

VETTER, I., PUJIC, Z. & GOODHILL, G. J. 2010. The response of dorsal root ganglion axons to nerve growth factor gradients depends on spinal level. *J Neurotrauma,* 27**,** 1379-86.

VISKOCHIL, D., CAWTHON, R., O'CONNELL, P., XU, G., STEVENS, J., CULVER, M., CAREY, J. & WHITE, R. 1991. The gene encoding the oligodendrocyte-myelin glycoprotein is embedded within the neurofibromatosis type 1 gene. *Molecular and cellular biology,* 11**,** 906-912.

VOELTZ, G. K., PRINZ, W. A., SHIBATA, Y., RIST, J. M. & RAPOPORT, T. A. 2006. A class of membrane proteins shaping the tubular endoplasmic reticulum. *Cell,* 124**,** 573-86.

WAHLQUIST, C., JEONG, D., ROJAS-MUNOZ, A., KHO, C., LEE, A., MITSUYAMA, S., VAN MIL, A., PARK, W. J., SLUIJTER, J. P., DOEVENDANS, P. A., HAJJAR, R. J. & MERCOLA, M. 2014. Inhibition of miR-25 improves cardiac contractility in the failing heart. *Nature,* 508**,** 531-5.

WAILE, P., TRACEY, D. & PAXINOS, G. 1995. Somatosensory system. *The Rat Nervous System***,** 689-724.

WAKANA, Y., KOYAMA, S., NAKAJIMA, K., HATSUZAWA, K., NAGAHAMA, M., TANI, K., HAURI, H. P., MELANCON, P. & TAGAYA, M. 2005. Reticulon 3 is involved in membrane trafficking between the endoplasmic reticulum and Golgi. *Biochem Biophys Res Commun,* 334**,** 1198-205.

WALL, P. 1992. Sensory mechanisms of the spinal cord. *Journal of anatomy,* 180**,** 352.

WALLQUIST, W., ZELANO, J., PLANTMAN, S., KAUFMAN, S. J., CULLHEIM, S. & HAMMARBERG, H. 2004. Dorsal root ganglion neurons up-regulate the expression of laminin-associated integrins after peripheral but not central axotomy. *J Comp Neurol,* 480**,** 162-9.

WANG, X., HASAN, O., ARZENO, A., BENOWITZ, L. I., CAFFERTY, W. B. & STRITTMATTER, S. M. 2012a. Axonal regeneration induced by blockade of glial inhibitors coupled with activation of intrinsic neuronal growth pathways. *Exp Neurol,* 237**,** 55-69.

WANG, Y., APARA, A., BLACKMORE, M., BROWN, D., LEBLANC, M., TRILLO, A. & GOLDBERG, J. 2013. Regulation of Krüppel-like Transcription Factor (KLF's) Family Members Promotes Potent Axon Regeneration in the Adult Rat Optic Nerve. *Investigative Ophthalmology & Visual Science,* 54**,** 4693-4693.

WANG, Y., ZHANG, W., ZHU, X., WANG, Y., MAO, X., XU, X. & WANG, Y. 2016. Upregulation of AEG-1 Involves in Schwann Cell Proliferation and Migration After Sciatic Nerve Crush. *J Mol Neurosci,* 60**,** 248-57.

WANG, Z., YANG, L. & ZHENG, H. 2012b. Role of APP and Abeta in synaptic physiology. *Curr Alzheimer Res,* 9**,** 217-26.

WARNER, F. M., CRAGG, J. J., JUTZELER, C. R., ROHRICH, F., WEIDNER, N., SAUR, M., MAIER, D. D., SCHULD, C., SITES, E., CURT, A. & KRAMER, J. K. 2017. Early Administration of Gabapentinoids Improves Motor Recovery after Human Spinal Cord Injury. *Cell Rep,* 18**,** 1614-1618.

WATANABE, M., TOYAMA, Y. & NISHIYAMA, A. 2002. Differentiation of proliferated NG2-positive glial progenitor cells in a remyelinating lesion. *J Neurosci Res,* 69**,** 826-36.

WELLER, R. O., GALEA, I., CARARE, R. O. & MINAGAR, A. 2010. Pathophysiology of the lymphatic drainage of the central nervous system: Implications for pathogenesis and therapy of multiple sclerosis. *Pathophysiology,* 17**,** 295-306.

WIDENFALK, J., LUNDSTROMER, K., JUBRAN, M., BRENE, S. & OLSON, L. 2001. Neurotrophic factors and receptors in the immature and adult spinal cord after mechanical injury or kainic acid. *J Neurosci,* 21**,** 3457-75.

WIGHTMAN, L., KIRCHEIS, R., ROSSLER, V., CAROTTA, S., RUZICKA, R., KURSA, M. & WAGNER, E. 2001. Different behavior of branched and linear polyethylenimine for gene delivery in vitro and in vivo. *J Gene Med,* 3**,** 362-72.

WILLIS JR, W. D. & COGGESHALL, R. E. 2004. Sensory pathways in the dorsal funiculus. *Sensory mechanisms of the spinal cord.* Springer.

WILLSON, C. A., IRIZARRY-RAMIREZ, M., GASKINS, H. E., CRUZ-ORENGO, L., FIGUEROA, J. D., WHITTEMORE, S. R. & MIRANDA, J. D. 2002. Upregulation of EphA receptor expression in the injured adult rat spinal cord. *Cell Transplant,* 11**,** 229-39.

WILLYARD, C. 2013. Stem cells: a time to heal. *Nature,* 503**,** S4-S6.

WISEMAN, J. W., GODDARD, C. A., MCLELLAND, D. & COLLEDGE, W. H. 2003. A comparison of linear and branched polyethylenimine (PEI) with DCChol/DOPE liposomes for gene delivery to epithelial cells in vitro and in vivo. *Gene Ther,* 10**,** 1654-62.

WONG, S. T., HENLEY, J. R., KANNING, K. C., HUANG, K. H., BOTHWELL, M. & POO, M. M. 2002. A p75(NTR) and Nogo receptor complex mediates repulsive signaling by myelin-associated glycoprotein. *Nat Neurosci,* 5**,** 1302-8.

WU, K., MEYERS, C. A., BENNETT, J. A., KING, M. A., MEYER, E. M. & HUGHES, J. A. 2004. Polyethylenimine-mediated NGF gene delivery protects transected septal cholinergic neurons. *Brain Res,* 1008**,** 284-7.

XIANG, R., LIU, Y., ZHU, L., DONG, W. & QI, Y. 2006. Adaptor FADD is recruited by RTN3/HAP in ER-bound signaling complexes. *Apoptosis,* 11**,** 1923-32.

XIANG, R. & ZHAO, S. 2009. RTN3 inducing apoptosis is modulated by an adhesion protein CRELD1. *Mol Cell Biochem,* 331**,** 225-30.

XU, X. M., GUÉNARD, V., KLEITMAN, N., AEBISCHER, P. & BUNGE, M. B. 1995. A combination of BDNF and NT-3 promotes supraspinal axonal regeneration into Schwann cell grafts in adult rat thoracic spinal cord. *Experimental neurology,* 134**,** 261-272.

YANG, M. L., LI, J. J., SO, K. F., CHEN, J. Y., CHENG, W. S., WU, J., WANG, Z. M., GAO, F. & YOUNG, W. 2012. Efficacy and safety of lithium carbonate treatment of chronic spinal cord

injuries: a double-blind, randomized, placebo-controlled clinical trial. *Spinal Cord,* 50**,** 141-6.

YANG, N. 2015. An overview of viral and nonviral delivery systems for microRNA. *Int J Pharm Investig,* 5**,** 179-81.

YANG, N., HIGUCHI, O., OHASHI, K., NAGATA, K., WADA, A., KANGAWA, K., NISHIDA, E. & MIZUNO, K. 1998. Cofilin phosphorylation by LIM-kinase 1 and its role in Rac-mediated actin reorganization. *Nature,* 393**,** 809-12.

YANG, Y. S. & STRITTMATTER, S. M. 2007. The reticulons: a family of proteins with diverse functions. *Genome Biol,* 8**,** 234.

YE, Z. C. & SONTHEIMER, H. 1999. Glioma cells release excitotoxic concentrations of glutamate. *Cancer Res,* 59**,** 4383-91.

YIN, X., REN, M., JIANG, H., CUI, S., WANG, S., JIANG, H., QI, Y., WANG, J., WANG, X. & DONG, G. 2015. Downregulated AEG-1 together with inhibited PI3K/Akt pathway is associated with reduced viability of motor neurons in an ALS model. *Molecular and Cellular Neuroscience,* 68**,** 303-313.

YISHENG, W., FUYING, Z., LIMIN, W., JUNWEI, L., GUOFU, P. & WEIDONG, W. 2007. First aid and treatment for cervical spinal cord injury with fracture and dislocation. *Indian J Orthop,* 41**,** 300-4.

YOO, B. K., EMDAD, L., LEE, S. G., SU, Z. Z., SANTHEKADUR, P., CHEN, D., GREDLER, R., FISHER, P. B. & SARKAR, D. 2011. Astrocyte elevated gene-1 (AEG-1): A multifunctional regulator of normal and abnormal physiology. *Pharmacol Ther,* 130**,** 1-8.

ZHANG, Y., ZHANG, Y. P., PEPINSKY, B., HUANG, G., SHIELDS, L. B., SHIELDS, C. B. & MI, S. 2015. Inhibition of LINGO-1 promotes functional recovery after experimental spinal cord demyelination. *Exp Neurol,* 266**,** 68-73.

ZHAO, X. 2016. HMGB1 (AMPHOTERIN) AND AMIGO1 IN BRAIN DEVELOPMENT.

ZHAO, Z.-S. & MANSER, E. 2005. PAK and other Rho-associated kinases–effectors with surprisingly diverse mechanisms of regulation. *Biochemical Journal,* 386**,** 201-214.

ZHOU, L., BAUMGARTNER, B. J., HILL-FELBERG, S. J., MCGOWEN, L. R. & SHINE, H. D. 2003. Neurotrophin-3 expressed in situ induces axonal plasticity in the adult injured spinal cord. *J Neurosci,* 23**,** 1424-31.

ZHOU, Z. D., SATHIYAMOORTHY, S. & TAN, E. K. 2012. LINGO-1 and Neurodegeneration: Pathophysiologic Clues for Essential Tremor. *Tremor Other Hyperkinet Mov (N Y),* 2.

ZILLER, C., LINCET, H., MULLER, C. D., STAEDEL, C., BEHR, J. P. & POULAIN, L. 2004. The cyclin-dependent kinase inhibitor p21(cip1/waf1) enhances the cytotoxicity of ganciclovir in HSV-tk transfected ovarian carcinoma cells. *Cancer Lett,* 212**,** 43-52.

ZORNER, B. & SCHWAB, M. E. 2010. Anti-Nogo on the go: from animal models to a clinical trial. *Ann N Y Acad Sci,* 1198 Suppl 1**,** E22-34.

ZUCKERMANN, M., HOVESTADT, V., KNOBBE-THOMSEN, C. B., ZAPATKA, M., NORTHCOTT, P. A., SCHRAMM, K., BELIC, J., JONES, D. T., TSCHIDA, B., MORIARITY, B., LARGAESPADA, D., ROUSSEL, M. F., KORSHUNOV, A., REIFENBERGER, G., PFISTER, S. M., LICHTER, P., KAWAUCHI, D. & GRONYCH, J. 2015. Somatic CRISPR/Cas9-mediated tumour suppressor disruption enables versatile brain tumour modelling. *Nat Commun,* 6**,** 7391.

ZUREK, N., SPARKS, L. & VOELTZ, G. 2011. Reticulon short hairpin transmembrane domains are used to shape ER tubules. *Traffic,* 12**,** 28-41.